

# TCAD Parameters for 4H-SiC: A Review

Jürgen Burin,<sup>1</sup> Philipp Gaggl,<sup>1</sup> Simon Waid,<sup>1</sup> Andreas Gsponer,<sup>1</sup> and Thomas Bergauer<sup>1</sup>

*Institute of High Energy Physics, Austrian Academy of Sciences, Nikolsdorfer Gasse 18, 1050 Wien*

(\*e-mail: [juergen.burin@oeaw.ac.at](mailto:juergen.burin@oeaw.ac.at))

(Dated: 11 February 2025)

In this paper we review the models and their parameters to describe the relative permittivity, bandgap, impact ionization, mobility, charge carrier recombination/effective masses and incomplete dopant ionization of 4H silicon carbide in computer simulations. We aim to lower the entrance barrier for newcomers and provide a critical evaluation of the status quo to identify shortcomings and guide future research. The review reveals a rich set of often diverging values in literature based on a variety of calculation and measurement methods. Although research for all the selected parameters is still active, we show that sometimes old values or those determined for other kinds of silicon carbide are commonly used.

Keywords: 4H-SiC, TCAD simulations, simulation parameters, silicon carbide

## CONTENTS

<b>I. Relative Permittivity</b>	4
A. Theory	4
B. Results	5
C. Discussion	7
<b>II. Density-of-States Effective Mass</b>	11
A. Theory	12
1. Effective Masses along Principal Directions	12
2. Density-of-States (DOS) Mass	12
3. Conductivity Effective Mass	13
4. Polaron Mass	14
B. Results	15
1. Effective Mass along Principal Directions	15
2. DOS Mass	17
3. Temperature	20
4. Effective DOS Mass for TCAD Tools	21
C. Discussion	21
<b>III. Band Gap</b>	23
A. Theory	25
1. Temperature Dependency	26
2. Doping Dependency	27
B. Results & Discussion	29
1. Temperature Dependency	31
2. Doping Dependency	34
3. TCAD Values	36
<b>IV. Impact Ionization</b>	40
A. Theory	41
B. Results	43
C. Discussion	49

<b>V. Charge Carrier Recombination</b>	51
A. Theory	52
1. Shockley-Read-Hall Recombination	52
2. Bimolecular Recombination	57
3. Auger Recombination	58
4. Analysis	59
B. Results & Discussion	60
1. SRH Lifetime	61
2. Doping Dependency of SRH Lifetime	65
3. Temperature Dependency of SRH Lifetime	69
4. Surface Recombination Velocity	71
5. Bimolecular Recombination	74
6. Auger Recombination	74
<b>VI. Incomplete Ionization</b>	77
A. Theory	79
B. Results	81
C. Discussion	86
<b>VII. Mobility</b>	92
A. Theory	92
1. Low-Field Mobility	93
2. High-Field Mobility	96
3. Carrier-Carrier Scattering	97
4. Hall Scattering Factor	97
B. Results & Discussion	98
1. Measurements	98
2. Low-Field Mobility	100
3. High-Field Mobility	114
4. Carrier-Carrier Scattering	119
<b>References</b>	121

## I. RELATIVE PERMITTIVITY

The permittivity  $\epsilon$  describes the dielectric properties that influence electromagnetic wave propagation within a material and their reflections on interfaces<sup>2</sup>. These effects are, for example, essential to describe the impact of an external electric field, which determines the capacitance values in a device. In general, the user has to provide the relative permittivity  $\epsilon_r = \epsilon/\epsilon_0$ , i.e., the ratio compared to the vacuum permittivity  $\epsilon_0 = 8.854 \times 10^{-12} \text{ F/m}$ , to the TCAD tools.

### A. Theory

In the frequency domain, the complex relative permittivity can be written as

$$\epsilon_r^*(\omega) = \epsilon'(\omega) + i\epsilon''(\omega).$$

The real part  $\epsilon'$  represents the energy stored in the material when exposed to an electric field and the imaginary part  $\epsilon''$  the losses (e.g., absorption and attenuation)<sup>2</sup>.  $\epsilon'$  and  $\epsilon''$  are tightly interconnected via the Kramers-Kronig (KK) relation<sup>3</sup>

$$\epsilon'(\omega) = 1 + \frac{2}{\pi} \int_0^\infty \frac{\omega' \epsilon''(\omega')}{\omega'^2 - \omega^2} d\omega' \quad (1a)$$

$$\epsilon''(\omega) = -\frac{2\omega}{\pi} \int_0^\infty \frac{\epsilon'(\omega')}{\omega'^2 - \omega^2} d\omega' \quad (1b)$$

In TCAD simulations of semiconductor devices  $\epsilon''$  is of diminishing importance, but  $\epsilon'$  is required to calculate capacitances or the electric field distribution. Consequently, we will focus on  $\epsilon'$  in the sequel.

In the literature the static ( $\epsilon_s$ ) and high-frequency resp. optical ( $\epsilon_\infty$ ) relative permittivity are distinguished. The former is  $\epsilon'(\omega \rightarrow 0)$  but a definition of the latter is more complicated. It denotes  $\epsilon'$  at the end of the reststrahlen range towards higher frequencies, where the real part of the refractive index is null<sup>4</sup>. In publications that focus on optical high-frequency analysis  $\epsilon_\infty$  is sometimes denoted as  $\epsilon'(0)$ <sup>5</sup>, which must not be confused with  $\epsilon_s$ . These inconsistencies were explained in the following fashion<sup>6</sup>: “We shall use  $\epsilon_\infty$  to denote the extrapolation … to zero frequency. This somewhat contradictory notation arose because  $\epsilon_\infty$  the “optical” dielectric constant, was often set … at a frequency much higher than the lattice frequency, but low compared with electronic transition frequencies. In many substances no suitable frequency exists, and it is preferable to extrapolate optical data to zero frequency …”

To clarify:  $\epsilon_\infty$  is measured at frequencies well above the long-wavelength longitudinal optical (LO) phonon frequency  $\omega_{\text{LO}}$ <sup>3</sup>.  $\omega_{\text{LO}}$  translates  $\epsilon_s$  into  $\epsilon_\infty$  and vice versa in conjunction with the transversal optical (TO) phonon frequency  $\omega_{\text{TO}}$  and the Lyddane-Sachs-Teller (LST) relationship<sup>7</sup>

$$\frac{\epsilon_s}{\epsilon_\infty} = \left( \frac{\omega_{\text{LO}}}{\omega_{\text{TO}}} \right)^2. \quad (2)$$

For  $\omega_{\text{LO}}$  we encountered the energy values 120 meV (approximately 29 THz)<sup>8–12</sup>, 104 to 121 meV<sup>13</sup> and 104.2 meV<sup>14</sup> in our search. Instead of the energy often the respective wave numbers are presented, i.e., (in  $\text{cm}^{-1}$ )  $\omega_{\text{TO}} = 793$  and  $\omega_{\text{LO}} = 974$ <sup>15</sup>,  $\omega_{\text{LO}}^{\parallel} = 964.2$ ,  $\omega_{\text{LO}}^{\perp} = 966.4$ ,  $\omega_{\text{TO}}^{\parallel} = 783$  and  $\omega_{\text{TO}}^{\perp} = 798$ <sup>16</sup>,  $\omega_{\text{TO}} = 783$  and  $\omega_{\text{LO}} = 964$ <sup>17</sup> and  $\omega_{\text{LO}} \in [967, 971]$ <sup>18</sup>.

## B. Results

Various approaches have been used to determine the relative permittivity: One possibility are calculations using the density functional theory (DFT) based local density approximation (LDA)<sup>5,8,19–24</sup> or the effective mass theory<sup>25</sup>. With these the band structure and, thus,  $\epsilon''$  is calculated and then transformed into  $\epsilon'$  using the Kramers-Kronig relations (Eq. (1)). Measurements use either some form of resonator (RES)<sup>26–28</sup>, spectroscopy (SPEC)<sup>29–31</sup>, spectroscopic ellipsometry (SE)<sup>32,33</sup> or the refractive index (RI)<sup>6,16,34</sup>. In some cases the transversal and longitudinal optical phonon frequencies are determined and used in the LST relationship (Eq. (2))<sup>32,33</sup>. Furthermore, the tight relationship between relative permittivity and complex refractive index, i.e.,  $n^*(E) = \sqrt{\epsilon(E)}$ <sup>3</sup>, with  $E = \hbar\omega$ , is utilized if  $\epsilon''$  is negligible. For fitting purposes the representation

$$n^2 = 1 + \frac{\epsilon_g}{1 - (hf/E_g)^2} \approx \epsilon_\infty + \epsilon_g \left( \frac{hf}{E_g} \right),$$

with  $hf$  the photon energy,  $E_g$  an "average band gap" and  $\epsilon_g$  proportional to the oscillator strength<sup>6</sup>, is used to extract  $\epsilon_\infty$ <sup>6,16,30,34</sup>. Finally, fitting to  $\ln(J/E)$ <sup>35</sup>, with  $J$  the current density, is also deployed.

The relative permittivity was furthermore investigated at mm-wave frequencies (MM) (10 GHz to 10 THz)<sup>27,36–39</sup> (nicely summarized by Li *et al.*<sup>28</sup>, Yanagimoto *et al.*<sup>40</sup>). Unfortunately, there are often fluctuations in the data or just single data points available, which makes an interpolation to zero frequency ( $= \epsilon_s$ ) not possible. For these reasons we had to discard most of the respective data. We also excluded publications whose values got refined in succeeding experiments<sup>41,42</sup>, that

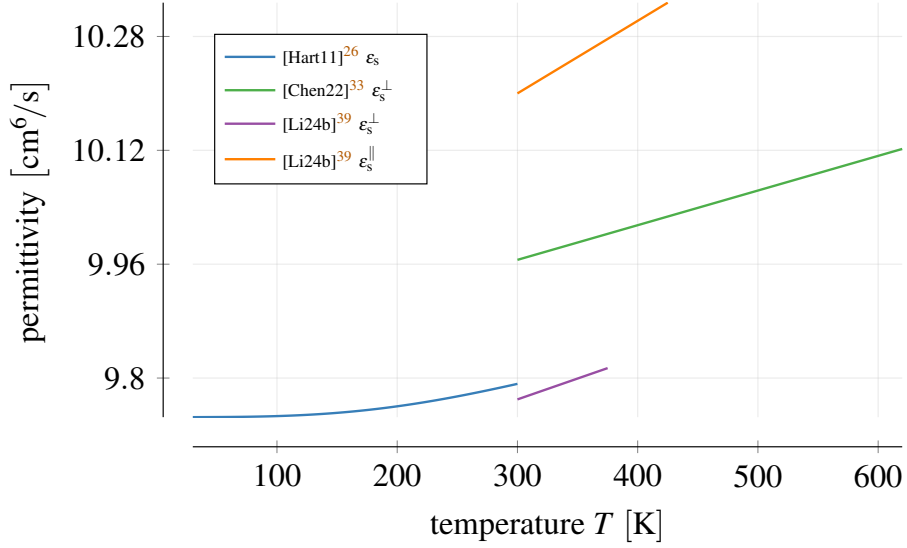


FIG. 1. Temperature dependency of the permittivity.

did not specify the investigated polytype<sup>43–46</sup> or where an extraction of the data values was not possible<sup>47</sup>.

With the listed characterization approaches values in the range of [9.6, 10.65] for the static relative permittivity and [6.25, 7.61] for the high-frequency one have been achieved (Table I). In the table we also show two references that exclusively provide 6H values because these are often referenced for 4H investigations. Wherever necessary we calculated the relative permittivity according to  $\epsilon_s = (\epsilon_s^{\parallel} \epsilon_s^{\perp 2})^{1/3}$  resp.  $\epsilon_{\infty} = (\epsilon_{\infty}^{\parallel} \epsilon_{\infty}^{\perp 2})^{1/3}$ <sup>48–52</sup>, which far more often used than  $\epsilon_s = (\epsilon_s^{\parallel} \epsilon_s^{\perp})^{1/2}$  proposed by Ivanov *et al.*<sup>25</sup>.

In TCAD tools the permittivity is a constant although research showed that there is a frequency<sup>26</sup> and temperature<sup>26,33</sup> dependency. For a frequency around 40 GHz Hartnett *et al.*<sup>26</sup> provided the approximation

$$\epsilon_s(T) = 9.7445 + 3.1862 \times 10^{-5} T - 6.3026 \times 10^{-7} T^2 + 5.9848 \times 10^{-9} T^3 - 8.2821 \times 10^{-12} T^4 ,$$

with the temperature  $T$  in K. Cheng, Yang, and Zheng<sup>33</sup> approximated  $\epsilon_s^{\perp} = 9.82 + 4.87 \times 10^{-4} T$  and Li *et al.*<sup>39</sup>  $\epsilon_s^{\perp} = 9.77 * (1 + 6 \times 10^{-5} (T - 300 \text{ K}))$  and  $\epsilon_s^{\parallel} = 10.2 * (1 + 1 \times 10^{-4} (T - 300 \text{ K}))$ . All approximations show an increase of the permittivity with temperature (Fig. 1).

TABLE I. Published relative permittivity values.

ref.	$\epsilon_s$	$\epsilon_s^{\parallel}$	$\epsilon_s^{\perp}$	$\epsilon_{\infty}$	$\epsilon_{\infty}^{\parallel}$	$\epsilon_{\infty}^{\perp}$	method <sup>a</sup>	SiC	doping
[Patr70] <sup>5</sup>	9.78 <sup>c</sup>	10.03	9.66	6.58 <sup>c</sup>	6.7	6.52	RI	6H	-
[Ikeda80] <sup>34</sup>	9.94 <sup>c</sup>	10.32	9.76	-	-	-	RI	4H	-
[Nino94] <sup>32</sup>	9.83 <sup>c</sup>	9.98	9.76	6.62 <sup>c</sup>	6.67	6.59	SE	6H	-
[Hari95] <sup>16</sup>	-	-	-	6.63 <sup>c</sup>	6.78	6.56	RI	4H	-
[Karc96] <sup>19</sup>	10.53 <sup>c</sup>	10.9	10.352	7.02 <sup>c</sup>	7.169	6.946	DFT-LDA	4H	-
[Well96] <sup>20</sup>	-	-	-	7.02 <sup>c</sup>	7.17	6.95	DFT-LDA	4H	-
[Adol97] <sup>21</sup>	-	-	-	7.56 <sup>c</sup>	7.61	7.54	DFT-LDA	4H	-
[Ahuja02] <sup>8</sup>	-	-	-	7.11 <sup>c</sup>	7.47	6.94	DFT-LDA	4H	n-type
[Peng04] <sup>22</sup>	-	-	-	6.31 <sup>c</sup>	6.44	6.25	DFT	4H	-
[Pers05] <sup>53</sup>	9.73 <sup>c</sup>	9.94	9.63	6.47 <sup>c</sup>	6.62	6.4	DFT-LDA	4H	intrinsic
[Chin06] <sup>5</sup>	-	-	-	6.81	-	-	DFT-LDA	4H	intrinsic
[Dutt06] <sup>36</sup>	9.97 $\pm$ 0.02 <sup>b</sup>	-	-	-	-	-	MM	4H	high purity
[Ivan06] <sup>25</sup>	9.93 $\pm$ 0.01	-	-	-	-	-	EMT	4H	intrinsic
[Hart11] <sup>26</sup>	9.77 <sup>d</sup>	-	-	-	-	-	RES	4H	high purity
[Jone11] <sup>27</sup>	9.6	-	-	-	-	-	RES	4H	high purity
[Naft16] <sup>29</sup>	10.11 <sup>c</sup>	10.53 <sup>f</sup>	9.91 <sup>f</sup>	-	-	-	SPEC	4H	undoped
[Cout17] <sup>24</sup>	10.13 <sup>c</sup>	10.65	9.88	-	-	-	DFT-LDA	4H	-
[Tare19] <sup>30</sup>	-	-	-	6.587 $\pm$ 0.003	-	-	SPEC	4H	-
[Chen22] <sup>33</sup>	9.97 <sup>g</sup>	-	-	-	-	-	SE	4H	-
[Gao22a] <sup>31</sup>	-	-	-	6.51	-	-	SPEC	4H	-
[Yang22a] <sup>35</sup>	10.21	-	-	-	-	-	$\ln(J/E)$	4H	p-type
[Li23] <sup>28</sup>	-	10.27 $\pm$ 0.03	-	-	-	-	RES	4H	high purity
[Li24b] <sup>39</sup>	9.91 <sup>c</sup>	10.20 $\pm$ 0.05	9.77 $\pm$ 0.01	-	-	-	RES	4H	high purity

<sup>a</sup> description of the single methods in the text

<sup>b</sup> frequency range 131–145 GHz, for lower resp. higher frequencies  $\epsilon_s = 9.74$  was achieved

<sup>c</sup>  $\epsilon_s = (\epsilon_s^{\perp 2} \epsilon_s^{\parallel})^{1/3}$

<sup>d</sup> temperature and frequency dependent

<sup>e</sup> calculated from refractive index  $n$  as  $\epsilon_s = n^2$

<sup>f</sup> wavelength-dependent refractive index presented

<sup>g</sup> temperature dependent

## C. Discussion

We identified two very influential publications, largely dominating the permittivity values found in literature. Ikeda, Matsunami, and Tanaka<sup>34</sup> published, based on measurements from Shaffer<sup>58</sup>, in 1980 the first 4H-SiC permittivity data. Although these values are broadly used in liter-

ature<sup>23,59–63</sup>, we never found a citation of that particular paper. Not even cross-references among the citing publications exist.

In 1970, so ten years prior to the first 4H values, Patrick and Choyke<sup>6</sup> determined, based on measurements published in 1944<sup>64</sup>, the permittivity of the 6H polytype. Many publications on 4H-SiC used these results (see Fig. 2) despite the deviating polytype. Some authors claimed that dedicated 4H values were not available<sup>13,49,65–68</sup>, a mistake as we showed before. Nevertheless, it is still claimed up to this day<sup>33</sup>. This shows, how hard it is to get a comprehensive overview over 4H-SiC TCAD parameters. In contrast to early analysis, that clearly highlight that 6H values were used<sup>69</sup>, the majority of publications simply adopts the parameters without further remark, which leaves the false impression that proper 4H values were used.

Rounding of the original values, e.g.,  $9.66 \rightarrow 9.7 \rightarrow 10^{72,83}$  (see Fig. 2), and mere typographical errors, e.g., turning 9.66 into 9.67<sup>92</sup> (a comprehensive analysis of all encountered inconsistencies is shown in ??), expanded the range of available values (see Figs. 3 and 4). In these figures we connected those values where at least one direct connection could be found. Due to missing references we can, however, not guarantee that all authors made their selection based on the same data. In many cases, e.g., for the prominent values  $\epsilon_s = 9.7$  or  $\epsilon_s = 10$ , it is not unreasonable to assume that simply the permittivity in one principal direction was picked.

An interesting case is  $\epsilon_s = 8.5584^{93,94}$ , which is supposed to be based on  $\epsilon_s^\perp = 9.66$  and  $\epsilon_s^\parallel = 10.03^{57}$ . We were not able to achieve this value analytically since the result is lower than both constituents. Only when we added the high-frequency relative permittivity to the calculations we achieved a somewhat close value of 8. Such a combination is, however, not justifiable.

Overall, the missing awareness regarding 4H related permittivity values is striking. One explanation why the same old values are reused over and over again are the often very long citation (see Fig. 2). Combined with often missing references this makes it difficult to pinpoint the origin of a value and thus assess its suitability. Another interpretation of the achieved results is that the permittivity has little impact in TCAD simulations, such that somewhat accurate 6H values are already sufficient. Nevertheless, even if this was the case, we highly encourage the scientific community to adopt the most recent measurement 4H-SiC in future publications to make these values more prominently known and, thus, lead to a wider distribution.

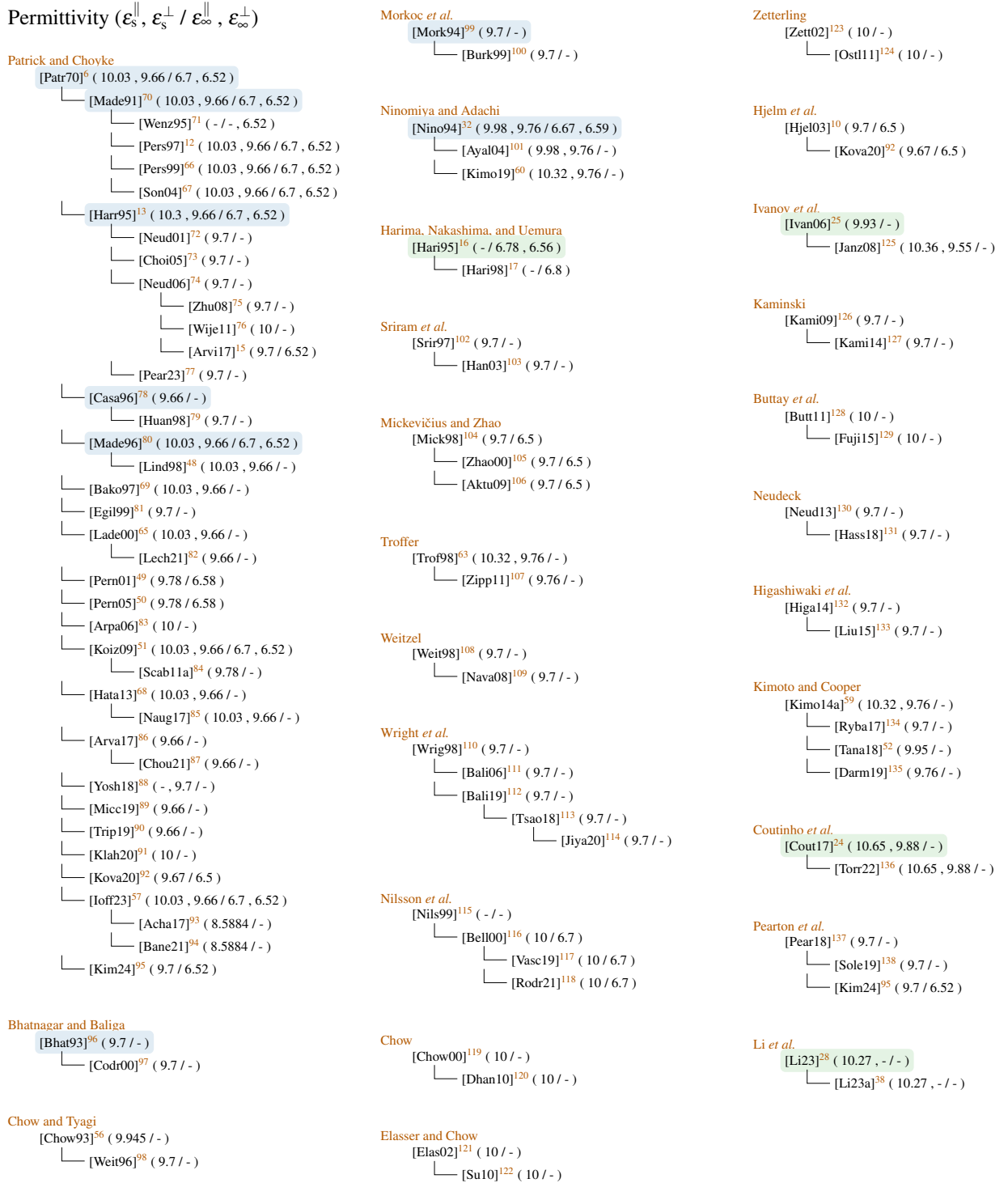


FIG. 2. Reference chains found for the relative permittivity. Publications with blue background are not focused on 4H-SiC, while those in green are novel analyses on 4H-SiC.

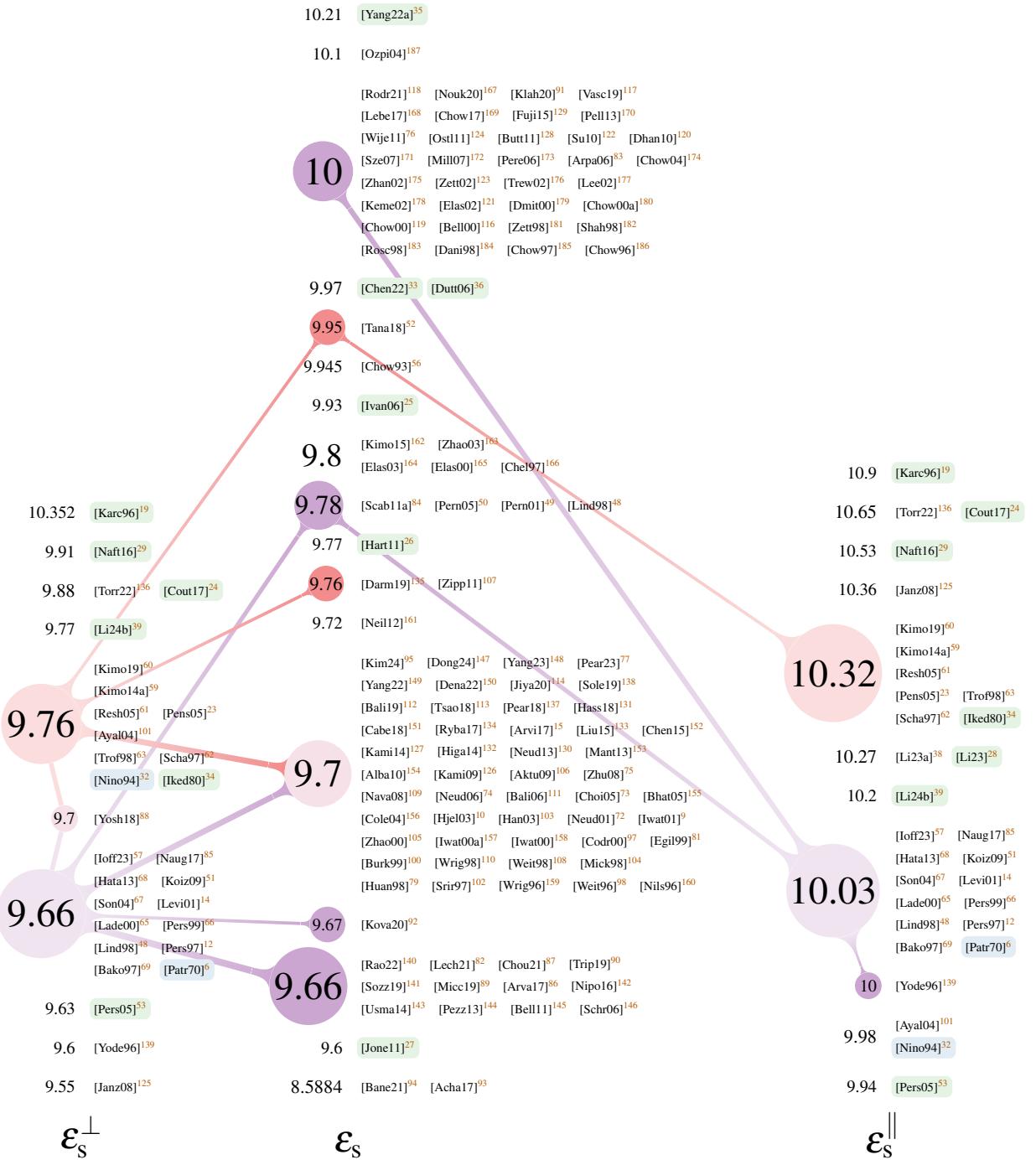


FIG. 3. Published values for the static permittivity. Connected values indicated that at least one connection has been found. References with blue background indicate investigations of non-4H silicon carbide while green background denotes basic 4H-SiC investigations.

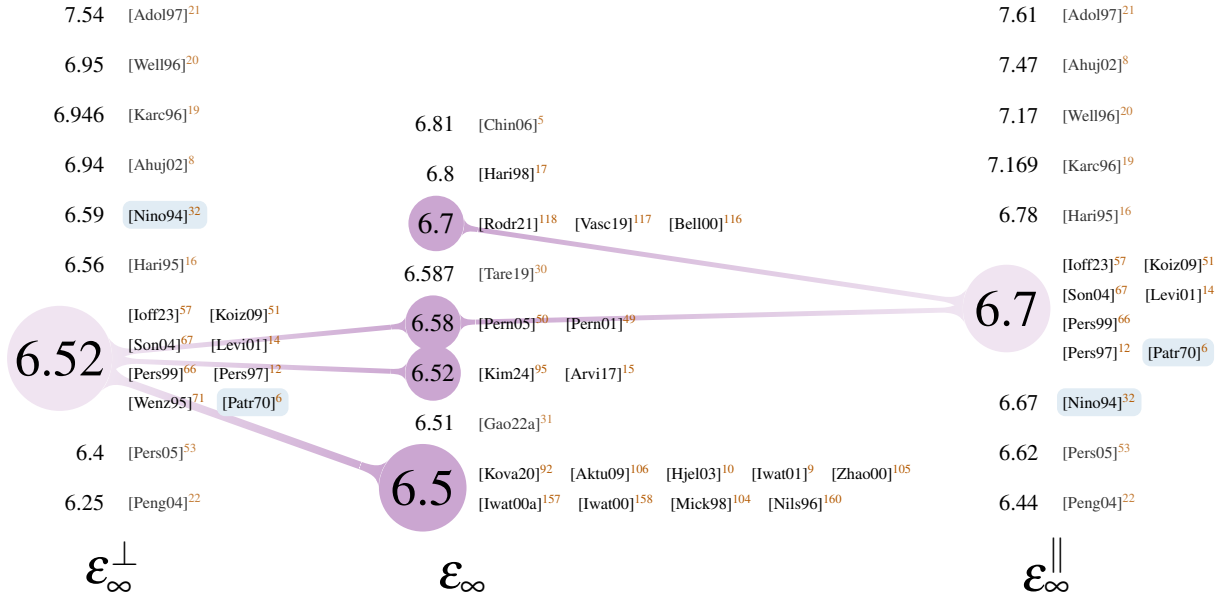


FIG. 4. Published values for the high-frequency permittivity. Connected values indicated that that at least one connection has been found. References with green background indicate investigations of non-4H silicon carbide while blue background denotes basic 4H-SiC investigations.

## II. DENSITY-OF-STATES EFFECTIVE MASS

The effective mass of charge carriers is defined as the reciprocal of the second derivative of the spherically averaged dispersion relation<sup>48</sup> and, thus, dependent on the shape of the conduction/valence band. Because the latter are not uniform in a semiconductor deviating masses for each principal direction are achieved. These direction-dependent values are then further combined to end up with more simplistic descriptions<sup>3</sup>.

In this section we investigate the effective mass of electrons and holes in each principal direction and how these get merged into the density-of-states (DOS) and conductivity mass. We extend earlier overview publications<sup>13,23,62,63,188–190</sup> and focus primarily on the DOS masses because they are used in TCAD simulations in various occasions, e.g., the calculation of the charge carrier concentration or impact and incomplete ionization. We want to highlight that in TCAD tools many additional effective masses are used, e.g., tunneling masses, quantum well masses, effective mass at the contact or in a channel or thermionic relative masses, which must not be confused.

## A. Theory

In the sequel we start with a short theoretical analysis of effective masses. For further information the interested reader is referred to the dedicated literature<sup>3,13,23,53,62,67,188,189,191</sup>. To increase the readability the effective masses are denoted relative to the free electron mass  $m_0$ , i.e.,  $m^* = m/m_0$ <sup>192</sup>.

### 1. Effective Masses along Principal Directions

For electrons the mass is specified in the directions starting in the conduction band minimum at the M point<sup>101,189,193–195</sup> (cp. ??) towards the  $\Gamma$ , K and L point, denoted in the sequel as  $m_{\text{MF}}^*$ ,  $m_{\text{MK}}^*$  and  $m_{\text{ML}}^*$ . The first two are perpendicular to the c-axis and the last one parallel<sup>69,101,196,197</sup>. In the M point two conduction bands are very close together, such that both can influence the effective mass<sup>62,195</sup>. Zhao *et al.*<sup>105</sup> even used three conduction bands. If not otherwise stated we will focus in this paper solely on the lowest one.

The valence band maximum is in the  $\Gamma$  point<sup>63,69,101</sup>. Consequently, the three relative masses are termed  $m_{\text{GM}}^*$ ,  $m_{\text{GK}}^*$  (perpendicular) and  $m_{\text{GA}}^*$  (parallel) indicating the directions towards the M, K and A point<sup>195,198</sup>. At the  $\Gamma$  point three separate bands meet<sup>67,69,193,198,199</sup>, whereat the two topmost are called heavy-hole (hh) and light-hole (lh) and the third one crystal split off (so)<sup>67,199</sup>. Although all have to be considered for an accurate estimation often only a subset is used.

### 2. Density-of-States (DOS) Mass

The effective density of states for conduction ( $N_C$ ) and valence ( $N_V$ ) band<sup>65,84,107,201,202</sup>

$$N_C = 2 M_C \left( \frac{2\pi m_{\text{de}}^* k_B T}{h^2} \right)^{3/2}$$

$$N_V = 2 \left( \frac{2\pi m_{\text{dh}}^* k_B T}{h^2} \right)^{3/2},$$

with  $M_C$  the number of conduction band minima in the first Brillouin zone<sup>202</sup>, is, for example, used to evaluate the electron and hole concentration. The utilized effective density-of-states masses  $m_{\text{de}}^*$  and  $m_{\text{dh}}^*$  are defined as<sup>23,69,81,191</sup>

$$m_{\text{de}}^* = (m_{\text{de}\perp}^* m_{\text{de}\parallel}^*)^{1/3} = (m_{\text{MF}}^* m_{\text{MK}}^* m_{\text{ML}}^*)^{1/3}$$

$$m_{\text{dh}}^* = (m_{\text{dh}\perp}^* m_{\text{dh}\parallel}^*)^{1/3} = (m_{\text{GM}}^* m_{\text{GK}}^* m_{\text{GA}}^*)^{1/3}$$

with<sup>67</sup>

$$\begin{aligned} m_{de\perp}^* &= \sqrt{m_{MI}^* m_{MK}^*}, & m_{de\parallel}^* &= m_{ML}^* \\ m_{dh\perp}^* &= \sqrt{m_{TM}^* m_{TK}^*}, & m_{dh\parallel}^* &= m_{TA}^*. \end{aligned}$$

In this case  $m_{de}^*$  is called the *single valley* DOS electron effective mass<sup>23,68,81,101</sup>, as the factor  $M_C$  is not considered. It is also very common, e.g., in some TCAD tools, to add  $M_C$  to the effective mass<sup>3,69,154,204,205</sup>, i.e.,

$$m_{de}^* = (M_C^2 m_{de\perp}^* {}^2 m_{de\parallel}^*)^{1/3}.$$

In this review we will only present the single valley values and highlight all publications where we found expressions including  $M_C$ .

For an effective mass of the holes it is also necessary to combine the masses of heavy ( $m_{hh}^*$ ) and light ( $m_{lh}^*$ ) holes, which can be achieved by<sup>48,50,171</sup>

$$m_{dh}^* = \left( m_{hh}^* {}^{3/2} + m_{lh}^* {}^{3/2} \right)^{2/3}. \quad (3)$$

This expression is already a simplification, because for accurate results the energy difference between the bands has to be considered<sup>69</sup>. This leads to

$$m_h^*(T) = \left[ m_{h1}^{3/2} + m_{h2}^{3/2} \exp\left(-\frac{\Delta E_2}{k_B T}\right) + m_{h3}^{3/2} \exp\left(-\frac{\Delta E_3}{k_B T}\right) \right]^{2/3} \quad (4)$$

where  $\Delta E_2$  and  $\Delta E_3$  denote the energy separation between the bands.

*a. Temperature Dependency* The changing amount of charge carriers with temperature can be compactly modeled by using a *thermal DOS effective mass*<sup>191,206</sup>. There is no explicit form available but it was calculated by Wellenhofer and Rössler<sup>191</sup> (electrons and holes separately) and Tanaka *et al.*<sup>52</sup> (average effective mass). Later Schadt<sup>62</sup>, Hatakeyama, Fukuda, and Okumura<sup>68</sup> fitted the results from Wellenhofer and Rössler<sup>191</sup> with an equation of the form

$$m^*(T) = \left( \frac{z_0 + z_1 T + z_2 T^2 + z_3 T^3 + z_4 T^4}{1 + n_1 T + n_2 T^2 + n_3 T^3 + n_4 T^4} \right)^\eta \quad (5)$$

for both electrons and holes. Such a change in the effective DOS mass is not yet covered in TCAD simulations suites.

### 3. Conductivity Effective Mass

For investigations of the mobility in 4H-SiC<sup>9,52,62,79,157,158,207–211</sup> the mobility mass is a crucial simplification, e.g., in<sup>189</sup>

$$\mu = \frac{e\tau}{m_c^*},$$

with  $\mu$  the mobility,  $e$  the elementary charge and  $\tau$  the lifetime (see Section VII). The conductivity mass must not be confused with the DOS mass since its definition<sup>3,212</sup>

$$m_{ce}^* = \frac{3m_{ce\perp}^* m_{ce\parallel}^*}{m_{ce\perp}^* + 2m_{ce\parallel}^*}$$

$$m_{ch}^* = \frac{3m_{ch\perp}^* m_{ch\parallel}^*}{m_{ch\perp}^* + 2m_{ch\parallel}^*}$$

with<sup>207,208</sup>

$$\frac{2}{m_{ce\perp}^*} = \frac{1}{m_{MK}^*} + \frac{1}{m_{M\Gamma}^*}, \quad m_{ce\parallel}^* = m_{ML}^*$$

$$\frac{2}{m_{ch\perp}^*} = \frac{1}{m_{\Gamma M}^*} + \frac{1}{m_{\Gamma K}^*}, \quad m_{ch\parallel}^* = m_{\Gamma A}^*$$

which results in<sup>79</sup>

$$\frac{3}{m_{ce}^*} = \frac{1}{m_{M\Gamma}^*} + \frac{1}{m_{MK}^*} + \frac{1}{m_{ML}^*}$$

$$\frac{3}{m_{ch}^*} = \frac{1}{m_{\Gamma M}^*} + \frac{1}{m_{\Gamma K}^*} + \frac{1}{m_{\Gamma A}^*}.$$

is fundamentally different. In the sequel we will solely concentrate on the DOS mass.

#### 4. Polaron Mass

In the Si-C bond of silicon carbide, carbon atoms are more electronegative than silicon ones. This results in a partly ionic crystal<sup>67</sup>. Within this surrounding a charge carrier, together with its self-induced polarization, forms a quasiparticle, which is called a polaron<sup>213</sup>. This can also be described by longitudinal optical vibrations that generate an electric field along the direction of the vibration which interacts with the charge carriers<sup>67,192</sup>. Effectively, the carrier is “dressed” by a charge leading to a deviating effective mass<sup>12</sup>. The adapted mass  $m_p$ , called *polaron mass*, is slightly higher than the bare mass  $m$  and can be calculated as<sup>12,53,67</sup>

$$m_p = m \frac{1 - 8 \times 10^{-4} \alpha^2}{1 - \alpha/6 + 3.4 \times 10^{-3} \alpha^2} \approx m \left(1 - \frac{\alpha}{6}\right)^{-1}$$

with the Fröhlich constant  $\alpha$  defined as

$$\alpha = \frac{1}{2} \left( \frac{1}{\epsilon_\infty} - \frac{1}{\epsilon_s} \right) \frac{e^2}{\hbar \omega_{LO}} \left( \frac{2m\omega_{LO}}{\hbar} \right)^{1/2} \frac{1}{4\pi\epsilon_s}.$$

In the latter  $e$  denotes the elementary charge,  $\epsilon_s/\epsilon_\infty$  the static/high-frequency dielectric constant and  $\omega_{\text{LO}}$  the longitudinal optical phonon frequency (see Section I). We want to highlight that in some definitions in literature<sup>213–215</sup> the last term  $1/4\pi\epsilon_s$  is missing due to a differing unit system.

Note that in (optically detected) cyclotron resonance measurements always the polaron mass is extracted. For a better comparability it is thus necessary to adapt non-polaron masses, e.g., those achieved by calculations<sup>195</sup>.

## B. Results

In the following we show the results of our investigations. Note that we discarded conductivity masses, e.g., by Mikami, Kaneko, and Kimoto<sup>217</sup>, and solely concentrate on the DOS mass here. We also did not include the results by Son *et al.*<sup>218</sup> since Son *et al.*<sup>67</sup> later stated that the smaller values are due to “errors caused by a broad and asymmetric ODCR line shape with the peak position slightly shifted to lower magnetic fields”.

### 1. Effective Mass along Principal Directions

To determine the effective masses mainly band structure calculations are used. The most common ones are based on the density functional theory (DFT) local density approximation (LDA)<sup>71,106,160,191,194–196,219</sup>. Differing methods, e.g., projector augmented wave (PAW)<sup>198,220</sup>, (full-potential) linearized augmented plane wave ((FP)LAPW)<sup>12,53,67,193,221</sup>, (orthogonalized) linear combination of atomic orbital ((O)LCAO)<sup>5,222</sup>, full-potential linear muffin-tin orbital method (FPLMTO)<sup>223</sup> and hybrid pseudo-potential and tight-binding (HPT)<sup>224</sup>, were utilized in this context. Other calculations include empirical pseudo potentials (EPM)<sup>116,225</sup> and RSP Hamiltonians (RSPH)<sup>199</sup>.

Results achieved by these calculations are sometimes combined using Monte Carlo (MC)<sup>106,160</sup> simulations or genetic algorithm fitting (GAF)<sup>228,229</sup>. In some cases the literature values were used as starting point for further analyses. Based on the data from Son *et al.*<sup>218</sup> such a refinement was executed by Nilsson, Sannemo, and Petersson<sup>160</sup>, whose results then served as starting point for a fitting by Mickevičius and Zhao<sup>104</sup>. Similarly, Mikami, Kaneko, and Kimoto<sup>217</sup> calculated the hole mass as the second derivative of the E-k dispersion by Persson and Lindefelt<sup>193</sup>.

The calculations are complemented by measurements, for example by optically detected cy-

TABLE II. Effective masses in principal directions. Multiple values for the same band are calculated by differing algorithms.

ref.	electron				hole				method <sup>a</sup>	polaron
	$m_{\text{MF}}^*$ [ $m_0$ ]	$m_{\text{MK}}^*$ [ $m_0$ ]	$m_{\text{ML}}^*$ [ $m_0$ ]	band	$m_{\Gamma\text{M}}^*$ [ $m_0$ ]	$m_{\Gamma\text{K}}^*$ [ $m_0$ ]	$m_{\Gamma\text{A}}^*$ [ $m_0$ ]	band		
[Kack94] <sup>219</sup>	0.62	0.13	0.39	-	4.23	2.41	1.73	hh	DFT-LDA	-
	-	-	-	-	0.45	0.77	1.73	lh	DFT-LDA	-
	-	-	-	-	0.74	0.51	0.21	so	DFT-LDA	-
[Karc95] <sup>194</sup>	0.66	0.31	0.3	-	-	-	-	-	DFT-LDA	-
[Lamb95] <sup>223</sup>	0.58	0.28	0.31	-	-	-	-	-	DFT-LDA	-
[Wenz95] <sup>71</sup>	0.6	0.28	0.19	-	-	-	-	-	DFT-LDA	-
[Nils96] <sup>160</sup>	0.43	0.43	0.28	1	-	-	-	-	DFT-LDA	-
	0.52	0.21	0.45	2	-	-	-	-	DFT-LDA	-
[Pers96] <sup>193</sup>	0.57	0.28	0.31	-	-	-	-	-	DFT-LDA	-
[Volm96] <sup>226</sup>	$0.58 \pm 0.01$	$0.31 \pm 0.01$	$0.33 \pm 0.01$	-	-	-	-	-	ODCR	y
[Chen97] <sup>224</sup>	1.2	0.19	0.33	-	-	-	-	-	DFT-LDA	-
[Pers97] <sup>12</sup>	0.57	0.28	0.31	1	-	-	-	-	DFT-LDA	-
	0.59	0.31	0.34	1	-	-	-	-	DFT-LDA	-
	0.61	0.29	0.33	1	-	-	-	-	DFT-LDA	y
	0.78	0.16	0.71	2	-	-	-	-	DFT-LDA	-
	0.8	0.18	0.75	2	-	-	-	-	DFT-LDA	-
	0.85	0.17	0.77	2	-	-	-	-	DFT-LDA	y
[Pers98a] <sup>227</sup>	-	-	-	-	0.7	3.04	1.64	1	fit	-
	-	-	-	-	0.6	0.34	1.64	2	fit	-
[Bell00] <sup>116</sup>	0.57	0.23	0.27	-	-	-	-	-	EPM	-
[Zhao00a] <sup>222</sup>	$0.62 \pm 0.03$	$0.27 \pm 0.02$	$0.31 \pm 0.02$	-	-	-	-	-	DFT-LDA	-
[Penn01] <sup>225</sup>	$0.60 \pm 0.05$	$0.20 \pm 0.02$	$0.36 \pm 0.02$	-	-	-	-	-	EPM	-
[Iwat03] <sup>196</sup>	0.59	0.29	-	-	-	-	-	-	DFT-LDA	-
[Iwat03a] <sup>209</sup>	0.58	0.3	-	-	-	-	-	-	Hall	-
[Dong04] <sup>195</sup>	0.53	0.27	0.3	-	0.86	0.95	1.58	1	DFT-LDA	-
	-	-	-	-	0.55	0.52	1.32	2	DFT-LDA	-
	-	-	-	-	1.13	1.30	0.21	3	DFT-LDA	-
[Chin06] <sup>5</sup>	0.47	-	0.38	-	-	-	-	-	DFT-LDA	-
[Ng10] <sup>228</sup>	0.66	0.31	0.34	-	-	-	-	-	GAF	-
[Kuro19] <sup>198</sup>	0.54	0.28	0.31	-	0.54	0.54	1.48	-	DFT-LDA	-
[Lu21] <sup>220</sup>	0.54	0.3	-	-	2.77	1.82	1.52	-	DFT-LDA	-

<sup>a</sup> for explanation see text

clotron resonance (ODCR)<sup>192,211,218,226,230</sup>, photoluminescence<sup>81</sup>, infrared absorption (IR)<sup>202</sup>, Raman scattering<sup>16</sup> and Hall effect measurements<sup>51,209,231,232</sup>. However, for the relative masses in the principal directions (see Table II) calculations clearly dominate. Only two measurements<sup>209,226</sup> could be found for the electron masses whereat not a single experimental evaluation for hole masses was achieved.

In literature the hole bands are either denoted as heavy-hole (hh), light-hole (lh) and crystal split-off (so) or simply as 1, 2, 3. According to the found values we are confident to say that  $1 \equiv \text{hh}$ ,  $2 \equiv \text{lh}$  and  $3 \equiv \text{so}$ .

## 2. DOS Mass

For a comprehensive overview on DOS masses we combine calculations based on the effective masses in the principal directions and values presented in literature (see Table III and Table IV). Again, calculations clearly dominate, however, an increased amount of measurements<sup>51,192,209,218,226,231,232</sup>, including some for the hole mass, could be acquired.

The values show significant deviation. In addition Schadt<sup>62</sup> stated that they are only valid close to the band minimum/maximum as they are calculated there or at very low temperature. Furthermore, Son *et al.*<sup>67</sup> claimed that if the polaron effect is added to the results from Persson and Lindefelt<sup>193,221</sup> the values  $m_{\text{dh}\perp}^* = 0.66$  and  $m_{\text{dh}\parallel}^* = 1.76$  are achieved, which fit the results from ODCR measurements well. In the opinion of these authors it is also important to consider spin-orbit couplings for holes. Zhao *et al.*<sup>105</sup> is the only publication that also provided parameters for a third conduction band, which is, however, 2 eV above the lowest one in the M-point.

According was achieved over the last decades regarding the value of  $M_C$ . Although in early publications rather high values of  $M_C = 12^{233,234}$  or  $M_C = 6^{190,235,236}$  were encountered, almost all more recent publications agree upon  $M_C = 3^{9,14,23,48,57,62,65,68,69,84,107,142,204,206,227,237-239}$ .

We found some deviations among the utilized formalisms. Pennington and Goldsman<sup>240</sup> used  $\sqrt{m_{\text{MR}}^* m_{\text{MK}}^*}$  as the DOS effective mass of electrons, i.e.,  $m_{\text{de}}^* = m_{\text{de}\perp}^*$ . Tilak, Matocha, and Dunne<sup>241</sup> reused the value of  $m_{\text{de}}^*$  but calculated the perpendicular one themselves, which lead to almost identical values. Persson and Lindefelt<sup>227</sup> used for the calculation of the effective mass, i.e.,  $m_{\text{de}}^* = (m_{\text{de}\perp 1}^* m_{\text{de}\parallel}^*)^{1/3}$  only one of the perpendicular masses, which was in the sequel reused<sup>50</sup>. In contrary, Gao *et al.*<sup>31</sup> used  $m_{\text{de}}^* = m_{\text{de}\parallel}^*$ . Ivanov, Magnusson, and Janzén<sup>42</sup> used  $m_{\text{de}\perp}^* = \sqrt{m_{\text{ML}}^* m_{\text{MK}}^*} = 0.32$  resp  $m_{\text{de}\parallel}^* = m_{\text{ML}}^* + 0.58$  by citing Faulkner<sup>242</sup>. We were unable

TABLE III. First half of DOS masses. Multiple values for the same band are calculated by differing algorithms.

ref.	electron				hole				method <sup>h</sup>	polaron
	$m_{de}^*$ [ $m_0$ ]	$m_{de\perp}^*$ [ $m_0$ ]	$m_{de\parallel}^*$ [ $m_0$ ]	band	$m_{dh}^*$ [ $m_0$ ]	$m_{dh\perp}^*$ [ $m_0$ ]	$m_{dh\parallel}^*$ [ $m_0$ ]	band		
[Loma73] <sup>231</sup>	0.20 <sup>a</sup>	0.21	0.19	-	-	-	-	-	Hall	-
[Loma74] <sup>232</sup>	0.20 <sup>a</sup>	0.21	0.19	-	-	-	-	-	Hall	-
[Gotz93] <sup>202</sup>	0.19	0.176	0.224	-	-	-	-	-	IR	-
[Kack94] <sup>219</sup>	0.31 <sup>a</sup>	0.28 <sup>b</sup>	0.39 <sup>c</sup>	-	2.60 <sup>a</sup>	3.19 <sup>b</sup>	1.73 <sup>c</sup>	hh	DFT-LDA	-
	-	-	-	-	0.84 <sup>a</sup>	0.59 <sup>b</sup>	1.73 <sup>c</sup>	lh	DFT-LDA	-
	-	-	-	-	0.43 <sup>a</sup>	0.61 <sup>b</sup>	0.21 <sup>c</sup>	so	DFT-LDA	-
[Hari95] <sup>16</sup>	0.35 <sup>a</sup>	$0.30 \pm 0.07$	$0.48 \pm 0.12$	-	-	-	-	-	Raman	-
[Karc95] <sup>194</sup>	0.39 <sup>a</sup>	0.45 <sup>b</sup>	0.30 <sup>c</sup>	-	-	-	-	-	DFT-LDA	-
[Kord95] <sup>211</sup>	-	0.42	-	-	-	-	-	-	ODCR	y
[Lamb95] <sup>223</sup>	0.35 <sup>a</sup>	0.4	0.27	-	-	-	-	-	DFT-LDA	-
[Son95] <sup>218</sup>	0.37 <sup>a</sup>	0.42	$0.29 \pm 0.03$	-	-	-	-	-	ODCR	y
[Wenz95] <sup>71</sup>	0.32 <sup>a</sup>	0.41 <sup>b</sup>	0.19 <sup>c</sup>	-	-	-	-	-	DFT-LDA	-
[Nils96] <sup>160</sup>	0.37 <sup>a</sup>	0.43 <sup>b</sup>	0.28 <sup>c</sup>	1	-	-	-	-	DFT-LDA	-
	0.37 <sup>a</sup>	0.33 <sup>b</sup>	0.45 <sup>c</sup>	2	-	-	-	-	DFT-LDA	-
[Pers96] <sup>193</sup>	0.37 <sup>a</sup>	0.40 <sup>b</sup>	0.31 <sup>c</sup>	-	-	-	-	-	DFT-LDA	-
[Volm96] <sup>226</sup>	0.39 <sup>a</sup>	0.42 <sup>b</sup>	0.33 <sup>c</sup>	-	-	-	-	-	ODCR	y
[Bako97] <sup>69</sup>	-	-	-	-	0.84	-	-	1	-	-
	-	-	-	-	0.79	-	-	2	-	-
	-	-	-	-	0.78	-	-	3	-	-
[Chen97] <sup>224</sup>	0.42 <sup>a</sup>	0.48 <sup>b</sup>	0.33 <sup>c</sup>	-	-	-	-	-	DFT-LDA	-
[Hemm97] <sup>204</sup>	-	-	-	-	1	-	-	-	-	-
[Lamb97] <sup>199</sup>	-	-	-	-	0.85 <sup>a</sup>	0.62	1.6	hh	RSPH	-
	-	-	-	-	0.84 <sup>a</sup>	0.62	1.55	lh	RSPH	-
	-	-	-	-	0.81 <sup>a</sup>	1.58	0.21	so	RSPH	-
[Pers97] <sup>12</sup>	0.37 <sup>a</sup>	0.40 <sup>b</sup>	0.31 <sup>c</sup>	1	0.82 <sup>a</sup>	0.59	1.56	1	DFT-LDA	-
	0.40 <sup>a</sup>	0.43 <sup>b</sup>	0.34 <sup>c</sup>	1	0.82 <sup>a</sup>	0.59	1.6	1	DFT-LDA	-
	0.39 <sup>a</sup>	0.42 <sup>b</sup>	0.33 <sup>c</sup>	1	0.82 <sup>a</sup>	0.59	1.56	2	DFT-LDA	y
	0.44 <sup>a</sup>	0.35 <sup>b</sup>	0.71 <sup>c</sup>	2	0.82 <sup>a</sup>	0.59	1.6	2	DFT-LDA	-
	0.48 <sup>a</sup>	0.38 <sup>b</sup>	0.75 <sup>c</sup>	2	0.78 <sup>a</sup>	1.49	0.21	3	DFT-LDA	-
	0.48 <sup>a</sup>	0.38 <sup>b</sup>	0.77 <sup>c</sup>	2	0.79 <sup>a</sup>	1.49	0.22	3	DFT-LDA	y

$$^a m_{de}^* = (m_{de\perp}^* m_{de\parallel}^*)^{1/3}$$

$$^b m_{de\perp}^* = \sqrt{m_{MI}^* m_{MK}^*}$$

$$^c m_{de\parallel}^* = m_{ML}^*$$

$$^d m_{dh}^* = (m_{dh\perp}^* m_{dh\parallel}^*)^{1/3}$$

$$^e m_{dh\perp}^* = \sqrt{m_{TM}^* m_{TK}^*}$$

$$^f m_{dh\parallel}^* = m_{TA}^*$$

<sup>h</sup> explanation see text

TABLE IV. Second half of DOS masses. Multiple values for the same band are calculated by differing algorithms.

ref.	electron				hole				method <sup>h</sup>	polaron
	$m_{de}^*$ [ $m_0$ ]	$m_{de\perp}^*$ [ $m_0$ ]	$m_{de\parallel}^*$ [ $m_0$ ]	band	$m_{dh}^*$ [ $m_0$ ]	$m_{dh\perp}^*$ [ $m_0$ ]	$m_{dh\parallel}^*$ [ $m_0$ ]	band		
[Well97] <sup>191</sup>	0.394	-	-	-	-	-	-	-	DFT-LDA	-
[Lind98] <sup>48</sup>	-	-	-	-	1.7	-	-	hh	DFT-LDA	-
-	-	-	-	-	0.48	-	-	lh	DFT-LDA	-
[Pers98a] <sup>227</sup>	-	-	-	-	0.94	1.46 <sup>b</sup>	1.64 <sup>c</sup>	1	fit	-
-	-	-	-	-	0.84	0.45 <sup>b</sup>	1.64 <sup>c</sup>	2	fit	-
-	-	-	-	-	0.88	-	-	3	fit	-
[Egil99] <sup>81</sup>	0.37	-	-	-	-	-	-	-	PL	-
[Pers99b] <sup>221</sup>	-	-	-	-	0.85 <sup>a</sup>	0.62	1.61	1	DFT-LDA	-
-	-	-	-	-	0.84 <sup>a</sup>	0.61	1.62	1	DFT-LDA	-
-	-	-	-	-	0.78 <sup>a</sup>	0.56	1.52	2	DFT-LDA	-
-	-	-	-	-	0.78 <sup>a</sup>	0.58	1.42	2	DFT-LDA	-
-	-	-	-	-	0.78 <sup>a</sup>	1.5	0.21	3	DFT-LDA	-
-	-	-	-	-	0.76 <sup>a</sup>	1.46	0.21	3	DFT-LDA	-
[Bell00] <sup>116</sup>	0.33 <sup>a</sup>	0.36 <sup>b</sup>	0.27 <sup>c</sup>	-	-	-	-	-	EPM	-
[Son00] <sup>192</sup>	0.39 <sup>a</sup>	$0.45 \pm 0.02$	$0.30 \pm 0.02$	-	0.91 <sup>a</sup>	$0.66 \pm 0.02$	$1.75 \pm 0.02$	-	ODCR	y
[Zhao00] <sup>105</sup>	0.37 <sup>a</sup>	0.42	0.28	1	-	-	-	-	-	-
-	0.44 <sup>a</sup>	0.35	0.71	2	-	-	-	-	-	-
-	0.40 <sup>a</sup>	0.66	0.15	3	-	-	-	-	-	-
[Zhao00a] <sup>222</sup>	0.37 <sup>a</sup>	$0.41 \pm 0.02$	0.31 <sup>c</sup>	-	-	-	-	-	DFT-LDA	-
[Penn01] <sup>225</sup>	0.34 <sup>a</sup>	$0.35 \pm 0.02$	$0.31 \pm 0.05$	-	-	-	-	-	EPM	-
[Iwat03] <sup>196</sup>	-	0.41 <sup>b</sup>	-	-	-	-	-	-	DFT-LDA	-
[Iwat03a] <sup>209</sup>	-	0.42 <sup>b</sup>	-	-	-	-	-	-	Hall	-
[Dong04] <sup>195</sup>	0.35 <sup>a</sup>	0.38 <sup>b</sup>	0.30 <sup>c</sup>	-	1.09 <sup>a</sup>	0.90 <sup>b</sup>	1.58 <sup>c</sup>	1	DFT-LDA	-
-	-	-	-	-	0.72 <sup>a</sup>	0.53 <sup>b</sup>	1.32 <sup>c</sup>	2	DFT-LDA	-
-	-	-	-	-	0.67 <sup>a</sup>	1.21 <sup>b</sup>	0.21 <sup>c</sup>	3	DFT-LDA	-
[Chin06] <sup>5</sup>	-	-	0.38 <sup>c</sup>	-	-	-	-	-	DFT-LDA	-
[Aktu09] <sup>106</sup>	0.40	-	-	-	-	-	-	-	DFT-LDA	-
[Koiz09] <sup>51</sup>	-	-	-	-	0.5	-	-	-	Hall	-
[Ng10] <sup>228</sup>	0.41 <sup>a</sup>	0.45 <sup>b</sup>	0.34 <sup>c</sup>	-	-	-	-	-	GAF	-
[Kuro19] <sup>198</sup>	0.36 <sup>a</sup>	0.39 <sup>b</sup>	0.31 <sup>c</sup>	-	0.76 <sup>a</sup>	0.54 <sup>b</sup>	1.48 <sup>c</sup>	-	DFT-LDA	-
[Lu21] <sup>220</sup>	-	0.40 <sup>b</sup>	-	-	1.97 <sup>a</sup>	2.25 <sup>b</sup>	1.52 <sup>c</sup>	-	DFT-LDA	-

$$^a m_{de}^* = (m_{de\perp}^*{}^2 m_{de\parallel}^*)^{1/3}$$

$$^b m_{de\perp}^* = \sqrt{m_{\Gamma M}^* m_{MK}^*}$$

$$^c m_{de\parallel}^* = m_{ML}^*$$

$$^d m_{dh}^* = (m_{dh\perp}^*{}^2 m_{dh\parallel}^*)^{1/3}$$

$$^e m_{dh\perp}^* = \sqrt{m_{\Gamma M}^* m_{\Gamma K}^*}$$

$$^f m_{dh\parallel}^* = m_{\Gamma A}^*$$

<sup>h</sup> explanation see text

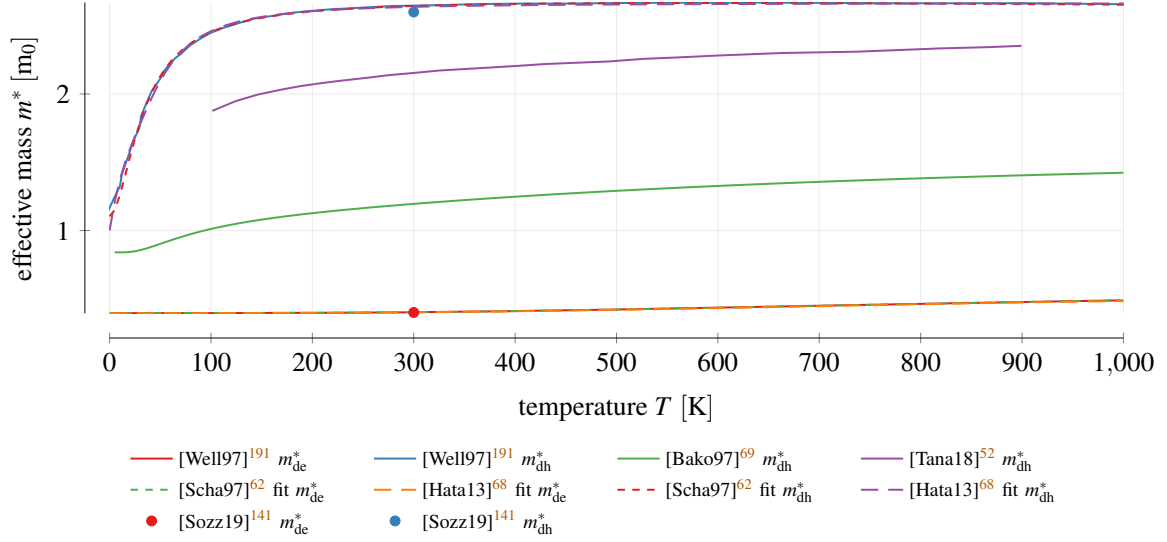


FIG. 5. Temperature dependency of the DOS mass.

TABLE V. Fitting parameters in Eq. (5) to calculations by Wellenhofer and Rössler<sup>[191]</sup>.

ref.	mass	$z_0$	$z_1$	$z_2$	$z_3$	$z_4$	$n_1$	$n_2$	$n_3$	$n_4$	$\eta$
[Scha97] <sup>[62]</sup>	$m_{de}^*$	0.3944	$-6.822 \times 10^{-4}$	$1.335 \times 10^{-6}$	$3.597 \times 10^{-10}$	0	$-1.776 \times 10^{-3}$	$3.65 \times 10^{-6}$	0	0	1
[Scha97] <sup>[62]</sup>	$m_{dh}^*$	1.104	$1.578 \times 10^{-2}$	$3.087 \times 10^{-3}$	$-7.635 \times 10^{-8}$	0	$1.387 \times 10^{-2}$	$1.126 \times 10^{-3}$	0	0	1
[Hata13] <sup>[68]</sup>	$m_{de}^*$	0.394	0	$3.09 \times 10^{-8}$	$2.23 \times 10^{-10}$	$-1.65 \times 10^{-13}$	0	0	0	0	1
[Hata13] <sup>[68]</sup>	$m_{dh}^*$	1	$6.92 \times 10^{-2}$	0	0	$1.88 \times 10^{-6}$	0	$6.58 \times 10^{-4}$	0	$4.32 \times 10^{-7}$	2/3

to retrace these equations. Transformed to the set of equations used in this paper we, thus, get  $m_{de\perp}^* = 0.42$  and  $m_{de\parallel}^* = 0.33$ . A more comprehensive listing of all inconsistencies is presented in ??.

### 3. Temperature

The temperature dependency of the DOS masses was calculated by Tanaka *et al.*<sup>[52]</sup> and Wellenhofer and Rössler<sup>[191]</sup> (see Fig. 5). Since these calculations can not be described implicitly there exist two fittings for the latter<sup>[62,68]</sup> using Eq. (5). The respective parameters are shown in Table V.

The temperature scaling of the hole mass considering the separation between the three valence bands in the  $\Gamma$  point<sup>[69]</sup> (see Eq. (4), also shown in the figure) is described by the coefficients  $m_{h1} = 0.84$ ,  $m_{h2} = 0.79$ ,  $m_{h3} = 0.78$ ,  $\Delta E_2 = 9$  meV and  $\Delta E_3 = 73$  meV. Bakowski, Gustafsson, and Lindefelt<sup>[69]</sup> stated that these are only valid for low temperatures, which might explain the big

deviations compared to the calculations by Wellenhofer and Rössler<sup>191</sup>. Also shown in the figure are the parameters extracted by Sozzi *et al.*<sup>141</sup> from Wellenhofer and Rössler<sup>191</sup> at 300 K, i.e.,  $m_{de}^* = 0.4$  and  $m_{dh}^* = 2.6$ .

#### 4. Effective DOS Mass for TCAD Tools

For TCAD simulations solely the effective electron and hole masses are interesting. We, therefore, collected all values found for  $m_{de}^*$  and  $m_{dh}^*$  (see Fig. 6). We also added values that we calculated from fundamental masses according to the formalism presented earlier. We just used the first conduction band for  $m_{de}^*$  and Eq. (3) to calculate  $m_{dh}^*$  considering the first two valence bands only.

For electrons the masses are dominantly using values of  $0.37 \pm 0.05$ . For holes the spread is more significant. Although the majority used  $1 \pm 3$  there are also values  $> 2.6$  available. This can be retraced to the significant temperature dependency. Ambivalent in this context is  $m_{dh}^* = 1.2$ . While Bakowski, Gustafsson, and Lindefelt<sup>69</sup> calculated this value for the mass at 300 K others<sup>154,243</sup> seemingly calculated  $m_{dh}^* = \sqrt{m_{dh\perp}^* m_{dh\parallel}^*}$ , i.e., twice the parallel instead of the perpendicular component, resulting in  $m_{dh}^* = 1.26^{61}$  based on the masses by Son *et al.*<sup>192</sup>. Crude rounding then leads to the desired value.

### C. Discussion

The majority of the investigations on the density-of-states masses in 4H-SiC have been conducted in a time frame of one decade between 1994 and 2004. Although the earliest studies in the 70s were measurements, nowadays dominantly calculations are utilized. For the hole mass, actually, up to this day only two measurements could be identified.

Our investigations showed that the value for  $m_{dh}^*$  has to be carefully picked, as a significant change with temperature was observed. Many of the available values, especially those based on calculations, are only valid close to 0 K. For more realistic results a much higher mass has to be used. Nevertheless, almost all temperature dependency fittings are based on the same calculation by Wellenhofer and Rössler<sup>191</sup>. Despite these large variations, temperature is rarely considered<sup>63,107</sup>. Rakheja *et al.*<sup>247</sup> explicitly claims the presented values to correspond to 300 K, although the reference investigation<sup>192</sup> was carried out at 4.4 K.

From the references (see Fig. 8 and Fig. 7) we are able to identify the publications by Persson

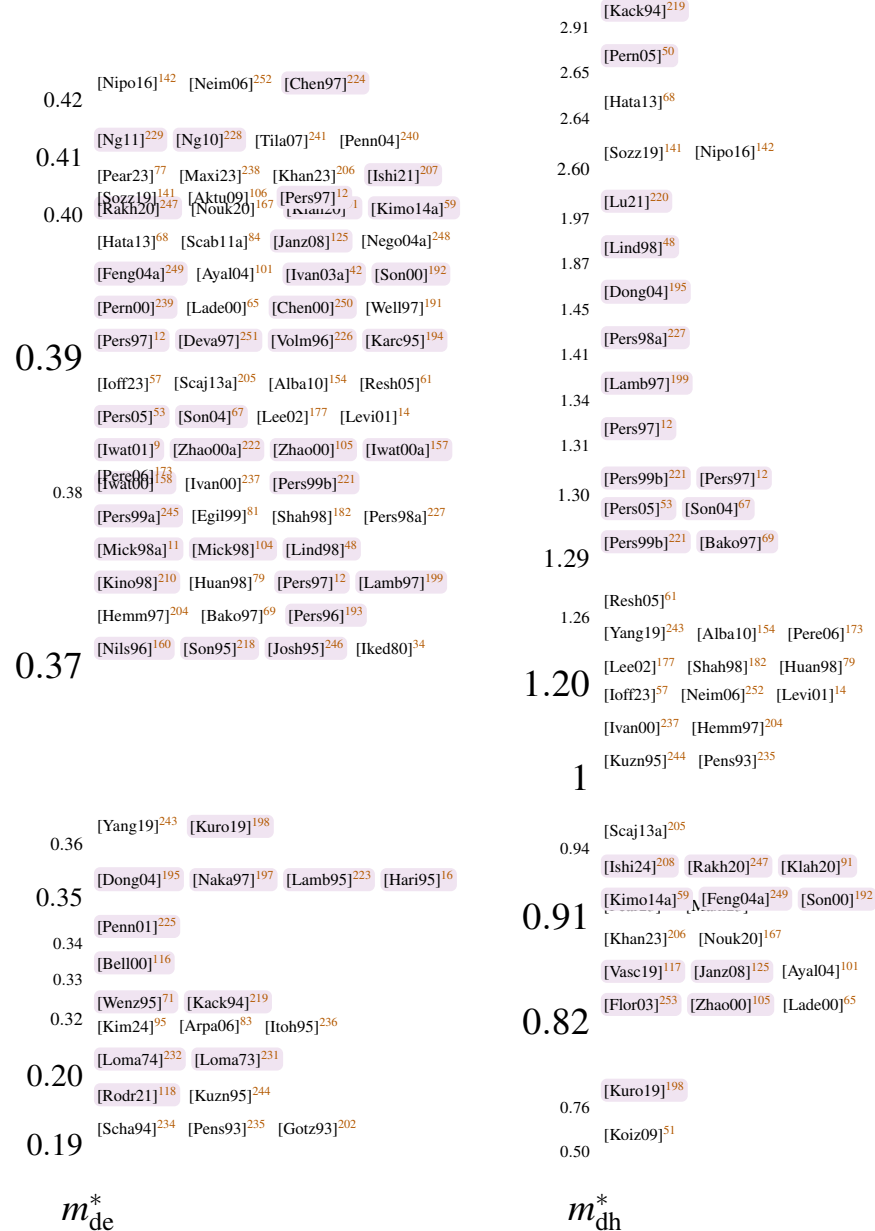


FIG. 6. Effective DOS masses for TCAD tools. A purple background denotes values that we calculated from more fundamental masses using the equations presented in this paper.

*et al.*<sup>12,193,221,227</sup> but also by Volm *et al.*<sup>226,191</sup> and<sup>192</sup> as very influential.

At last we shortly want to notice that there have been hints that the DOS mass is also doping dependent<sup>3</sup>. This was shown for 6H-SiC<sup>245</sup> but not yet for 4H.

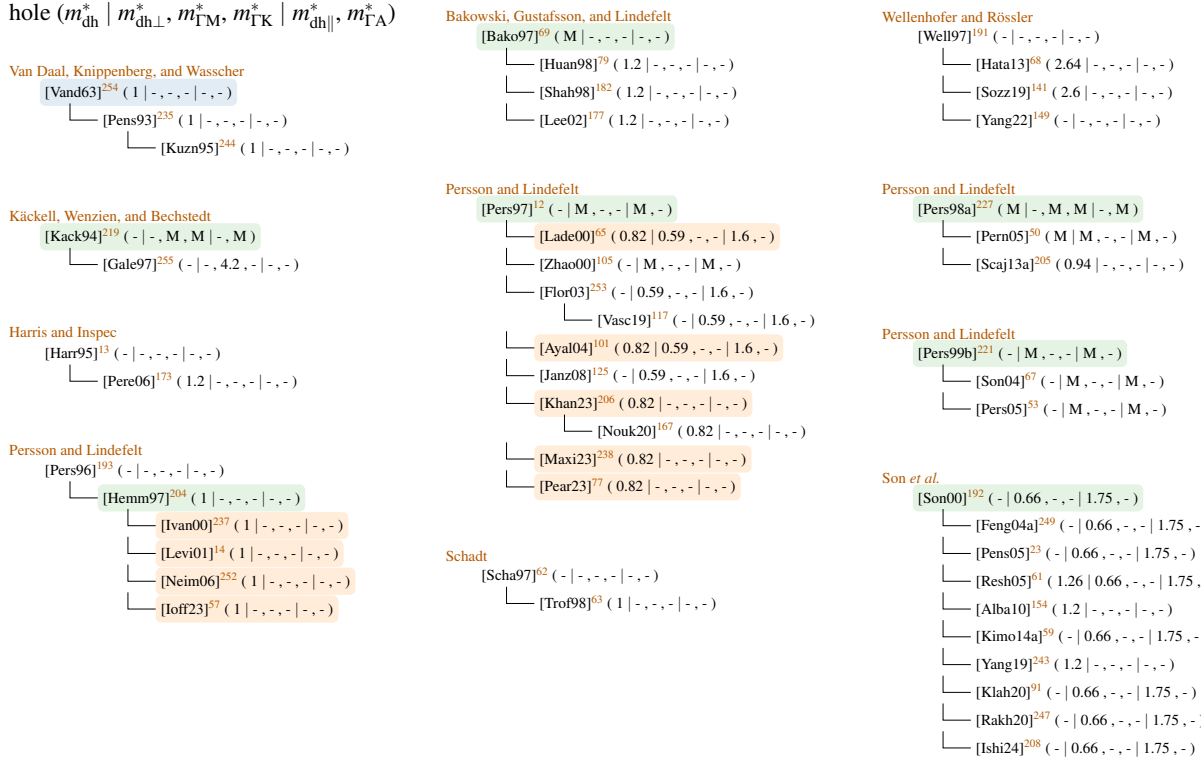


FIG. 7. DOS reference chain for holes. 'M' denotes that multiple values are found in the publication. Entries with green background show fundamental investigations, orange references we inferred based on the used data.

### III. BAND GAP

The band diagram of a material specifies the energy of a charge carrier for a given direction-dependent momentum. The electrons are described by the *conduction band* and the holes by the *valence band*. If both touch the material is called a conductor while a large gap, called the *band gap*, characterizes an insulator. Materials having a band gap in between these two extremes are called semiconductors. This shows that an exact knowledge of the band gap is instrumental to describe the electronic properties of 4H-SiC.

In TCAD simulations the band gap  $E_g$  is essential for the carrier concentration, in the drift diffusion equation and also for the barrier heights in Schottky contacts. Because  $E_g$  is often stated in the exponent, where small changes can have a huge impact, a high accuracy is desired. In this section we are, thus, going to investigate band gap energies published in literature by extending existing overviews<sup>130,257</sup>. Overall, we conclude that the majority of the currently used values are, with high confidence, based on measurement from the year 1964. Despite various variations and

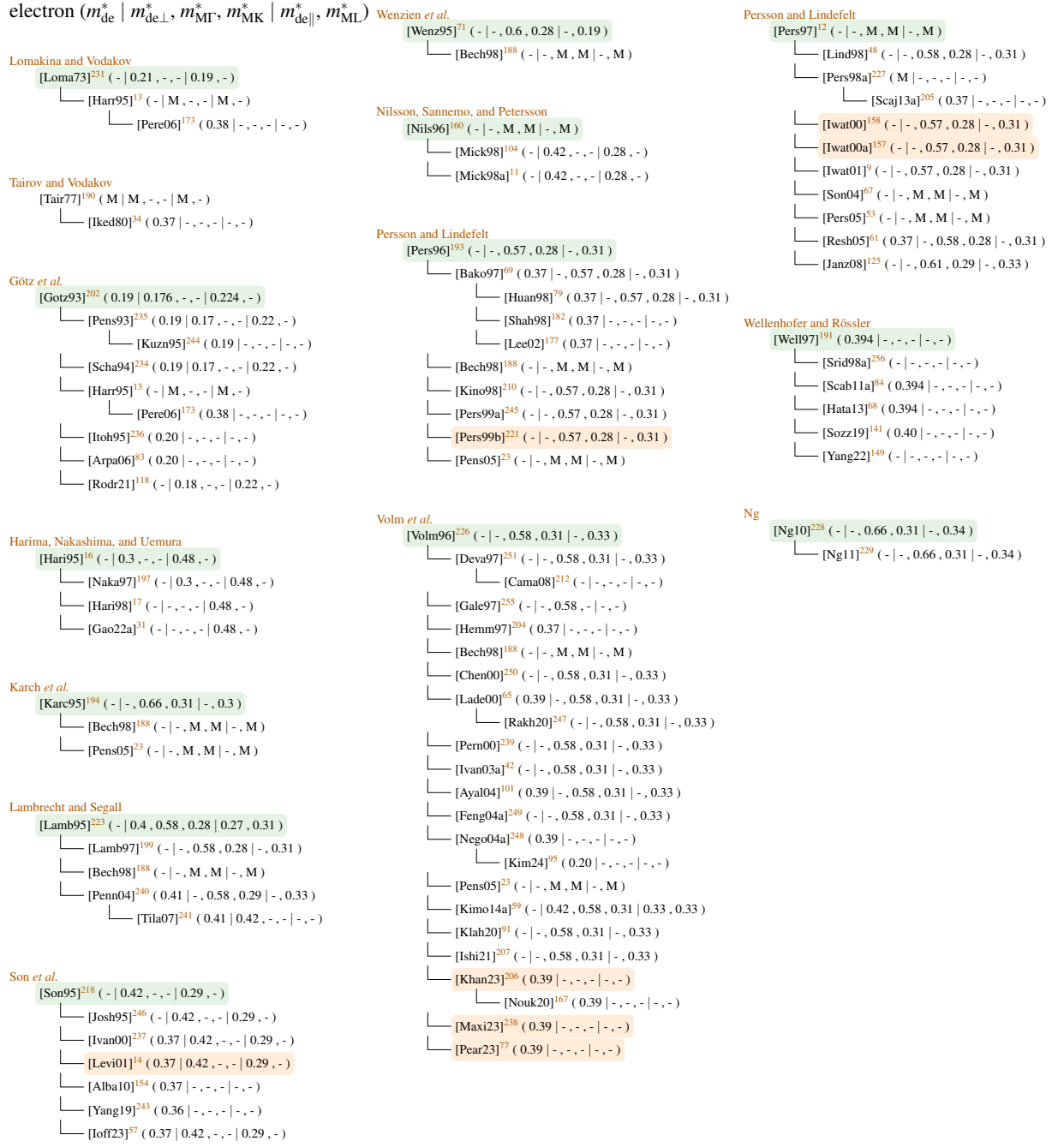


FIG. 8. DOS reference chain for electrons. 'M' denotes that multiple values are found in the publication. Entries with green background show fundamental investigations, orange references we inferred based on the used data and blue investigation based not on 4H.

changes the most commonly used value coincidentally fits latest measurements, however further investigations are required for proper confirmation.

## A. Theory

The band gap is measured between the highest energy value of the valence band in the  $\Gamma$  point (see ??) and the lowest one of the conduction band in the M-point<sup>5,57,67</sup>. Because these are not at the same location 4H-SiC is a so-called indirect semiconductor, which means that some transfer of moment, e.g., by a phonon, is required for the minimum energy difference. Electrons can also be lifted from the valence to the conduction band in the  $\Gamma$  point and then gradually relax towards the minimum, however, in that case more than the band gap energy is required to create an electron-hole pair. An overview of ionization energies for these cases is provided by Gsponer *et al.*<sup>258</sup>, who extracted a value of  $(7.83 \pm 0.02)$  eV from their own measurements.

Our statement that electrons are lifted from the valence to the conduction is not completely correct. Actually, the electron first forms an exciton by Coulomb interactions with the hole it left behind<sup>259–262</sup>. This setup can be compared to the hydrogen atom but with much larger radii due to the much lower effective masses. Additional energy has to be provided before the electron can move freely within the conduction band. Consequently, the band gap energy  $E_g$  is the sum of the energy required to generate the exciton, i.e., the exciton band gap energy  $E_{gx}$ , and the energy to free the electron from the exciton, i.e., the *free exciton binding energy*  $E_x$  (see Eq. (6)<sup>154</sup>).

$$E_g = E_{gx} + E_x \quad (6)$$

The free exciton binding energy  $E_x$  must not be confused with the *bound* exciton binding energy<sup>34,91,202,211,233,259,263–268</sup>. An exciton, which is neutral and thus can relatively easily travel through the lattice, can achieve an energetically better configuration when attaching itself to an impurity<sup>259</sup>. The energy reduction relative to  $E_{gx}$  is represented by the bound exciton binding energy, which depends on the impurity atom, the lattice site and the charge state<sup>269</sup>. Typical values reported in literature are comparable to the free exciton binding energy (in the range of a few meV). Because the same symbol  $E_x$  is used it is challenging to distinguish bound and free exciton binding energy.

The band gap energy is not a constant. First and foremost it varies among the polytypes of silicon carbide. It was empirically shown that the band gap scales linearly with the degree of

hexagonality, i.e., the ratio of hexagonal to cubic lattice sites<sup>59,270–272</sup>. Because 4H-SiC has a hexagonality of 50 %<sup>273</sup> (cp. Section VI) its band gap energy is located halfway between the extreme values. In addition the band gap changes with pressure<sup>3</sup>, under strain<sup>198</sup> and for varying temperature and doping concentrations. These have a significant effect on the device behaviour as the shift in the band edges create, for example, potential barriers which influence the carrier transport across junctions<sup>274</sup>.

In the sequel we are going to investigate band gap narrowing described by Eq. (7), whereat  $E_g(T)$  denotes the temperature induced variation and  $\Delta E_g(N_D^+, N_A^-)$  the doping-induced one.

$$E_g(T, N_D^+, N_A^-) = E_g(T) - \Delta E_g(N_D^+, N_A^-) \quad (7)$$

## 1. Temperature Dependency

Lattice vibrations cause a shift of the band energies and changes in the electron-lattice interaction energy<sup>275</sup>. Because these changes differ among energy levels the effective band gap changes<sup>276</sup>. The temperature dependent band gap (see Eq. (8))<sup>3</sup> contains effects from thermal expansion ( $\Delta E_{\text{th}}(T)$ ) and electron-phonon interaction ( $\Delta E_{\text{ph}}(T)$ ).

$$E_g(T) = E_g(0) - \Delta E_{\text{th}}(T) - \Delta E_{\text{ph}}(T) \quad (8)$$

These effects are hard to separate in experiments<sup>3</sup>, which was, so far, only achieved by Cheng, Yang, and Zheng<sup>33</sup>. Because  $\Delta E_{\text{th}}(T)$  has a much weaker impact<sup>277</sup> and the scaling of both contributions is comparable<sup>278</sup> the models for  $\Delta E_{\text{ph}}(T)$  are, in general, used to describe both with reasonable accuracy. Arvanitopoulos *et al.*<sup>86</sup> extended Eq. (8) by adding an additive term  $\Delta_g^{\text{Fermi}}$  to account for carrier statistics. This is, however, only necessary for devices whose size is close to the de-Broglie wavelength.

For high temperatures the band gap decreases linearly<sup>65,279,280</sup> while for low temperatures non-linear behavior, i.e., quadratic<sup>280</sup> or plateau-like behavior<sup>281</sup> is observed. Quadratic behavior is described by the empirical Varshni relation in Eq. (9)<sup>282</sup> with  $T_g$  some arbitrary characterization temperature.

$$E_g(T) = E_g(T_g) + \alpha \left( \frac{T_g^2}{T_g + \beta} - \frac{T^2}{T + \beta} \right) \quad (9)$$

Multiple authors<sup>277,278,281</sup> criticize that it is not possible to retrace the parameters of this model to physical mechanism-specific quantities (e.g.,  $\beta$  was said to be approximately the Debye temperature which turned out to be not the case, since it sometimes even got negative<sup>143,283,284</sup>) and

the model is unable to provide adequate interpretation of available data sets at low and high temperature<sup>285,286</sup>. For example, Pässler<sup>286</sup> tried to match the values from Choyke, Hamilton, and Patrick<sup>270</sup> but achieved only unrealistic results.

A physically based approach describing a plateau-like behavior at cryogenic temperature is a model of Bose-Einstein type in Eq. (10)<sup>281,287</sup> with  $\Theta_B$  the mean frequency of the involved phonons and  $\alpha_B$  the strength of the electron-phonon interaction<sup>3</sup>.

$$E_g(T) = E_B - \alpha_B \left( 1 + \frac{2}{e^{\Theta_B/T} - 1} \right) \quad (10)$$

The rate of change of the band gap at low temperatures is strongly material specific and depends on the phonon dispersion  $\Delta$ <sup>286</sup>. Eq. (9) is most accurate for  $\Delta \gg 1$ <sup>280,288</sup>, while Eq. (10) represents the lower limit ( $\Delta \rightarrow 0$ ) and is most suitable for  $\Delta < \frac{1}{3}$ <sup>286</sup>. Because most semiconductors show a dispersion in the range of 0.3–0.6<sup>286</sup> Pässler<sup>277,286</sup> proposed the model shown in Eq. (11) with  $\varepsilon$  the entropy and  $\Theta_p$  the average phonon temperature.

$$E_g(T) = E_g(0) - \frac{\varepsilon \Theta_p}{2} \left[ \sqrt[p]{1 + \left( \frac{2T}{\Theta_p} \right)^p} - 1 \right] \quad (11)$$

$$p \approx \sqrt{\frac{1}{\Delta^2} + 1}$$

This model was subsequently extended by Pässler<sup>280</sup> to cover a wider range of the phonon dispersion  $\Delta$  and, thus, promises to bridge the gap between Eq. (9) and Eq. (10).

## 2. Doping Dependency

The band gap also changes due to many-body effects of free carriers, i.e., their interactions among each other and with dopants, which become dominant for small carrier-to-carrier distances (high doping concentrations)<sup>289</sup>. Examples are interactions within a band, across bands and with ionized dopants<sup>48,289,290</sup>. The single effects were investigated extensively on their own<sup>289</sup> and got eventually merged, based on a similar analysis for silicon<sup>290</sup>, for 4H-SiC by Lindefelt<sup>48</sup> to the

model shown in Eq. (12).

$$\begin{aligned}
\Delta E_g(N_D^+, N_A^-) &= -\Delta E_{(n/p)c}(N_D^+) + \Delta E_{(n/p)v}(N_A^-) \\
\Delta E_{nc}(N_D^+) &= A_{nc} \left( \frac{N_D^+}{10^{18}} \right)^{1/3} + B_{nc} \left( \frac{N_D^+}{10^{18}} \right)^{1/2} < 0 \\
\Delta E_{nv}(N_D^+) &= A_{nv} \left( \frac{N_D^+}{10^{18}} \right)^{1/4} + B_{nv} \left( \frac{N_D^+}{10^{18}} \right)^{1/2} > 0 \\
\Delta E_{pc}(N_D^+) &= A_{pc} \left( \frac{N_A^-}{10^{18}} \right)^{1/4} + B_{pc} \left( \frac{N_A^-}{10^{18}} \right)^{1/2} < 0 \\
\Delta E_{pv}(N_D^+) &= A_{pv} \left( \frac{N_A^-}{10^{18}} \right)^{1/3} + B_{pv} \left( \frac{N_A^-}{10^{18}} \right)^{1/2} + C_{pv} \left( \frac{N_A^-}{N_{A0}} \right)^{1/4} > 0
\end{aligned} \tag{12}$$

$\Delta E_{nc}$  and  $\Delta E_{pc}$  denote the change of the conduction band due to *n* and *p* type doping. Because the conduction band energy level drops these factors are negative and thus have to be subtracted from the increase of the valence band denoted by  $\Delta E_{nv}$  and  $\Delta E_{pv}$ .

The term featuring  $C_{pv}$  was added in an extension proposed by Persson, Lindefelt, and Sernelius<sup>66</sup>. The authors define the validity of this model for ionized charge carrier concentrations (see Section VI) above a few  $10^{18}/\text{cm}^3$  and claim that a larger displacement is observable in 4H compared to other polytypes. More specifically, the valence band displacement is larger than the conduction band one. Other publications distribute the band gap narrowing equally across valence and conduction band<sup>86</sup> or chose a contribution of  $\Delta E_c/E_g = 0.7$ <sup>291</sup>.

Some TCAD tools merge the prefactor and the denominator  $10^{18}$  often called Jain-Roulston model<sup>290</sup>, as shown in Eq. (13). We get  $A_{xc}^j/A_{xc} = 10^{-6}$  and  $B_{xy}^j/B_{xy} = 10^{-9}$  with  $x \in \{n, p\}, y \in \{c, v\}$ . For the remaining parameters the correlation is not so simply, i.e., we get  $A_{xc}^j/A_{xc} = \approx 3.162 \times 10^{-5}$ . For better comparison we transferred all parameters of Eq. (13) back to their respective counterparts in Eq. (12), except the sum of  $B_{xy}$ , which could obviously not be separated.

$$\begin{aligned}
\Delta E_{gn} &= -A_{nc}^j (N_D^+)^{1/3} + (B_{nv}^j - B_{nc}^j) (N_D^+)^{1/2} + A_{nv}^j (N_D^+)^{1/4} \\
-\Delta E_{gp} &= A_{pc}^j (N_A^-)^{1/3} + (B_{pv}^j - B_{pc}^j) (N_A^-)^{1/2} + A_{pv}^j (N_A^-)^{1/4}
\end{aligned} \tag{13}$$

An alternative approach to describe the doping dependency is to use the Slotboom model (see Eq. (14)), which was originally developed for Si. Ruff, Mitlehner, and Helbig<sup>292</sup> first did it for 6H and Lades<sup>65</sup> later followed for 4H-SiC by fitting to the results in Eq. (12) with  $N$  the and  $N_{n,p}$ .

$$\Delta E_g = C_{n,p} \left( \ln \left( \frac{N}{N_{n,p}} \right) + \sqrt{\left( \ln \left( \frac{N}{N_{n,p}} \right) \right)^2 + G} \right) \tag{14}$$

A more physically based approach is to interpret the band gap reduction as renormalization due to electron-electron interactions alone. To describe this effect Schubert<sup>289</sup> proposed the band gap narrowing described by Eq. (15).

$$\Delta E_g = \frac{e^2}{4\pi\epsilon r_s} \quad (15)$$

The screening radius  $r_s$  is given by the Debye and Thomas-Fermi radii leading to the descriptions for the non-degenerate (see Eq. (16)) and degenerate (see Eq. (17)) case with  $n$  the charge carrier concentration.

$$\Delta E_g = \frac{e^3 \sqrt{n}}{4\pi\epsilon^{3/2} \sqrt{k_B T}} \quad (\text{Debye, non-degenerate}) \quad (16)$$

$$\Delta E_g = \frac{e^3 \sqrt{m_{de}^*(3n)^{1/3}}}{4\pi^{5/3} \epsilon^{3/2} \hbar} \quad (\text{Thomas-Fermi, degenerate}) \quad (17)$$

We want to highlight that in state-of-the-art TCAD tools only Eq. (9) and Eq. (14) are supported out of the box, although some feature the possibility to write custom code for band gap narrowing.

## B. Results & Discussion

Multiple methods to determine the band gap, which were partially discussed by Nava *et al.*<sup>109</sup>, De Napoli<sup>150</sup>, were used in literature. Most of them focus on measurements, e.g., transmission spectroscopy (TS)<sup>8,33</sup>, spectroscopic ellipsometry<sup>293</sup>, photo absorption (PA)<sup>269,270,285,294</sup>, optical admittance (OA)<sup>295</sup>, exciton electroabsorption (EE)<sup>268</sup>, free carrier absorption (FCA)<sup>279</sup>, free exciton luminescence (FEL)<sup>267</sup>, photoluminescence (PL)<sup>211,266,296</sup>, photoconductivity (PC)<sup>297</sup> and wavelength-modulated absorption (WMA)<sup>91,298</sup>. Sometimes the results of multiple measurements are combined to improve the accuracy<sup>263</sup>. Stefanakis and Zekentes<sup>299</sup> states that the free carrier absorption method overestimates the band gap while optical absorption studies deliver more accurate results.

An alternative are calculations, which include empirical pseudopotentials (EP)<sup>116,300–302</sup>, density functional theory local density approximation (DFT-LDA)<sup>5,12,67,136,195,198,220,222,224,303</sup>, rectangular barrier of finite height (RB)<sup>304</sup>, fitting (FT)<sup>14,59,65,68</sup> and genetic algorithm fitting (GAF)<sup>228</sup>.

With these methods mainly results for low temperatures were achieved (see Table VI). Predominantly the exciton band gap energy was measured, whereat the achieved values seem to agree on  $E_{gx} = (3.265 \pm 0.002)$  eV. For the band gap energy only two investigations could be found which deliver  $E_g = 3.285$  eV respectively  $E_g = 3.28$  eV. The calculations show a much larger spread,

however, the latest investigations all propose significantly lower values of  $E_g = (3.15 \pm 0.03)$  eV. For room temperature only few dedicated measurements are available<sup>8,279,285,293,305</sup>, whereas the ones by Ahuja *et al.*<sup>8</sup> have a quite big uncertainty of 98 meV. We only found one publication that investigated the anisotropy<sup>285</sup> achieving the same exciton (band gap) energy for fields parallel resp. perpendicular to the c-axis. The doping induced band gap narrowing is in general not known for these measurements.

TABLE VI: Band gap energies and their temperature dependency fittings. If no temperature dependency parameters (for Eq. (9)) are shown  $T_g$  represents the measurement temperature for the shown energies. Highlighted lines represent no 4H results and calculations.

ref.	band gap			temperature dep.			interval	method <sup>306</sup>
	$E_g$ [eV]	$E_{gx}$ [eV]	$E_x$ [meV]	$T_g$ [K]	$\alpha$ [eV/K]	$\beta$ [K]		
[Choy57] <sup>294 307</sup>	-	-	-	-	$3.3 \times 10^{-4}$	-	-	PA
[Choy64] <sup>270</sup>	-	$3.263 \pm 0.003$	-	4	-	-	-	PA
[Choy64a] <sup>269 308</sup>	-	3.265	-	4.7	-	-	-	PA
[Jung70] <sup>301</sup>	2.8	-	-	0	-	-	-	EP
[Dubr75] <sup>268</sup>	-	-	$20 \pm 15$	2	-	-	-	EE
[Dubr77] <sup>304</sup>	3.2	-	-	0	-	-	-	RB
[Ikeda80b] <sup>267</sup>	-	3.2639	10	77	-	-	-	FEL
[Gavr90] <sup>309</sup>	2.89	-	-	0	-	-	-	DFT-LDA
[Back94] <sup>300</sup>	3.28	-	-	0	-	-	-	EP
[Park94] <sup>310</sup>	2.14	-	-	0	-	-	-	EP
[Kord95] <sup>211</sup>	-	3.265	-	4.2	-	-	-	PL
[Wenz95] <sup>71</sup>	3.56	-	-	0	-	-	-	DFT-LDA
[Evwa96] <sup>295</sup>	$3.41 \pm 0.03$	-	-	40	-	-	-	OA
[Itoh96] <sup>266 308</sup>	-	3.265	-	4.25	-	-	-	PL
[Kaec96] <sup>311</sup>	2.18	-	-	0	-	-	-	DFT-LDA
[Bako97] <sup>69</sup>	3.19	-	-	300	$3.3 \times 10^{-4}$	0	300–700	FT
[Chen97] <sup>224</sup>	3.27	-	-	0	-	-	-	DFT-LDA
[Pers97] <sup>12</sup>	2.9	-	-	0	-	-	-	DFT-LDA
[Vanh97] <sup>302</sup>	3.28	-	-	0	-	-	-	EP
[Ivan98] <sup>296</sup>	-	3.266	-	2	-	-	-	PL
[Bell00] <sup>116</sup>	3.05	-	-	0	-	-	-	EP
[Lade00] <sup>65 312</sup>	-	3.265	40	0	$3.3 \times 10^{-4}$	$1.05 \times 10^3$	4–200	FT
	-	3.265	40	0	$3.3 \times 10^{-2}$	$1 \times 10^5$	4–600	FT
	-	3.342	40	0	$3.3 \times 10^{-4}$	0	300–700	FT
[Srid00] <sup>298</sup>	-	3.267	-	2	-	-	-	WMA
[Zhao00a] <sup>222</sup>	3.11	-	-	0	-	-	-	DFT-LDA
[Levi01] <sup>14 313</sup>	3.23	-	-	300	$6.5 \times 10^{-4}$	1300	-	FT
[Ahuja02] <sup>8</sup>	$3.260 \pm 0.098$	-	-	300	-	-	-	TS
[Gale02] <sup>279</sup>	3.285	-	-	0	$3.5 \times 10^{-4}$	1100	0–650	FCA
	3.2625	-	-	300	$2.4 \times 10^{-4}$	0	300–650	FCA
[Ivan02] <sup>297</sup>	3.285	-	$20.5 \pm 1.0$	2	-	-	-	PC

[Shal02] <sup>305</sup>	3.18	-	-	300	-	-	-	-	PL
[Dong04] <sup>195</sup>	2.194	-	-	0	-	-	-	-	DFT-LDA
[Son04] <sup>67</sup>	3.35	-	-	0	-	-	-	-	DFT-LDA
[Bala05] <sup>283 314</sup>	3.26	-	-	300	$4.15 \times 10^{-4}$	-131	-	-	-
[Chin06] <sup>5</sup>	2.433	-	-	0	-	-	-	-	DFT-LDA
[Griv07] <sup>285</sup>	-	3.267	$30 \pm 10$	0	-	-	0–500	-	PA
[Tama08a] <sup>315 314</sup>	3.23	-	-	300	$7.036 \times 10^{-4}$	1509	-	-	-
[Ng10] <sup>228</sup>	3.28	-	-	0	-	-	-	-	GAF
[Hata13] <sup>68 313</sup>	3.285	3.265	20	0	$9.06 \times 10^{-4}$	2030	0–800	-	FT
[Kimo14a] <sup>59 313</sup>	-	3.265	20	2	$8.2 \times 10^{-4}$	1800	-	-	FT
[Yama18] <sup>303</sup>	3.12	-	-	0	-	-	-	-	DFT-LDA
[Kuro19] <sup>198</sup>	3.15	-	-	0	-	-	-	-	DFT-LDA
[Klah20] <sup>91</sup>	-	3.2659	40	1.4	-	-	-	-	WMA
[Lech21] <sup>82 314</sup>	3.265	-	-	0	$10.988 \times 10^{-3}$	32744.3	-	-	FT
[Lu21] <sup>220</sup>	3.17	-	-	0	-	-	-	-	DFT-LDA
[Chen22] <sup>33</sup>	3.44	-	-	0	$5.27 \times 10^{-4}$	0	300–620	-	TS
[Huan22b] <sup>316</sup>	3.18	-	-	0	-	-	-	-	DFT-LDA
[Torr22] <sup>136</sup>	3.17	-	-	0	-	-	-	-	DFT-LDA
[Khan23] <sup>206 314</sup>	3.285	-	-	0	$3.3 \times 10^{-4}$	240	-	-	-
[Main24] <sup>293</sup>	$3.30 \pm 0.02$	-	-	300	-	-	-	-	SE

The free exciton binding energy  $E_x$  was first estimated by Hagen, Van Kemenade, and Van Der Does De Bye<sup>317</sup> to be around 20 meV, with the side note that further investigations are needed. Later, five measurements were published<sup>91,267,268,285,297</sup>. The achieved values range from 10–40 meV. The value of 10 meV<sup>267</sup> was determined for the activation energy for thermal quenching of free excitons, however, Devaty and Choyke<sup>251</sup> argue that these values are too low to be free exciton binding energies.

## 1. Temperature Dependency

Very few measurements on the temperature dependency are available<sup>33,269,279,285</sup>. The remaining models<sup>14,59,65,68</sup> fit the data published by Choyke<sup>263</sup>, Choyke, Patrick, and Hamilton<sup>269</sup>, Choyke, Hamilton, and Patrick<sup>270</sup> from the 1960s. Surprisingly, the model development only started at the beginning of the 2000s. In 1997 Bakowski, Gustafsson, and Lindefelt<sup>69</sup> were still forced to use the 6H values. In 2004 Ayalew<sup>101</sup> stated that not reliable data are available.

The origin of some of the proposed model parameters<sup>82,206,283</sup> could not be traced back to any scientific publication. Occasionally, we were able to them back to prominent TCAD simulation suites, where these were used as default values. Although Tamaki *et al.*<sup>315</sup> provides a reference

for the used model<sup>78</sup>, we were unable to verify the parameters. By comparison we found that the results are very close to those predicted by Kimoto and Cooper<sup>59</sup> (see Fig. 9).

To describe the temperature dependency the majority resorts to the Varshni model (see Eq. (9)). We would like to highlight that the value  $\alpha = 3.3 \times 10^{-4}$  eV/K was determined by Choyke and Patrick<sup>294</sup> for an undefined polytype of SiC. According to the utilized band gap we suspect it to be 21R-SiC device although Bakowski, Gustafsson, and Lindefelt<sup>69</sup> argued that it was 6H. Nevertheless, a wide range of fittings utilizes this value, i.e., that 4H and 6H share the same temperature dependency<sup>163</sup>. Nallet *et al.*<sup>318</sup> even references 6H values directly<sup>292</sup>, which, however, go back to the same data by Choyke and Patrick<sup>294</sup>.

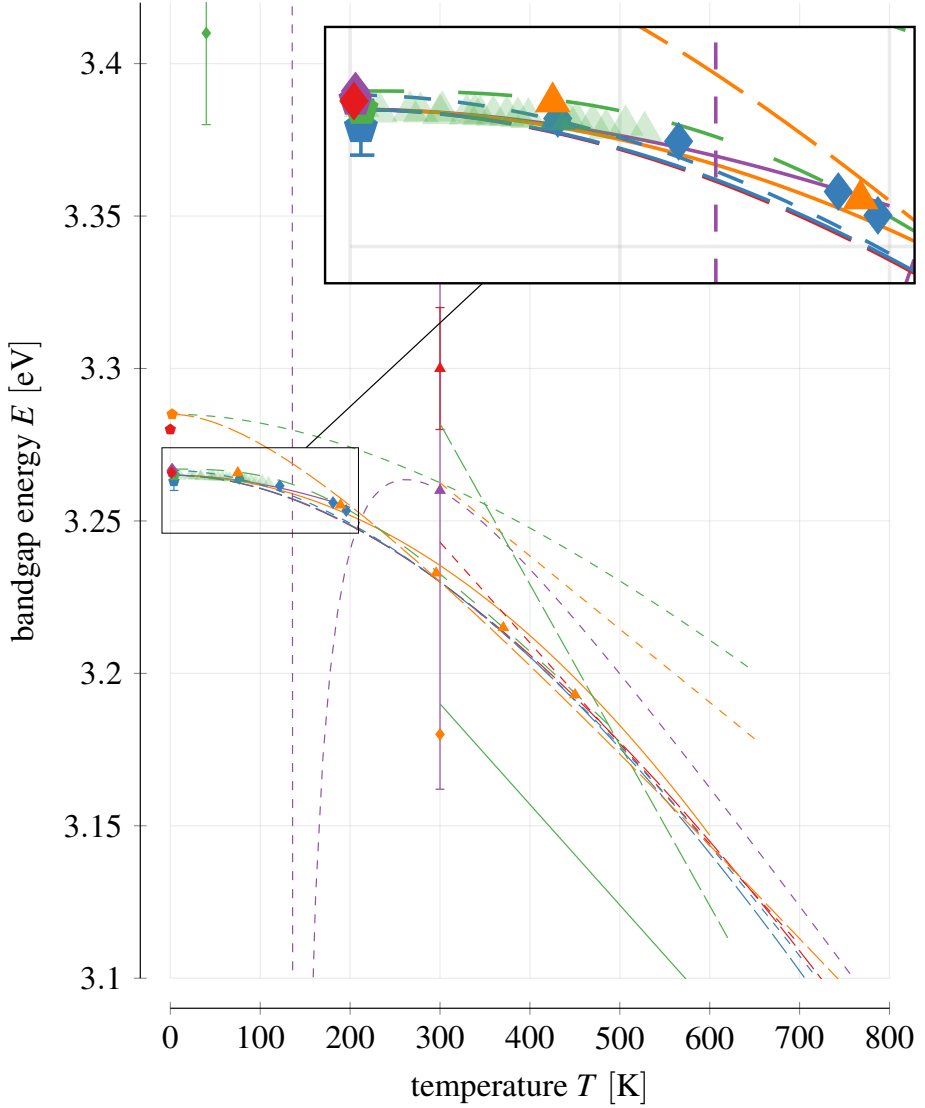
The model presented in Eq. (11) is solely used by Grivickas *et al.*<sup>285</sup> with the parameters shown in Eq. (18).

$$\Theta_p = 450\text{ K}, \quad \epsilon = 3 \times 10^{-4} \text{ eV/K}, \quad p = 2.9 . \quad (18)$$

From a graphical representation of the band gap energy versus temperature (see Fig. 9) the deviations of the models becomes evident. We do not show the fitting by Hatakeyama, Fukuda, and Okumura<sup>68</sup> which is identical to the one by Kimoto and Cooper<sup>59</sup>. Similarly, the parameters provided by Lechner<sup>82</sup> reproduce the fitting from Lades<sup>65</sup> (4–600 K).

First of all it has to be noted that the measurements nicely distinguish  $E_g$  and  $E_{gx}$ . The same can not be said for the fittings. For example, Levinstejn, Rumyantsev, and Shur<sup>14</sup> denoted to describe  $E_g$  but the values agree more to  $E_{gx}$ . Also the fitting by Bakowski, Gustafsson, and Lindefelt<sup>69</sup>, who simply took the band gap at 0 K and applied the scaling factor  $\alpha$ , turns out to underestimate the band gap. Newer models, e.g., the one by Cheng, Yang, and Zheng<sup>33</sup>, suggest a much different slope with temperature, actually crossing the traces of  $E_{gx}$  with  $E_g$ . The model by Khanna<sup>206</sup> matches  $E_g$  at low temperatures but at around 200 K it is equal to  $E_{gx}$  and follows that value from there onward. The fitting by Balachandran, Chow, and Agarwal<sup>283</sup> is only feasible for  $T \geq 300\text{ K}$  as it has a singularity at 131 K.

The plateau achieved by the Pässler model in Eq. (11) is barely visible, showing that the deviations are only subtle. Lades<sup>65</sup> approximated the shape with the Varshni model by just fitting it in a very narrow temperature range. The phonon dispersion of 4H-SiC  $\Delta = 0.29^{285}$  is rather low, which would actually indicates that Eq. (10) is the most suitable, however, Eq. (11) seems to be accurate as well. Even more, Stefanakis and Zekentes<sup>299</sup> compared the single models and identifies Eq. (9) as the most suitable one. In fact, we did not find a single instance where Eq. (10) was used to describe 4H-SiC.



- |  |   |  |
|--|---|--|
| • [Choy64] <sup>270</sup> $E_{gx}$         | • [Choy64a] <sup>269</sup> $E_{gx}$     | • [Ikeda80b] <sup>267</sup> $E_{gx}$     |
| • [Kord95] <sup>211</sup> $E_{gx}$         | • [Evwa96] <sup>295</sup> $E_g$         | • [Itoh96] <sup>266</sup> $E_{gx}$       |
| • [Ivan98] <sup>296</sup> $E_{gx}$         | • [Srid00] <sup>298</sup> $E_{gx}$      | • [Ahuja02] <sup>8</sup> $E_g$           |
| • [Ivan02] <sup>297</sup> $E_g$            | • [Shal02] <sup>305</sup> $E_g$         | • [Griv07] <sup>285</sup> $E_{gx}$       |
| • [Ng10] <sup>228</sup> $E_g$              | • [Klah20] <sup>91</sup> $E_{gx}$       | • [Main24] <sup>293</sup> $E_g$          |
| — [Bako97] <sup>69</sup> $E_g$ (V)         | — [Lade00] <sup>65</sup> $E_{gx}$ (V)   | — [Lade00] <sup>65</sup> $E_{gx}$ (V)    |
| - - - [Lade00] <sup>65</sup> $E_{gx}$ (V)  | - - - [Levi01] <sup>14</sup> $E_g$ (V)  | - - - [Gale02] <sup>279</sup> $E_g$ (V)  |
| - - - [Gale02] <sup>279</sup> $E_g$ (V)    | - - - [Bala05] <sup>283</sup> $E_g$ (V) | - - - [Tama08a] <sup>315</sup> $E_g$ (V) |
| - - - [Hata13] <sup>68</sup> $E_{gx}$ (V)  | - - - [Chen22] <sup>33</sup> $E_g$ (V)  | - - - [Khan23] <sup>206</sup> $E_g$ (V)  |
| - - - [Griv07] <sup>285</sup> $E_{gx}$ (P) |   |  |

FIG. 9. Band gap measurements and models. The latter are, if available, only shown in the specified confidence interval. (V) denotes a fitting using the Varshni model and (P) fitting with the Pässler model.

TABLE VII. Parameters for ionized dopants induced band gap narrowing.

ref.	method	n-type				p-type				
		$A_{nc}$	$B_{nc}$	$A_{nv}$	$B_{nv}$	$A_{pc}$	$B_{pc}$	$A_{pv}$	$B_{pv}$	$C_{pv}$
		[meV]								
[Lind98] <sup>48</sup>	calculation	-15	-2.93	19	8.74	-15.70	-0.39	13	1.15	-
[Pers99] <sup>66</sup>	calculation	-17.91	-2.20	28.23	6.24	-16.15	-1.07	-35.07	6.74	56.96

TABLE VIII. Parameters for ionized dopants induced band gap narrowing Slotboom model.

ref.	type	$C$	$N$	$G$
		[eV]	[1/cm <sup>3</sup> ]	[1]
[Lade00] <sup>65</sup>	n	$2 \times 10^{-2}$	$10^{17}$	0.5
	p	$9 \times 10^{-3}$	$10^{17}$	0.5

## 2. Doping Dependency

Two fittings for the doping dependent narrowing model in Eq. (12) could be found (see Table VII). We want to highlight that these are solely based on calculations. Measurement results are available<sup>285,319</sup>, but due to their sparsity (see Fig. 11) they are not suitable to verify the calculations.

The main issue we identified regarding the parameters is an incorrect sign, as often all parameters become negative (see Fig. 10). The fact that in some cases, e.g., by Lophitis *et al.*<sup>320</sup>, the Jain-Roulston form is used (see Eq. (13)) makes a direct comparison of the parameters challenging. Furthermore, the parameter for the term with exponent 1/2 are sometimes combined<sup>144,145,154</sup>, which makes it potentially impossible to apply them accurately in certain TCAD tools. A detailed analysis of all the inconsistencies we found in literature is provided in ??.

For the Slotboom model, that is used by various publications<sup>65,82,101</sup>, one set of parameters is available<sup>65</sup> (see Table VIII). In contrast to the other models the band gap narrowing is linear in the semi-logarithmic plot (see Fig. 11). In a reasonable doping concentration range the deviation for p-type material is quite low but for n-type material considerable. The models of<sup>48</sup> and<sup>66</sup> only differ by a small amount.

Lindfelft ( $A_{\text{nc}}, A_{\text{nv}}$ ) ( $B_{\text{nc}}, B_{\text{nv}}$ ) ( $A_{\text{pc}}, A_{\text{pv}}$ ) ( $B_{\text{pc}}, B_{\text{pv}}$ ) ( $C_{\text{pv}}$ )

**Lindfelft**

- [Lind98]<sup>48</sup> ( $-1.5 \times 10^{-2}, 1.9 \times 10^{-2}$ ) ( $-2.93 \times 10^{-3}, 8.74 \times 10^{-3}$ ) ( $-1.57 \times 10^{-2}, 1.3 \times 10^{-2}$ ) ( $-3.87 \times 10^{-4}, 1.15 \times 10^{-3}$ ) (-)
  - └─ [Levi01]<sup>14</sup> ( $-1.5 \times 10^{-2}, 1.9 \times 10^{-2}$ ) ( $-2.93 \times 10^{-3}, 8.74 \times 10^{-3}$ ) ( $-1.57 \times 10^{-2}, 1.3 \times 10^{-2}$ ) ( $-3.87 \times 10^{-4}, 1.15 \times 10^{-3}$ ) (-)
  - └─ [Well01]<sup>321</sup> (-, -) (-, -) (-, -) (-)
  - └─ [Cha08]<sup>322</sup> ( $-1.5 \times 10^{-2}, 1.9 \times 10^{-2}$ ) ( $-2.93 \times 10^{-3}, 8.74 \times 10^{-3}$ ) (-, -) (-, -) (-)
    - └─ [Chen12]<sup>323</sup> ( $-1.5 \times 10^{-2}, 1.9 \times 10^{-2}$ ) ( $-2.93 \times 10^{-3}, 8.74 \times 10^{-3}$ ) (-, -) (-, -) (-)
  - └─ [Alba10]<sup>154</sup> ( $-1.5 \times 10^{-2}, 1.9 \times 10^{-2}$ ) ( $1.7 \times 10^{-2}$ ) ( $1.57 \times 10^{-2}, 1.3 \times 10^{-2}$ ) ( $1.54 \times 10^{-2}$ ) (-)
  - └─ [Zhan10]<sup>324</sup> ( $-1.5 \times 10^{-2}, 1.9 \times 10^{-2}$ ) ( $-2.93 \times 10^{-3}, 8.74 \times 10^{-3}$ ) (-, -) (-, -) (-)
  - └─ [Bell11]<sup>145</sup> ( $-1.5 \times 10^{-2}, 1.9 \times 10^{-2}$ ) ( $1.17 \times 10^{-2}$ ) ( $1.57 \times 10^{-2}, 1.3 \times 10^{-2}$ ) ( $1.54 \times 10^{-3}$ ) (-)
  - └─ [Habi11]<sup>274</sup> ( $-1.5 \times 10^{-2}, 1.9 \times 10^{-2}$ ) ( $-2.93 \times 10^{-3}, 8.74 \times 10^{-3}$ ) ( $-1.57 \times 10^{-2}, 1.3 \times 10^{-2}$ ) ( $-3.87 \times 10^{-4}, 1.15 \times 10^{-3}$ ) (-)
  - └─ [Buon12]<sup>325</sup> ( $-1.5 \times 10^{-2}, -1.9 \times 10^{-2}$ ) ( $-2.93 \times 10^{-3}, -8.74 \times 10^{-3}$ ) (-, -) (-, -) (-)
  - └─ [Pezz13]<sup>144</sup> ( $1.5 \times 10^{-2}, 1.9 \times 10^{-2}$ ) ( $1.17 \times 10^{-2}$ ) ( $1.57 \times 10^{-2}, 1.3 \times 10^{-2}$ ) ( $1.54 \times 10^{-3}$ ) (-)
  - └─ [Stef14]<sup>299</sup> ( $-1.5 \times 10^{-2}, 1.9 \times 10^{-2}$ ) ( $-2.93 \times 10^{-3}, 8.74 \times 10^{-3}$ ) ( $-1.57 \times 10^{-2}, 1.3 \times 10^{-2}$ ) ( $-3.87 \times 10^{-4}, 1.15 \times 10^{-3}$ ) (-)
  - └─ [Zegh19]<sup>326</sup> ( $-1.5 \times 10^{-2}, 1.9 \times 10^{-2}$ ) ( $1.17 \times 10^{-2}$ ) ( $-1.37 \times 10^{-2}, 1.3 \times 10^{-2}$ ) ( $1.54 \times 10^{-3}$ ) (-)
  - └─ [Zegh20]<sup>327</sup> ( $-1.5 \times 10^{-2}, 1.9 \times 10^{-2}$ ) ( $1.17 \times 10^{-2}$ ) ( $-1.37 \times 10^{-2}, 1.3 \times 10^{-2}$ ) ( $1.54 \times 10^{-3}$ ) (-)
  - └─ [Ioff23]<sup>57</sup> ( $-1.5 \times 10^{-2}, -1.9 \times 10^{-2}$ ) ( $-2.93 \times 10^{-3}, -8.74 \times 10^{-3}$ ) ( $-1.57 \times 10^{-2}, -1.3 \times 10^{-2}$ ) ( $-3.87 \times 10^{-4}, -1.15 \times 10^{-3}$ ) (-)
  - └─ [Maxi23]<sup>238</sup> ( $-1.5 \times 10^{-2}, -1.9 \times 10^{-2}$ ) ( $-2.93 \times 10^{-3}, -8.74 \times 10^{-3}$ ) ( $-1.57 \times 10^{-2}, -1.3 \times 10^{-2}$ ) ( $-3.87 \times 10^{-4}, -1.15 \times 10^{-3}$ ) (-)

**Persson, Lindfelft, and Sernelius**

- [Pers99]<sup>60</sup> ( $-1.791 \times 10^{-2}, 2.823 \times 10^{-2}$ ) ( $-2.2 \times 10^{-3}, 6.24 \times 10^{-3}$ ) ( $-1.615 \times 10^{-2}, -3.507 \times 10^{-2}$ ) ( $-1.07 \times 10^{-3}, 6.74 \times 10^{-3}$ ) ( $5.696 \times 10^{-2}$ )
  - └─ [Nipo16]<sup>142</sup> (-, -) (-, -) (-, -) (-, -) (-)
  - └─ [Loph18]<sup>320</sup> ( $-1.791 \times 10^{-2}, 2.823 \times 10^{-2}$ ) ( $-2.2 \times 10^{-3}, 6.24 \times 10^{-3}$ ) ( $-7.311 \times 10^{-2}, 3.507 \times 10^{-2}$ ) ( $-1.07 \times 10^{-3}, 6.74 \times 10^{-3}$ ) (-)

Slotboom ( $C_{\text{n}}, N_{\text{n}} \mid C_{\text{p}}, N_{\text{p}} \mid G$ )

**Lades**

- [Lade00]<sup>65</sup> ( $2 \times 10^{-2}, 1 \times 10^{17} \mid 9 \times 10^{-3}, 1 \times 10^{17} \mid 5 \times 10^{-1}$ )
  - └─ [Ayal04]<sup>101</sup> ( $2 \times 10^{-2}, 1 \times 10^{17} \mid 9 \times 10^{-3}, 1 \times 10^{17} \mid 5 \times 10^{-1}$ )
  - └─ [Lech21]<sup>82</sup> ( $2 \times 10^{-2}, 1 \times 10^{17} \mid -, - \mid 5 \times 10^{-1}$ )

FIG. 10. Citations and extracted parameters for the doping dependency of the band gap. If solely a single value is shown for parameter  $B$  then the publication only provides  $B_c + B_v$ .   are fundamental investigations and   connections predicted from the used values.

The band gap narrowing according to Eq. (17) is also shown, because it also occasionally used<sup>291,299</sup>, whereas Stefanakis and Zekentes<sup>299</sup> used a slightly different form of the Thomas-Fermi radius shown in Eq. (19) with  $n_0$  the equilibrium carrier density.

$$\Delta E_g = \frac{e^2}{4\pi\epsilon_0\epsilon_s} \left( \frac{3n_0 e^2}{2\epsilon_0 E_F} \right)^{1/2} \quad (19)$$

Unfortunately our calculations did not succeed to reproduce the results achieved in these publications so we extracted the curve from Donnarumma, Palankovski, and Selberherr<sup>291</sup>. Surprising for us is also the shape of the narrowing, which becomes almost linear in the semi-logarithmic plot for high doping concentrations. With the simple assumption  $n = N_D^+$  resp.  $n = N_A^-$  this does not

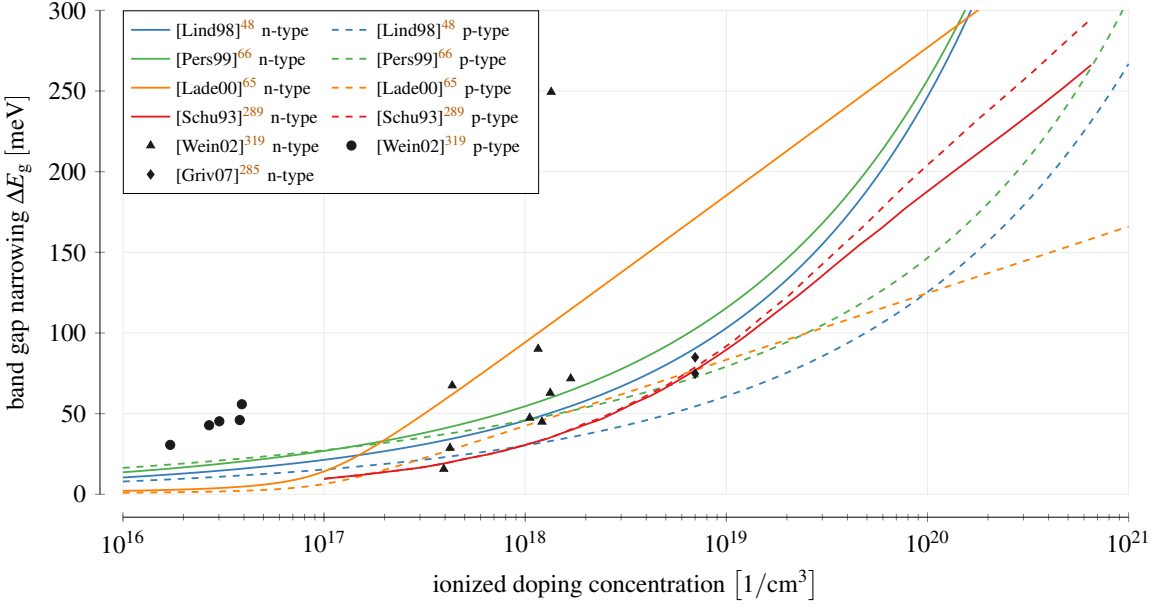


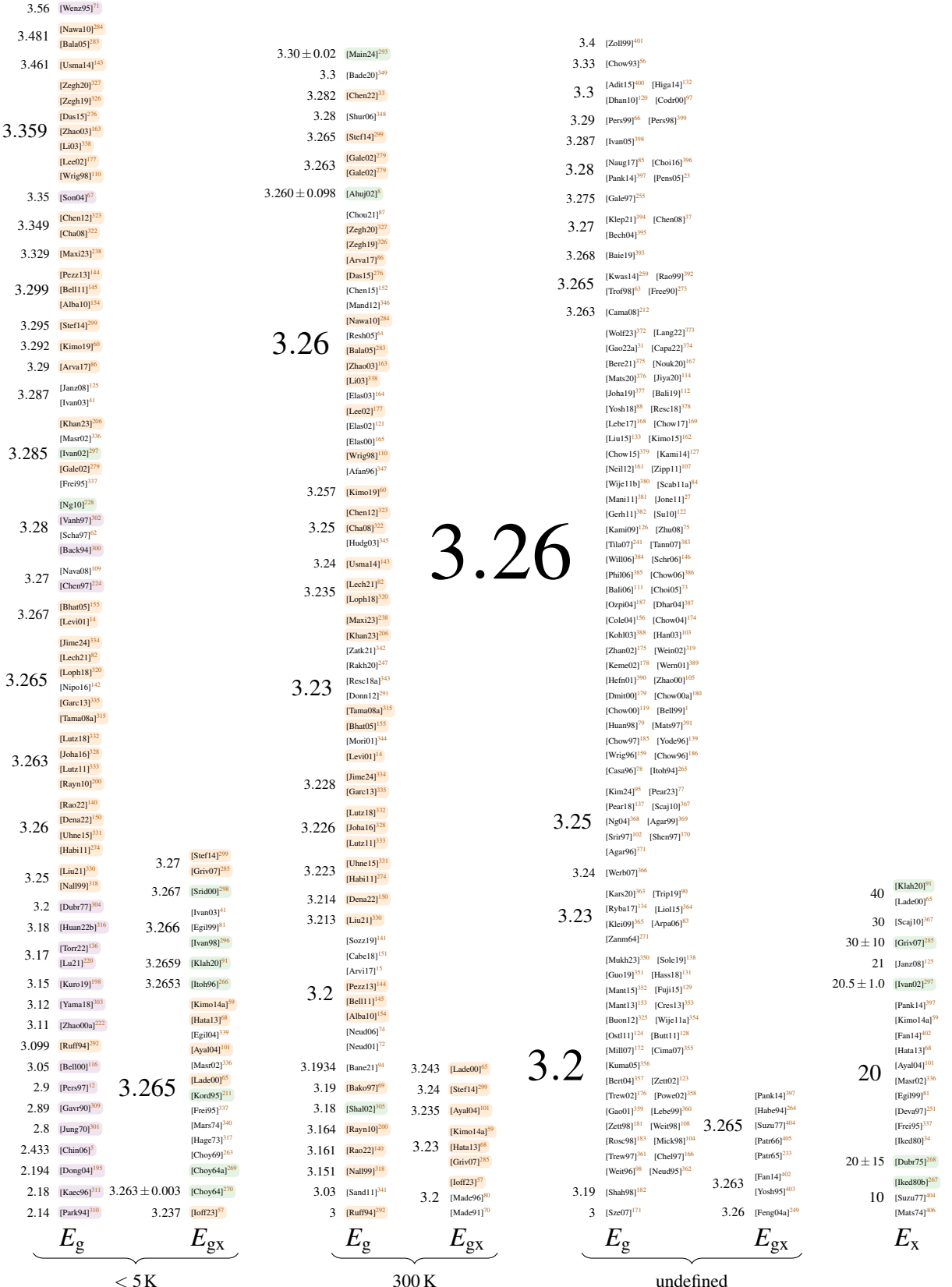
FIG. 11. Doping induced band gap narrowing. The different models complemented by measurement results for p- and n-type material are shown.

seem to be possible. Last Johannesson and Nawaz<sup>328</sup> used the Debye radius from Eq. (16), based on the calculations by Lanyon and Tuft<sup>329</sup>.

### 3. TCAD Values

An overwhelming amount of band gap values can be found in literature (see Fig. 12). Measurements mainly focused on the exciton band gap energy  $E_{gx}$  at low temperatures, resulting in values of  $(3.265 \pm 0.002)$  eV. Using the broadly accepted value of  $E_x = 20$  meV (see also Fig. 15) a band gap energy of  $E_g = 3.285$  eV is achieved, which has also been confirmed by dedicated measurements. The additional higher and lower values mainly stem from temperature dependency models, which were designed for higher temperatures and, thus, lack accuracy at low one. In general, only a few values for the parameters  $\alpha$  and  $\beta$  are used (see Fig. 13), however, the energy value ( $E_g(T_g)$ ) in Eq. (8)) is varied resulting in this wide range of values. Also calculations often deviate significantly. At room temperature few measurements are available such that values are dominated by model fitting.

The question that remains to be answered is on which values the various models for the band gap  $E_g$  are based upon, since there are very few measurements available. Our analysis revealed



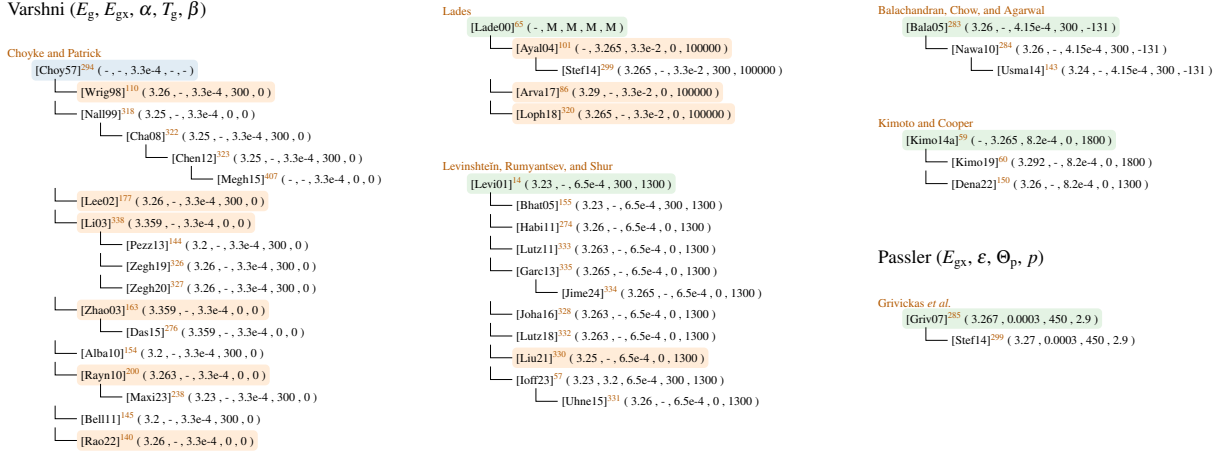


FIG. 13. Citations and the respective values for the temperature dependency.  entries indicate values that have not been determined for 4H-SiC,  are fundamental investigations and  connections predicted from the used values.

that it sounds to assume, that all the values currently in use go back to the investigations of  $E_{\text{gx}}$  by Choyke, Patrick, and Hamilton<sup>269</sup>, Choyke, Hamilton, and Patrick<sup>270</sup> in 1964. Already in 1970 Junginger and Van Haeringen<sup>301</sup> rounded the achieved values of  $E_{\text{gx}} = 3.263 \text{ eV}$  to  $E_g = 3.26 \text{ eV}$ . The same things were observed for the results from Choyke, Patrick, and Hamilton<sup>269</sup>, i.e.,  $E_{\text{gx}} = 3.263 \text{ eV}$ . Stunningly, not only the value was changed but the exciton band gap energy was turned into the band gap energy, completely neglecting the free exciton binding energy. In fact, the excitonic values are nowadays only encountered in sophisticated publications.

Zanmarchi<sup>271</sup> introduced in 1964 for the first time the value  $E_g = 3.23 \text{ eV}$ , which is also commonly used today. Due to missing data at that time it is reasonable to assume that it was derived based on low temperature measurements of the exciton band gap. Also  $E_g = 3.2 \text{ eV}$  seems to result from rounding  $E_g = 3.265 \text{ eV}$ . This was also achieved by Dubrovskii and Lepneva<sup>304</sup> who added the excitation band gap  $E_{\text{gx}} = 3.265 \text{ eV}$ <sup>263</sup> and  $E_x = 20 \text{ meV}$  to achieve  $E_g = 3.2 \text{ eV}$ . Solely for  $E_g = 3.25 \text{ eV}$  we have no clear explanation, but maybe it is simply the result of a typographical error when transferring  $E_g = 3.265 \text{ eV}$ .

The outcome of our analysis is thus, that it is possible that the room temperature band gap energies commonly used in literature go back to low temperature exciton band gap energy measurements six decades ago. The fact that Ahuja *et al.*<sup>8</sup> achieved the same value of  $E_g = 3.23 \text{ eV}$  as Zanmarchi<sup>271</sup> 60 years ago shows, that multiple avenues to a specific value are possible and thus such statements not easy to prove. Nevertheless, since we did not find any other derivations,

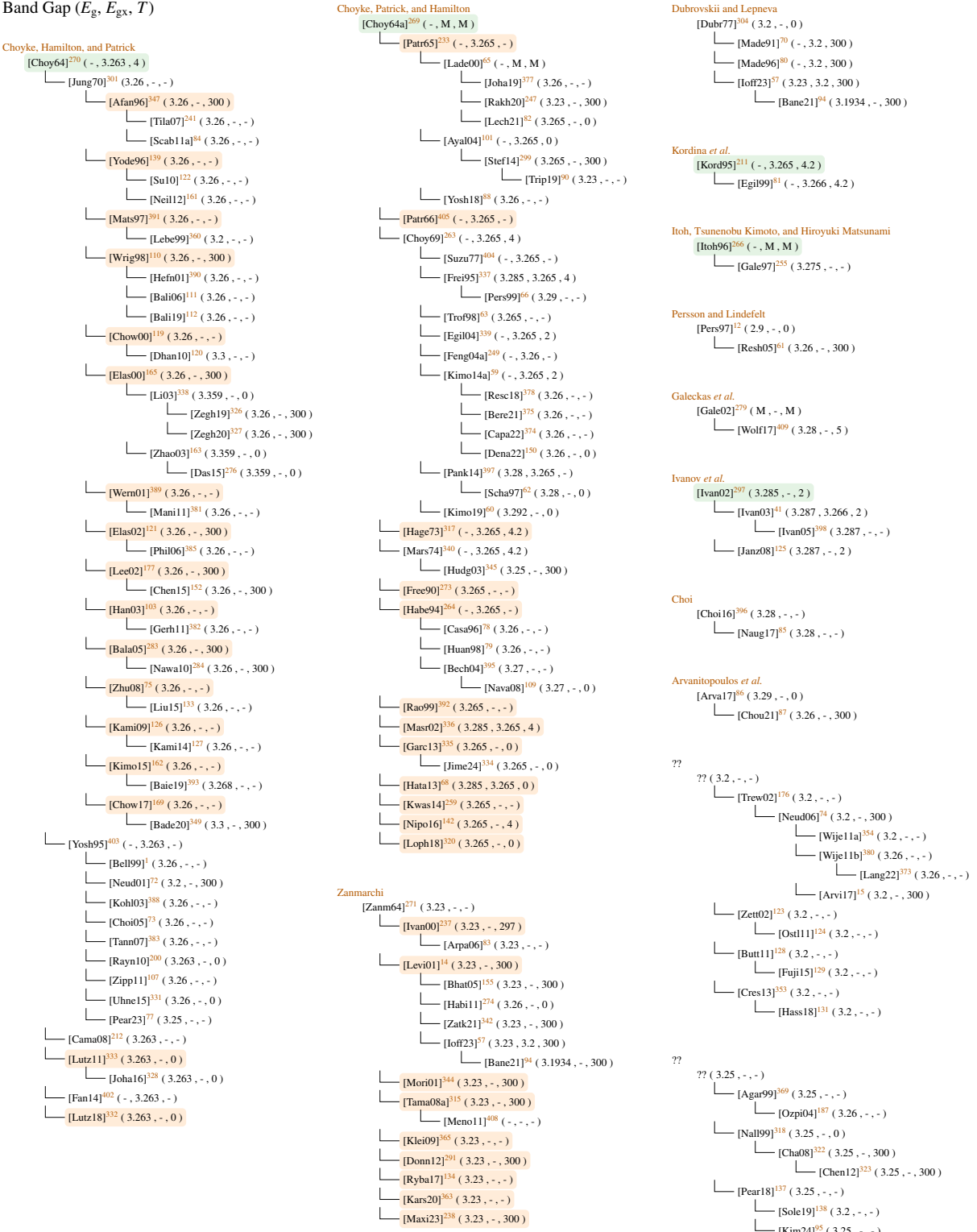


FIG. 14. Citations and values for band gap energies.  are fundamental investigations and  connections predicted from the used values. We collect publications that share the same value but that do not provide a reference under ??.

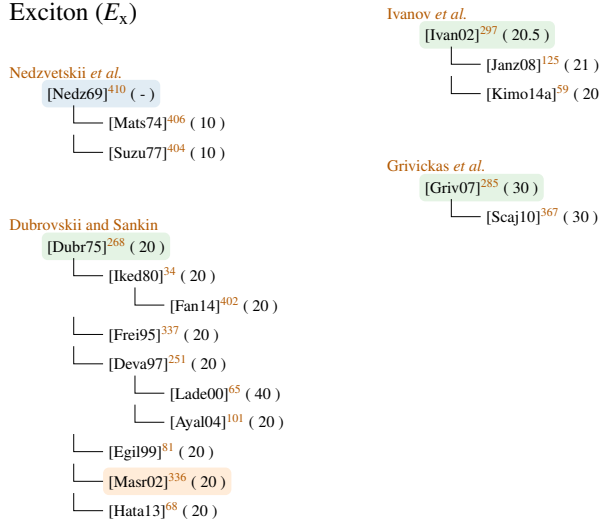


FIG. 15. Citations and values of the free exciton binding energy  $E_x$ . entries indicate values that have not been determined for 4H-SiC, are fundamental investigations and connections predicted from the used values.

we think that the chances that our hypothesis is true is quite high.

Aren't that horrifying news? Well, coincidentally recent measurements by Galeckas *et al.*<sup>279</sup> and Ahuja *et al.*<sup>8</sup> actually suggest that the band gap energy at 300 K is approximately 3.26 eV, whereat it has to be noted that the result by the latter have an uncertainty of 98 meV and thus have to be handled with care. To confirm that  $E_{gx}(0) \approx E_g(300)$  holds, additional verifications are required. In our opinion this also includes an investigation of  $E_x$  versus temperature, which is assumed constant at the moment. The newest models (see Fig. 9), however, suggest an increasing distance between the band gap energies.

An additional avenue for future research would be an investigation of the differences between measurements and calculations. If the latter achieve the actually more accurate results the band gap energy for 4H-SiC might need significant corrections.

#### IV. IMPACT IONIZATION

In high electric fields, charge carriers are able to pick up enough kinetic energy to create an additional electron-hole pair, which is called impact ionization. This effect is sometimes deliberately used, e.g., in avalanche diodes, to increase the responsiveness<sup>3</sup> but often is an undesired effect that leads to breakdown and the destruction of the device. Consequently, impact ionization

simulations are crucial to predict the safe operation regions of a device. In TCAD tools impact ionization is modeled as a (electric field dependent) multiplicative factor that denotes the increase of charge carriers per unit distance.

## A. Theory

The impact ionization is described by the charge carrier generation rate<sup>69,325</sup>

$$G_{II} = \frac{1}{q} (\alpha J_n + \beta J_p) = \frac{1}{q} (\alpha n v_n + \beta p v_p)$$

with  $n$  resp.  $p$  the amount of electron resp. holes,  $v_n$  resp.  $v_p$  their velocity and  $J_n$  resp.  $J_p$  the electron resp. hole current. The impact ionization coefficients for electrons ( $\alpha$ ) and holes ( $\beta$ ) represent the number of secondary carriers a single charge carrier generates per cm in an electric field  $F$ , i.e.,<sup>3</sup>

$$\alpha = \frac{1}{n} \frac{dn}{dx} 1/\text{cm} , \quad \beta = \frac{1}{p} \frac{dp}{dx} 1/\text{cm} .$$

Many models to describe  $\alpha$  and  $\beta$  were proposed. We will provide a short introduction to the topic, whereat more detailed descriptions are available in literature<sup>3,161,249,411,412</sup>. One of the earliest models is the still very popular empirical Chynoweth's law<sup>413,414</sup>

$$\alpha, \beta(F) = a \exp\left[-\frac{b}{F}\right] , \quad (20)$$

often also called Van Overstraeten-de Man model<sup>415</sup>. This empirical fitting was a necessity at the time of its publication because a physical explanation was only available for strong electric fields as<sup>416</sup>

$$\alpha, \beta(F) = \frac{eF}{E_i} \exp\left[-\frac{3E_p E_i}{(eF\lambda)^2}\right] .$$

This changed with Shockley<sup>417</sup> who modeled the impact ionization coefficient by

$$\alpha, \beta(F) = \frac{eF}{E_i} \exp\left[-\frac{E_i}{eF\lambda}\right] , \quad (21)$$

In this case,  $e$  denotes the electron charge,  $\lambda$  the mean free path and  $E_i$  the ionization energy, i.e., the energy to create an electron-hole pair. The prefactor is the inverse of the length required to gain the ionization energy, i.e., how often per unit length this energy is reached, while the exponential term denotes the chance of doing that without collisions. This model is often called Shockley's "lucky electron"<sup>418</sup>. In Lackner<sup>419</sup> the close relationship between Eq. (20) and Eq. (21), which can

be easily retraced by setting  $a = eF/E_i$  and  $b = E_i/e\lambda$ , is highlighted, leading to a physically based calculation of parameters  $a$  and  $b$ . The author suggests an additional scaling factor, depending on the electric field and the parameter  $b$  for both  $\alpha$  and  $\beta$ , to cover the parameter variations with changing electric field strength.

The low- and high-field cases were finally combined in Baraff's theory<sup>420</sup>, which expresses  $\alpha, \beta \propto \exp[-b/F]$  for low fields and  $\alpha, \beta \propto \exp[-c/F^2]$  for high ones. It was later extended by Thornber<sup>421</sup> to the expression<sup>411</sup>

$$\alpha, \beta(F) = \frac{eF}{\langle E_i \rangle} \exp \left[ -\frac{\langle E_i \rangle}{[(eF\lambda)^2/3E_p] + eF\lambda + E_{k_B T}} \right], \quad (22)$$

with  $\langle E_i \rangle$  the effective ionization threshold<sup>411</sup>,  $E_p$  the optical phonon energy and  $E_{k_B T}$  a temperature contribution that is often neglected in the literature. Konstantinov *et al.*<sup>418</sup> even only used the high-field part for the electrons and dropped the factor  $3E_p$  for the holes in the equation presented in the paper. We assume a typographical error as the division sign is still visible. For the ionization energy  $E_i$  originally a value of  $3/2E_g$  ( $E_g$  the band gap; see Section III) was assumed, which represents the ideal case<sup>167</sup>. Recent measurements, however, revealed for 4H-SiC values between 7.28 and 8.6 eV<sup>258</sup>.

Since Baraff's theory was not able to satisfy all demands<sup>422</sup>, Okuto and Crowell<sup>423</sup> extended Chynoweth's law by adding the electric field as a multiplicative factor, an exponential parameter  $m$  and a temperature dependency via  $c$  and  $d$ . The overall fitting model has the form

$$\alpha, \beta(F) = a\{1 + c(T - 300)\} F^n \exp \left[ -\left( \frac{b\{1 + d(T - 300)\}}{F} \right)^m \right] \quad (23)$$

where  $T$  denotes the temperature in Kelvin. In all investigated publications  $n = 0$  so we will not consider this parameter any further, leading to a simplified model that is often referred to as Selberherr model<sup>412</sup>.

More advanced models were also proposed, which are, however, not yet used in TCAD simulations. These include a more sophisticated temperature dependency in Eq. (23)<sup>424</sup> and models based on multi-stage<sup>425</sup> and inelastic collision events<sup>93</sup>. Other popular methods to investigate the effects of impact ionization are Monte Carlo simulations<sup>10,104–106,116,426–431</sup>, non-localized models<sup>432,433</sup> and the impact of defects<sup>434</sup> in the presence of a magnetic field<sup>435,436</sup>. Some researchers<sup>333,437,438</sup> even combine  $\alpha$  and  $\beta$  to an effective coefficient and model it by a power law, i.e.,  $\alpha, \beta \propto E^n$ , to achieve an analytic expression suitable for calculations.

The impact ionization is anisotropic, meaning that the breakdown field in  $\langle 11\bar{2}0 \rangle$  is about three quarters of the one in  $\langle 0001 \rangle$  direction<sup>439</sup>. For that reason the impact ionization coefficients have

been determined parallel and perpendicular to the c-axis. These can be combined, using a formalism introduced by Hatakeyama<sup>440</sup>, to achieve suitable amplification factors for any desired lattice direction. Jin *et al.*<sup>441</sup> reused the parameter values but introduced a new approach to calculate the "driving force" by considering also the field direction for constant carrier temperature. Nida and Grossner<sup>442</sup> adapted the field strength to an effective  $F^* = (m/m_{\parallel})^{1/2}F$ , with  $m$  resp  $m_{\parallel}$  the effective masses (see Section II).

To depict the changing behavior with temperature either the built-in parameters, as is the case for the Okuto-Crowell model (see Eq. (23)), or a multiplicative factor<sup>443</sup>

$$\gamma = \frac{\tanh\left(\frac{\hbar\omega_{\text{OP}}}{2k_B T_0}\right)}{\tanh\left(\frac{\hbar\omega_{\text{OP}}}{2k_B T_L}\right)} \quad (24)$$

to scale the parameters  $a$  and  $b$  of Eq. (20) is used<sup>65,101,318,440</sup> with  $T_0$  a reference temperature (often 300 K),  $T_L$  the lattice temperature and  $\omega_{\text{OP}}$  the optical phonon energy. We are very confident that the latter corresponds to the longitudinal optical phonon energy  $\omega_{\text{LO}}$  (see Section I) as their respective values match well. Hatakeyama<sup>440</sup>, however, pointed out that for a good fit  $\omega_{\text{OP}} = 190$  meV had to be used, which contradicts experimental results of  $\omega_{\text{LO}} = 120$  meV. Niwa, Suda, and Kimoto<sup>444</sup> use a polynomial of degree two to scale the parameters while Bartsch, Schörner, and Dohnke<sup>437</sup> utilize the ratio  $T/300$  K for this purpose. In contrast, Hamad *et al.*<sup>445</sup> explicitly present parameter values for different temperatures. Nida and Grossner<sup>442</sup> scaled the mean free path by  $\sqrt{\gamma}$  and the ionization energy by the ratio of the bandgap at temperature  $T_L$  and at 300 K.

## B. Results

To measure the impact ionization coefficients an equal amount of charge carriers is generated in a space charge region, either by (pulsed) electron (electron beam induced current (EBIC))<sup>448</sup> or optical beams (optical beam induced current (OBIC))<sup>418,444,445,449–455</sup>. Defects have a significant impact on the coefficients such that EBIC is used to extract parameters at defect-free regions<sup>112</sup>.

The charge carrier generation is executed at varying field strengths. Recording the respective terminal currents enables a comparison against the no-field current and, thus, the determination of the effective amplification. The readout of the current can be executed in DC mode<sup>418,449</sup> (whereat Raghunathan and Baliga<sup>448</sup> state that elimination of leakage current in this case is hard), AC mode<sup>448,452,453</sup> or both combined<sup>450,451</sup>. Additional challenges are the selection of a suitable

test structure, e.g., p-n/n-p diodes or pnp/npn transistors) and the proper separation of electron and hole multiplication phenomena, which we will not further cover in this review. Instead we refer the interested reader to the dedicated literature<sup>418,444,452,454,456,457</sup>.

Monte Carlo simulations are also used for the investigation of the impact ionization. While some are able to extract the impact coefficients as the reciprocal of the average distance<sup>431,458</sup> others solely present simulated values without fitting to any of the earlier presented model<sup>10,104–106,116,426–430,459</sup>. Fitting is, however, crucial to use the results in TCAD simulations tools. For this purpose Stefanakis *et al.*<sup>460</sup> provides fittings to Monte Carlo simulation<sup>116,461</sup>, Nouketcha *et al.*<sup>167</sup> used a genetic algorithm to fit to multiple sources<sup>442,449–451,462,463</sup>, Nida and Grossner<sup>442</sup> fitted their model to values from<sup>418,440,448,450,462</sup> and Stefanakis *et al.*<sup>460</sup> achieved a "global fit" in regard to many 4H investigations<sup>418,450,451,453,455,463</sup>, but also a 6H one<sup>292</sup>, and Monte Carlo simulations<sup>116,461</sup>. Kyuregyan<sup>456</sup> calculated the average of available parameter values without conducting any fitting. According to the authors this is supposed to remove statistical inaccuracies and uncertainties introduced by the characterization methods. Even multiple fittings on the same data were executed. Choi *et al.*<sup>73</sup>, Banerjee<sup>94</sup>, Baliga<sup>112</sup>, Zhao *et al.*<sup>163</sup>, Morisette<sup>344</sup>, Sheridan *et al.*<sup>464</sup> all used the data from Konstantinov *et al.*<sup>418</sup>, however, the ones for Sheridan *et al.*<sup>464</sup> exactly match values achieved for 6H by Ruff, Mitlehner, and Helbig<sup>292</sup>.

TABLE IX. Parameters for fundamental fittings of the Okuto-Crowell model found in literature. If only a single value spanning across two columns is presented the crystal direction was not specified.

ref.	electron							hole							$F$ region
	$a_{\parallel}$	$a_{\perp}$	$b_{\parallel}$	$b_{\perp}$	$c$	$d$	$m$	$a_{\parallel}$	$a_{\perp}$	$b_{\parallel}$	$b_{\perp}$	$c$	$d$	$m$	
	[ $10^6/\text{cm}$ ]	[MV/cm]	[ $10^{-3}$ ]	[ $10^{-3}$ ]	[1]			[ $10^6/\text{cm}$ ]	[MV/cm]	[ $10^{-3}$ ]	[ $10^{-3}$ ]	[1]			[MV/cm]
[Ragh99] <sup>448</sup>	-	-	-	-	0	0	1	3.09		$17.9 \pm 0.4$		-3.46	0	1	2.5–3.2
[Bert00] <sup>465j</sup>	0.4	48	15		0	0	1.15	1.8	45	15		0	0	1	-
[Sher00] <sup>464dl</sup>	-	-	-	-	0	0	1	5.18	-	14	-	0	0	1	-
[Mori01] <sup>344d</sup>	-	-	-	-	0	0	1	-	-	-	-	0	0	1	-
[Ng03] <sup>451</sup>	1.98		9.46	-2.02 <sup>a</sup>	0	1.42		4.38		11.4	-0.913 <sup>a</sup>	0	1.06		1.8–4
[Zhao03] <sup>163d</sup>	7.26		23.4	0	0	1		6.85		14.1	0	0	0	1	-
[Hata04] <sup>466</sup>	176	21	33	17	0	0	1	341	29.6	25	16	0	0	1	2–5
[Choi05] <sup>73d</sup>	16.5		25.8	0	0	1		5.5		13.5	0	0	0	1	1.5–5
[Loh08] <sup>450</sup>	2.78		10.5	0	0	1.37		3.51		10.3	0	0	0	1.09	1–5
[Loh09] <sup>467</sup>	-	-	-	-	0	0	1	3.321		10.385	-2.78	0.48 <sup>k</sup>	1.09		1.33–2
[Nguy11] <sup>452</sup>	0.46		17.8	0	0	1		15.6		17.2	0	0	0	1	1.5–2.7
[Gree12] <sup>457h</sup>	0.019		2.888	0	0	4.828		0.06		1.387	0	0	0	0.96	1.6–4
[Nguy12] <sup>453</sup>	3.36		22.6	0	0	1		8.5		15.97	0	0	0	1	1.5–4.8
[Sun12] <sup>431</sup>	1.803		13.52	0	0	1.2		1.861		9.986	0	0	0	1.11	1.5–5
[Niwa14] <sup>444</sup>	8190		39.4	0	0	1		4.513		12.82	0 <sup>f</sup>	0	0	1	1.4–2.7
[Hama15] <sup>445</sup>	0.99		12.9	0	0	1		1.61		11.5	0	0	0	1	2.5–7
[Niwa15] <sup>462</sup>	0.143	-	4.93	-	0 <sup>e</sup>	0 <sup>e</sup>	2.37	3.14	-	11.8	-	6.3 <sup>c</sup>	1.23 <sup>c</sup>	1.02	1–2.8
[Shar15] <sup>468</sup>	186	-	28	-	0	0	1	301	-	20.5	-	0	0	1	-
[Kyur16] <sup>456i</sup>	$38.6 \pm 15.0$		$25.6 \pm 0.1$	0	0	1		$5.31 \pm 0.30$		$13.10 \pm 0.01$	0	0	0	1	1–5
[Zhan18] <sup>469</sup>	1.31		13	-1.47	0	1		2.98		13	-1.56	0	1		-
[Bali19] <sup>112d</sup>	313		34.5	0	0	1		8.07		15	0	0	0	1	1.1–5
[Zhao19] <sup>455</sup>	0.339	-	5.15	-	0	0	2.37	3.56	-	11.7	-	6.19	1.15	1.02	1–3.2
[Stef20] <sup>454</sup>	-	6.4	-	12.5	0	0	1	-	6	-	13.3	0	0	1	1.3–2
[Bane21] <sup>94d</sup>	100		40.268	0	0	1		41.915		46.428	0	0	0	1	0.1–1
[Chea21] <sup>458g</sup>	0.932		7.19	0	0	1.95		1.75		6.56	0	0	0	1.45	1.6–10
[Stef21] <sup>460e</sup>	2.8	-	20.7	-	-1 <sup>b</sup>	-0.29 <sup>b</sup>	1	2.5	-	12.1	-	1.74 <sup>b</sup>	0.59 <sup>b</sup>	1	-

<sup>a</sup> provided by Cha *et al.*<sup>470</sup>

<sup>b</sup> provided by Steinmann *et al.*<sup>471</sup>

<sup>c</sup> different values suggested by Steinmann *et al.*<sup>471</sup>

<sup>d</sup> values fitted to Konstantinov *et al.*<sup>418</sup>

<sup>e</sup> values fitted to<sup>116,292,418,450,451,453,455,461,463</sup>

<sup>f</sup> temperature dependency stated in the paper that could not be transferred to model formalism

<sup>g</sup>  $a$  and  $b$  presumably stated in 1/m and MV/m in paper, converted to 1/cm and MV/cm

<sup>h</sup> for  $F > 2.5$  MV/cm the parameters  $\alpha$  from Ng *et al.*<sup>451</sup> are used

<sup>i</sup> values achieved by averaging of<sup>368,418,444,449–451,457,467</sup>

<sup>j</sup> fitted to Nilsson *et al.*<sup>115</sup>

<sup>k</sup> we changed  $b = 8.9 \times 10^6 - 4.95 \times 10^3 T$  to  $b = 8.9 \times 10^6 + 4.95 \times 10^3 T$  to better match the results in the paper

<sup>l</sup> same values achieved as 6H investigation by Ruff, Mitlehner, and Helbig<sup>292</sup>

TABLE X. Parameters for fundamental fittings of the Thurnber model found in literature. For  $E_{k_B T} = k_B T$  this parameter scales with temperature.

ref.	dir	electron				hole				$F$ region
		$\langle E_i \rangle$ [eV]	$\lambda$ [Å]	$E_p$ [meV]	$E_{k_B T}$ [meV]	$\langle E_i \rangle$ [eV]	$\lambda$ [Å]	$E_p$ [meV]	$E_{k_B T}$ [meV]	
[Kons97] <sup>418f</sup>		10	29.9	120	0	7	32.5	120	0	1.5–10
[Nida19] <sup>442a</sup>		10.61	27	120	$k_B T$	10.87	39.49	85	$k_B T$	1–10
[Nouk20] <sup>167c</sup>	-	7.5	10	92.5	14	6.62	4.8	9	102	0.9–10
[Stei23] <sup>471e</sup>	-	10.6	27	87	$k_B T$	10.9	80	87	$k_B T$	1–10

<sup>a</sup> values picked from specified ranges, fitting to<sup>418,440,448,450,462</sup>

<sup>c</sup>  $3/2 E_g$  instead of  $\langle E_i \rangle$  used in the exponential, fitting to<sup>442,449–451,462,463</sup>

<sup>e</sup> initial values taken from Nida and Grossner<sup>442</sup>

<sup>f</sup> linear term in denominator not used for  $\alpha$

A wide range of Okuto-Crowell (see Table IX) and Thornber (see Table X) model parameters could be identified in literature. In one case we were unable to match the temperature variation of  $\beta$  with  $b = 8.9 \times 10^6 - 4.95 \times 10^3 T^{467}$  with the data presented in the same publication. We achieved much better results with  $d = 8.9 \times 10^6 + 4.95 \times 10^3 T$  with  $T$  the temperature in Kelvin. In Stefanakis *et al.*<sup>454</sup> the fitting for  $\alpha$  also deviates slightly from the plots in the paper. Due to the minor deviation we kept the values as they were. In Cheang, Wong, and Teo<sup>458</sup> the values of parameters  $a$  and  $b$  are two orders of magnitude too high. We suspect that they are specified in 1/m resp. MV/m although in the paper it is explicitly stated as 1/cm resp. MV/cm. Despite these changes we were not able to exactly recreate the plots shown in the paper. We had to exclude the publication by Ng *et al.*<sup>368</sup> as no data are shown in the paper and Cheong *et al.*<sup>447</sup>, Kimoto *et al.*<sup>472</sup> who only specify that SiC is investigated but not the polytype.

A graphical representation of the models describing the impact ionization coefficient for electrons (see Fig. 16) show a spread of approximately one order of magnitude, whereat the deviations increase for low fields. For the crystal direction perpendicular to the c-axis much higher values are determined. This matches qualitatively early estimations, however, the quantities of  $\alpha_\perp/\alpha_\parallel = 3.5$  used by Lades<sup>65</sup>, Bakowski, Gustafsson, and Lindefelt<sup>69</sup> seems to be too low. For low resp. high fields the fittings of Zhang and You<sup>469</sup> resp. Sharma, Hazdra, and Popelka<sup>468</sup> are too high meaning that the models have to be handled with care in these regions.

For holes (see Fig. 17) the spread in values is much smaller, especially close to a field strength

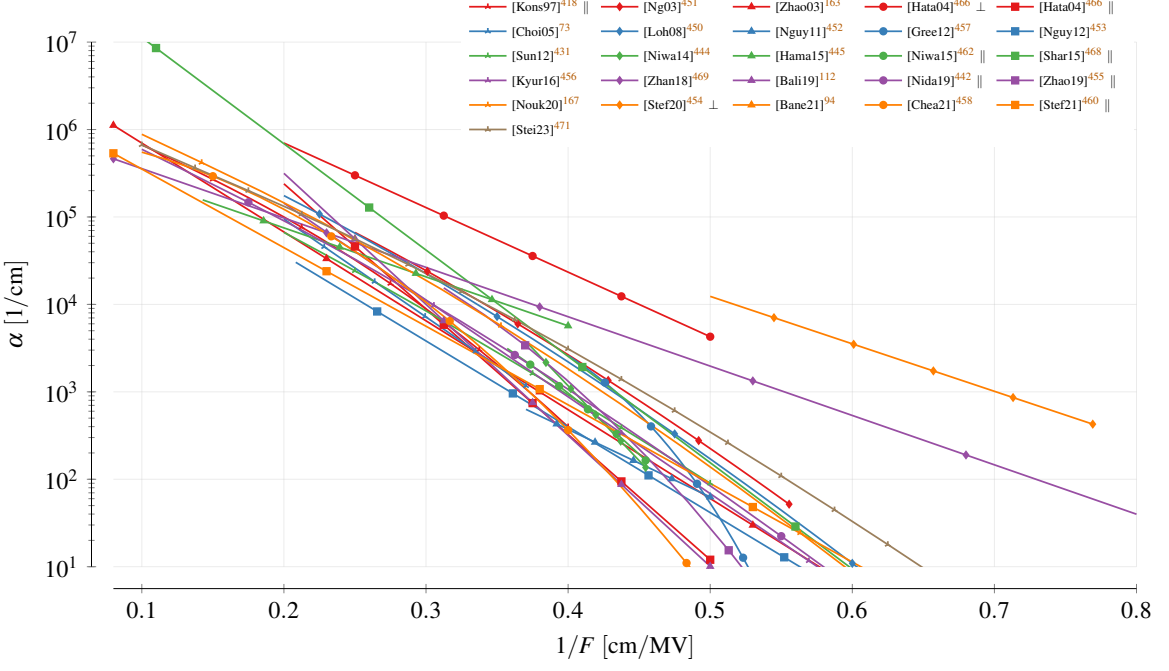


FIG. 16. Impact ionization coefficient  $\alpha$  for electrons. Each model is limited to the interval used for characterization. The colors are altered to increase the readability.

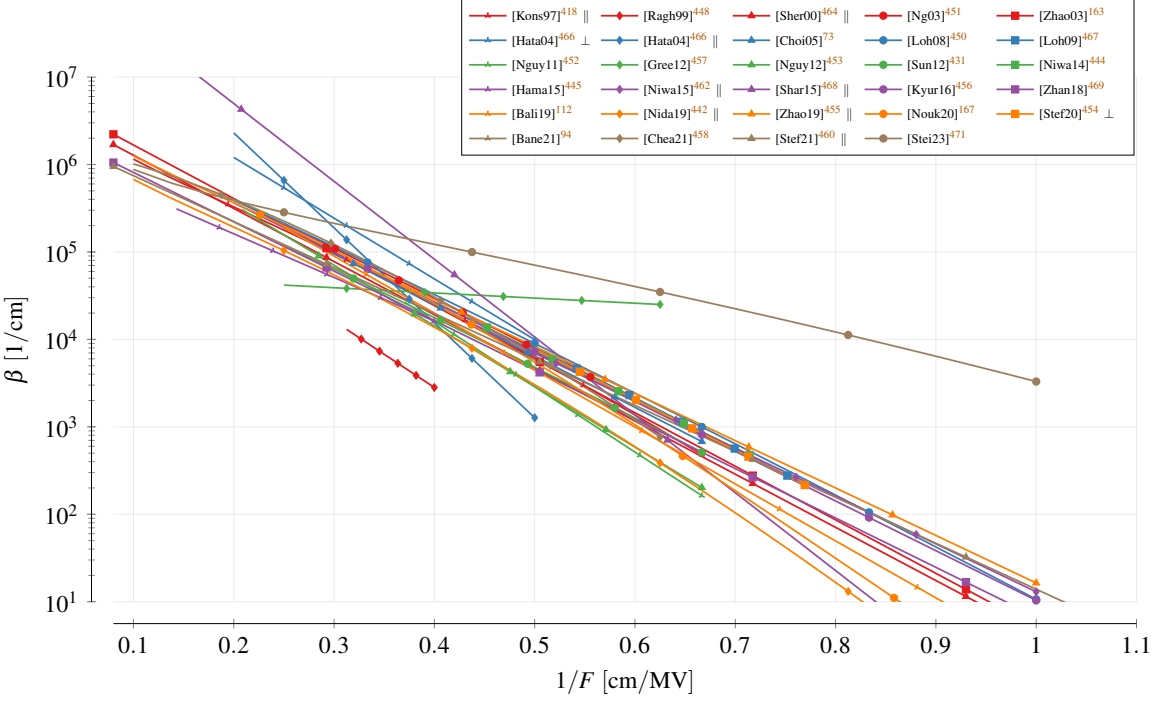


FIG. 17. Impact ionization coefficient  $\beta$  for electrons. Each model is limited to the interval used for characterization. The colors are altered to increase the readability.

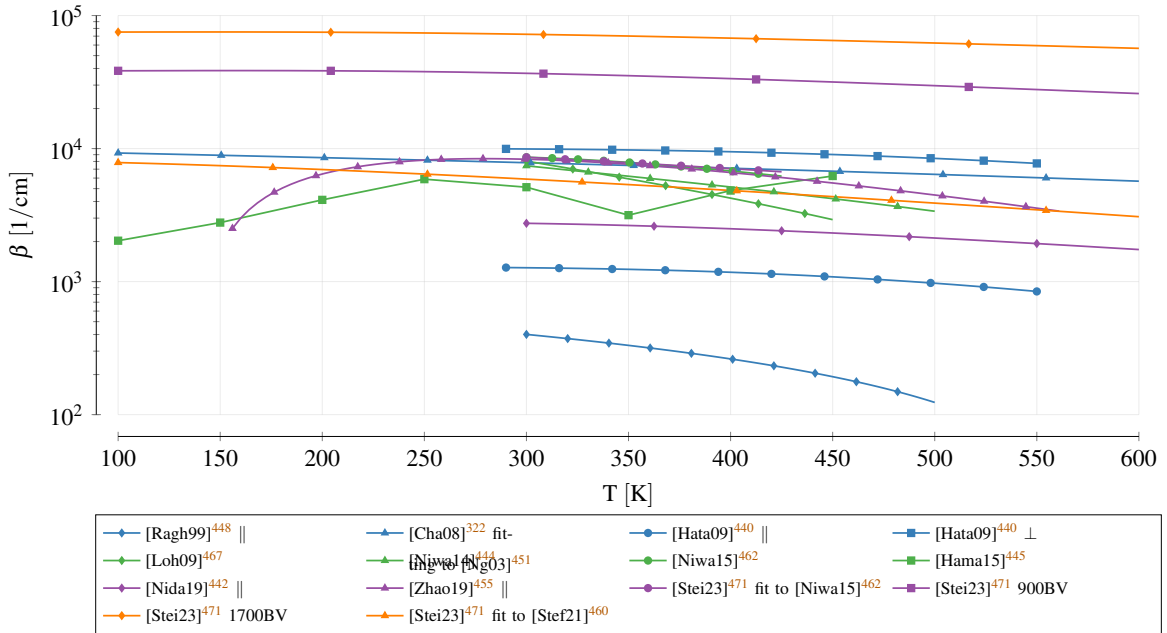


FIG. 18. Temperature dependence of the hole impact ionization coefficient. The single models are evaluated for an electric field of 2 MV/cm and are ordered according to their publication date. The colors simply are used to improve the readability.

around 2 MV/cm. Nevertheless, there are also fittings we want to highlight. The results of Steinmann *et al.*<sup>471</sup> are too high possibly correlating to the fitting of a rather high breakdown voltage. The values from Raghunathan and Baliga<sup>448</sup> are too low, which was attributed to the direction dependency of  $\alpha$ <sup>249,465</sup>, i.e., that the coefficient in the direction perpendicular to the c-axis is much stronger. Feng and Zhao<sup>249</sup> thus conclude that the results in<sup>448</sup> deviate from practical results since the focused beam used in the analyses caused them to miss a large share of the intrinsic defects. Although Fig. 17 supports this statement, the statement that the perpendicular impact ionization of holes is a lot stronger, could not be confirmed. The results suggest rather  $\beta_{\perp} = \beta_{||}$ , which was also used for 6H<sup>69</sup>. Finally, the fittings by Green *et al.*<sup>457</sup> show a significantly slower increase with field than all other models.

Important for TCAD simulations is also the temperature dependency of the impact ionization coefficients. For holes (see Fig. 18) all models predict a decreasing value, which matches the reports of increasing breakdown voltage with increasing temperature<sup>322,473</sup> and prevents thermal runaway. Hatakeyama<sup>440</sup> uses the temperature scaling shown in Eq. (24) (multiplication with  $\gamma$ ), which is also used by Lades<sup>65</sup>, Schröder<sup>146</sup>. Clearly visible is the decline of  $\beta$  with increasing temperature. Steinmann *et al.*<sup>471</sup> proposed two fittings for two different breakdown voltages of

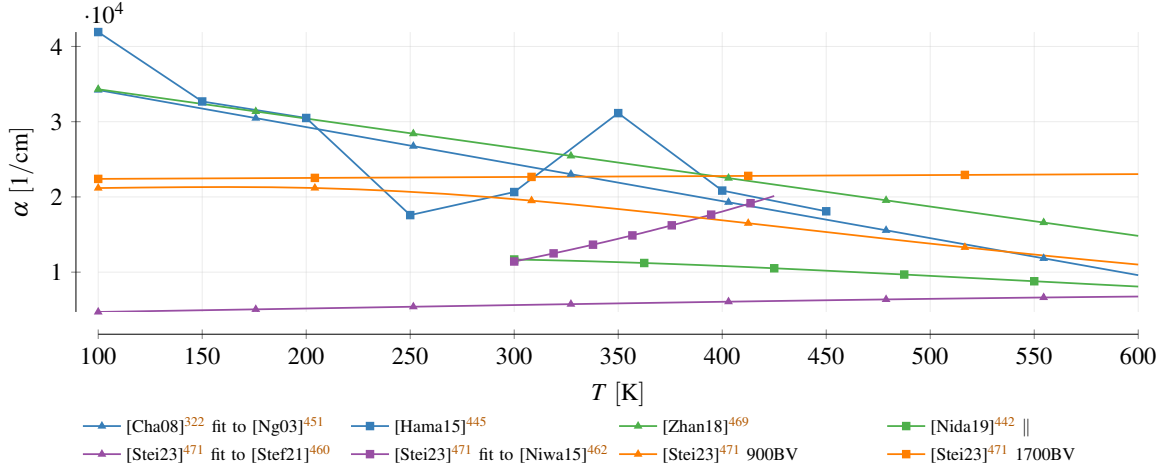


FIG. 19. Temperature dependence of the electron impact ionization coefficient. The single models are evaluated for an electric field of 3.33 MV/cm and are ordered according to their publication date. The colors simply are used to improve the readability.

the investigated device, i.e., 900 V and 1700 V.

For electrons (see Fig. 19) the results are quite inconclusive. Some models even propose an increase of  $\alpha$  with temperature. This is, however, compensated by the decrease in  $\beta$  with increasing temperature due to the relatively small variations of  $\alpha$  compared to  $\beta$  (linear vs. logarithmic y-axis).

### C. Discussion

The majority of the currently utilized impact ionization coefficients are based on 4H measurements (see Fig. 20). Care has to be taken especially for publications prior to the year 2000, as those often are based on 6H<sup>69,292,474,475</sup>. These outdated results have later found their way in various publications<sup>65,110,155,159,161</sup>. In early publications<sup>69</sup> 6H was still used because 4H values were not available or simply<sup>163,476</sup> because the early available fittings from Konstantinov *et al.*<sup>449</sup>, Raghunathan and Baliga<sup>463</sup> deviated significantly. The results from Bakowski, Gustafsson, and Lindefelt<sup>69</sup> were later further changed by Lades<sup>65</sup> who calculated the parameters at 273 K and introduced a typographical error for the hole coefficient  $a$ , which was stated as  $2.24 \times 10^6$ /cm instead of  $3.24 \times 10^6$ /cm. We found additional more or less critical inaccuracies, which we all summarize in ??.

The most influential publications are arguably by Raghunathan and Baliga<sup>448,463</sup> and Hatakeyama

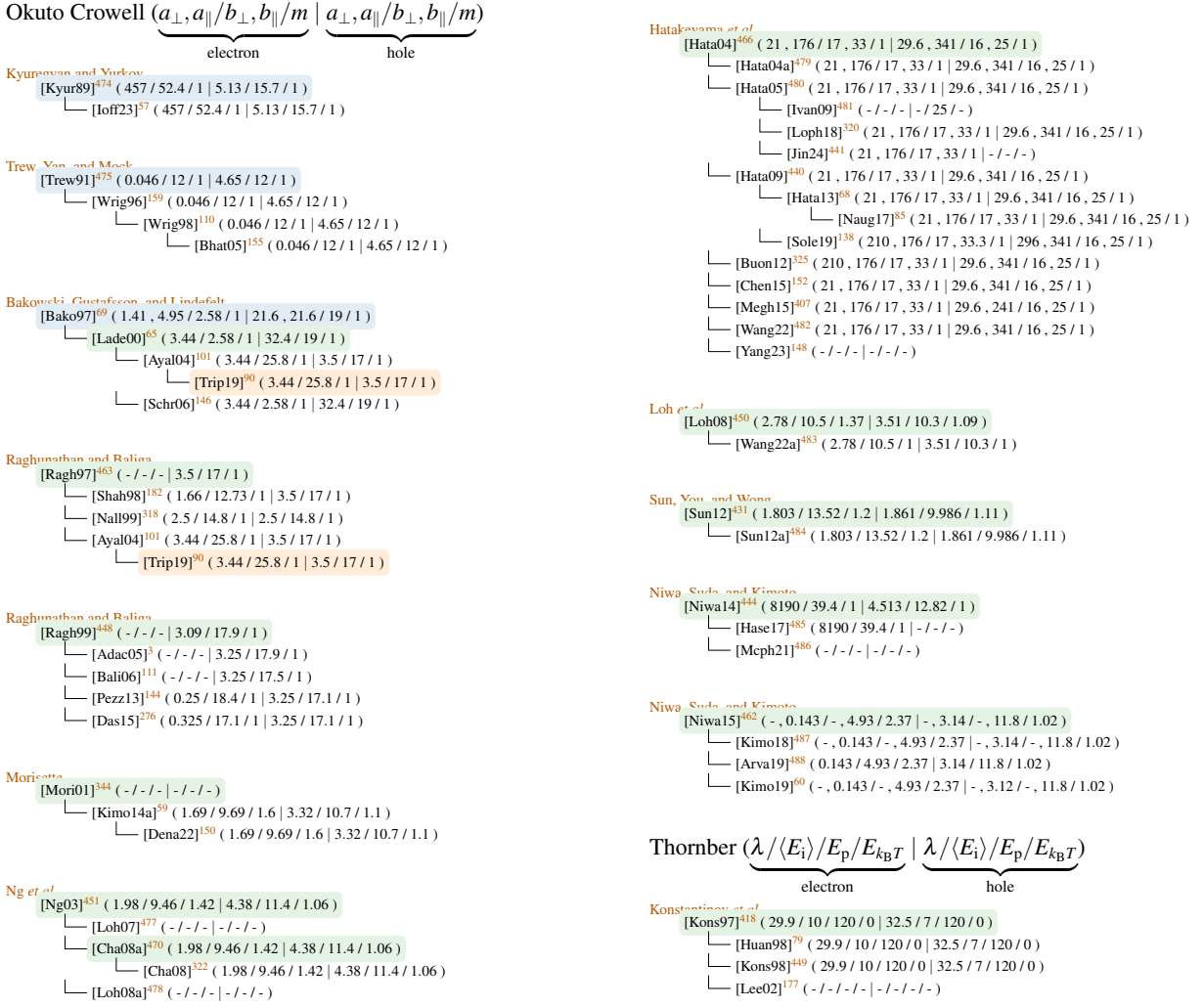


FIG. 20. Reference chain for impact ionization parameters. Publications with blue background are not focused on 4H-SiC, those in green are novel analyses on 4H-SiC and orange color indicates that the reference was guessed based on the values but not explicitly stated in the publication. The values for  $a$  and  $b$  were scaled by  $1 \times 10^6$  for improved readability.

*et al.*<sup>466</sup>. However, twelve investigations in the last decade indicate that impact ionization is still an active area of research. Nevertheless, only few values for the impact ionization perpendicular to the c-axis are available. Since the available parameters suggest a higher multiplication and thus earlier breakdown in these directions, further in detail investigations are required in the future.

In contrast to Silicon, 4H-SiC shows higher hole than electron current amplification, i.e.,  $\beta > \alpha$ <sup>3,180</sup>, which is attributed to discontinuities in the electron spectrum<sup>160</sup>. Consequently, the Shockley approximation of the "lucky electron" can only be applied to holes, as the electrons

energy can not continuously increase<sup>418</sup>. Kimoto *et al.*<sup>487</sup> name these "minigaps" as the reason for the low temperature dependence of  $\alpha$ . Temperature analyses are, however, sparsely available. Some of the available data were years after the original publication proposed by other authors, e.g., by Cha and Sandvik<sup>322</sup> or by Steinmann *et al.*<sup>471</sup>, who fitted the linear and quadratic temperature coefficients of the breakdown voltage. Nida and Grossner<sup>442</sup> present the high temperature evolution of some models.

Although models can be used for any arbitrary field strengths, they are most accurate within their often very narrow characterization range. In general, the highest accuracy is required around the critical electric field, i.e., where breakdown occurs. In the literature commonly 2–3 MV/cm<sup>23,72,103,121,123,137,139,389,490</sup> are used, whereat some explicitly state a dependence on the doping concentration<sup>60,112,333,348,390,418,439,448,455,462,487,491–493</sup>. Be advised that these values are, most commonly, determined for uniformly doped non-punch through diodes using power law approximations of the impact coefficients<sup>448</sup>. Consequently such values have to be interpreted with a grain of salt and have to be corrected according to the actual structure and doping level<sup>462,494</sup>. Over short distances a higher field is required to achieve breakdown than for thick devices, where charges can multiply over long distances.

## V. CHARGE CARRIER RECOMBINATION

In a semiconductor electron-hole pairs are continuously created, for example due to thermal processes, adding additional charge carriers. Their concentration is denoted as excess carrier  $\Delta_N$ , non-equilibrium, generated<sup>495,496</sup> or solely carrier concentration<sup>252</sup>. Simultaneously to the generation, electron-hole pairs also recombine, such that the rate of change can be described as shown in Eq. (25)<sup>497–499</sup>.

$$\frac{d\Delta_N}{dt} = D \frac{d^2\Delta_N}{dx^2} - R + G \quad (25)$$

The first term denotes the diffusion of charge carriers ( $D$  equals the ambipolar diffusion coefficient),  $R$  the recombination and  $G$  the generation rate. One of the effects accounting to the latter is impact ionization, which we already investigated in Section IV, or optical generation. In equilibrium, all the contributions compensate and the net change is zero.

In TCAD simulations it is essential to correctly model the localized change in charge carrier concentration, as it influences, among others, the conductivity and the internal electric fields. In this section we are, thus, going to review the relevant charge carrier recombination mechanisms

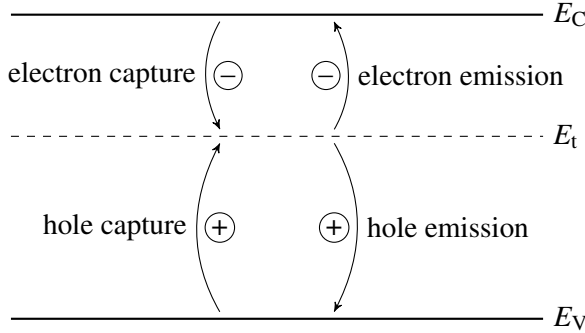


FIG. 21. Capture and emission of charge carriers described by  $R_{\text{SRH}}$ .  $E_t$  denotes the trap level energy.

in 4H-SiC. The time between two recombination events depends on several parameters that have to be clearly distinguished. Partially, the values are very sample depend and thus a wide range of values were found in the literature.

### A. Theory

The decay of excess charge carriers towards the equilibrium value is described by the recombination rate  $R^{500}$ . It can be written as shown in Eq. (26)<sup>243,367,498,501,502</sup> where  $R_{\text{SRH}}$  denotes the trap-assisted Shockley-Read-Hall,  $R_{\text{bim}}$  the bimolecular and  $R_{\text{Auger}}$  the Auger recombination rate<sup>255</sup>.

$$\begin{aligned} R &= R_{\text{SRH}} + R_{\text{bim}} + R_{\text{Auger}} \\ &= \frac{\Delta_N}{\tau_{\text{SRH}}} + \frac{\Delta_N}{\tau_{\text{bim}}} + \frac{\Delta_N}{\tau_{\text{Auger}}} = \frac{\Delta_N}{\tau_r} \end{aligned} \quad (26)$$

In the second line an alternative representation using lifetimes  $\tau_x$  is shown<sup>154</sup>, which denote the average time between two recombination events. The single contributions to the recombination will be shortly investigated in the sequel. For a more comprehensive description the interested reader is referred to the dedicated literature<sup>171,260,501,503</sup>.

#### 1. Shockley-Read-Hall Recombination

The term  $R_{\text{SRH}}$  denotes the successive capturing of a hole and an electron in a trap level with energy  $E_t$  inside the band gap<sup>501,504</sup>, sometimes also called monomolecular recombination<sup>255</sup>. Due to the lower energy difference between trap and energy bands compared to the overall band

gap, the transition of a charge carrier to a trap is much more likely than a band-to-band transition. To describe this process in detail specific terms have been proposed in literature (see also Fig. 21)<sup>505–507</sup>: *electron capture* denotes the transition of an electron from the conduction band into the trap while *electron emission* describes the reverse process. Similarly, during *hole capture* a hole rises from the valence band to the trap level, i.e., an electron drops from the trap into the valence band. *Hole emission* denotes the reverse case. Overall, during any capture process the electron loses energy, while during emission it gains some. In this context the electron/hole *capture cross sections* are used to quantify the possibility for an electron/hole capture.

The excessive energy released/consumed during these transitions is exchanged with lattice vibrations<sup>501</sup>, whereat different phonon interactions are distinguished, e.g., multi- or cascade-phonon interaction<sup>503,508</sup>. Among these the capture cross section and their respective temperature dependencies differ<sup>506</sup>.

The recombination rate  $R$  heavily depends on the material quality<sup>501</sup>. Certain defects, e.g., impurities or damages in the lattice, are very effective "lifetime killers"<sup>509</sup>, meaning that they increase the recombination rate significantly. Lots of effort is undertaken to refine growth conditions to achieve cleaner samples and, thus, higher lifetimes<sup>243,510–528</sup>. The recombination rate even varies across a single wafer. Typically it is smallest in the middle where the best growth conditions are available<sup>512,525,527,529–539</sup>, but also in thick 4H-SiC layers variations were reported<sup>540</sup>. In fact, the recombination rate decreases at structural defect positions<sup>541</sup> but increases inversely linear with temperature<sup>542–544</sup>.

For an accurate description of  $R_{\text{SRH}}$  detailed information, i.e., energy level, type (acceptor or donor) and cross section of the defects in the device are required. Many investigations in regard to these parameters have been published<sup>9,13–15,23,24,34,41,49–51,53,57,59–63,65,68–70,72,74–77,81,86,88,90,101,104,107,111,123,124</sup>, making a comprehensive analysis within this review infeasible. Instead, we refer the interested reader to an analysis by Gaggl *et al.*<sup>612</sup>, who investigated defects in 4H-SiC. In regard to recombination, the most important ones are called  $Z_{1/2}$  and  $\text{EH}_{6/7}$ <sup>604,610,613,614</sup> and, presumably, denote different charge states of a carbon vacancy<sup>553</sup>.

The trap-assisted recombination can be split into the recombination in the bulk ( $R_{\text{SRH}}^{\text{b}}$ ) and on the surface ( $R_{\text{SRH}}^{\text{s}}$ ). Both occur simultaneously and are therefore often hard to separate<sup>501,615</sup>. In the sequel we are going to investigate these in more detail.

*a. Bulk Recombination Rate* The Shockley-Read-Hall recombination of the bulk was mathematically first described by Shockley and Read<sup>505</sup>, Hall<sup>616</sup> as shown in Eq. (27)<sup>86,260,333,412,505,507,616</sup>.

$$R_{\text{SRH}}^{\text{b}} = \frac{np - n_i^2}{\tau_p(n + n_1) + \tau_n(p + p_1)} \quad (27)$$

$$n_1 = \frac{1}{g_t} N_C \exp\left(-\frac{E_C - E_t}{k_B T}\right) \quad (28)$$

$$p_1 = g_t N_V \exp\left(-\frac{E_t - E_V}{k_B T}\right) \quad (29)$$

$$n_i = \sqrt{n_1 p_1} = \sqrt{N_C N_V} \exp\left(-\frac{E_C - E_V}{2k_B T}\right) = \sqrt{N_C N_V} \exp\left(-\frac{E_g}{2k_B T}\right) \quad (30)$$

$$\tau_{n,p} = (\sigma_{n,p} v_{\text{th}} N_t)^{-1} \quad (31)$$

Here,  $n_i$  denotes the intrinsic carrier concentration,  $\tau_{n,p}$  the electron resp. hole lifetime,  $\sigma_{n,p}$  the electron resp. hole cross section,  $N_t$  the trap concentration,  $v_{\text{th}} = \sqrt{3k_B T/m_d^*}$ <sup>203,507</sup> the thermal velocity and  $g_t$  the trap degeneracy factor, which is often neglected as they are usually one<sup>325</sup>.  $E_t$  denotes the trap energy level, whereat Shockley and Read<sup>505</sup> stated that this is actually an effective energy level that is derived from the actual one by considering the degeneracies of the empty ( $w_p$ ) and full ( $w$ ) trap, i.e.,  $E_t = E_t(\text{true}) + k_B T \ln(w_p/w)$ . In TCAD tools either the lifetimes  $\tau_{n,p}$  or the cross sections  $\sigma_{n,p}$  can be provided as input, however, none of the investigated tools allows to specify the degeneracy factor at the moment.

It is also possible to define  $p_1$  and  $n_1$  as shown in Eq. (32)<sup>154,177,508</sup>, i.e., by using the intrinsic carrier concentration and an effective Fermi level  $E_i$ , which must not be confused with the intrinsic Fermi level  $E_F$  used to calculate the actual carrier concentration  $n = N_C \exp[(E_F - E_C)/k_B T]$  and  $p = N_V \exp[(E_V - E_F)/k_B T]$ . Care has to be taken in this case as the intrinsic carrier concentration  $n_i$  changes with the doping concentration due to band gap narrowing effects (see Section III).

$$\begin{aligned} n_1 &= \frac{1}{g_t} n_i \exp\left(-\frac{E_t - E_i}{k_B T}\right) \\ p_1 &= g_t n_i \exp\left(-\frac{E_i - E_t}{k_B T}\right) \end{aligned} \quad (32)$$

The SRH carrier lifetime is not constant but depends on the temperature and doping concentration  $N_{A,D}$ <sup>617</sup>. The latter describes the increase of lattice defects, i.e., recombination centers, that accompany the doping process<sup>412</sup> and has to be clearly distinguished from the excess carrier concentration  $\Delta_N$ . The reduction of the lifetime can be described for each charge carrier separately using the empirical Scharfetter relation<sup>86,145,292,412,508,618–622</sup> shown in Eq. (33). A more detailed analysis on the change of the lifetime for various relations of donor and acceptor concentrations

was recently provided by Shao *et al.*<sup>623</sup>. We want to highlight that dopants (see Section VI) themselves are a special form of defects, i.e., recombination centers, whose impact on the recombination can be described also with Eq. (27)<sup>247</sup>.

$$\tau = \frac{\tau_{\max}}{1 + \left(\frac{N_A + N_D}{N_{\text{ref}}}\right)^{\gamma}} \quad (33)$$

It is also common practice to determine the reduced lifetime in a more simplistic fashion from the defect concentration, e.g.,  $\tau(\mu\text{s}) = 1.5 \times 10^{13}/N_{\text{VC}}$ <sup>613,624</sup> and  $\tau(\mu\text{s}) = 1.8 \times 10^{13}/N_{\text{VC}}$ <sup>487</sup> for carbon vacancies, and  $\tau(\mu\text{s}) = 1.6 \times 10^{13}/N_{Z_{1/2}}$ <sup>59</sup> and  $\tau(\mu\text{s}) = 2 \times 10^{13}/N_{Z_{1/2}}$ <sup>518</sup> for the  $Z_{1/2}$  defect, instead of using Eq. (31)<sup>625</sup>.

At high temperatures the energetic charge carrier has to approach the center of the defect more closely to be captured<sup>621</sup>. This implies that the lifetime increases with increasing temperature<sup>521,524,537,626</sup>, which was extensively analyzed by Udal and Velmre<sup>627</sup>. The cross section changes in the order of  $T^{-x}$ <sup>628</sup>, which leads, in conjunction with the change of the thermal velocity according to  $\sqrt{T}$ , to a power law description<sup>624</sup>. In TCAD tools the model shown in Eq. (34)<sup>629–631</sup> is used, whereat  $\tau_{T_0}$  denotes the lifetime at some reference temperature  $T_0$ .

$$\tau_{\max} = \tau_{T_0} \left( \frac{T}{T_0} \right)^{\alpha} \quad (34)$$

Because the lifetime approaches zero for  $T \rightarrow 0$  in this approximation a slightly modified version<sup>247</sup> shown in Eq. (35) was proposed. By comparison we find  $\tau_0 = \tau_{T_0}/2$  that is achieved for  $T = 0\text{K}$ .

$$\tau_{\max} = \tau_0 \left( 1 + \left( \frac{T}{T_0} \right)^{\alpha} \right) \quad (35)$$

We also found an exponential description using an activation energy  $E_{\text{act}}$  shown in Eq. (36)<sup>627</sup>, where  $\tau_{\infty}$  denotes the lifetime for  $T \rightarrow \infty$ .

$$\tau_{\max} = \tau_{\infty} \exp \left( \frac{-E_{\text{act}}}{k_B T} \right) \quad (36)$$

Since the meaning of  $\tau_{\infty}$  is hard to grasp, it can be replaced by  $\tau_{T_0} \exp(E_{\text{act}}/k_B T_0)$ <sup>59,632</sup>, with  $\tau_{T_0}$  the lifetime at  $T = T_0$ . For  $E_{\text{act}} = 0.105\text{eV}$  and  $T_0 = 300\text{K}$  we get  $\exp(E_{\text{act}}/k_B T_0) = 57.9$ <sup>59,632</sup>. A very similar approach shown in Eq. (37)<sup>497</sup> approaches a value of  $51\tau_0$  for  $T \rightarrow \infty$ .

$$\tau_{\max} = \tau_0 \left( 1 + \frac{100}{1 + \exp(E_{\text{act}}/k_B T)} \right) \quad (37)$$

The models in Eq. (36) and Eq. (37) have the disadvantage that the lifetime stalls for high temperatures. Consequently these are only suitable for moderate temperatures between 300–500 K<sup>627</sup>, which circumvented by the model shown in Eq. (38)<sup>82,318</sup>.

$$\tau_{\max} = \tau_{T_0} \exp^{C\left(\frac{T}{T_0} - 1\right)} \quad (38)$$

A recent investigation by Lechner<sup>82</sup> identified an initial increase in the lifetime followed by a decrease at high temperatures. Based on the research by Schenk<sup>631</sup> the fitting shown in Eq. (39)<sup>82</sup> was proposed.

$$\tau_{\max} = \tau_{T_0} \left( \frac{T}{T_0} \right)^{T_{\text{coeff}}} \exp \left[ -\alpha_{\tau} \left( \frac{T}{T_0} - 1 \right)^{\beta_{\tau}} \right] \quad (39)$$

Be aware that in state-of-the-art simulation tools only Eq. (34) and Eq. (38) are included.

*b. Surface Recombination Rate* Surface recombination includes mechanisms that occur on surfaces or interfaces due to imperfections or impurities at the transition between two materials. It includes many different surface types and thus also effects, such as semiconductor-oxide, semiconductor-semiconductor or oxides across the latter. Naturally, these can be heavily influenced by the chosen materials and growth conditions. The share of surfaces recombination on the overall recombination rate decreases with the thickness of the samples, because the ratio of surface to bulk volume decreases<sup>625</sup>.

In general, the surface recombination is written as the boundary condition of the diffusion term<sup>633–636</sup> as shown in Eq. (40). A fantastic review on the causes, characterization methods and possible countermeasures of surface recombination is presented by Mao *et al.*<sup>499</sup> and a theoretical analysis by Gulbinas *et al.*<sup>633</sup>.

$$D \frac{d\Delta_N(\mathbf{x}, t)}{d\mathbf{x}} = S_0 \Delta_N(\mathbf{x}, t) \quad (40)$$

Despite the tight correlation to the diffusion the surface recombination is described in TCAD tools by the SRH formalism, with the sole difference that instead of lifetimes the *surface recombination velocities*  $s_{n,p}$  (see Eq. (41))<sup>260,325,412,501</sup> that depend on the interface trap density  $N_{\text{it}}$  are used.

$$R_{\text{SRH}}^s = \frac{(n_s p_s - n_i^2)}{(n_s + n_i)/s_p + (p_s + p_i)/s_n} \quad (41)$$

$$s_n = \sigma_{ns} v_{\text{th}} N_{\text{it}} \quad (42)$$

$$s_p = \sigma_{ps} v_{\text{th}} N_{\text{it}} \quad (43)$$

As inputs, the TCAD tools expect  $s_n$  and  $s_p$ . Their dependency on the crystal faces<sup>535,615,634–636</sup> is not included in state-of-the-art simulation tools yet. Some, however, provide the possibility to model a doping dependency but we found no reliable data for 4H-SiC in literature.

The surface recombination velocity again depends on the surface quality and the neighboring material. Therefore, there have been studies to improve the material quality<sup>495,615,633,637–643</sup> by differing growth mechanisms or by irradiation<sup>568</sup>. Even a more elaborate model using trap regions inside the band gap was developed<sup>347,644,645</sup>.

The temperature dependency of the surface recombination velocity was described by Klein *et al.*<sup>625</sup>, Kato *et al.*<sup>635</sup> and can be modeled by Eq. (44)<sup>646,647</sup>.  $-E_{bb}$  denotes the band bending near the surface, which leads to accumulation of charge carriers of one type at the surface and effectively repelling the other type<sup>517,647</sup>.

$$s_{\text{eff}}(T) = s_\infty \exp\left(\frac{-E_{bb}}{k_B T}\right) \quad (44)$$

## 2. Bimolecular Recombination

The term  $R_{\text{bim}}$  denotes the recombination rate due to the interaction of two particles, which can be described by Eq. (45)<sup>333,412</sup> with  $B$  the bimolecular recombination coefficient<sup>154,498</sup>.

$$R_{\text{bim}} = B(np - n_i^2) \quad (45)$$

We want to highlight that in literature this type of recombination is sometimes reduced to the radiative band-to-band recombination process emitting a photon<sup>367</sup>. Since 4H-SiC is an indirect semiconductor (see Section III) and this process, thus, always requires a phonon to absorb the momentum, radiative recombination is less important<sup>154,497,498,506,536</sup>. In addition to the radiative band-to-band recombinations  $R_{\text{bim}}$  includes (i) recombinations between donor-acceptor pairs (DAP)<sup>243,648</sup> (ii) the recombination of a charge carrier from the conduction/valence band and an unionized dopant (e.g. e-A)<sup>648,649</sup> and (iii) the recombination of excitons (see Section III)<sup>367</sup>.

Trap-assisted Auger recombination (TAA)<sup>650</sup> is also a bimolecular process but it is handled in differing fashions in the literature. TAA denotes the process when an electron (hole) interacts with a trap (capture resp. emission) and the additional/missing energy is exchanged with a particle of the same kind. Since two particles are involved many authors include this process in the bimolecular recombination coefficient<sup>31,255,367,651</sup>, some in the Auger process<sup>61,652</sup>, whereat others add it to SRH<sup>503,650,653</sup>. The latter is also the only option to model TAA in existing TCAD tools, however,

for 4H-SiC no suitable values have been found. TAA is also used to explain the rather high values of the bimolecular recombination coefficient<sup>367</sup>. We want to highlight that in the literature a lot of additional trap-assisted Auger processes are mentioned, which have to be handled with care. For example, the excitonic Auger capture process described by Hangleiter<sup>504</sup> is denoted as "markedly different" from TAA and should be regarded as an alternative explanation for multi-phonon/SRH recombination<sup>651</sup>. Booker *et al.*<sup>553</sup> describe a trap-Auger mechanism, where the energy of a hole captured in a neutral EH<sub>6,7</sub> trap, which contains two electrons, is transferred to the other electron in the trap, ejecting it to the conduction band.

Little data about the temperature dependency of  $B$  is available. Tawara *et al.*<sup>524</sup> present measurements for six different temperatures and state, that the value stays constant. If one would assume, however, the first data point as flawed, a clear decrease would be visible. Ščajev *et al.*<sup>205</sup> state that the radiative recombination coefficient doubles in the range of 10–1000 K, which could also lead to an increase of  $B$ . For more definite statements, however, further investigations would be necessary.

### 3. Auger Recombination

At last, the term  $R_{\text{Auger}}$ , also called Auger recombination "(first discovered in atomic systems by Pierre Auger; soft g, please, the gentleman is French not German!)"<sup>503</sup>, denotes a three particle interaction where the excessive resp. missing energy and momentum is taken from/transferred to a third particle (either hole or electron). This process is an intrinsic property of the material<sup>501</sup> and dominates for high excessive charge carrier densities. It is described by Eq. (46)<sup>86,333,412,654</sup> where  $C_n$  denotes the energy transfer to an electron and  $C_p$  the transfer to a hole<sup>255</sup>.

$$R_{\text{Auger}} = (C_n n + C_p p)(np - n_i^2) \quad (46)$$

The Auger recombination coefficients are also temperature dependent<sup>285,524</sup>. Galeckas *et al.*<sup>255</sup> describes this effect by Eq. (47).

$$C_n + C_p = \gamma_{30} \exp\left(-\frac{\alpha(T - 300\text{K})}{k_B T}\right) \quad (47)$$

Ščajev and Jarašiūnas<sup>497</sup> received quite different results, as they argue that Galeckas *et al.*<sup>255</sup> did not consider the in-depth profile. Instead the authors propose the model in Eq. (48), with

$B_{CE}(T) \propto T^{-1.5}$  the Coulomb enhancement coefficient and  $a_{SC}$  the screening parameter.

$$C(T, \Delta_N) = \left( C_0 + \frac{B_{CE}(T)}{\Delta_N} \right) / \left( 1 + \frac{\Delta_N}{a_{SC} \times T} \right)^2 \quad (48)$$

Ščajev *et al.*<sup>367</sup> mentioned a dependency of  $C$  with  $\Delta_N^{-0.3}$  due to the screening of the Coulomb enhancement coefficient and Tanaka, Nagaya, and Kato<sup>652</sup> derived a dependency of  $\Delta_N^{-0.68}$ . The differences can be explained due to a deviating fitting.

Also the model used to describe the temperature induced changes of the Auger recombination coefficients in Silicon (shown in Eq. (49)) is used<sup>320,469</sup>.

$$C_{n,p} = \left( A_{n,p} + B_{n,p} \left( \frac{T}{T_0} \right) + D_{n,p} \left( \frac{T}{T_0} \right)^2 \right) \left[ 1 + H_{n,p} \exp \left( -\frac{n,p}{N_{0n,p}} \right) \right] \quad (49)$$

#### 4. Analysis

In the sequel we want to analyze the presented equations and extract further useful information. Some reader might have already noticed that all recombination rates contain the multiplicative factor shown in Eq. (50) with  $n_0, p_0$  the intrinsic- and  $\Delta_n, \Delta_p$  the excessive carrier concentrations for electrons resp. holes.

$$(np - n_i^2) = (n_0 + \Delta_n)(p_0 + \Delta_p) - n_0 p_0 = n_0 \Delta_p + p_0 \Delta_n + \Delta_n \Delta_p \quad (50)$$

For a device without traps, i.e.,  $\Delta_p = \Delta_n = \Delta$ , and for low-level (ll,  $\Delta \ll n_0, p_0$ ) resp. high-level (hl,  $\Delta \gg n_0, p_0$ ) injections the models can be significantly simplified<sup>171,260,333,501,651</sup>, which is also important to correctly interpret the measurements results<sup>501</sup>. After a short calculation we get, due to  $R = \Delta_N / \tau_r$  (see Eq. (26)), for low-level injections the results shown in Eq. (51) and high-level in Eq. (52).

$$\tau_{SRH}^{ll} = \frac{\tau_p(n_0 + n_1) + \tau_n(p_0 + p_1)}{n_0 + p_0} \quad (51a)$$

$$\tau_{bim}^{ll} = \frac{1}{B(n_0 + p_0)} \quad (51b)$$

$$\tau_{Auger}^{ll} = \frac{1}{(C_n n_0 + C_p p_0)(n_0 + p_0)} \quad (51c)$$

$$\tau_{SRH}^{hl} = \tau_p + \tau_n \quad (52a)$$

$$\tau_{bim}^{hl} = \frac{1}{B\Delta} \quad (52b)$$

$$\tau_{Auger}^{hl} = \frac{1}{(C_n + C_p)\Delta^2} \quad (52c)$$

The results show that for SRH and Auger at high-injection levels always the sum of electron and hole parameters is achieved, whereat  $\tau_p + \tau_n$  in Eq. (52) is also denoted as ambipolar lifetime<sup>59,400</sup>. Separate measurements are only possible at low-injection level and with doped semiconductors, i.e., either  $n_0 \gg p_0, p_1, n_1$  or  $p_0 \gg n_0, n_1, p_1$ . In that case one of the summands gets significantly smaller and can be ignored.

For doped semiconductors we can rewrite the high-level injection results from Eq. (52) as shown in Eq. (53)<sup>154,255,333,367,498,501–503,563,651</sup>, which highlights that the introduced recombination terms actually represent a polynomial approximation of the recombination rate up to degree three in respect to the excess carrier concentration.

$$\begin{aligned} R &= \Delta\tau^{-1} = \Delta(\tau_{\text{SRH}}^{-1} + \tau_{\text{bim}}^{-1} + \tau_{\text{Auger}}^{-1}) \\ &= A\Delta + B\Delta^2 + C\Delta^3 \end{aligned} \quad (53)$$

Note that for no excess charge carriers, i.e.,  $\Delta = 0$ , also  $R = 0$ . For relatively low excess charge carrier densities the SRH term dominates while for high densities the Auger process is most important.

All these simplifications are only valid for  $\Delta \geq 0$ . If  $(np - n_i^2) < 0$  the recombination rate becomes negative, meaning that according to Eq. (25) charge carriers are generated. The corresponding rate of change can be described by using the so-called generation lifetime  $\tau_g$ <sup>260,333,500,614,655</sup>.

However, a simple inversion is only meaningful for the SRH and Auger descriptions, because for bimolecular generation incoming photons are mandatory<sup>500</sup>. We want to highlight that often impact ionization (see Section IV) is stated as the inverse of Auger recombination<sup>171,508,656</sup>. However, Selberherr<sup>412</sup> states that there is a difference, namely the source of the energy. While impact ionization requires high current densities the inverse process of the Auger recombination only requires high charge carrier concentrations with negligible current flow. Due to these facts the recombination rates in TCAD tools, specifically bimolecular and Auger, often get deactivated when they drop below zero. For the Auger process some simulation tools allow to explicitly enable generation while the optical generation of charge carriers (inverse of bimolecular recombination) is implemented separately in the tools.

## B. Results & Discussion

In the sequel the results of our analyses are presented. We did not include values when solely the effective lifetime was proposed<sup>366,534,655</sup> or if it was not possible to clearly distinguish  $\tau_n$  and

$\tau_p$ <sup>367,657,658</sup>. We also do not show values for different faces inside the crystal<sup>523,635</sup>.

## 1. SRH Lifetime

The recombination lifetime can be measured either optically or electrically. Commonly used optical techniques include photoluminescence decay (PLD)<sup>537,575,617</sup>, (transient) (time-resolved) free carrier absorption ((T)(TR-)FCA)<sup>205,255,367,497,502,511,536,651,659,660</sup>, electron beam induced current (EBIC)<sup>510</sup>, time-resolved photoinduced absorption (TRPA)<sup>255</sup>, time-resolved photoluminescence (TRPL)<sup>499,512,519,522–524,536,539,604,610,625,661</sup>, time-resolved transient absorption (RTA), transient absorption spectroscopy (TAS)<sup>498</sup>, four wave mixing (FWM)<sup>252</sup>, low-temperature photoluminescence (LTPL)<sup>617,622</sup>, capacitance transient (C-t)<sup>638</sup>, differential transmittivity (DT)<sup>622</sup> and (microwave) photoconductance decay (( $\mu$ )-PCD)<sup>379,487,495,496,499,513–518,520,521,527–529,531,536,563,615,635,642,657,666</sup>. For electrical measurements possible techniques are reverse recovery (RR)<sup>490,627,665,666</sup>, thyristor turned off gate current (TTOGC)<sup>542</sup>, short-circuit current/open-circuit voltage decay (SCCVD/OCVD)<sup>61,154,543,624,667–670</sup>, diode current density (DCD)<sup>485,671,672</sup>, bipolar transistor emitter current (BTEC)<sup>673</sup> and diode forward voltage degradation (DFVD)<sup>674</sup>. Also utilized is fitting to measurement results in literature (FT)<sup>143,238,291</sup> or simulations (SIM)<sup>544</sup>.

The achieved lifetime values depend on the utilized method<sup>61</sup>. Overall it has to be assured that the same quantity is measured, and that injection level and temperature are taken into account<sup>61</sup>. For example, Kato, Mori, and Ichimura<sup>675</sup> claim that  $\mu$ -PCD tends to overestimate the carrier lifetimes in high injection conditions and, similarly, Tawara *et al.*<sup>604</sup> experienced that  $\mu$ -PCD achieves longer lifetimes than the ones by TRPL. Deviations might also result from improper measurement setups, because, e.g., OCVD is limited to low and high injection regions only<sup>154</sup>. For more detailed information, e.g., which carrier lifetime is extracted from the decay time for high and low injection by each measurement technique, the interested reader is referred to the dedicated literature<sup>59,536</sup>.

A wide range of values for  $\tau_n$  (see Table XI) and  $\tau_p$  (see Table XII) are available in literature, whereat much more results for holes are available. In early days, Bakowski, Gustafsson, and Lindefelt<sup>69</sup> still had to use Silicon values due to a lack of data but since then many investigations have been conducted. Despite the wide range of values, the relation  $\tau_n = 5\tau_p$ , which was originally used for Si, is still utilized<sup>146,163,182,292,324,338,377,476,676,677</sup>. Recently,  $\tau_n = \tau_p$  was observed as well<sup>140,144,315,318,678–680</sup>.

TABLE XI. Electron lifetime results. Column *inj.* denotes the carrier injection level, i.e., low (ll) resp. high (hl), and column *excess* the exact amount. A *y* in column *impr.* highlights that the shown value is the highest lifetime achieved in an optimization process.

ref.	$\tau_n$	dop	conc.	T	inj.	excess	impr.	method
	[s]		[1/cm <sup>3</sup> ]	[K]		[1/cm <sup>3</sup> ]		
[Agar01] <sup>542</sup>	$6 \times 10^{-7}$	p	$7 \times 10^{14}$	293	hl	-	-	TTOGC
[Ivan06a] <sup>544</sup>	$6.6 \times 10^{-8}$	p	$2 \times 10^{17}$	300	-	-	-	SIM
[Alba10] <sup>154</sup>	$8 \times 10^{-9}$	-	$2.04 \times 10^{17}$	300	-	-	-	OCVD
[Haya11] <sup>495</sup>	$1.3 \times 10^{-6}$	Al	$9 \times 10^{14}$	-	ll	$1.5 \times 10^{14}$	y	uPCD
[Haya11a] <sup>496</sup>	$1.6 \times 10^{-6}$	p	$9 \times 10^{14}$	300–525	ll	$1.5 \times 10^{14}$	y	uPCD
[Haya12] <sup>513</sup>	$1.7 \times 10^{-6}$	p	$5.6 \times 10^{14}$	-	ll	$1 \times 10^{15}$	y	uPCD
[Okud13a] <sup>520</sup>	$3.1 \times 10^{-7}$	Al	$1 \times 10^{18}$	300	-	$9.1 \times 10^{15}$	-	uPCD
[Dibe14] <sup>671</sup>	$1 \times 10^{-9}$	-	-	-	hl	-	-	DCD
[Okud14] <sup>521</sup>	$1 \times 10^{-5}$	Al	$2 \times 10^{14}$	300	-	$3.6 \times 10^{16}$	y	uPCD
[Liau15] <sup>622</sup>	$2 \times 10^{-8}$	Al	$1 \times 10^{17}$	300	hl	-	-	DT
[Okud16] <sup>663</sup>	$1.2 \times 10^{-5}$	Al	$1 \times 10^{15}$	300	-	$3.6 \times 10^{14}$	y	uPCD
[Hase17] <sup>485</sup>	$4 \times 10^{-7}$	p	$8 \times 10^{14}$	-	-	-	-	DCD
[Kato20] <sup>635</sup>	$1.2 \times 10^{-6}$	Al	$6 \times 10^{14}$	300	ll	-	y	uPCD
[Koya20] <sup>674</sup>	$1.3 \times 10^{-7}$	p	$1 \times 10^{19}$	-	-	-	-	DFVD
[Maxi23] <sup>238 a</sup>	$6 \times 10^{-6}$	-	-	-	-	-	-	FT
[Zhan23a] <sup>527</sup>	$3.14 \times 10^{-6}$	Al	$2 \times 10^{14}$	300	-	-	y	uPCD

<sup>a</sup> value fitted to measurements by Kimoto *et al.*<sup>487</sup>

TABLE XII: Hole lifetime results. Column *inj.* denotes the carrier injection level, i.e., low (ll) resp. high (hl), and column *excess* the exact amount. A *y* in column *impr.* highlights that the shown value is the highest lifetime achieved in an optimization process.

ref.	$\tau_p$	dop	conc.	T	inj.	excess	impr.	method
	[s]		[1/cm <sup>3</sup> ]	[K]		[1/cm <sup>3</sup> ]		
[Kord96] <sup>537</sup>	$2.1 \times 10^{-6}$	n	-	300	-	-	-	PLD
[Gale97] <sup>255</sup>	$2.6 \times 10^{-7}$	N	$5 \times 10^{15}$	-	hl	-	-	TRPA
[Neud98] <sup>490</sup>	$7 \times 10^{-7}$	N	$(2\text{--}4) \times 10^{16}$	-	-	-	-	RR
[Gale99a] <sup>533</sup>	$5 \times 10^{-7}$	N	<1e16	-	-	-	-	FCA
[Ivan99] <sup>543</sup>	$6 \times 10^{-7}$	n	$6 \times 10^{14}$	293	hl	-	-	OCVD
	$3.8 \times 10^{-6}$	n	$6 \times 10^{14}$	550	hl	-	-	OCVD
[Kimo99] <sup>665</sup>	$3.3 \times 10^{-7}$	N	$5 \times 10^{14}$	-	-	-	-	RR

[Udal00] <sup>66</sup>	$5.2 \times 10^{-8}$	n	$(0.9\text{--}2.6) \times 10^{15}$	-	-	-	-	RR
[Cheo03] <sup>638</sup>	$1 \times 10^{-6}$	N	$(1\text{--}1.8) \times 10^{16}$	300	-	-	-	Ct
[Dome03] <sup>673</sup>	$3.5 \times 10^{-9}$	n	$8.6 \times 10^{15}$	-	hl	-	-	BTEC
[Zhan03] <sup>610</sup>	$3 \times 10^{-7}$	n	$(1\text{--}200) \times 10^{14}$	-	-	-	-	TRPL
[Levi04] <sup>669</sup>	$1.55 \times 10^{-6}$	n	$3 \times 10^{14}$	293	hl	-	-	OCVD
[Tawa04] <sup>604</sup>	$(0.26\text{--}6.8) \times 10^{-6}$	n	$(1.8\text{--}34) \times 10^{14}$	300\text{--}500	-	$(1.1\text{--}4.2) \times 10^{15}$	-	TRPL
[Resh05] <sup>61</sup>	$1 \times 10^{-6}$	n	$7 \times 10^{15}$	-	-	-	-	OCVD
[Huh06] <sup>575</sup>	$5 \times 10^{-7}$	n	$1 \times 10^{14}$	-	ll	$1 \times 10^{13}$	-	PLD
[Ivan06b] <sup>668</sup>	$3.7 \times 10^{-6}$	n	$2 \times 10^{14}$	300	hl	-	-	OCVD
[Jenn06] <sup>510</sup>	$1.55 \times 10^{-5}$	N	$5 \times 10^{15}$	-	-	-	-	EBIC
[Neim06] <sup>252</sup>	$1.2 \times 10^{-8}$	N	$1 \times 10^{16}$	-	-	-	-	FWM
[Dann07] <sup>563</sup>	$2.5 \times 10^{-6}$	N	$1.5 \times 10^{15}$	300	hl	$(2\text{--}20) \times 10^{16}$	y	uPCD
[Stor07] <sup>522</sup>	$2.18 \times 10^{-7}$	N	$5 \times 10^{15}$	300	-	-	y	TRPL
[Udal07] <sup>627</sup>	$4.4 \times 10^{-9}$	n	$7 \times 10^{15}$	297	-	-	-	RR
[Kimo08] <sup>517</sup>	$8.6 \times 10^{-6}$	n	$(1\text{--}2) \times 10^{15}$	-	ll	$5 \times 10^{12}$	-	uPCD
[Stor08] <sup>523</sup>	$9.9 \times 10^{-7}$	n	$1 \times 10^{14}$	300	-	-	y	TRPL
[Hiyo09] <sup>528</sup>	$1.62 \times 10^{-6}$	N	$(1\text{--}5) \times 10^{15}$	-	hl	$(2\text{--}20) \times 10^{16}$	y	uPCD
[Resh09] <sup>667</sup>	$2.13 \times 10^{-6}$	n	$(1\text{--}1.2) \times 10^{15}$	-	hl	-	-	OCVD
[Alba10] <sup>154</sup>	$1.5 \times 10^{-11}$	-	$2.21 \times 10^{17}$	300	-	-	-	OCVD
[Kimo10] <sup>518</sup>	$9.5 \times 10^{-6}$	n	$(0.9\text{--}1) \times 10^{15}$	-	hl	$(5\text{--}50) \times 10^{15}$	y	uPCD
[Kimo10a] <sup>642</sup>	$1.31 \times 10^{-5}$	N	$7 \times 10^{14}$	-	hl	$(5\text{--}50) \times 10^{15}$	y	uPCD
[Klei10] <sup>625</sup>	$>100e-6$	N	$<1e16$	222	ll	$2 \times 10^{14}$	-	TRPL
[Miya10] <sup>662</sup>	$1.85 \times 10^{-5}$	N	$7 \times 10^{13}$	-	ll	$3 \times 10^{12}$	-	uPCD
[Haya11a] <sup>496</sup>	$4.6 \times 10^{-6}$	n	$1.2 \times 10^{15}$	300\text{--}525	ll	$1.5 \times 10^{14}$	y	uPCD
[Donn12] <sup>291</sup> ?	$2.4 \times 10^{-7}$	N	$1 \times 10^{16}$	-	-	-	-	FT
[Ichi12] <sup>514</sup>	$3.32 \times 10^{-5}$	N	$(3\text{--}8) \times 10^{14}$	-	-	$(1\text{--}10) \times 10^{15}$	y	uPCD
[Kawa12] <sup>516</sup>	$6.5 \times 10^{-6}$	n	$1 \times 10^{16}$	300	-	$1 \times 10^{16}$	y	uPCD
[Lilj13] <sup>512</sup>	$1.6 \times 10^{-6}$	N	$3 \times 10^{15}$	300	ll	-	y	TRPL
[Miya13] <sup>519</sup>	$1.3 \times 10^{-5}$	N	$(2\text{--}3) \times 10^{14}$	300	-	-	y	TRPL
[Scaj13] <sup>497</sup>	$5.5 \times 10^{-7}$	n	$4 \times 10^{14}$	-	ll	-	-	FCA
[Dibe14] <sup>671</sup>	$1 \times 10^{-8}$	-	-	-	hl	-	-	DCD
[Usma14] <sup>143</sup> ?	$1.3 \times 10^{-6}$	n	$2 \times 10^{14}$	-	-	-	-	FT
[Chow15] <sup>379</sup>	$2.5 \times 10^{-6}$	n	$2.5 \times 10^{14}$	300	hl	-	-	uPCD
[Kaji15] <sup>515</sup>	$2.16 \times 10^{-5}$	N	$2 \times 10^{14}$	-	-	$1 \times 10^{14}$	y	uPCD
[Suva15] <sup>659</sup>	$3.5 \times 10^{-7}$	N	$8 \times 10^{15}$	-	hl	$6 \times 10^{17}$	-	FCA
[Puzz16] <sup>672</sup>	$1 \times 10^{-6}$	n	$3 \times 10^{15}$	400	-	-	-	DCD
[Sait16] <sup>664</sup>	$2.6 \times 10^{-5}$	n	$1 \times 10^{14}$	300	-	$1.8 \times 10^{17}$	-	uPCD
[Tawa16] <sup>524</sup>	$3 \times 10^{-7}$	N	$7.7 \times 10^{17}$	300	ll	-	-	TRPL
[Tsuc16] <sup>661</sup>	$2.6 \times 10^{-6}$	n	$1.4 \times 10^{14}$	-	-	-	-	TRPL
[Ayed17] <sup>509</sup>	$2 \times 10^{-5}$	N	$1 \times 10^{15}$	-	-	-	y	-
[Lilj17] <sup>617</sup>	$3.5 \times 10^{-6}$	N	$1.3 \times 10^{15}$	300	ll	-	-	PLD
[Fang18] <sup>498</sup>	$(11\pm3) \times 10^{-9}$	N	$9.1 \times 10^{18}$	300	-	-	-	TAS
[Kimo18] <sup>487</sup>	0.00011	n	$1 \times 10^{14}$	-	-	$(1\text{--}10) \times 10^{14}$	y	uPCD
[Cui19] <sup>529</sup>	$1.05 \times 10^{-6}$	N	$2 \times 10^{13}$	300	-	$4 \times 10^{16}$	-	uPCD
[Mura19] <sup>539</sup>	$9.9 \times 10^{-6}$	N	$1 \times 10^{15}$	293	ll	-	-	TRPL
[Kato20] <sup>635</sup>	$7 \times 10^{-7}$	N	$(1\text{--}10) \times 10^{15}$	300	ll	-	y	uPCD

[Naga20] <sup>502</sup>	$1 \times 10^{-5}$	N	$1 \times 10^{18}$	293	hl	$1.5 \times 10^{18}$	-	TR-FCA
[Sapi20] <sup>624</sup>	$1.9 \times 10^{-5}$	n	$1 \times 10^{16}$	300	hl	-	-	OCVD
[Erle21] <sup>531</sup>	$5 \times 10^{-6}$	N	$(5-10) \times 10^{14}$	-	ll	-	-	uPCD
[Mura21] <sup>648</sup>	$1.4 \times 10^{-7}$	N	$2 \times 10^{17}$	293	ll	$7 \times 10^{14}$	-	TRPL
[Maxi23] <sup>238</sup> ?	$2 \times 10^{-6}$	-	-	-	-	-	-	FT
[Kato24] <sup>615</sup>	$4.5 \times 10^{-6}$	n	$1 \times 10^{15}$	300	-	$(5-50) \times 10^{15}$	-	uPCD
[Sozz24] <sup>670</sup>	$6.09 \times 10^{-6}$	n	$1.5 \times 10^{14}$	298	hl	$4 \times 10^{17}$	-	OCVD

This overview is already a simplification, as many publications present values for multiple operating conditions, i.e., temperature, doping concentration or excess carrier concentration. Only the best achieved values are shown here. For example Hayashi *et al.*<sup>496</sup> provides measurements over injection level for two temperatures (300 K and 525 K). Grivickas *et al.*<sup>511</sup> show measurements with different intensities but no actual values. The lifetime depends on all the mentioned parameters simultaneously, which makes a proper presentation very challenging. Therefore, we highlight each single dependency separately. For example, we depict the measured lifetimes with the respective doping densities if specified in the paper (see Fig. 22). A decreasing lifetime with increasing doping density can be observed, but no actual difference between electron and hole lifetime. However, all these values were most probably measured with differing excess carrier concentrations and at deviating temperatures.

Note that we explicitly show the injection level during the measurements, because for a high level only the sum  $\tau_n + \tau_p$  is achieved<sup>575,659</sup> (cp. Eq. (52)). Consequently, it can be expected that the lifetime increases when going from low to high injection level, until it eventually starts to decrease when the bimolecular or Auger recombination become dominant. This effect was explicitly shown in literature<sup>495,496,513,615</sup>. Despite that, Kimoto *et al.*<sup>681</sup> stated in 2016 that the injection-level dependence of SRH lifetimes is not known in SiC, calling for further research. In contrast, Ščajev and Jarašiūnas<sup>497</sup> stated that the lifetime is almost injection level independent. Very different results were reported by Tawara *et al.*<sup>524</sup>, who saw a lifetime decrease, eventually approaching a constant value.

For thin samples the achieved recombination rate has diminishing resemblance to the bulk contribution  $R_{SRH}^b$ <sup>501</sup>, since the surface recombination  $R_{SRH}^s$  dominates. In any case it is always important to consider the impact of the surface during measurements<sup>536</sup>. Optimally the surface contribution is measured separately<sup>490,625,662,665</sup>, which is, however, not always practical<sup>536</sup>. For sufficiently thick samples  $R_{SRH}^b$  can be determined directly, however, this demands extraordinarily

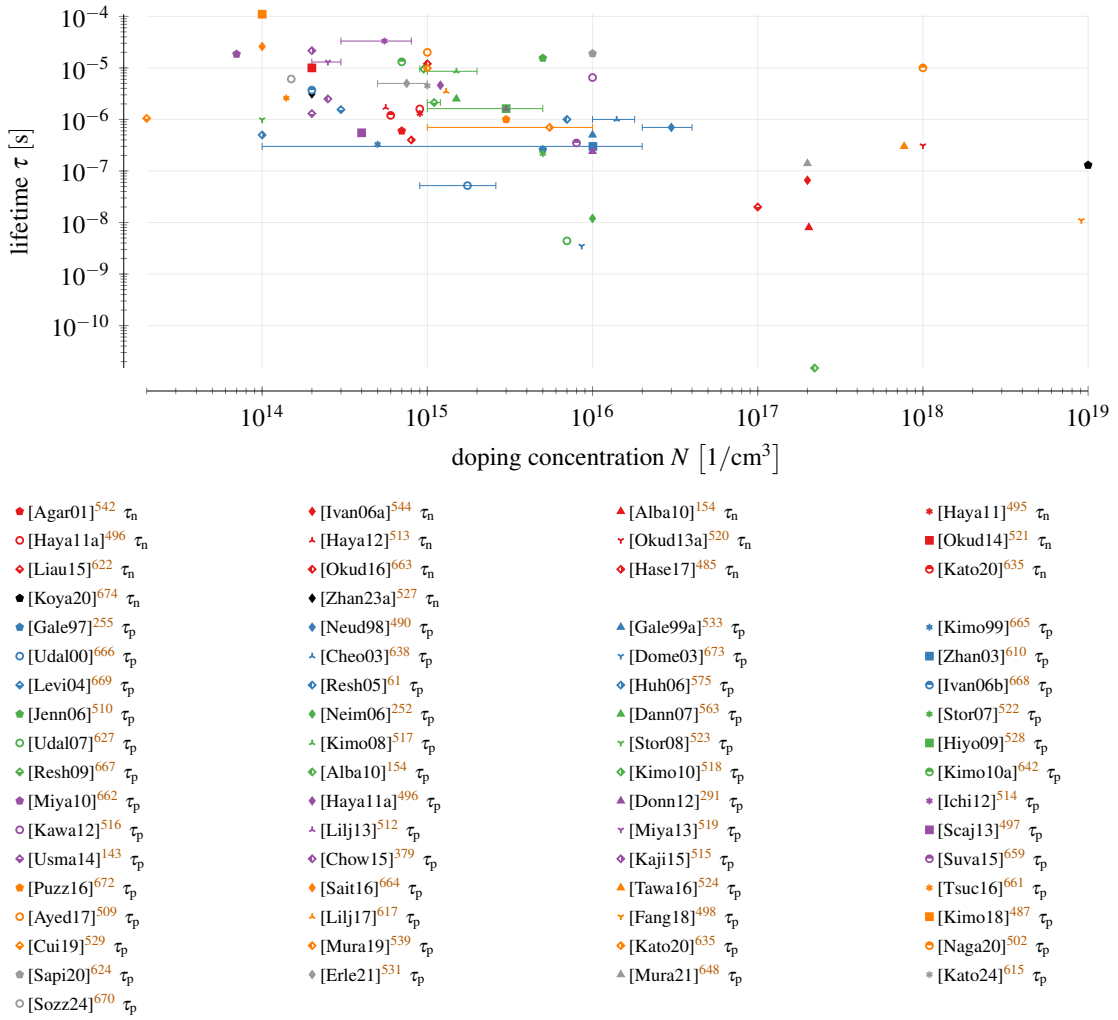


FIG. 22. Measurements of the minority charge carrier lifetime for the respective doping densities.

thick ones<sup>501</sup>: Depending on the surface recombination velocity, thicknesses in the range of mm or even cm would be required<sup>260</sup>.

Finally, we also investigated the values that are referenced in literature (see Fig. 23). Overall, there are only very few references compared to the amount of fundamental investigations. This shows that the lifetime depends on many parameters and may differ considerably among samples. As mentioned before, very similar values for  $\tau_n$  and  $\tau_p$  are encountered.

## 2. Doping Dependency of SRH Lifetime

The decrease of the minority carrier lifetimes with doping concentration (cp. Fig. 22) is described by additional recombination centers (Scharfetter relation, Eq. (33)). We acquired multiple

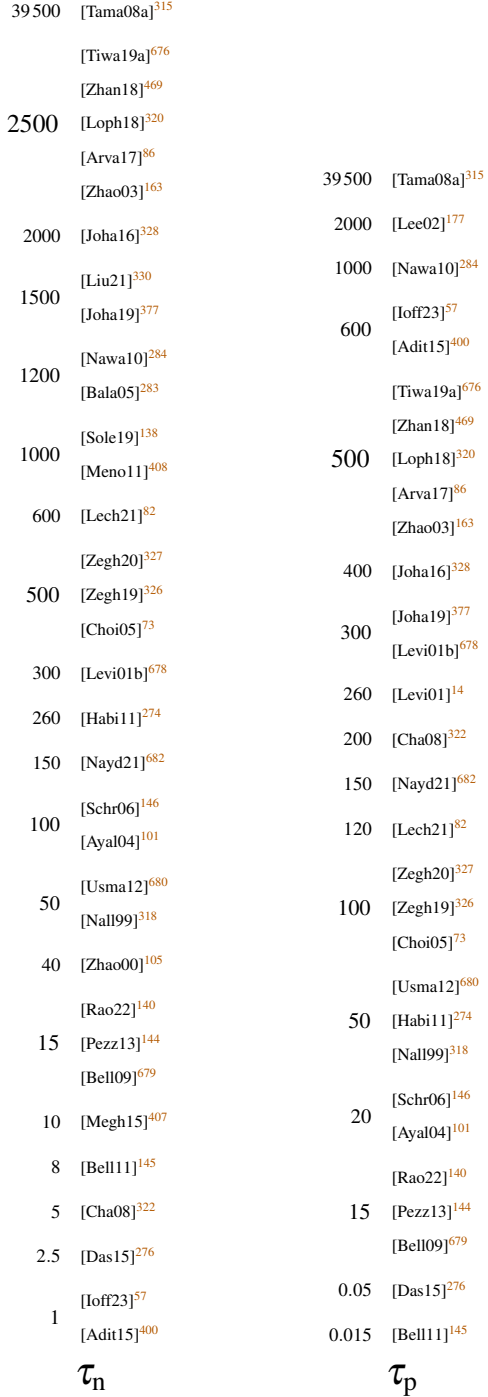


FIG. 23. Lifetime values referenced in literature.

parameter sets (see Table XIII) for the latter. In the 1990s no values for 4H-SiC values were available, so Ruff, Mitlehner, and Helbig<sup>292</sup> settled for a combination of Silicon based values gathered from various sources. Surprisingly, these parameters are still the most commonly ones used in literature (see Fig. 25). While some publications are well aware that Silicon data are used<sup>101,325,644</sup>

TABLE XIII. Parameters for doping dependency according to the Scharfetter relation in Eq. (33). are fittings to suitable measurements and fittings to the excessive carrier concentrations.

ref.	electrons		holes	
	$N_{\text{ref}}$ [1/cm <sup>3</sup> ]	$\gamma$ [1]	$N_{\text{ref}}$ [1/cm <sup>3</sup> ]	$\gamma$ [1]
[Ruff94] <sup>292 a</sup>	$3 \times 10^{17}$	0.3	$3 \times 10^{17}$	0.3
[Nall99] <sup>318 c</sup>	$1 \times 10^{16}$	1	$1 \times 10^{16}$	1
[Levi01b] <sup>678</sup>	$7 \times 10^{17}$	1	-	-
[Choi05] <sup>73 b</sup>	$5 \times 10^{16}$	1	$5 \times 10^{16}$	1
[Donn12] <sup>291 b f</sup>	$2 \times 10^{18}$	1.9	$2 \times 10^{18}$	1.9
<sup>g</sup>	$4 \times 10^{18}$	1.4	$4 \times 10^{18}$	1.4
[Liau15] <sup>622 e</sup>	$5 \times 10^{18}$	1.2	-	-
[Lech21] <sup>82</sup>	$7 \times 10^{16}$	1	$7 \times 10^{16}$	1
[Maxi23] <sup>238 d</sup>	$5 \times 10^{15}$	0.55	$5 \times 10^{15}$	0.67

<sup>a</sup> Silicon data from multiple sources combined

<sup>b</sup> References Harris and Inspec <sup>13</sup> but no data found there. According to Albanese <sup>154</sup> based on Silicon data.

<sup>c</sup> fit to lifetime over excessive charge carrier densities <sup>255</sup>

<sup>d</sup> fit to measurements for changing doping concentration by Kimoto *et al.* <sup>487</sup>

<sup>e</sup> fit to own measurements for changing doping concentration

<sup>f</sup> fit to lifetime over excessive charge carrier densities <sup>683</sup>

<sup>g</sup> fit to lifetime over excessive charge carrier densities <sup>252</sup>

this information seems to was lost over the years.

The only fittings we could actually trace back to measurements of  $\tau_{\text{SRH}}$  with varying doping concentration are the investigations by Liaugaudas *et al.* <sup>622</sup>, who did their own differential transmittivity measurements, and Maximenko <sup>238</sup>, who fitted to the results of the  $\mu$ -PCD measurements by Kimoto *et al.* <sup>487</sup>. We also found dedicated measurements by Lilja *et al.* <sup>617</sup> and Murata *et al.* <sup>648</sup>, which, seemingly, were not yet used in any fitting. For other publications <sup>73,82,678</sup> we were simply unable to retrace the origin of the values, although often explicit references were provided.

There are often confusions between the doping and the excess charge carrier concentration. While both lead to a decrease in lifetime with increasing concentration the physical process causing that are fundamentally different. While more doping causes more recombination centers, more excess charge carrier lead to a higher contribution of bimolecular and Auger recombination. For

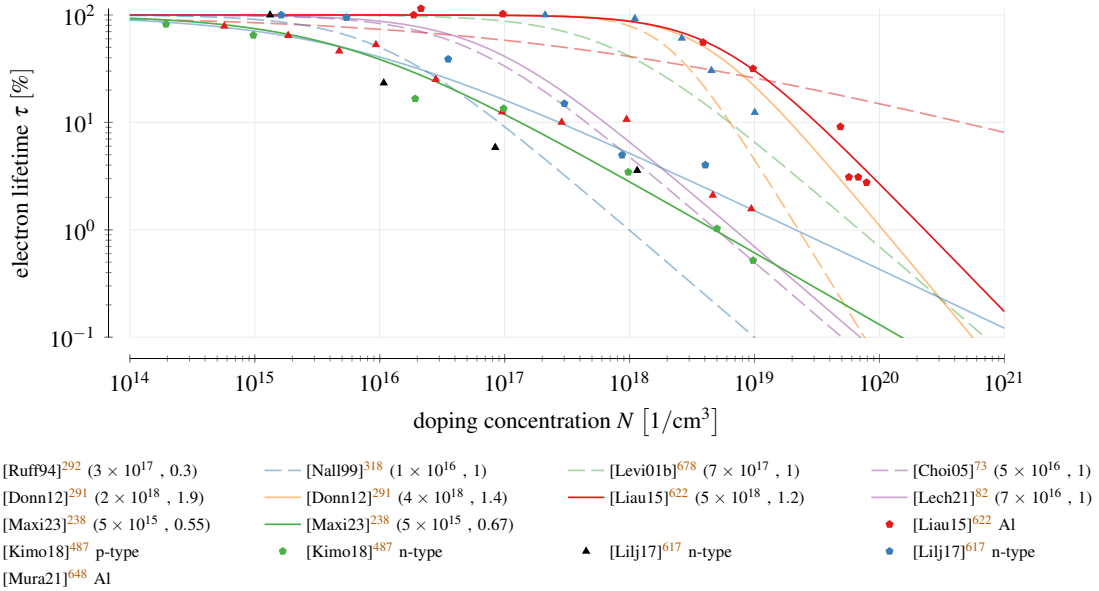


FIG. 24. Doping dependency according to the Scharfetter relation in Eq. (33). In brackets are the values for  $(N_{\text{ref}}, \gamma)$ . Only one graph is shown if electron and hole parameters are equal (see Table XIII). Solid non-opaque lines represent fitting to 4H-SiC measurement data.

example, Kimoto *et al.*<sup>487</sup> adds bimolecular and Auger coefficients to a plot over the doping concentration. In addition, fittings of the Scharfetter relation versus an increasing excess charge carrier concentration were proposed<sup>291,318</sup>. Although we believe that such a fitting is not reasonable we included the respective results in the table but highlighted them accordingly.

In a double logarithmic plot (see Fig. 24) the differences are well observable. There are differences in the onset of lifetime degradation, i.e., the value  $N_{\text{ref}}$ . For a specific reduction of the lifetime the respective doping can vary by up to three orders of magnitude. Also the rate of change deviates, whereat for the Silicon based model proposed by Ruff, Mitlehner, and Helbig<sup>292</sup> a significantly lower transition rate is observable. Interestingly also the models based on the measurements differ quite significantly. We also added some measurement result, which show significant variations and thus also lead to deviating fitting results.

In the literature the values by Ruff, Mitlehner, and Helbig<sup>292</sup> are still heavily utilized to describe the doping dependency (see Fig. 25), although these are not based on 4H. The dedicated fittings to 4H measurements have not been referenced so far.



FIG. 25. Reference chain for charge carrier recombination. ■ are fundamental investigations, ■ research not focused on 4H and ■ connections predicted from the used values.

### 3. Temperature Dependency of SRH Lifetime

There are various fantastic investigations on the changes of the lifetime with temperature<sup>615,635</sup> some even distinguishing between surface and bulk lifetime<sup>625</sup>. Even various excess charge carriers in the range ( $1-1000$ )  $\times 10^{16}$  1/cm<sup>3</sup> were investigated<sup>649</sup>, whereat the behavior varies.

In the literature predominantly the power law descriptions of Eq. (34) and Eq. (35) are used (see Table XIV). The values for the exponent  $\alpha$  thereby commonly vary between 1 and 2. Udal and Velmre<sup>627</sup> stated a fitting in two regions, as the lifetime started to increase faster above 700 K.

TABLE XIV. temperature dependency parameters in literature. If only one value for  $\alpha_{n,p}$  is stated no charge carrier specification was made in the publication.

ref.	$\alpha_n$	$\alpha_p$	$T_0$	$E_{act}$	$C$	conf.	equ.	method
	[1]	[1]	[K]	[eV]	[1]	[K]		
[Kord96] <sup>537 a</sup>	-	1.72	300	-	-	0–200	(34)	PLD
[Ivan99] <sup>543 d</sup>	-	-	-	0.11	-	300–500	(36)	OCVD
[Nall99] <sup>318 b</sup>	-	-	300	-	2.55	-	(38)	-
[Udal00] <sup>666</sup>	-	2.2	300	-	-	200–450	(34)	RR
[Agar01] <sup>542 d</sup>	-	-	-	0.12	-	300–500	(36)	TTOGC
[Bala05] <sup>283</sup>	5	-	300	-	-	-	(34)	-
[Levi05] <sup>626 d</sup>	-	-	-	0.08	-	300–500	(36)	-
[Ivan06a] <sup>544 e</sup>	-	-	-	0.105	-	300–500	(36)	SIM
[Udal07] <sup>627</sup>	-	1.9	300	-	-	300–700	(34)	RR
	-	4.4	300	-	-	700–1000	(34)	RR
[Scaj13] <sup>497</sup>	-	-	-	0.125	-	70–1000	(37)	FCA
[Dibe14] <sup>671</sup>	2.15	-	300	-	-	250–500	(34)	DCD
[Chow15] <sup>379 c</sup>	1.2	-	300	-	-	300–525	(34)	uPCD
[Rakh20] <sup>247</sup>	-	8	450	-	-	100–700	(35)	-
	-	14	530	-	-	100–700	(35)	-
[Sapi20] <sup>624</sup>	1.5	-	300	-	-	300–450	(34)	OCVD
[Tian20] <sup>677</sup>	1.84	1.84	300	-	-	300–573	(34)	-
[Maxi23] <sup>238</sup>	1.72	1.72	300	-	-	-	(34)	FT
[Sozz24] <sup>670</sup>	1.7	-	298	-	-	300–450	(34)	OCVD

<sup>a</sup> fitting provided in citing articles (see Fig. 25), Sapienza *et al.*<sup>624</sup> fitted  $\alpha = 1.9$

<sup>b</sup> default value of many simulation tools, according to Lechner<sup>82</sup> based on the research from Grasser *et al.*<sup>690</sup>

<sup>c</sup> fitting done by Sapienza *et al.*<sup>624</sup>

<sup>d</sup> fitting done by Udal and Velmre<sup>627</sup>

<sup>e</sup> fitting done by Tamaki *et al.*<sup>632</sup>

Sapienza *et al.*<sup>624</sup> achieved  $\alpha = 1.5$  which is exactly the value expected for Coulomb-attractive charge recombination centers<sup>627</sup>.

More complex is the situation for the value  $\alpha_{n,p} = 5^{143,283,284}$ . Although we stated Balachandran, Chow, and Agarwal<sup>283</sup> as the origin here we were actually not able to determine the origin

of this parameter. We suspect that it might have been the default value of a TCAD tool but we could not even confirm that. In the same sense we were not able to pinpoint the origin of the value  $C = 2.55^{318}$  for Eq. (38). Although Lechner<sup>82</sup> provided a reference<sup>690</sup> we were not able to find anything in there either.

For the exponential based approaches the value of  $E_{\text{act}}$  is between 110–125 meV. Please note that for Eq. (39) a lot of parameters have been presented<sup>82</sup>. We calculated the average from the single sets and achieved the values shown in Eq. (54), where an initial increase followed by a decrease in the lifetime is visible.

$$T_{\text{coeff}} = 0.666, \quad \alpha_{\tau} = 0.06385, \quad \beta_{\tau} = 5.716 \quad (54)$$

A comparison of the single models (see Fig. 26) shows that for all the lifetime increases with increasing temperature. We also added some temperature measurements and scaled them such that the room temperature values are around  $1\mu\text{s}$ , which we fixed. Please be aware that we had to dismiss the values by Lophitis *et al.*<sup>320</sup> as only the parameters but not the according equations were defined. We also do not show the results by Puzzanghera and Nipoti<sup>672</sup> as only minor deviations around the value at room temperature were achieved. Again we want to highlight that the plots have to be considered with a grain of salt as temperature changes depend on doping<sup>648</sup>. For high-level injection the sum of hole and electron lifetime is measured<sup>379</sup>, which, again, can have a differing temperature dependency. Sapienza *et al.*<sup>624</sup> compares various sources in this respect<sup>87,537,627</sup>.

The most prominent model in literature is the one proposed by Kordina *et al.*<sup>537</sup> (see Fig. 25), which, was, however, only characterized up to 200 K.

#### 4. Surface Recombination Velocity

The surface recombination velocity is, as the name indicates, not a bulk property but depends on many parameters such as crystal faces, i.e., Si-, C-, a- or m-face<sup>635,636</sup>, and interface treatment. For these reasons we will only roughly cover this topic. Interesting analyses of the surface recombination velocity were published by Ščajev *et al.*<sup>367</sup>, Gulbinas *et al.*<sup>633</sup>, Mori, Kato, and Ichimura<sup>636</sup>.

In general, the surface recombination velocity has to be determined for each sample separately, due to the dependency on so many factors. It was pointed out that the injection level during

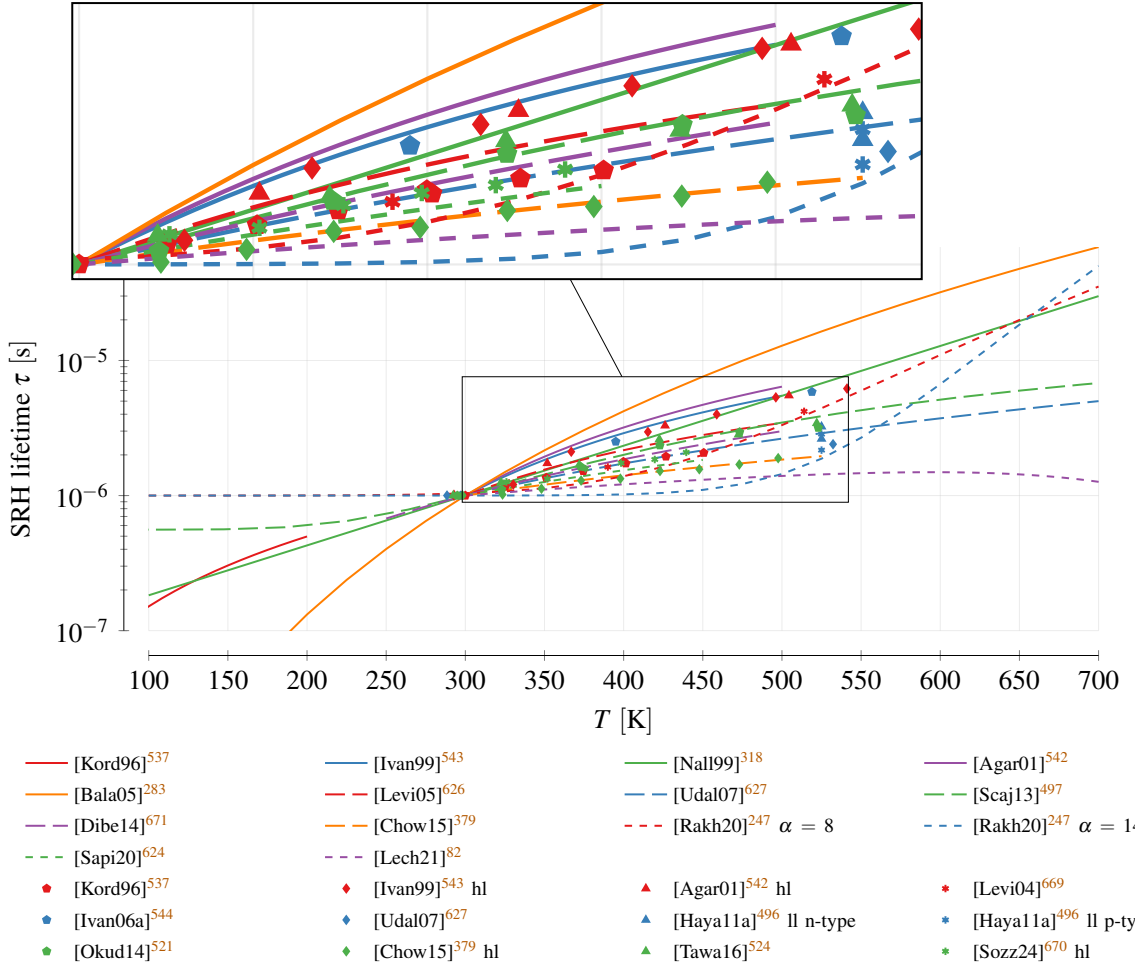


FIG. 26. Temperature Dependency of the SRH lifetime. Models are calibrated to hit 1  $\mu$ s at 300 K. Measurement results are scaled such that 1  $\mu$ s at  $(296 \pm 4)$  K is achieved.

measurements has an impact<sup>260,367,615</sup>, which was possibly explained by a band banding near the interface<sup>517</sup>. Furthermore the surface recombination velocity is temperature dependent and increases with increasing temperature<sup>625,635</sup>. Overall, suitable values in literature are mainly based on dedicated investigations (see Table XV) or are simply assumed, e.g.,  $s = 2.2 \times 10^5$  cm/s<sup>643</sup>,  $s = 1 \times 10^3$  cm/s<sup>514</sup>.

For the surface recombination velocity additional measurement methods to the earlier explained ones were used, for example colinear pump probe (CPP)<sup>633</sup>, non-equilibrium free-carrier density (NFCD)<sup>285</sup>, via the exponential prefactor in the current density (CD)<sup>639,692</sup> or reverse recovery (RR)<sup>665</sup>. By changing the thickness of the devices the impact of the surfaces and their recombination velocities was extracted<sup>633</sup> and sometimes even eliminated<sup>490,662</sup>. An effective bulk lifetime of more than 1  $\mu$ s can, however, only directly measured within epitaxial layers thicker than

TABLE XV. Surface recombination velocity. A y in column *impr.* indicates that the velocities were achieved at the end of an optimization process.

ref.	$s$ [cm/s]	$s_n$ [cm/s]	$s_p$ [cm/s]	type <sup>a</sup>	impr.	method
[Gale97] <sup>255</sup>	-	-	$4 \times 10^4 / 1 \times 10^4$	S/I	-	FCA
[Neud98] <sup>490</sup>	-	-	$5 \times 10^4$	M	-	RR
[Gale99a] <sup>533</sup>	-	-	$(5\text{--}8) \times 10^3$	S	y	FCA
[Kimo99] <sup>665</sup>	-	-	$5 \times 10^4$	M	-	CD
[Gale01] <sup>534</sup>	$(5\text{--}500) \times 10^3$	-	-	S	y	TA
[Cheo03] <sup>638</sup>	-	-	1–1000	S	y	Ct
[Huh06] <sup>575</sup>	-	-	$2.50 \times 10^3$	S	-	TRPL
[Ivan06a] <sup>544</sup>	4200	-	-	M	-	CD
[Neim06] <sup>252</sup>	-	-	$(4 \pm 1) \times 10^4$	S	-	FWM
[Griv07] <sup>285</sup>	$1 \times 10^4$	-	-	S	-	NFCD
[Klei08] <sup>536</sup>	-	-	$(5\text{--}500) \times 10^3$	S	y	TFCA
[Klei10] <sup>625</sup>	-	-	400–6940	S	-	TRPL
[Scaj10] <sup>367</sup>	$(2\text{--}13) \times 10^3$	-	-	S	-	FCA
[Gulb11] <sup>633</sup>	-	$(1.5\text{--}3) \times 10^4$	$(1\text{--}100) \times 10^4$	S	y	CPP
[Pour11] <sup>691</sup>	-	$1.07 \times 10^3$	$(1.07\text{--}57) \times 10^3$	S	y	FCA
[Kato12] <sup>634</sup>	-	-	$(1\text{--}2) \times 10^3$	S	y	uPCD
[Mori14] <sup>636</sup>	-	-	1500–7500	S	y	uPCD
[Suva15] <sup>659</sup>	-	-	$(3.5\text{--}200) \times 10^4$	S/I	y	FCA
[Asad18] <sup>639</sup>	$(6\text{--}120) \times 10^5$	-	-	M	y	CD
[Ichi18] <sup>641</sup>	-	300–6000	200–2500	S	y	uPCD
[Kato20] <sup>635</sup>	-	400–1950	150–750	S	y	uPCD
[Xian21] <sup>692</sup>	$((6 \pm 7)\text{--}58 \pm 5) \times 10^5$	-	-	M	y	CD
[Kato24] <sup>615</sup>	-	-	100–2500	S	y	uPCD

<sup>a</sup> mesa structure (M), surface (S) or interface (I)

100 µm<sup>59</sup>. Due to the numerous growth parameters<sup>691</sup> a wide range of growth optimizations and surface treatments were proposed. Nevertheless, it seems that mechanically polishing surfaces, which leads to a significant roughness, delivers bad results (high velocities)<sup>536</sup>. The most recent values of < 200 cm/s indicate high surface qualities. The amount of publications in the recent years also shows that this is an active field of research.

Publications referencing other publications often combine multiple values to achieve reasonable values, e.g.,  $s = (1-100) \times 10^3 \text{ cm/s}$ <sup>14,57</sup>,  $s = 2 \times 10^3 \text{ cm/s}$ <sup>377</sup>,  $s = 1 \times 10^4 \text{ cm/s}$ <sup>622</sup>,  $s = 1 \times 10^3 \text{ cm/s}$ <sup>502,652</sup>,  $s = 4 \times 10^4 \text{ cm/s}$ <sup>497</sup> and  $s_n = s_p = 1 \times 10^5 \text{ cm/s}$ <sup>673</sup>. Finally, we want to highlight that the values for 4H and 6H are fairly similar<sup>533</sup>.

## 5. Bimolecular Recombination

The bimolecular coefficient  $B$  was determined in several investigations (see Table XVI). The most influential is the one of Galeckas *et al.*<sup>255</sup> (cp. Fig. 25), whereat Institute<sup>57</sup> states that the bimolecular factor is just an estimation. All the studies achieve a value of  $(1.5 \pm 0.5) \times 10^{-12} \text{ cm}^3/\text{s}$ . Exceptions were the investigation by Neimontas *et al.*<sup>252</sup>, whose value is one order of magnitude bigger, and Murata *et al.*<sup>648</sup>, who achieved 3-4 times higher values. In some investigations<sup>497,502,635</sup> deliberately only the radiative component with a value of  $(1-3) \times 10^{-14} \text{ cm}^3/\text{s}$ <sup>205</sup> was used for the bimolecular parameter  $B$ . The rather high values of  $B$  compared to the radiative part is explained by the additionally included trap-assisted Auger recombination<sup>255</sup> and electron-acceptor (e-A) recombination<sup>648</sup>.

## 6. Auger Recombination

The most fundamental research on Auger coefficients in 4H-SiC was conducted by Galeckas *et al.*<sup>255</sup>, who provided separate values for electrons ( $C_n$ ) and holes ( $C_p$ ). This is, so far, the only publications that did that. Following publications achieved, in general, similar combined coefficients (see Table XVII) and thus confirmed the results. Solely Grivickas *et al.*<sup>285</sup> and Tawara *et al.*<sup>524</sup> derived parameters that are one order of magnitude smaller. Interesting are also the results by Tanaka, Nagaya, and Kato<sup>652</sup>, who identified a dependency of the Auger parameter on the excess carrier concentration  $\Delta_N$ . In the investigations by Murata *et al.*<sup>648</sup> Auger recombination turned out to be not important for an Aluminum doping concentration of  $1 \times 10^{19}/\text{cm}^3$  but

TABLE XVI. Fundamental investigations of the bimolecular recombination parameter.

ref.	$B$ [cm <sup>3</sup> /s]	$T$ [K]	interval [1/cm <sup>3</sup> ]	method
[Gale97] <sup>255</sup>	$1.50 \times 10^{-12}$	300	$(1\text{--}1000) \times 10^{16}$	FCA
[Neim06] <sup>252</sup>	$(3 \pm 1) \times 10^{-11}$	-	$(1\text{--}2000) \times 10^{16}$	FWM
[Scaj10] <sup>367</sup>	$(1.2 \pm 0.2) \times 10^{-12}$	298	-	FCA
[Tawa16] <sup>524</sup>	$1.3 \times 10^{-12}$	300	$(3\text{--}70) \times 10^{17}$	TRPL
	$0.94 \times 10^{-12}$	523	$(3\text{--}70) \times 10^{17}$	TRPL
[Mura21] <sup>648</sup>	$5.6 \times 10^{-12}$	293	$(1\text{--}100) \times 10^{17}$	TRPL
	$4.5 \times 10^{-12}$	523	$(1\text{--}100) \times 10^{17}$	TRPL
[Tana23a] <sup>660</sup>	$<2 \times 10^{-12}$	-	$(2\text{--}10) \times 10^{18}$	FCA

TABLE XVII. Auger recombination parameters.

ref.	$C_n$ [cm <sup>6</sup> /s]	$C_p$ [cm <sup>6</sup> /s]	$T$ [K]	method	$\Delta_N$ [1/cm <sup>3</sup> ]
[Gale97] <sup>255</sup>	$(5 \pm 1) \times 10^{-31}$	$(2 \pm 1) \times 10^{-31}$	300	FCA	-
[Griv07] <sup>285</sup>	$2 \times 10^{-30}$	-	75	FCA	-
[Scaj10] <sup>367</sup>	$(7 \pm 4) \times 10^{-31}$		298	FCA	$(1\text{--}3) \times 10^{18}$
	$(0.8 \pm 0.2) \times 10^{-31}$		298	FCA	$(1\text{--}10) \times 10^{19}$
[Scaj13] <sup>497</sup>	$(5 \pm 1) \times 10^{-31}$	-		FCA	-
[Tawa16] <sup>524</sup>	$1.6 \times 10^{-30}$	-	300	TRPL	-
	$0.44 \times 10^{-30}$	-	523	TRPL	-
[Zhan18] <sup>469</sup>	$7.25 \times 10^{-31}$	$1.21 \times 10^{-31}$	-	-	-
[Tana23] <sup>652 a</sup>	$7.4 \times 10^{-19}$	$\Delta_N^{-0.68}$	-	FT	-
[Tana23a] <sup>660</sup>	$<3 \times 10^{-31}$	-		FCA	-

<sup>a</sup> fitting to measurements by Ščajev *et al.*<sup>367</sup>

considerable for a Nitrogen doping in mid  $1 \times 10^{18}/\text{cm}^3$  range.

We want to highlight that there were also some values based on 6H<sup>688</sup> used for 4H<sup>82,101</sup> and even some based on Silicon<sup>182,292</sup> for 4H<sup>276</sup>. Zhao *et al.*<sup>105</sup> simply assumed  $C_n = C_p = 1 \times 10^{-28} \text{ cm}^6/\text{s}$ . For the results presented by Tawara *et al.*<sup>524</sup> we concluded from the description of

TABLE XVIII. Parameters for Auger model shown in Eq. (49)

ref	type	$A$ [cm <sup>6</sup> /s]	$B$ [cm <sup>6</sup> /s]	$D$ [cm <sup>6</sup> /s]	$H$	$N_0$ [1/cm <sup>3</sup> ]	$T_0$ [K]
. [Loph18] <sup>320</sup>	electron	$6.7 \times 10^{-32}$	$2.45 \times 10^{-31}$	$-2.2 \times 10^{-32}$	3.47	$10^{18}$	300
	hole	$7.2 \times 10^{-32}$	$4.5 \times 10^{-33}$	$2.63 \times 10^{-32}$	8.26	$10^{18}$	300
[Zhan18] <sup>469</sup>	electron	$5 \times 10^{-31}$	$2.45 \times 10^{-31}$	$-2.2 \times 10^{-32}$	0	-	-
	hole	$9.9 \times 10^{-32}$	$4.5 \times 10^{-33}$	$2.63 \times 10^{-32}$	0	-	-

samples and measurement (low injection and highly n-doped material) that  $C_n$  was measured and added it appropriately to the table.

For a comparison of the temperature dependency models in Eq. (47) and Eq. (48) we use the parameters shown in Eq. (55), Eq. (56) and Eq. (57).

$$\alpha = 0.45 \text{ meV/K} \quad (55)$$

$$B_{CE}(T) = 3.5 \times 10^{-9} T^{-3/2} \text{ cm}^3/\text{s} \quad (56)$$

$$a_{SC} = 7.8 \times 10^{16} \text{ K/cm}^3 \quad (57)$$

In a graphical representation (see Fig. 27) a contradiction among the models can be observed. Dedicated 4H-SiC models and measurements predict a decrease of  $C$  with increasing temperature, which confirms the prediction that Auger recombination is not significant for power devices operated at high temperatures Bellone *et al.*<sup>145</sup>. In contrast, the models used for Silicon predict an increase of  $C$ .

Finally, Lophitis *et al.*<sup>320</sup> present parameters for the model shown in Eq. (49) (see Table XVIII). We found these values also as default in some TCAD simulation suites, which, in general, correspond to Silicon. Thus, these values have to be handled with care.

For Auger recombination there is one main reference in literature, namely Galeckas *et al.*<sup>255</sup> (see Fig. 25).

Finally, we combine all contributions to the lifetime into one plot, showing the lifetime over the excess carrier concentration (see Fig. 28). For the SRH lifetimes we added all measurements that clearly specified the excess carrier concentrations. In this log-log representation the bimolecular and Auger coefficients only cause a horizontal shift while the derivative (-1 for bimolecular, -2 for Auger) stays constant. Overall, it can be noted that the higher the value of  $\tau_{SRH}$  the earlier and more pronounced the impact of the bimolecular recombination. A decrease due to Auger recombination

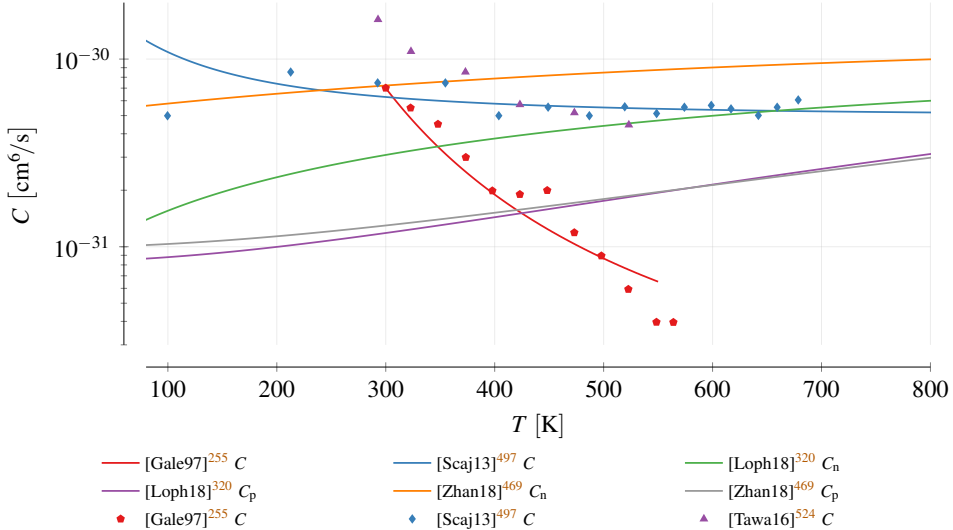


FIG. 27. Temperature dependency of the Auger recombination coefficients  $C_n$  and  $C_p$  for  $\Delta_N = 2.5 \times 10^{18}/\text{cm}^3$

only gets significant for  $\Delta_N > 10^{18}/\text{cm}^3$ . Interestingly, there seem to be measurements that extract SRH values in regions where bimolecular resp. Auger recombination should be already very pronounced.

## VI. INCOMPLETE IONIZATION

It is indispensable to add a doping to a semiconductor, i.e., to introduce impurity atoms, in order to create sophisticated electronic devices. These so-called dopants add energy levels near to the conduction (n-type doping) resp. valence band (p-type doping) such that free charge carrier can be injected at moderate temperatures. In this fashion the electrical characteristics of the material can be altered. Partial overviews on available doping elements and their respective activation energies in 4H-SiC are available<sup>13,14,23,53,72,74,75,120,123,162,249,259,332,333,360,397,552,562,607,694,695</sup>. Uncommon elements were also investigated. Ab initio calculations by Miyata, Higashiguchi, and Hayafuji<sup>696</sup> identified Arsenic<sup>697</sup>, Gallium<sup>698</sup> or Antimony as, energy level wise, fitting. Group IV elements were investigated by Krieger *et al.*<sup>699</sup>, Feng and Zhao<sup>249</sup>, Huang *et al.*<sup>574</sup> focused on Tantalum and Chromium and Dalibor *et al.*<sup>561</sup>, Dalibor and Schulz<sup>562</sup> on Vanadium. Additional factors such as the activation rates<sup>700</sup> or the impact of hydrogen<sup>573</sup> might, however, prevent the deployment of these dopants.

Due to the wide bandgap of 4H-SiC the respective dopant activation energies are large such

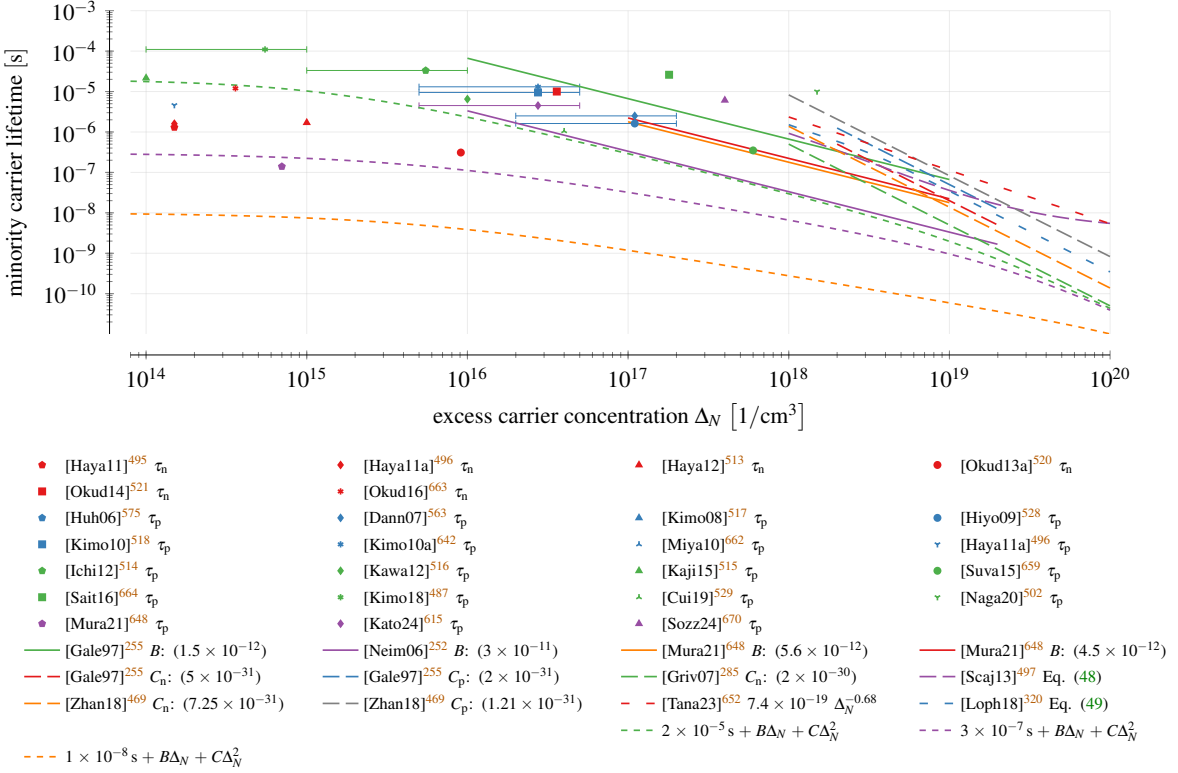


FIG. 28. Charge carrier lifetime considering the contributions of SRH, bimolecular (solid lines) and Auger (dashed lines). The overall recombination lifetime  $\tau_r$  (dotted line) is shown for different values of  $\tau_{\text{SRH}}$ ,  $\tau_{\text{bim}} = 3 \times 10^{-11} \text{ s}$ <sup>252</sup> and  $\tau_{\text{Auger}} = 2 \times 10^{-30} \text{ s}$ .

that the often used assumption of full ionization is not applicable. Quite the opposite: incomplete ionization has to be carefully considered to correctly predict the amount of free charge carriers and, thus, achieve a realistic conductivity<sup>701,702</sup>.

In this section we will, thus, review measurements, models and TCAD parameters used to described the amount of ionized dopants depending on temperature and doping concentration. We focus on the four most common doping species in 4H-SiC<sup>84,154,703</sup>: Aluminum (analysis by Darmody and Goldsman<sup>135</sup>) and Boron for p-type resp. Nitrogen and Phosphorous for n-type doping. We limit ourselves to simple model, e.g., a single energy level per lattice site (cubic or hexagonal). Depending on various parameters, e.g., binding type and location<sup>136,395,584,598</sup> or whether the impurity is located in a non-neutral regions or not<sup>702</sup>, rather elaborate descriptions would be necessary to account otherwise<sup>235</sup>.

## A. Theory

A good overview on the the physical descriptions of incomplete ionization is provided by<sup>84</sup>. In brief, the amount of ionized dopants can be modeled by the Fermi-Dirac distribution<sup>171,274,331,333,704</sup>, also known as steady-state Gibbs distribution<sup>702</sup>, as

$$\begin{aligned} N_D^+ &= \frac{N_D}{1 + g_D \exp\left(\frac{E_{F,n} - E_D}{k_B T}\right)} \\ N_A^- &= \frac{N_A}{1 + g_A \exp\left(\frac{E_A - E_{F,p}}{k_B T}\right)} \end{aligned} \quad (58)$$

where  $N_A$  resp.  $N_D$  are the active acceptor resp. donor concentrations,  $E_A$  resp.  $E_D$  the acceptor resp. donor energy levels,  $E_{F,n}$  resp.  $E_{F,p}$  the electron resp. hole Fermi level and  $g_D$  resp.  $g_A$  the degeneracy factors. The latter denote the degeneracy of the energy levels<sup>201</sup>, whereat in the literature commonly the values  $g_A = 4$  (spin up and spin down plus two valence bands) and  $g_D = 2$  (spin up and down)<sup>596,701</sup> are used. There are, however, exception: Troffer<sup>63</sup> used  $g_D = 6$ , Scaburri<sup>84</sup>, Laube *et al.*<sup>705</sup> a spin degeneracy of  $g_D = 4$  for Phosphorous, Balachandran, Chow, and Agarwal<sup>283</sup>, Nawaz<sup>284</sup>  $g_A = g_D = 3$ , Persson and Lindefelt<sup>399</sup>  $g_A = 2$ , Lv *et al.*<sup>706</sup>  $g_A = g_D = 2$  and Pernot *et al.*<sup>239</sup>  $g_k = 6$  resp.  $g_h = 2$  for the cubic resp. hexagonal site of Nitrogen. There were also efforts to introduce a temperature dependency as  $G_A(T)$  and  $G_D(T)$ <sup>23,49,62,63,84,589,707</sup> based on the energy separation of excited states, whereat the description by Lophitis *et al.*<sup>320</sup> (equ. (11)) deviates significantly.

If solely Boltzmann statistics are considered Eq. (58) can be simplified to<sup>68,84,101,123,325</sup>

$$\begin{aligned} N_D^+ &= \frac{N_D}{1 + g_D \frac{n}{n_1}}, & n_1 &= N_C \exp\left(-\frac{\Delta E_D}{k_B T}\right) \\ N_A^- &= \frac{N_A}{1 + g_A \frac{p}{p_1}}, & p &= N_V \exp\left(-\frac{\Delta E_A}{k_B T}\right) \end{aligned} \quad (59)$$

with  $N_C$  resp.  $N_V$  the effective density of states in the conduction resp. valence band (see Section II) and  $\Delta E_D = E_C - E_D$  resp.  $\Delta E_A = E_A - E_V$  the ionization energies of donors and acceptors relative to the conduction ( $E_C$ ) and valence band ( $E_V$ ). This representation is often preferred in TCAD simulation tools, which commonly operate on charge carrier concentrations.

For completeness we want to highlight that using the neutrality equation<sup>84</sup>

$$N_D^+(E_F) + p(E_F) = N_A^-(E_F) + n(E_F) \quad (60)$$

it is possible to even get rid of the carrier concentration. If we assume a highly donor doped material ( $p(E_F)$  can be neglected) and no compensation ( $N_A^-(E_F) = 0$ ) Eq. (60) results, by inserting Eq. (59) for  $N_D^+$ , in a quadratic equation for  $n$  which can be solved to<sup>154,177,181,292,326,327,606</sup>

$$N_D^+ = N_D \frac{-1 + \sqrt{1 + 4 g_D \frac{N_D}{N_C} \exp\left(\frac{\Delta E_D}{k_B T}\right)}}{2 g_D \frac{N_D}{N_C} \exp\left(\frac{\Delta E_D}{k_B T}\right)} . \quad (61)$$

The ionization energies also depend on the doping concentration. This can be explained by the changing potential energy of the charge carriers when they are closer to the ionized atoms, effectively shielding them<sup>708</sup>. To model the decrease in the ionization energy the Pearson-Bardeen<sup>708</sup> expression

$$\Delta E(N) = \Delta E_0 - \alpha N^{1/3} \quad (62)$$

is used. Nice discussion of topic also by Schöner<sup>709</sup>, i.e., additional models described.

The literature is inconsistent on what dopants should be included into the overall doping concentration  $N$  in Eq. (62). Some authors include both donors and acceptors  $N_A + N_D$ <sup>68,325</sup>, others only the respective donor concentration ( $N_A$  or  $N_D$ )<sup>15,50,578,589,710,711</sup>, while a third group just uses the ionized ones<sup>52</sup>. Kajikawa<sup>712</sup> even argues that the compensating dopants, i.e., donors for the acceptor levels and vice versa, have the bigger impact and should be used instead of the overall donor and acceptor concentrations. There have also been proposals to include the compensating dopants into the factor  $\alpha$ <sup>84,713</sup>. Finally, a completely different approach focuses on the degree of compensation depicted by a screening of free charge carriers<sup>84,714</sup>, which introduces an additional temperature dependency.

An alternative approach to the Pearson-Bardeen expression in Eq. (62) is given by Altermatt, Schenk, and Heiser<sup>715</sup>, Altermatt *et al.*<sup>716</sup>, who used the logistic equation

$$\Delta E(N) = \frac{\Delta E_0}{1 + (N/N_E)^c} \quad (63)$$

to model the decrease in ionization energy, with  $N_E$  a reference concentration where the ionization energy is half its original value  $\Delta E_0$ . Darmody and Goldsman<sup>135</sup> argue that with Eq. (62) it is possible to shift the dopant level into the conduction/valence band and thus ionize all dopants immediately, which is neither physically reasonable nor possible with Eq. (63). Despite these arguments, the described approach has not yet found its way into the major simulation tools.

Dopants have differing ionization energies depending on whether they are located in a hexagonal or a cubic lattice site<sup>34</sup> (see ??). Consequently Eq. (59) has to be adapted to<sup>68,697</sup>

$$N_D^+ = \frac{\frac{1}{2}N_D}{1 + g_D \frac{p}{N_C} \left( \frac{\Delta E_{Dh}}{k_B T} \right)} + \frac{\frac{1}{2}N_D}{1 + g_D \frac{p}{N_C} \left( \frac{\Delta E_{Dc}}{k_B T} \right)}$$

$$N_A^- = \frac{\frac{1}{2}N_A}{1 + g_A \frac{p}{N_V} \left( \frac{\Delta E_{Ah}}{k_B T} \right)} + \frac{\frac{1}{2}N_A}{1 + g_A \frac{p}{N_V} \left( \frac{\Delta E_{Ac}}{k_B T} \right)}$$

with  $E_{Dc}$  and  $E_{Dh}$  the cubic resp. hexagonal ionization energies for donors and  $E_{Ac}$  and  $E_{Ah}$  for acceptors. The factors 1/2 denote that both lattice sites are equally probable<sup>101</sup>. In TCAD simulations it is often the case that these separate values are merged to an effective energy level, ending up once again in a description as shown in Eq. (59)<sup>69,155,292,325,332</sup>. The effects of such simplifications have been investigated by Lades<sup>65</sup>, Ayalew *et al.*<sup>549</sup>.

For more accurate approximation of dynamic processes around the dopant, i.e., (de)trapping of charge carriers, the electron and hole cross sections are crucial (see Section V). There are multiple description available in literature, which differ in their temperature scaling<sup>506</sup>. The multi-phonon capture model is independent of temperature<sup>709,717–719</sup> while the cascade capture model is proportional to  $T^{-2}$ <sup>256,709,720,721</sup> (also [78Aba] in Schöner<sup>709</sup>). Kaindl *et al.*<sup>722</sup> argue that the latter delivers a better fit. A scaling with  $T^{-3}$  was used by Kuznetsov and Zubrilov<sup>244</sup>. Note that we discovered large discrepancies between the single tools regarding which models are supported.

## B. Results

Gorban *et al.*<sup>723</sup> uses hexagonal value 66 of Ikeda, Matsunami, and Tanaka<sup>34</sup> to get cubic one. The most commonly method to determine the ionization energy of dopants in literature is to fit the neutrality equation, i.e., for p-type doping

$$p + N_K = \frac{N_A}{1 + \frac{g_A p}{N_V} \exp \left( \frac{\Delta E_A}{k_B T} \right)}.$$

to Hall measurements, e.g., conductivity or charge carrier concentration, for varying temperature<sup>15,49–51,62,63,202,231,239,256,392,557,560,576,579,580,584,586,590,594,596,603,605,606,698,711,712,724–738</sup>. The compensation doping density  $N_K$  is only required for fitting purposes, such that we solely use  $N_A$  as the doping density to present our results. Due to the anisotropy of the Hall effect it is possible to achieve direction dependent ionization energies this way<sup>62</sup>. Other approaches based on Hall measurements include the fitting to the activation ratio<sup>739</sup> or free carrier concentration spectroscopy

(FCCS)<sup>578,589,740</sup>. Further used electrical measurements are (thermal)<sup>295,741–743</sup> admittance spectroscopy (AS)<sup>61–63,256,580,698,711,722</sup>, electron spin resonance (ESR) measurement<sup>744</sup>, deep level transient spectroscopy (DLTS)<sup>62,244,610,745</sup> and minority carrier transient spectroscopy (MCTS)<sup>610</sup>, which are often combined with Hall measurements for more accurate results. Troffer<sup>63</sup> notes that DLTS is more sensitive but admittance spectroscopy allows to depict time constants below 1  $\mu$ s.

These electrical methods are complemented by optical ones, e.g., (fourier transform infrared) photothermal ionization spectroscopy (PTIS)<sup>250</sup>, donor-acceptor pair (DAP) luminescence<sup>34,41,251,398</sup>, free to acceptor (FTA) spectroscopy<sup>34</sup>, infrared absorption (IA)<sup>202</sup>, photoluminescence (PL)<sup>317,404,406,580,602</sup>, time-resolved spectroscopy (TRS)<sup>317</sup> or delay measurements (DM)<sup>317</sup>. In these cases electrons are empowered and the resulting photon emission is recorded. The latter can be cause by transitions among traps or between traps and the conduction/valence band<sup>62</sup>. Note that different methods lead to slightly deviating results, even when applied to the same device<sup>202</sup>. Also possible are calculations, e.g., Faulkner model (FM) calculations<sup>42</sup>, density functional theory (DFT)<sup>220,696</sup>, effective mass approximation (EMA)<sup>224</sup>, first principles calculations (FPC)<sup>136,573,574</sup> or *ab initio* supercell calculations (AISC)<sup>746</sup>. Finally, some authors define a value range based on measurements in literature<sup>65,101,154</sup>, calculate an average values<sup>588</sup> or fit to existing data<sup>68,82,135</sup>.

In the sequel we are going to present the ionization energies  $\Delta E_D$  resp.  $\Delta E_A$  found in literature with their respective doping concentration. In order to draw the measurements we dropped uncertainties and replaced the sometimes stated exciton energy  $E_X$  with 20 meV (see Section III). We had to discard results where the samples were solely described as "high purity" or "unintentional doping"<sup>404,406,560,602</sup> and Laube *et al.*<sup>705</sup>, which was superseded by a publication of the same authors. We mark results for the hexagonal lattice site by a trailing "h" and result for the cubic one by a trailing "c". The latter is often also denoted by the letter "k", which, most probably, corresponds to the german word "kubisch" for cubic. In fact, some of the literature is written in german<sup>62,63</sup>, making it hard to retrace the results for the international community.

For Aluminum (see Fig. 29) many measurements and model fittings have been proposed. The values are equally distributed across the last three decades, meaning that the improvements in material quality did not result in significant changes. The model proposed by Achatz *et al.*<sup>710</sup> uses the critical aluminum concentration for the doping-induced metal-insulator transition to set  $\Delta E_A = 0$  and then fit the parameters. This is in contrast to the logistic equation in Eq. (63) used by Darmody and Goldsman<sup>135</sup>, where a much slower decrease of  $\Delta E_A$  below 100 meV can be observed.

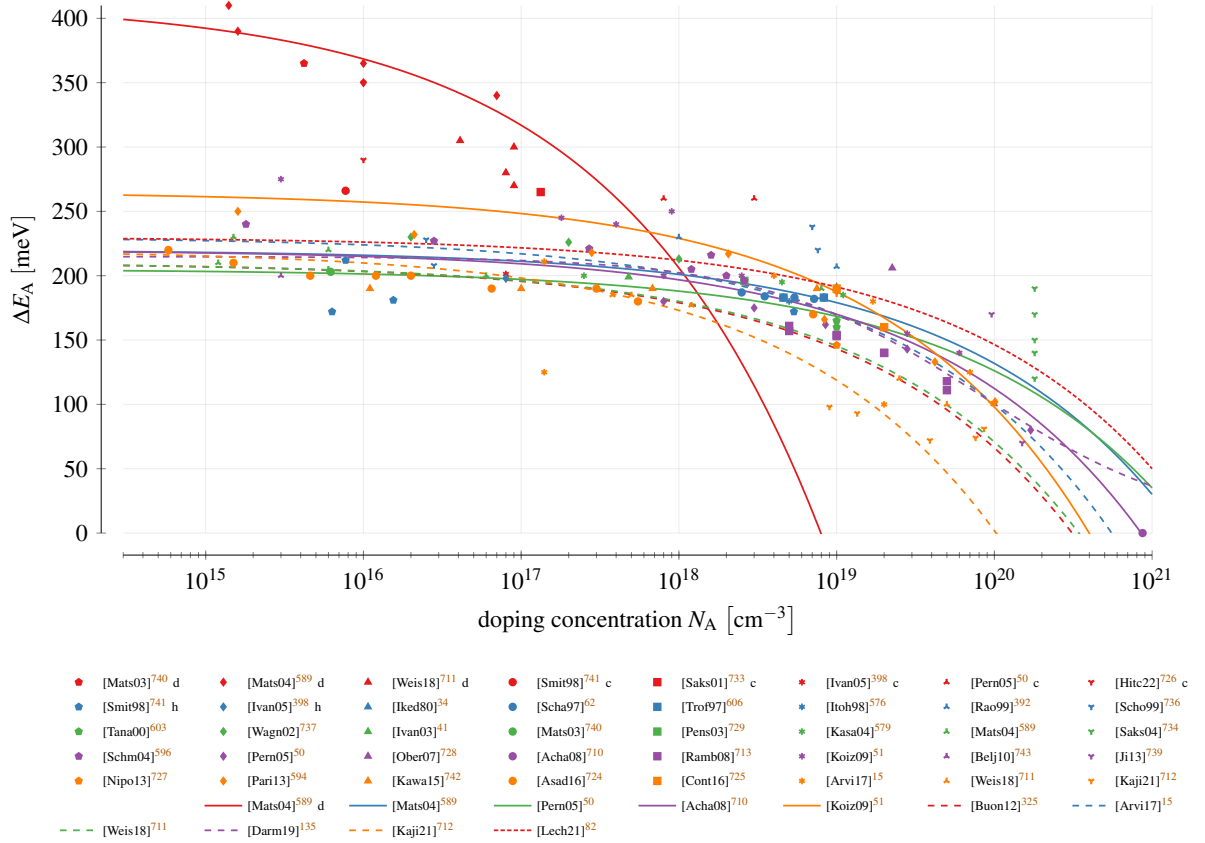


FIG. 29. Aluminum ionization energy. Marks refer to measurements and lines to fittings. The letter 'd' after the reference indicates a deep level whose origin is still discussed (see text). Colors are used solely to increase the readability.

For low-doped and compensated devices a second energy level is required to properly describe the measurements<sup>50</sup>. The origin of this deep level is still discussed in literature. Matsuura *et al.*<sup>589,740</sup> were not able to provide any explanation, Weiße *et al.*<sup>711</sup> suspect excited states of the aluminum ground state and Pernot, Contreras, and Camassel<sup>50</sup>, Smith, Evvaraye, and Mitchel<sup>741</sup> describe them as the cubic lattice site. In fact, Smith, Evvaraye, and Mitchel<sup>741</sup> states that for higher concentration only the hexagonal site is measured. Nevertheless, in our plots we show the data as presented by the original authors, with the exceptions of the ones by Saks *et al.*<sup>733</sup>, which Pernot, Contreras, and Camassel<sup>50</sup> pointed out to denote the cubic lattice site.

Aluminum is the single dopant where a fitting using the logistic approximation (see Eq. (63)) was used. Darmody and Goldsman<sup>135</sup> achieved  $\Delta E_0 = 214.86 \text{ meV}$ ,  $N_E = 8.12 \times 10^{19} / \text{cm}^3$  and  $c = 0.632$ .

The available measurements for Boron (see Fig. 30) are very few and date back to the last

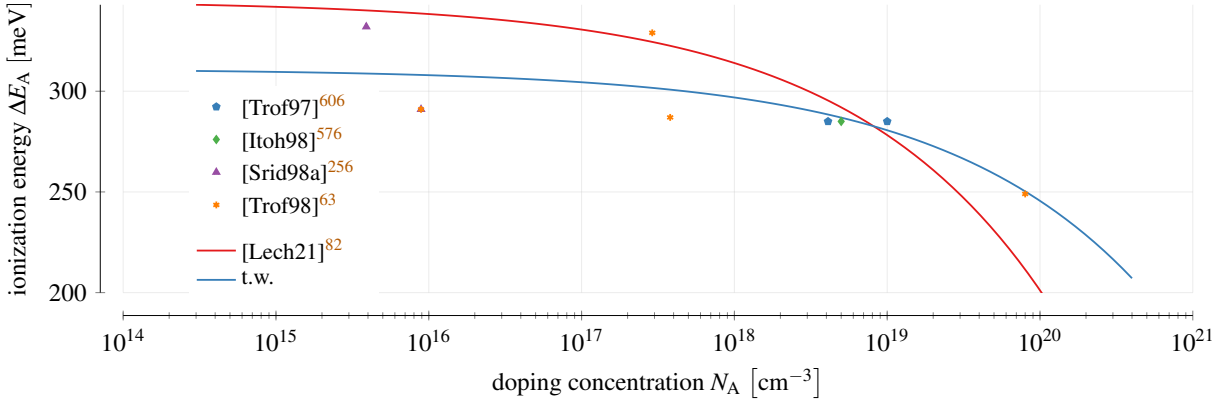


FIG. 30. Boron ionization energy. Marks refer to measurements and lines to fittings. Colors are used solely to increase the readability.

millennium. We suspect the main cause in the deep D-center<sup>63,135,136</sup> that comes with a Boron doping. It introduces an energy level in a range of 495–630 meV<sup>34,63,244,251,256,610</sup>, which results in a very effective recombination center. In some publications and also in some simulation tools the D-center level is used as the actual Boron one<sup>34,57,70,251,259,402,404,567</sup>. Since only a single fitting according to Eq. (62) is available for Boron we used all the available data to generate an additional one (t.w.).

For the n-type donor Nitrogen (shown in Fig. 31) almost all publications distinguish between cubic and hexagonal site. However, there is also a big spread in the data, especially towards higher doping concentrations. The results suggest that the ionization energy does not decrease (especially for the cubic lattice site) even as the solubility limit ( $1 \times 10^{19} \text{ cm}^3$  for annealing at 1700 K up to  $3 \times 10^{20} \text{ cm}^3$  for annealing at 2500 K<sup>60,70,397,398,747</sup>) is approached.

For Nitrogen only fittings according to Eq. (62) are available. Kagamihara *et al.*<sup>578</sup> provided a fitting for both hexagonal and cubic lattice site, which were combined by Hatakeyama, Fukuda, and Okumura<sup>68</sup> to an effective ionization energy model. The remaining fittings also represent effective levels but are surprisingly low. In the case of Buono<sup>325</sup> this can be explained by the selection of  $\Delta E_0$ , which was picked as the effective value of 65 meV determined by Bakowski, Gustafsson, and Lindefelt<sup>69</sup> based on the values from Götz *et al.*<sup>202</sup>. The latter, as can be seen in the figure, were, however, determined for a doping of  $1 \times 10^{17} / \text{cm}^3$  resp.  $1 \times 10^{18} / \text{cm}^3$ .

Compared to Nitrogen a lot less measurements are available for Phosphorous (see Fig. 32), all roughly two decades old. Again, hexagonal and cubic lattice site are always distinguished, but the results especially for the latter largely deviate. Due to the lack of fittings according to Eq. (62) we

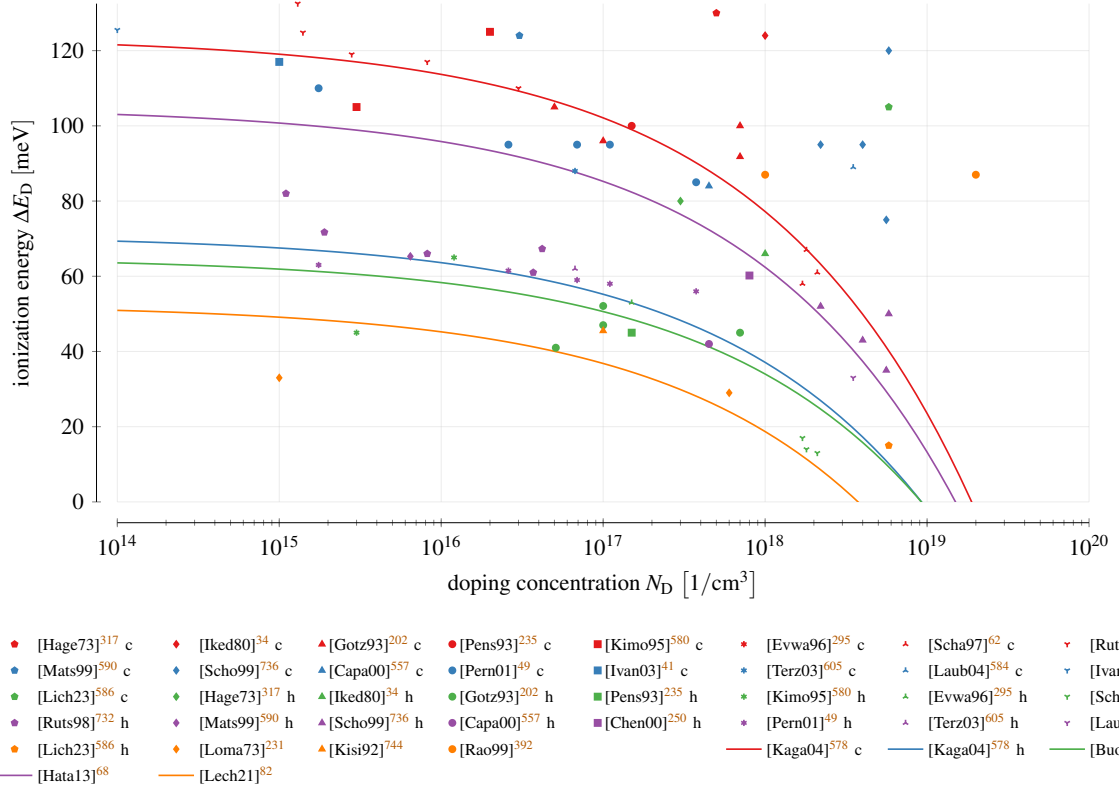


FIG. 31. Nitrogen ionization energy. Marks refer to measurements and lines to fittings. Colors are used solely to increase the readability.

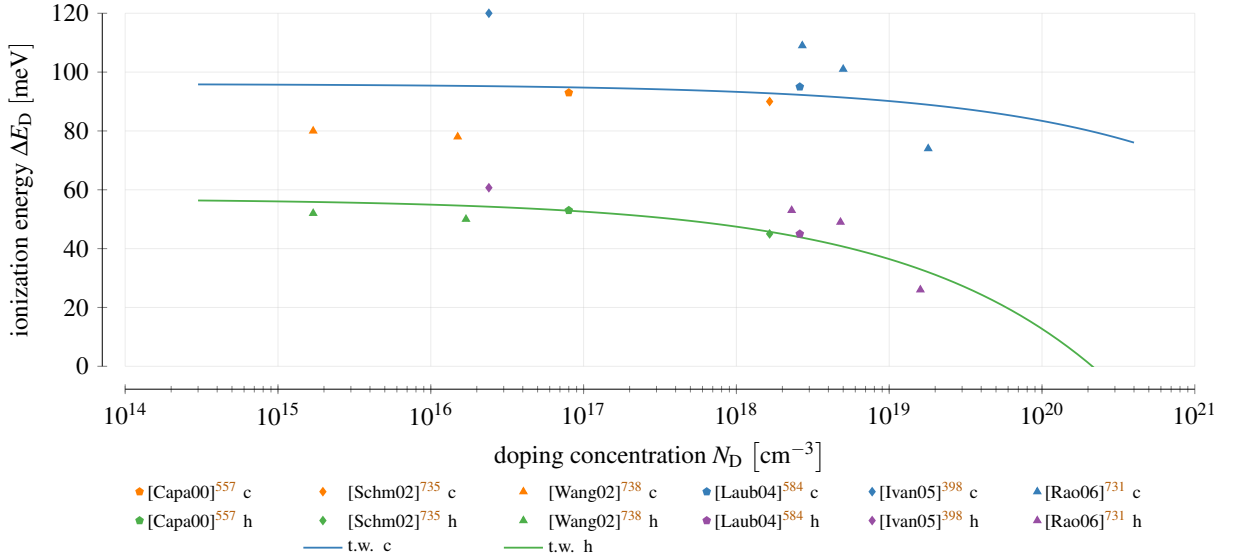


FIG. 32. Phosphorous ionization energy. Marks refer to measurements and lines to fittings. Colors are used solely to increase the readability.

used the available data to generate very crude fittings. Even as the solubility limit ( $6 \times 10^{18} \text{ cm}^3$  for annealing at 1700 K up to  $2 \times 10^{20} \text{ cm}^3$  for annealing at 2500 K<sup>60,70,397,398,747</sup>) is reached high ionization energies for the cubic lattice site are observable.

The parameters for the Pearson-Bardeen model (see Eq. (62)) fittings, which were shown in Figs. 29 to 32, are summarized in Table XIX. We also added our own fitting parameters (t.w.). To take the described inconsistency for  $N$  in Eq. (62) into account column N denotes either the total doping (tot), the n- resp. p-type doping (dop), the compensation (comp) or fitting (fit). For the figures we used uniformly the specific doping concentration  $N_A$  resp.  $N_D$  (x-axis).

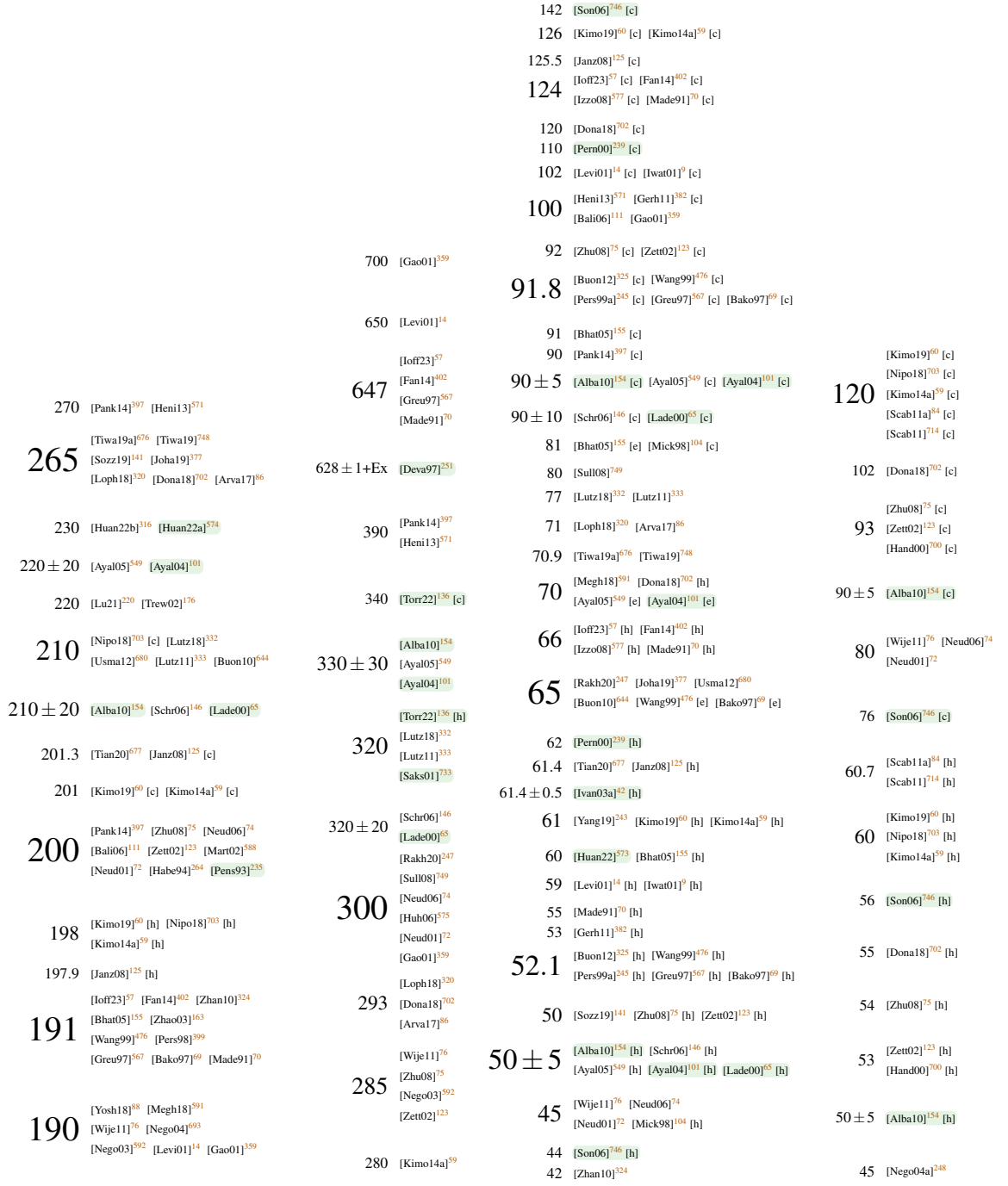
Cross-sections with varying temperature were heavily investigated at the end of the last century (see Table XX). The column  $\sigma$  denotes the cross section with the charge carrier in the energetically closer band (conduction or valence) because the interaction with the other band is significantly lower<sup>63,722</sup>.

Finally we also investigated single energy values used in overviews or in TCAD simulations (see Fig. 33). We do not show fundamental values here as these are always linked to a specific doping concentration. For Aluminum many publications use a value that corresponds to the deeper (cubic site?) energy level. Also for Boron some values refer to the deep D-center. Altogether, a wide range of values is used, especially for Nitrogen, where again hexagonal and cubic sites are almost always distinguished. We want to highlight that for the Boron ionization energy of 293 meV<sup>86,320,702</sup> no direct connection to any fundamental investigation could be inferred.

In some publications the dopant is not clearly specified. Instead only the acceptor and donor energy level are provided (see Fig. 34). While the acceptor values clearly correspond to Aluminum the n-type values could belong to both Nitrogen and Phosphorous.

## C. Discussion

In contrast to other properties that have been investigated within this review, there exist a lot of fundamental studies and measurements for incomplete ionization. Nevertheless, the results acquired over the last decades deviate sometimes significantly, making it impossible to distill them to common values. This is, by the way, not caused by less mature samples in the past. Even by limiting our analysis to the last two decades we did reveal a large spread in measurement results. The situation is worsened by the fact that values for hexagonal and cubic lattice sites are often used without appropriate notation. In this fashion significant errors can be introduced, especially



AI

B

N

P

FIG. 33. Energy levels used in literature for each investigated dopant shown at the bottom. [c] marks cubic, [h] hexagonal and [e] effective values, i.e., a combination of hexagonal and cubic. Nodes with green background indicate a fundamental publication.

TABLE XIX. Parameters for the Pearson-Bardeen model (see Eq. (62)). Column N denotes how the factor  $N$  is interpreted: either as active dopants (dop), all dopants (tot), just the compensating ones (comp) or simply used in a fitting (fit). The site denotes besides hexagonal and cubic also a combined effective energy level (eff) and the deep level for Aluminium (deep). If left blank no information were stated in the paper.

ref.	N	site	$\Delta E$	$\alpha$
			[meV]	[meV cm]
<b>Nitrogen</b>				
[Kaga04] <sup>578</sup>	dop	hex	70.9	$3.38 \times 10^{-5}$
		cubic	123.7	$4.65 \times 10^{-5}$
[Buon12] <sup>325</sup>	tot	eff	65	$3.1 \times 10^{-5}$
[Hata13] <sup>68</sup>	tot	eff	105	$4.26 \times 10^{-5}$
[Lech21] <sup>82</sup>	tot		52.5	$3.38 \times 10^{-5}$
<b>Phosphorous</b>				
t.w.	fit	hex	57	$9.54 \times 10^{-6}$
		cubic	96	$2.71 \times 10^{-6}$
<b>Aluminum</b>				
[Mats04] <sup>589</sup>	dop		220	$1.9 \times 10^{-5}$
[Pern05] <sup>50</sup>	dop		205	$1.7 \times 10^{-5}$
[Acha08] <sup>710</sup>	dop		220	$2.32 \times 10^{-5}$
[Koiz09] <sup>51</sup>	dop		265	$3.6 \times 10^{-5}$
[Buon12] <sup>325</sup>	tot	eff	210	$3.1 \times 10^{-5}$
[Arvi17] <sup>15</sup>	dop		$230 \pm 10$	$(2.8 \pm 0.3) \times 10^{-5}$
[Weis18] <sup>711</sup>	dop		210	$3 \times 10^{-5}$
[Kaji21] <sup>712</sup>	comp		220	$4.7 \times 10^{-5}$
[Lech21] <sup>82</sup>	tot		230	$1.8 \times 10^{-5}$
<b>Boron</b>				
[Lech21] <sup>82</sup>	tot		345	$3.1 \times 10^{-5}$
t.w.	fit		311	$1.41 \times 10^{-5}$

for Boron where the deep levels is approximately twice the shallow one.

Overall, almost all publications utilize values determined from 4H-SiC measurements. Only

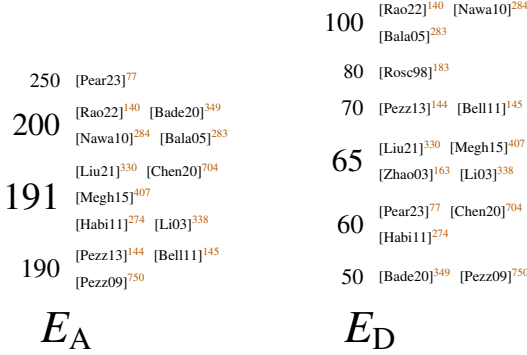


FIG. 34. Energy levels used in literature for acceptors and donors without closer specification of dopant element.

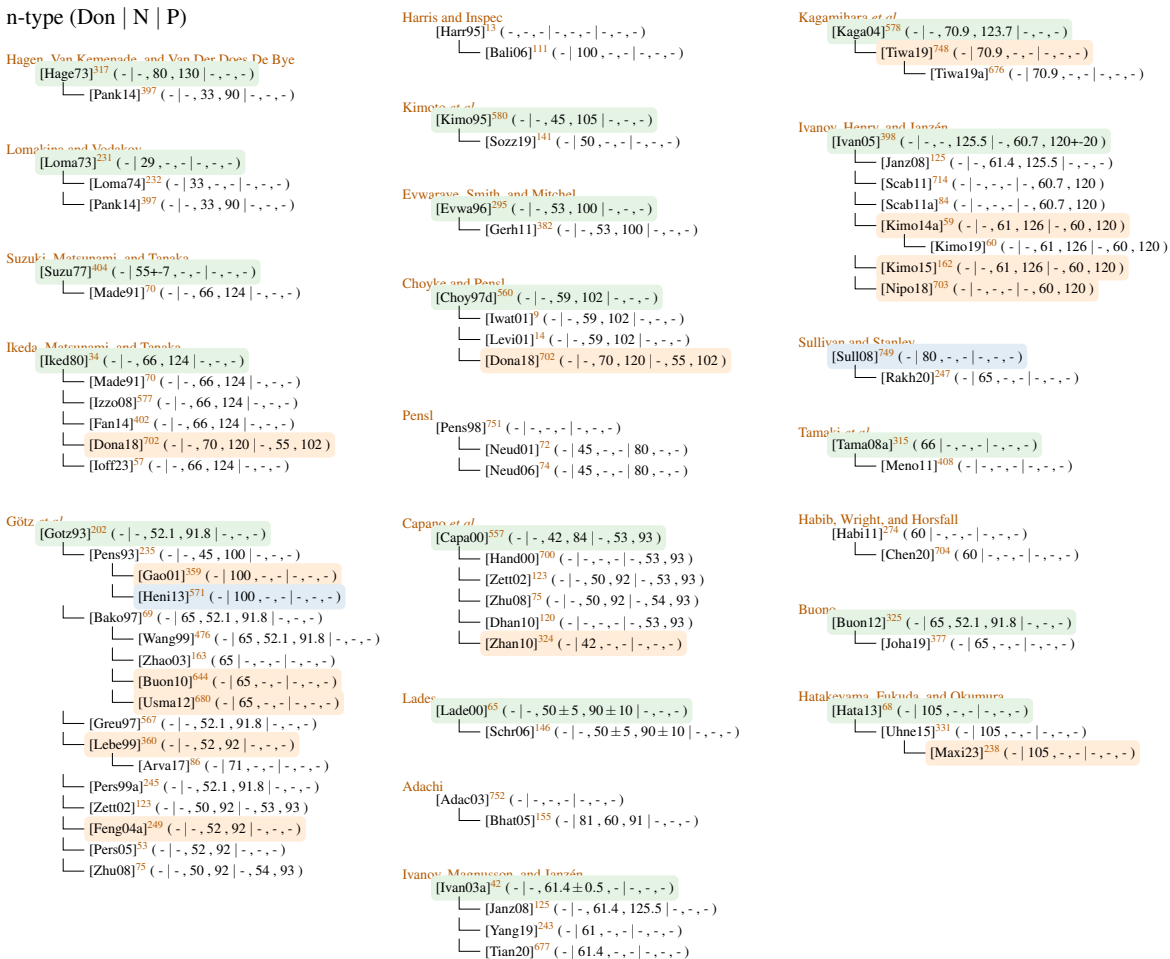


FIG. 35. Reference chain for n-type doping. Entries with green background show fundamental investigations, orange references we inferred based on the used data and blue investigation based not on 4H.

TABLE XX. Dopants and their respective cross sections with the charge carriers in the energetically closer band (conduction or valence). Different temperature dependencies are indicated in the column  $T^\alpha$ . We found no data for Nitrogen.

ref.	site	$T^\alpha$	$\Delta E$ [meV]	$\sigma$ [cm $^2$ ]
<b>Nitrogen</b>				
[Kain99] <sup>722</sup>	cubic	$T^0$	77	$7.92 \times 10^{-15}$
		$T^{-2}$	90	$3.57 \times 10^{-10}$
<b>Aluminum</b>				
[Kuzn95] <sup>244</sup>		$T^{-3}$	229	$8 \times 10^{-13}$
[Scha97] <sup>62</sup>		$T^0$	164–179	$2.2 \times 10^{-13}$
		$T^{-2}$	189–202	$1.7 \times 10^{-13}$
[Kain99] <sup>722</sup>		$T^0$	189	$2.58 \times 10^{-13}$
		$T^{-2}$	208	$2.57 \times 10^{-8}$
[Resh05] <sup>61</sup>		$T^0$	185	$1 \times 10^{-14}$
		$T^{-2}$	210	$1 \times 10^{-13}$
[Belj10] <sup>743</sup>		$T^0$	200	$1 \times 10^{-12}$
[Kawa15] <sup>742</sup>		$T^0$	190	$1.4 \times 10^{-13}$
[Kato22] <sup>745</sup>		$T^0$	120–170	$1 \times 10^{-13}$
<b>Boron</b>				
[Srid98a] <sup>256</sup>		$T^0$	259–262	-
		$T^{-2}$	284–295	-
[Trof98] <sup>63</sup>		$T^0$	292	$6 \times 10^{-15}$
		$T^{-2}$	314	$5 \times 10^{-14}$
[Kain99] <sup>722</sup>		$T^0$	312	$2.1 \times 10^{-14}$
		$T^{-2}$	375	$9.69 \times 10^{-9}$
[Zhan03] <sup>610</sup>		$T^0$	230–280	$2 \times 10^{-13}$

seldomly 6H data were used<sup>247,575</sup>, whereat the values match those from 4H publications<sup>86,320,702</sup>. However, since the latter did not provide a reference for the picked values it is impossible to retrace where and how these values have been determined. Nevertheless we tried to create causality chains for n-type (see Fig. 35) p-type (see Fig. 36) values, whereat quite some values had to be inferred due to missing information.

For n-type doping the values published by Ikeda, Matsunami, and Tanaka<sup>34</sup> are widely used up until this day. Similarly, for p-type doping Götz *et al.*<sup>202</sup> provided for some time the values. However, recently the values by Ivanov, Magnusson, and Janzén<sup>42</sup>, Ivanov, Henry, and Janzén<sup>398</sup>

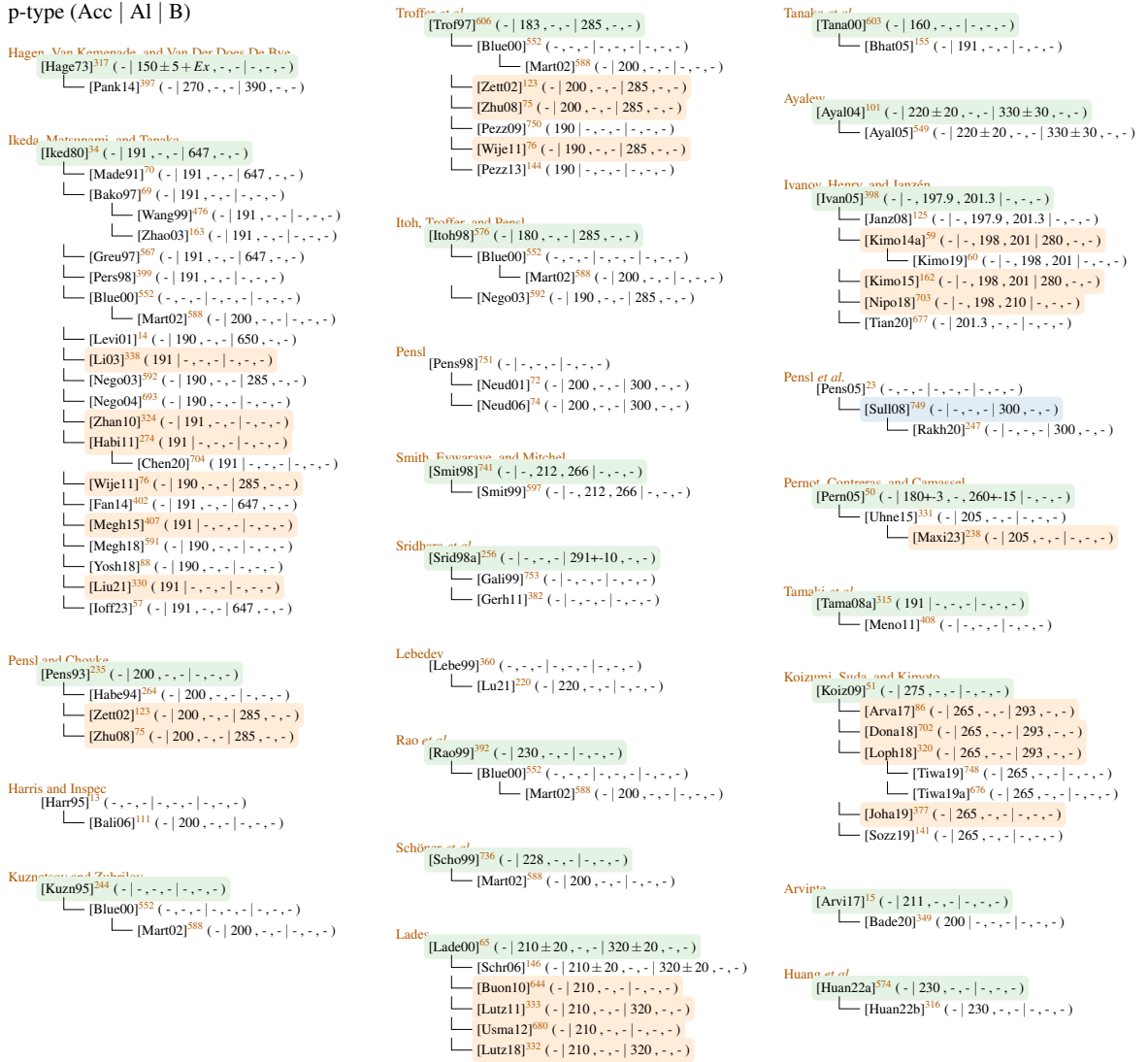


FIG. 36. Reference chain for p-type doping. Entries with green background show fundamental investigations, orange references we inferred based on the used data and blue investigation based not on 4H.

are dominantly cited.

The most research has been clearly directed towards Aluminum. Overall, future research should be denoted to (i) gather additional data for Phosphorous and Boron and (ii) condense the already achieved values. For this purpose we added our own fittings based on the gathered data for cubic and hexagonal lattice site as well as for all values together (effective value).

## VII. MOBILITY

To describe the conductivity  $\rho$  of a material<sup>82</sup>, which is relevant for any transient process, the charge carrier mobility  $\mu$  as shown in Eq. (64)<sup>111,112</sup> is used. In this case,  $n$  denotes the amount of charge carriers and  $\mu_n$  the respective mobility. Different mechanisms may influence the mobility such as the surface, the inversion channel in MOS structures and the bulk<sup>82</sup>, whereat we will investigate here solely the latter. We, thereby, build on the analysis of measurements by Darmody and Goldsman<sup>135</sup> and the summaries of mobility models published by Neila Inglesias<sup>161</sup>, Stefanakis and Zekentes<sup>299</sup> and Tian *et al.*<sup>677</sup>.

$$\rho = \frac{1}{nq\mu_n} \quad (64)$$

Overall, our analyses reveal many investigations targeted toward the mobility.

### A. Theory

Charge carriers in 4H-SiC accelerate along the electric field  $F$  until they are "scattered", i.e., they drastically change their velocity and/or direction by interacting with other particles. It is possible to distinguish (i) phonon (ii) defect and (iii) carrier-carrier scattering, which can be further divided<sup>3</sup>. The most prominent processes for 4H-SiC are acoustic phonon, (non-)polar optical phonon, zero and first order optical intervalley phonon, ionized/neutral impurity and carrier-carrier scattering<sup>50,51,207,515,754</sup>. The mobility defines the average time between two scattering event<sup>65</sup> and thus provides a link between charge carriers and scattering processes<sup>33</sup>. Detailed theoretical analyses of each single contribution is available in literature<sup>3,49–51,161,239,412,755</sup>.

In TCAD tools, however, such detailed models are not convenient<sup>51</sup>. Instead, empirical models are used to describe the mobility in the low-field and high-field region (a detailed explanation follows in the next sections). The mobility, thereby, depends on many factors such as doping concentration<sup>276</sup>, degree of compensation<sup>333</sup>, spatial direction<sup>9,16,158</sup>, temperature<sup>276</sup> and whether majority or minority charge carriers<sup>3</sup> are described. For holes even the separate valence bands (heavy-hole, light-hole, split-off; see Section II)<sup>3,50,105</sup> have to be considered.

In the past years hopping conduction, also denoted as nearest-neighbor-hopping (NNH)<sup>756</sup> or variable-range-hopping (VRH)<sup>756</sup> was described in 4H-SiC. This process describes the tunneling of charge carriers bound to a dopant from one impurity to the next, possibly alternated by some conventional drifting phases in the bands. This effect was described at temperatures below

100 K<sup>712</sup> ant at very high doping concentrations<sup>95,756</sup>. Darmody and Goldsman<sup>135</sup> calculated the critical limit for the latter to  $N_{\text{crit}} \approx 1 \times 10^{20}/\text{cm}^3$ . Since this is a relatively new effect the available information are very limited and we will, thus, not further consider it in this review.

## 1. Low-Field Mobility

For low electric fields exists a direct relationship between the carrier velocity  $v$  and the electric field strength  $F$ <sup>757</sup> as shown in Eq. (65). The impact of phonon and impurity scattering is thereby not independent<sup>146</sup>, meaning that both have to be implemented in the same model.

$$v = \mu(N, T)F \quad (65)$$

Each dopant represents a coulomb scattering center<sup>112</sup> that causes the charge carrier mobility to decrease. To account for this fact an empirical model shown in Eq. (66) was developed by Caughey and Thomas<sup>758</sup>.  $\mu_{\min}$  can be interpreted as the mobility for very high doping where impurity scattering is dominant<sup>161,299</sup> and  $\mu_{\max}$  the highest possible mobility at low doping, i.e., when lattice (phonon) scattering is dominant<sup>82,161,299</sup>.  $N_{\text{ref}}$  denotes the doping concentration where the mobility is exactly in between those values<sup>333,757</sup> and  $\delta$  just how quickly the change from one to the other occurs. Arora, Hauser, and Roulston<sup>759</sup> later simplified the model by replacing the expression  $\mu_{\max} - \mu_{\min}$  by  $\mu_0$ <sup>79</sup>, which will become interesting when we later investigate the temperature dependency.

$$\mu(N) = \mu_{\min} + \frac{\mu_{\max} - \mu_{\min}}{1 + (N/N_{\text{ref}})^{\delta}} \quad (66)$$

There is some disagreement in literature (discussed by Vasilevskiy *et al.*<sup>760</sup>) whether  $N$  denotes all dopants<sup>51,52,60,68,69,79,85,86,101,104,173,207,208,299,316,322,325,468,622,760–764</sup> or just the ionized ones<sup>52,97,324,338,591,693,754,765</sup>. An argument to use all dopants was that this model is just a fitting<sup>299,677</sup> or that also scattering on neutral dopants decreases the mobility. Roschke and Schwierz<sup>757</sup> stated that using something different than the absolute doping for  $N$  did not result in better results but led to convergence issues.

A similar dependency can be observed with changing temperatures. In hot samples more phonons are generated, which increases the probability of a charge carrier's scattering<sup>112,202,276</sup>. In contrast, at low temperatures and high doping concentration (un)ionized impurity scattering is dominant<sup>766</sup>. This is accounted for by scaling the respective parameters with temperature as

shown in Eq. (67)<sup>68,154</sup>. Note that  $\gamma_{\text{NNref}} = -\delta_{\text{ref}}$ .

$$\theta = \theta_{300} \left( \frac{T}{300} \right)^\zeta \quad (67)$$

$$\theta \in [\mu_{\min}, \mu_{\max}, \mu_0, N_{\text{ref}}, \delta, (N/N_{\text{ref}})^\delta] \quad (68)$$

$$\zeta \in [\gamma_{\min}, \gamma_{\max}, \gamma_0, \gamma_{\text{ref}}, \gamma_\delta, \gamma_{\text{NNref}}] \quad (69)$$

We want to highlight that many different names for this combined model exist in literature, featuring sometimes more and sometimes less of the shown temperature scaling factors. Referenced were, among others, the publications by Mohammad *et al.*<sup>767</sup> and Sotoodeh, Khalid, and Rezazadeh<sup>768</sup>. The term Masetti model<sup>276,338</sup> is also used for this model, although the expression proposed by Masetti, Severi, and Solmi<sup>769</sup> actually contains an additional additive term that leads to a further reduction of the mobility at high doping densities (see<sup>770</sup>). Except for Zhang and You<sup>469</sup> the parameters are, however, chosen in a fashion that the description in Eq. (66) is achieved<sup>82,318</sup>.

$$\mu(N) = \mu_{\min} + \frac{\mu_{\max} - \mu_{\min}}{1 + (N/N_{\text{ref}})^\delta} - \frac{\mu_1}{1 + (N_{\text{ref2}}/N)^\kappa} \quad (70)$$

In this model each parameter has a constant temperature scaling parameter. However, depending on the dominant scattering process vastly deviating temperature dependencies have been observed<sup>60</sup>. While acoustic phonon scattering shows a decrease proportional to  $T^{-1.5}$ <sup>65,713,730,761,771</sup> the decline proportional to  $T^{-2.6}$  was attributed to nonpolar optical phonon scattering<sup>51,771</sup> ( $T^{-2.5}$  for optical-mode phonons<sup>65</sup>). For the latter Adachi<sup>3</sup> states, however, a dependency according to  $T^{-1.5}$ . Ionized impurities scale with  $T^{3/2}$ <sup>207,622,713,730</sup> and neutral impurities with  $T^0$ <sup>3,207,622</sup> while coulomb scattering scales with  $T^1$  and phonon scattering with  $T^{-1}$ <sup>375</sup>. This makes the model presented in Eq. (66) not adequate for large temperature swings<sup>772</sup>. A different approach was shown by Schröder<sup>146</sup>, p. 668 who defined equations below/above 200 K with deviating temperature scaling, but only provided parameters for Si.

To account for the changing temperature behavior Izzo *et al.*<sup>577</sup> used the phenomenological function shown in Eq. (71), without however specifying the values of  $A$  and  $B$ . This description features an increasing mobility due to ionized impurity scattering at low temperature ( $T^{3/2}$ ) and a adjustable decrease for high temperatures, e.g.,  $n = 3.06$  in this case. This corresponds to the values by La Via *et al.*<sup>585</sup>.

$$\mu(T) = \left( \frac{A}{T^{3/2}} + \frac{B}{T^{-n}} \right)^{-1} \quad (71)$$

Rambach *et al.*<sup>713,730</sup> stated that the parameters of Eq. (66) should be dependent on the doping concentration, without, however, explicitly stating a mathematical expression for these. Rambach, Bauer, and Ryssel<sup>713</sup> also proposes a single temperature scaling for all parameters. Another possibility is to use only a single multiplicative factor for the temperature scaling, that is, however, structured according to the CT equation itself as shown in Eq. 72 and Eq. 73<sup>578,589</sup>.

$$\mu_p(T, N_A) = \mu_p(300, N_A) \left( \frac{T}{300} \right)^{\beta_p(N_A)} \quad (72)$$

$$\beta_p(N_A) = \beta_{\min} + \frac{\beta_{\max} - \beta_{\min}}{1 + (N_A/N_p)^\eta} \quad (73)$$

Uhnevionak<sup>331</sup> split  $\mu_{\max}$  into two additive parts with separate temperature scaling as shown in Eq. (74) to simulate the temperature dependent contribution of the bulk mobility on the channel mobility of a MOSFET. The author differentiates between this contribution and the mobility solely in bulk material.

$$\mu_{\max} \left( \frac{T}{300} \right)^{\gamma_{\max}} = \mu_{\max 1} \left( \frac{T}{300} \right)^{\gamma_{\max 1}} + \mu_{\max 2} \left( \frac{T}{300} \right)^{\gamma_{\max 2}} \quad (74)$$

Based on Eq. (66) Mnatsakanov *et al.*<sup>766</sup> separated the empirical description in the lattice and charge impurity scattering and scaled these independently with temperature. This leads to the expressions shown in Eq. 75 and Eq. 76 with  $\gamma_l$  the temperature scaling factor of the impurity scattering contribution. For  $T = T_0$  this expression collapses to Eq. (66). Mnatsakanov *et al.*<sup>766</sup> claims that this model describes the temperature behavior for low and high doping in an improved fashion. In our opinion the exponents  $\gamma_l + \gamma_{\max}$  and  $\gamma_l$  should be exchanged such that the nominator is scaled with  $(T/T_0)^{\gamma_l + \gamma_{\max}}$  and the denominator with  $(T/T_0)^{\gamma_l}$ . Also,  $\delta$  in the nominator of  $B(N)$  should be negative. We confirmed this by comparing the results to the figures by Neimontas *et al.*<sup>252</sup> and an analytic comparison to the equation presented by Mnatsakanov, Pomortseva, and Yurkov<sup>773</sup>.

$$\mu(N, T) = \mu_{\max}(T_0) \frac{B(N) \left( \frac{T}{T_0} \right)^{\gamma_l}}{1 + B(N) \left( \frac{T}{T_0} \right)^{\gamma_l + \gamma_{\max}}} \quad (75)$$

$$B(N) = \left[ \frac{\mu_{\min} + \mu_{\max} \left( \frac{N_{\text{ref}}}{N} \right)^\delta}{\mu_{\max} - \mu_{\min}} \right] \Big|_{T=T_0} \quad (76)$$

One final model was proposed by Klaassen<sup>774</sup> as a unified description of majority and minority charge carriers including screening effects, also called Philips model, which was recently used in

conjunction with 4H-SiC<sup>772</sup>. Although this model is already included in state of the art simulation frameworks we did not consider it in our review as no explicit parameters for 4H-SiC were found in literature.

## 2. High-Field Mobility

At high electric fields the charge carrier velocity approaches a maximum value, the so-called saturation velocity. Explanations for this behavior are an increasing amount of optical phonon scattering<sup>177,276,322</sup> or an increase in elastic and nonelastic scattering owing to the increase in carrier energy<sup>68</sup>. Because the velocity is modeled according to  $v = \mu F$ , the mobility has to decrease. This field dependency of the mobility was, again, modeled by Caughey and Thomas<sup>758</sup> as shown in Eq. (77). Chen *et al.*<sup>323</sup> used the hydrodynamic version instead.

$$\mu = \frac{\mu_{\text{low}}}{\left[ 1 + \left( \frac{\mu_{\text{low}} F}{v_{\text{sat}}} \right)^{\beta} \right]^{\frac{1}{\beta}}} \quad (77)$$

Here  $\mu_{\text{low}}$  denotes the low field mobility as described in the previous section and  $v_{\text{sat}}$  the saturation mobility (Kimoto and Cooper<sup>59</sup> calls the latter sound velocity). In some cases an additional additive factor  $\alpha$  is introduced in various spots of this equation<sup>86,320</sup> but is always set to 0 and, thus, irrelevant.

Because  $v_{\text{sat}}$  is temperature dependent<sup>3,94,112</sup> Canali *et al.*<sup>775</sup> suggested to scale the parameters  $\beta$  and  $v_{\text{sat}}$  with temperature, as shown for the low-field case in Eq. (67)<sup>65,68</sup>. This model is thus often called Canali model<sup>441,488</sup>. In some occasions<sup>154</sup> the temperature change of  $v_{\text{sat}}$  is modeled by the approach presented for Si shown in Eq. (78)<sup>476,776</sup>. Be aware that some publication<sup>161,754,757</sup> use a value of  $d = 0.6$ , while others use  $d = 0.8$  in the denominator, referencing an early edition of Sze and Ng<sup>171</sup>.

$$v_{\text{sat}} = \frac{v_{\text{max}}}{1 + d \exp\left(\frac{T}{600}\right)} . \quad (78)$$

Also for the temperature scaling of  $\beta$  a slightly different approach shown in Eq. (79) was proposed which is a combination of the modeling by Roschke and Schwierz<sup>757</sup> and Bertilsson, Harris, and Nilsson<sup>777</sup>.

$$\beta = \beta_0 + a \exp\left(\frac{T - T_{\text{ref}}}{b}\right) + c T \quad (79)$$

Recent Monte-Carlo simulations<sup>1,10,104,106,116,160,161,247,357,428,754,777</sup> revealed a velocity overshoot, i.e., negative differential mobility, at fields near  $1 \times 10^6$  V/cm<sup>757</sup>. Foutz, O’Leary, and

Shur<sup>778</sup> proposed a new model for wide band gap materials that better models mobility overshoot as shown in Eq. (80)<sup>754</sup>. This approach was used for GaN<sup>779</sup> and lately also for 4H-SiC<sup>754</sup> but is not yet available in TCAD tools. A simplified version ( $\alpha = -\infty$ ) is denoted as transferred-electron model<sup>412,780</sup>.

$$v(F) = \frac{\mu_0 F + \mu_1 F(F/F_0)^\alpha + v_{\text{sat}}(F/F_1)^\beta}{1 + (F/F_0)^\alpha + (F/F_1)^\beta} \quad (80)$$

We want to highlight that in any of the publications that presented these decreasing velocity the term "overshoot" was stated. In addition the peak value, i.e., the maximum, was denoted as the saturation velocity, which begs the question whether the decrease in velocity is not only a simulation artifact.

Baliga<sup>112</sup> used the presentation shown in Eq. (81) to describe the high field mobility. The parameters from Eq. (66) can be achieved by using  $v_{\text{sat}} = A$  and  $\mu_{\text{low}} = v_{\text{sat}}/B^{1/\beta}$ .

$$\mu = \frac{A}{[B + F^\beta]^{1/\beta}} \quad (81)$$

### 3. Carrier-Carrier Scattering

This scattering process decreases the mobility at high injections levels<sup>112,677,781</sup> and denotes interactions among the same type of charge carriers, e.g., electron-electron<sup>3</sup>, or between electrons and holes<sup>333</sup>. To describe this effect the Conwell-Weisskopf equation shown in Eq. (82) is used<sup>90,101,782,783</sup>.

$$\mu_{\text{ccs}} = \frac{D \left( \frac{T}{T_0} \right)^{\frac{3}{2}}}{\sqrt{np}} \left[ \ln \left( 1 + F \left( \frac{T}{T_0} \right)^2 (pn)^{-\frac{1}{3}} \right) \right]^{-1} \quad (82)$$

### 4. Hall Scattering Factor

The mobility can be experimentally extracted from conductivity measurements, called in that case conductivity or drift mobility, as shown in Eq. (64)<sup>3</sup>. Since the amount of charge carriers is required as well often Hall measurements are used to determine the mobility. In general it is said that the Hall mobility can be easier measured, while the conductivity mobility can be easier calculated<sup>3</sup>. However, for Hall measurements a slightly different mobility, the Hall mobility  $\mu_H$  is determined<sup>15</sup>. The relation between these two is called Hall factor  $r$  and defined as shown in Eq. (83)<sup>3,9,202,207,729,761</sup>. In Hall measurements the Hall coefficient  $R_H$  is determined, that is

defined as shown in Eq.(84) with  $n_H$  the Hall charge carrier count<sup>51,52,724,725,732</sup>.  $R_H$  is also used to connect the conductivity and the mobility as shown in Eq. (85)<sup>62,112,235</sup>. For holes the calculation of  $r_H$  requires to consider both light and heavy holes<sup>50,594</sup>.

$$r_H = \frac{\mu_H}{\mu_c} = \frac{n}{n_H} \quad (83)$$

$$R_H = \frac{1}{n_H e} = \frac{r_H}{ne} \quad (84)$$

$$\mu_H = \sigma R_H = \frac{1}{en_H \rho} \quad (85)$$

$$(86)$$

For this reason a clear distinction between Hall and conductivity mobility is shown in the sequel. For further theoretical analyses and overviews on Hall mobilities and measurements the interested reader is referred to the dedicated literature<sup>49,161,260,596</sup>.

## B. Results & Discussion

In the following we present the gathered results. We had to exclude publications that solely focused on channel mobilities<sup>73,79,349,441,784–788</sup>, that did not clearly specify the SiC polytype<sup>53,146,352,475,789</sup> or that deal with mobility over irradiation defects<sup>790</sup>. Furthermore, we did not consider Wright<sup>159</sup> that got superseded by Wright *et al.*<sup>110</sup>.

### 1. Measurements

Several approaches to determine the mobility have been proposed in the literature. These include simulations such as Monte Carlo<sup>10,104,106,160,246,357,428,791</sup>, full band monte carlo (FBMC)<sup>792</sup>, empirical pseudo potentials (EPM)<sup>1,10,116</sup>, monte carlo particle (MCP)<sup>105</sup>, non equilibrium statistical ensemble formalism (NESEF)<sup>117</sup>, linear augmented plane wave (LAPW)<sup>588</sup>, density functional theory (DFT)<sup>52</sup>, extraction from the diffusion coefficient (DIFF)<sup>252</sup>, conductivity tensor calculations (COTE)<sup>9,157,158,210</sup>, general calculations<sup>49,50,239</sup> and fitting (FIT)<sup>33,65,68,441,578,712,754,757,773</sup>. Measurements include collected charge (CCh)<sup>793</sup>, nanosecond pulsed conductance (NPC)<sup>787,794–797</sup>, resistance measurements (RES)<sup>577,585</sup>, Schottky barrier diode I-V fitting (SBD-IV)<sup>798</sup>, Raman scattering (Raman)<sup>16,197</sup>, low temperature photoluminescence (LTPL)<sup>622</sup>, spectroscopic ellipsometry (SE)<sup>293</sup>, optical detection of cyclotron resonance (ODCR)<sup>218,755</sup>, diode I-V (DIV)<sup>366,798</sup>, bipolar transistor I-V (BIV)<sup>799</sup> and Hall measurements<sup>15,23,51,62,202,207,208,234,265,279,376,391,560,579,584,589,605,693,709,720</sup>.

Regarding the type of mobility the majority of publications provided Hall mobility data<sup>23,49–51,62,157,158,207,208,2</sup> and only few directly the conductivity one<sup>16,104,197,755,792</sup>.

As outlined in the previous section, the results of the latter have to be scaled by the Hall scattering factor  $r_H$  to achieve the conductivity mobility. In early investigations  $r_H$  was assumed approximately unity<sup>65,135,757,784,804</sup> due to a lack of reliable data<sup>202</sup>. Later it was shown, however, that this is actually only the case for high magnetic fields<sup>596</sup>. More thorough investigations revealed a dependency on the magnetic field<sup>596,732,807</sup>, temperature<sup>9,23,50–52,62,274,594,596,727,729</sup> and doping concentration<sup>52,274,724</sup>.  $r_H$  thereby shows predominantly variations in the range of [0.5, 1.5].

Both an increase<sup>208</sup> and a decrease<sup>9,724</sup> of  $r_H$  with increasing temperature was observed in measurements, which may even depend on the doping concentration<sup>208</sup>. Pernot, Contreras, and Camassel<sup>50</sup> provided a fitting of the results by Pensl *et al.*<sup>729</sup> as shown in Eq. (87). Theoretical analyses predicted an increase of  $r_H$ <sup>9,51</sup>.

$$r_H = 1.748\,23 - 6.22 \times 10^{-3}T + 1.367\,29 \times 10^{-5}T^2 - 1.448\,37 \times 10^{-8}T^3 + 5.864\,98 \times 10^{-12}T^4 \quad (87)$$

Tanaka *et al.*<sup>52</sup> fitted both the Hall and conductivity mobility with the model shown in Eq. (66). A division of these fittings led to the expression for  $r_H$  shown in Eq. (88)

$$r_H = 1.16 \left( \frac{T}{300\text{K}} \right)^{-0.9} \frac{1 + \left( \frac{T}{300\text{K}} \right)^{-1.5} \left( \frac{N_A}{1 \times 10^{19}/\text{cm}^3} \right)^{0.7}}{1 + \left( \frac{T}{300\text{K}} \right)^{-1.8} \left( \frac{N_A}{3 \times 10^{18}/\text{cm}^3} \right)^{0.6}} \quad (88)$$

With increasing doping concentration the Hall scattering factor drops<sup>724</sup>. The impact of compensation is still under investigation<sup>51</sup> as well as the anisotropy<sup>732,807</sup>.

We want to discuss the publication by Darmody and Goldsman<sup>135</sup> in greater detail here, because it initially seems to provide a simple answer to the question raised above but, in our opinion, contradicts in various occasions the remaining literature. At first the ratio  $\mu_c/\mu_H$ , which is actually the definition of  $r_H$ , was defined as the ratio of the free charge carriers and the doping concentration. This is based on the assumption that all dopants contribute to the conductivity mobility, i.e., are ionized, which has to be doubted in 4H-SiC (cp. Section VI). The Hall scattering coefficient was set to 1 in this analysis. In the sequel the authors showed two plots, one for the Hall and one for the conductivity mobility, which revealed a significant difference. In detail the latter is much lower, which resulted from the fact that the authors gathered the values from resistivity measurements, assuming that the amount of charge carriers is equal to the doping concentration. Since the

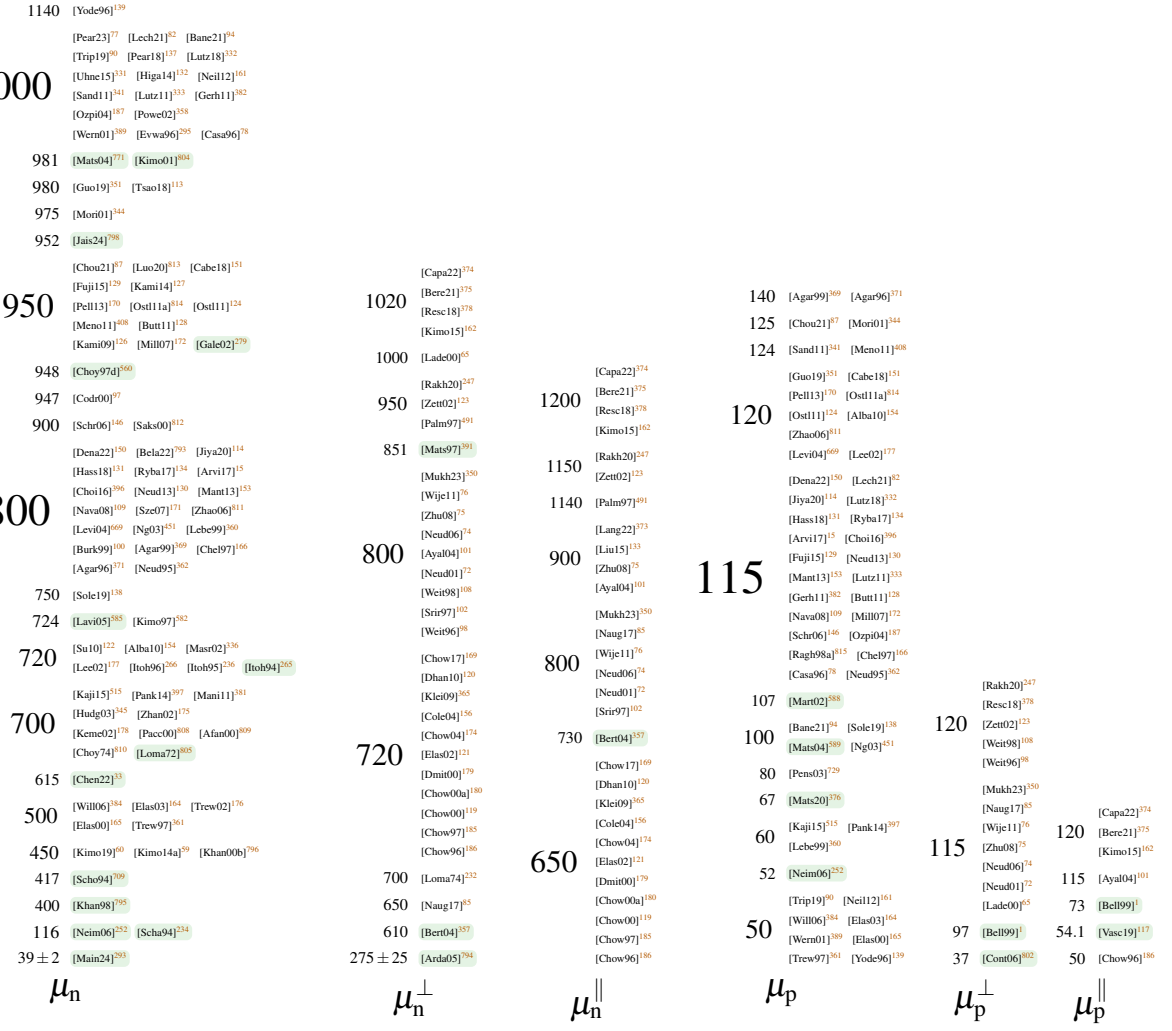


FIG. 37. Single mobility values for 4H-SiC in different spatial directions.

presented plots lead to  $r_H > 5$  according to the definitions shown in this publication the results of this paper have to be considered with care.

Since there is no simple translation between Hall and conductivity mobility we present the values as published and just denote their meaning with  $H$  resp.  $C$  in the sequel.

## 2. Low-Field Mobility

In literature often only single mobility value is found<sup>257</sup>. Although these can also be used in TCAD tools they often serve the purpose of a rough and quick comparison among different materials. Consequently often no information about doping concentration and temperature are provided. We found a wide range of values for the effective mobility, as well as in single spatial

TABLE XXI. Fundamental investigations of the ratio of electron and hole mobilities in the direction perpendicular ( $\perp$ ) and parallel ( $\parallel$ ) to the c-axis.

ref.	$\mu_n^\perp / \mu_n^\parallel$	$\mu_p^\perp / \mu_p^\parallel$	type <sup>a</sup>	method
	[1]	[1]		
[Scha94] <sup>234</sup>	$0.85 \pm 0.05$	-	H	Hall
[Scha94] <sup>761</sup>	0.83	-	H	Hall
[Hari95] <sup>16</sup>	$1.2 \pm 0.3$	-	C	Raman
[Josh95] <sup>246</sup>	$0.75 \pm 0.04$	-	C	MC
[Son95] <sup>218</sup>	0.7 <sup>b</sup>	-	C	ODCR
[Nils96] <sup>160</sup>	$0.825 \pm 0.025$	-	C	MC
[Choy97d] <sup>560</sup>	0.86	-	H	Hall
[Mats97] <sup>391</sup>	$(1.2)^{-1}$	-	H	Hall
[Mick98] <sup>104</sup>	$0.77 \pm 0.07$	-	C	MC
[Bell99] <sup>1</sup>	-	1.33	C	EPM
[Iwat00] <sup>158</sup>	0.7	-	H	COTE
[Bert01] <sup>791</sup>	0.85	-	C	MC
[Hata03] <sup>765</sup>	0.83	1.15	H	Hall
[Bert04] <sup>357</sup>	0.84	-	C	MC
[Chen20] <sup>792</sup>	$(1.75)^{-1} - (1.25)^{-1}$	-	C	FBMC
[Ishi21] <sup>207</sup>	$(1.15 \pm 0.03)^{-1}$	-	H	Hall
[Ishi24] <sup>208</sup>	-	$(0.90 \pm 0.05)^{-1}$	H	Hall

<sup>a</sup> type of mobility: Hall (H), conductivity (C)

<sup>b</sup> temperature range of 2–6 K

directions (see Fig. 37). The electron mobility is much higher than the hole one, whereas the direction parallel to the c-axis is slightly more beneficial. At least for electrons; for holes no clear distinction is possible. A wide range of values is used in the literature, which reflects the many dependencies of the mobility, e.g., doping concentration, temperature and field strength.

The analysis of the reference chain (see Fig. 38) shows that these values are not derived from a main source but rather smaller clusters are formed. This indicates that the authors assume this as common knowledge, without the need to provide proper references.

As shown before, the mobility shows an anisotropy. Some authors argue that due to low anisotropy (see Table XXI) just considering mobility in base plane is a reasonable approxima-

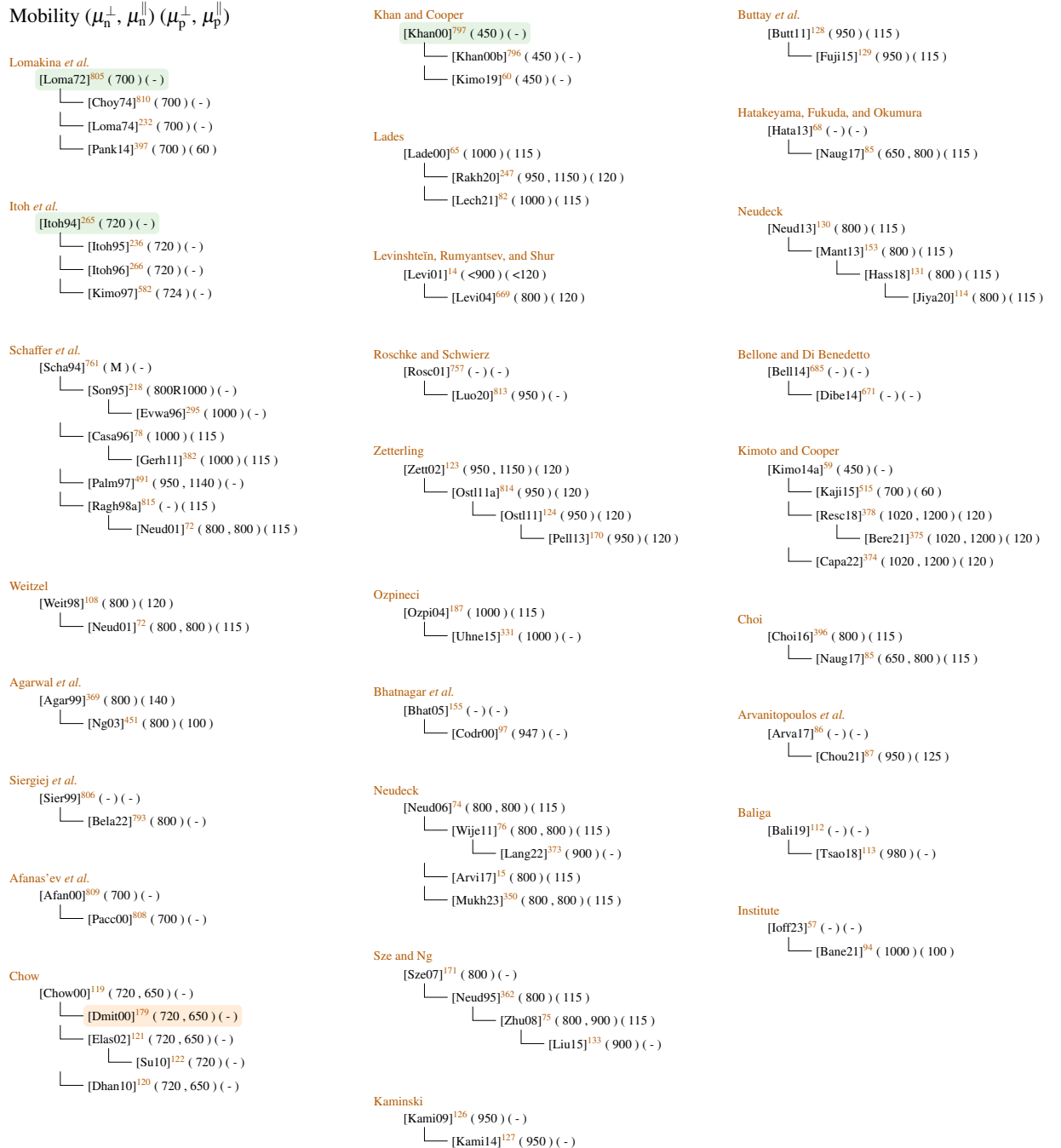


FIG. 38. Reference chain for single mobility values in different spatial directions. If only a single value is shown the value denotes the effective value without direction.

tion<sup>154</sup>, however, Hatakeyama *et al.*<sup>765</sup> showed that not even within the basal plane the mobility is constant. The anisotropy of the mobility is most probably caused by the anisotropy of the effective masses<sup>68,158,764</sup> and thus depends on additional parameters such as the temperature<sup>207</sup>. Although it was pointed out that the ratio changes from below to above one depending on the doping and



FIG. 39. Ratio of electron and hole mobilities in the direction perpendicular ( $\perp$ ) and parallel ( $\parallel$ ) to the c-axis used in literature.

thus constant values are not well suited<sup>357</sup>, almost exclusively constant factors are used in literature (see Fig. 39). Cheng and Vasileska<sup>792</sup> stated that previous publications<sup>761</sup> did not specify the exact perpendicular direction. Thus their values range between 1.25 and 1.75, compared to the previously achieved 1.2<sup>761</sup>. Iwata, Itoh, and Pensl<sup>158</sup> investigated the mobility in varying in-plane directions, revealing a maximum anisotropy factor for electrons of 0.7. The ratio was also investigated over temperature and doping concentration<sup>62,104,160,207,208,231,234,246,588,761</sup>. It was also extracted from ratio of resistivity to cancel the Hall scattering factor<sup>207,764</sup>.

For electrons all but one fundamental investigation predict a higher mobility parallel to the c-axis with  $\mu_n^\perp/\mu_n^\parallel = 0.83 \pm 0.07$ . Some predominantly qualitative overview papers state, however, the opposite<sup>120,121,156,169,174,179,185,186,365</sup>. Others predict no anisotropy at all<sup>72,74,76,102,350</sup>. For holes almost all references predict a ratio bigger than one with the most common values of  $1.15 \pm 0.04$ .

*a. Doping Dependency* A lot of publications investigated the impact of the doping concentration on the low-field mobility<sup>9,15,16,23,49–52,60,157,197,207,208,239,274,376,391,579,582,596,622,693,709,725,755,760,761,764</sup>.

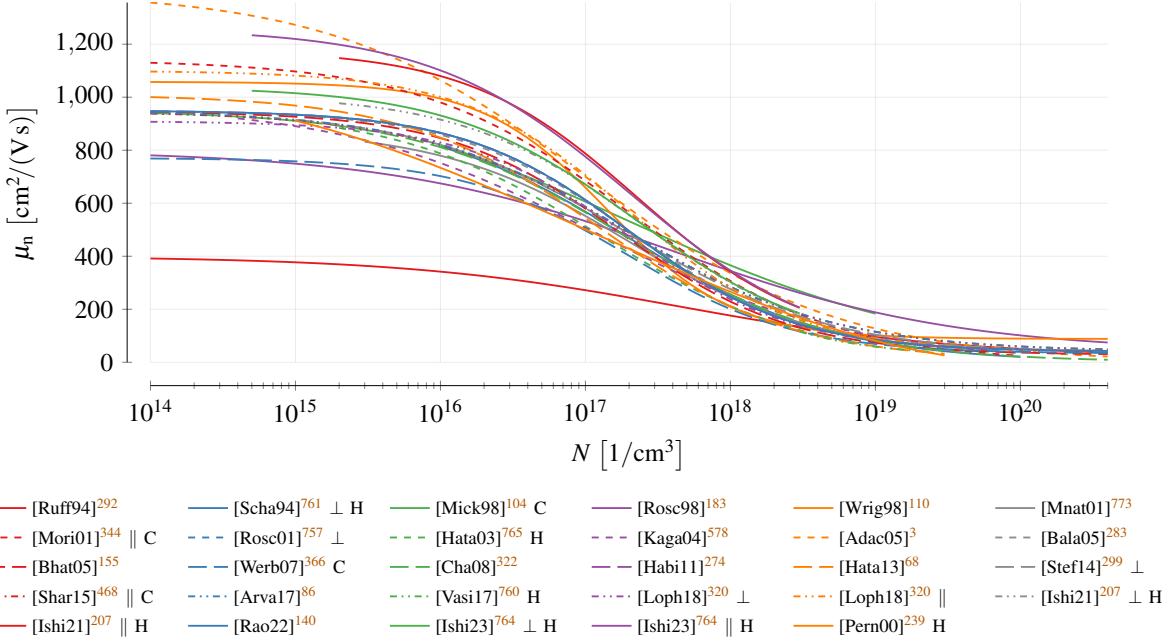


FIG. 40. Electron mobility approximations by the Caughey-Thomas model in Eq. (66) at  $T = 300\text{ K}$ . The models are only shown in the region used for characterization.

which makes it impossible to show all gathered results in this paper. Instead we focus on the models that were developed based on these data.

A wide range of parameters for Eq. (66) were proposed to describe the low-field mobility. The model parameters for the electron (see Table XXII) have been proposed over a range of three decades. The maximum mobility varies within a range of [800, 1240] and the reference doping concentration  $N_{\text{ref}}$  only minor in the low  $10^{17}$  range. There were several attempts to distinguish the spatial directions and to describe the temperature dependency of the single parameters. We also highlighted the deviating interpretation of parameter  $N$  in the table, which underlines the large discrepancy in literature.

In a graphical representation (see Fig. 40) the qualitative agreement among the models becomes evident, with the exception of the model by Stefanakis and Zekentes<sup>299</sup>. However, in this case we suspect a typographical error for the parameter  $\delta$  which should be 0.61 instead of  $-0.61$ . Indeed, we see the main difference among these models in the maximum mobility  $\mu_{\text{max}}$ .

For the hole mobility less models were proposed with a larger spread in the respective parameters (see Table XXIII). An extreme outlier is the value of  $\mu_{\text{max}}$  by Bhatnagar *et al.*<sup>155</sup> that supersedes all remaining values by almost 300 %. Qualitatively, the decrease of the hole mobility,

TABLE XXII. Parameters for the Caughey-Thomas model in Eq. (66) used to describe the electron mobility.

ref.	dir	$\mu_{\min}$	$\mu_{\max}$	$\mu_0$	$N_{\text{ref}}$	$\delta$	$\gamma_{\min}$	$\gamma_{\max}$	$\gamma_{\text{ref}}$	$\gamma_s$	$\gamma_0$	$\gamma_{N\text{ref}}$	$N^{\text{a}}$	$K^{\text{b}}$	method
		[cm <sup>2</sup> /(Vs)]	[cm <sup>2</sup> /(Vs)]	[cm <sup>2</sup> /(Vs)]	[1/cm <sup>3</sup> ]	[1]	[1]	[1]	[1]	[1]	[1]	[1]	[1]	[1]	
[Ruff94] <sup>292</sup>	-	20	-	380	$4.50 \times 10^{17}$	0.45	-	-	-	-	-3	-	-	-	-
[Scha94] <sup>761</sup>	$\perp$	-	947	-	$1.94 \times 10^{17}$	0.61	-	-2.15	-	-	-	-	S	H	Hall
[Mick98] <sup>104</sup>	-	-	1071	-	$1.94 \times 10^{17}$	0.4	-	-	-	-	-	-	S	C	MC
[Rosc98] <sup>183c</sup>	-	40	800	-	$4 \times 10^{17}$	0.44	-	-	-	-	-	-	D	-	FIT
[Wrig98] <sup>110</sup>	-	88	-	970	$1.43 \times 10^{17}$	1	-0.57	-	2.55	-	-2.7	-	I	-	-
[Mnat01] <sup>73d</sup>	-	30	880	-	$2 \times 10^{17}$	0.67	-	-	-	-	-	-	D	-	FIT
[Mori01] <sup>344</sup>	$\parallel$	-	1141	-	$1.94 \times 10^{17}$	0.61	-	-	-	-	-	-	S	C	DIV
[Rosc01] <sup>757e</sup>	$\perp$	40	950	-	$2 \times 10^{17}$	0.76	-0.5	-2.4	1	-	-	-	D	-	FIT
[Hata03] <sup>765</sup>	-	-	954	-	$1.28 \times 10^{17}$	0.61	-	-	-	-	-	-	I	H	Hall
[Kaga04] <sup>578f</sup>	-	-	977	-	$1.17 \times 10^{17}$	0.49	-	-	-	-	-	-	S	-	FIT
[Adac05] <sup>3</sup>	-	-	1400	-	$1 \times 10^{17}$	0.5	-	-	-	-	-	-	I	-	-
[Bala05] <sup>283</sup>	-	40	950	-	$2 \times 10^{17}$	0.73	-	-2.4	-	-	-0.76	-	-	-	-
[Bhat05] <sup>155</sup>	-	27.87	946.97	-	$1.75 \times 10^{17}$	0.73	-	-2.3	-3.8	-	-	-	-	-	-
[Werb07] <sup>366</sup>	-	33	771	-	$2 \times 10^{17}$	0.76	-	-	-	-	-	-	D	C	DIV
[Chao08] <sup>322</sup>	-	-	950	-	$1.90 \times 10^{17}$	0.6	1	-2.15	-	-	0.05	D	-	-	-
[Habi11] <sup>274g</sup>	-	40	-	910	$2 \times 10^{17}$	0.76	-1.538	-	0.75	0.722	-2.397	-	S	-	FIT
[Hata13] <sup>68h</sup>	-	5	1010	-	$1.25 \times 10^{17}$	0.65	-0.57	-2.6	2.4	-0.146	-	-	S	-	FIT
[Stef14] <sup>299i</sup>	$\perp$	28	950	-	$1.94 \times 10^{17}$	0.61 <sup>j</sup>	-	-2.4	-	-	0.73	I	-	FIT	
[Shar15] <sup>468</sup>	$\parallel$	40	947	-	$1.94 \times 10^{17}$	0.61	-0.5	-2.9	-	-	2.4	S	C	DIV	
[Arva17] <sup>86</sup>	-	40	950	-	$1.94 \times 10^{17}$	0.61	-1.536	-2.4	-	-	-	D	-	-	
[Vasi17] <sup>760</sup>	-	20	950	-	$2 \times 10^{17}$	0.8	-	-	-	-	-	D	H	Hall	
[Loph18] <sup>320</sup>	$\perp$	40	910	-	$2 \times 10^{17}$	0.76	-1.536	-2.4	0.75	0.722	-	-	-	-	-
	$\parallel$	40	1100	-	$2 \times 10^{17}$	0.76	-1.536	-2.4	0.75	0.722	-	-	-	-	-
[Ishi21] <sup>207</sup>	$\perp$	40	1010	-	$2.4 \times 10^{17}$	0.7	-	-	-	-	-2.58	-	D	H	Hall
	$\parallel$	60	1180	-	$2.3 \times 10^{17}$	0.74	-	-	-	-	-2.67	-	D	H	Hall
[Rao22] <sup>140</sup>	-	40	950	-	$2 \times 10^{17}$	0.76	-0.5	-2.15	-	-	-0.76	I	-	-	
[Ishi23] <sup>764</sup>	$\perp$	40	-	1000	$2.2 \times 10^{17}$	0.68	-0.7	-	-	-	-2.9	-2.5	D	H	Hall
	$\parallel$	20	-	1240	$2 \times 10^{17}$	0.64	0.3	-	-	-	-3.2	-2.7	D	H	Hall

<sup>a</sup> meaning of N: doping (D), ionized (I), sum of all dopants (S), intrinsic (N)

<sup>b</sup> type of mobility: Hall (H), conductivity (C)

<sup>c</sup> fitted to<sup>13</sup>

<sup>d</sup> fitted to<sup>761</sup>

<sup>e</sup> fitted to<sup>104,210,246,761,816,817</sup>

<sup>f</sup> fitted to<sup>202,239,391,736,761,816</sup>

<sup>g</sup> fitted to<sup>761,766,816,817</sup>

<sup>h</sup> fitted to<sup>391</sup>

<sup>i</sup> fitted to<sup>50,51,210,284</sup>

<sup>j</sup> In the paper  $\delta = -0.61$  was stated. This did, however, not fit the shown plots

TABLE XXIII. Parameters for the Caughey-Thomas model in Eq. (66) used to describe the hole mobility.

ref.	dir	$\mu_{\min}$	$\mu_{\max}$	$\mu_0$	$N_{\text{ref}}$	$\delta$	$\gamma_{\min}$	$\gamma_{\max}$	$\gamma_{\text{ref}}$	$\gamma_b$	$\gamma_0$	$\gamma_{N\text{ref}}$	$N^{\text{a}}$	$K^{\text{b}}$	method
		[cm <sup>2</sup> /(Vs)]	[cm <sup>2</sup> /(Vs)]	[cm <sup>2</sup> /(Vs)]	[1/cm <sup>3</sup> ]	[1]	[1]	[1]	[1]	[1]	[1]	[1]	[1]	[1]	
[Ruff94] <sup>292</sup>	-	5	-	70	$1 \times 10^{19}$	0.5	-	-	-	-	-3	-	-	-	-
[Scha94] <sup>761</sup>	$\perp$	15.9	124	-	$1.76 \times 10^{19}$	0.34	-	-	-	-	-	-	S	H	Hall
[Wrig98] <sup>110</sup>	-	74	-	43	$1.43 \times 10^{17}$	1	-0.57	-	2.55	-	-2.7	-	I	-	-
[Mnat01] <sup>773c</sup>	-	33	117	-	$1 \times 10^{19}$	0.5	-	-	-	-	-	-	D	-	FIT
[Hata03] <sup>765</sup>	-	15.9	120	-	$1.80 \times 10^{18}$	0.65	-	-	-	-	-	-	I	H	Hall
[Mats04] <sup>589</sup>	-	37.6	106	-	$2.97 \times 10^{18}$	0.356	-	-	-	-	-	-	S	H	Hall
[Bala05] <sup>283</sup>	-	53.3	105.4	-	$2.20 \times 10^{18}$	0.7	-	-2.1	-	-	-	-	-	-	-
[Bhat05] <sup>155</sup>	-	26.1	401.87	-	$1.04 \times 10^{18}$	0.7	-	-2.3	-3.8	-	-	-	-	-	-
[Werb07] <sup>366</sup>	-	10	-	81	$1 \times 10^{19}$	0.5	-	-	-	-	-	-	D	C	DIV
[Cha08] <sup>322</sup>	-	16	140	-	$1.70 \times 10^{19}$	0.34	-1.6	-2.14	-	-	-	0.17	D	-	-
[Koiz09] <sup>51d</sup>	-	-	114.1	-	$5.38 \times 10^{18}$	0.66	-	-2.1	-	-0.35	-	2.44	D	H	Hall
[Habi11] <sup>274e</sup>	-	40	-	82	$6.30 \times 10^{18}$	0.55	-1.538	-	0.75	0.722	-2.2397	-	S	-	FIT
[Hata13] <sup>68f</sup>	-	-	113.5	-	$2.40 \times 10^{18}$	0.69	-0.57	-2.6	2.9	-0.2	-	-	S	-	FIT
[Stef14] <sup>299g</sup>	$\perp$	-	114	-	$5.38 \times 10^{18}$	0.66	-	-2.72	-	-0.35	-	2.44	I	-	FIT
[Liau15] <sup>622</sup>	-	-	75	-	$2 \times 10^{19}$	0.7	-	-	-	-	-	-	D	C	LTPL
[Shar15] <sup>468</sup>	$\parallel$	15.9	124	-	$1.76 \times 10^{19}$	0.34	-0.5	-2.9	-	-	-	2.3	S	C	DIV
[Loph18] <sup>320</sup>	$\perp/\parallel$	-	114	-	$2.40 \times 10^{18}$	0.69	-0.57	-2.6	2.9	-0.2	-	-	-	-	-
[Tana18] <sup>52</sup>	-	-	110	-	$3 \times 10^{18}$	0.6	-	-3	-	-	-	-1.8	D	H	DFT
	-	-	95	-	$1 \times 10^{19}$	0.7	-	-2.1	-	-	-	-1.5	D	C	DFT
[Rao22] <sup>140</sup>	-	15.9	125	-	$1.76 \times 10^{19}$	0.76	-0.5	-2.15	-	-	-	-0.76	I	-	-
[Ishi24] <sup>208</sup>	$\perp$	20	-	74	$6.2 \times 10^{18}$	0.72	-2.2	-	-	-	-2.3	-0.9	D	H	Hall
	$\parallel$	20	-	63	$6.4 \times 10^{18}$	0.83	-2.2	-	-	-	-2.3	-0.9	D	H	Hall

<sup>a</sup> meaning of N: doping (D), ionized (I), sum of all dopants (S), intrinsic (N)

<sup>b</sup> type of mobility: Hall (H), conductivity (C)

<sup>c</sup> fitted to<sup>761</sup>

<sup>d</sup> fitting done by Stefanakis and Zekentes<sup>299</sup>

<sup>e</sup> fitted to<sup>761,766,816,817</sup>

<sup>f</sup> fitted to<sup>391</sup>

<sup>g</sup> fitted to<sup>50,51,210,284</sup>

<sup>h</sup> In the paper  $\delta = -0.61$  was stated. This did, however, not fit the shown plots

compared to the electron one, starts at a higher doping density (see Fig. 41), i.e., the maximum mobility can be maintained for a longer period of time.

There are bigger uncertainties in regard to the minimum/maximum mobility. For the former Negoro *et al.*<sup>693</sup> pointed out that the value  $\mu_{\min} = 16 \text{ cm}^2/(\text{Vs})$  proposed by Hatakeyama *et al.*<sup>765</sup> is too high. Similarly Stefanakis and Zekentes<sup>299</sup> argues that Schaffer *et al.*<sup>761</sup> overestimates the hole mobility at high doping values, although the latest studies again indicate a value larger than

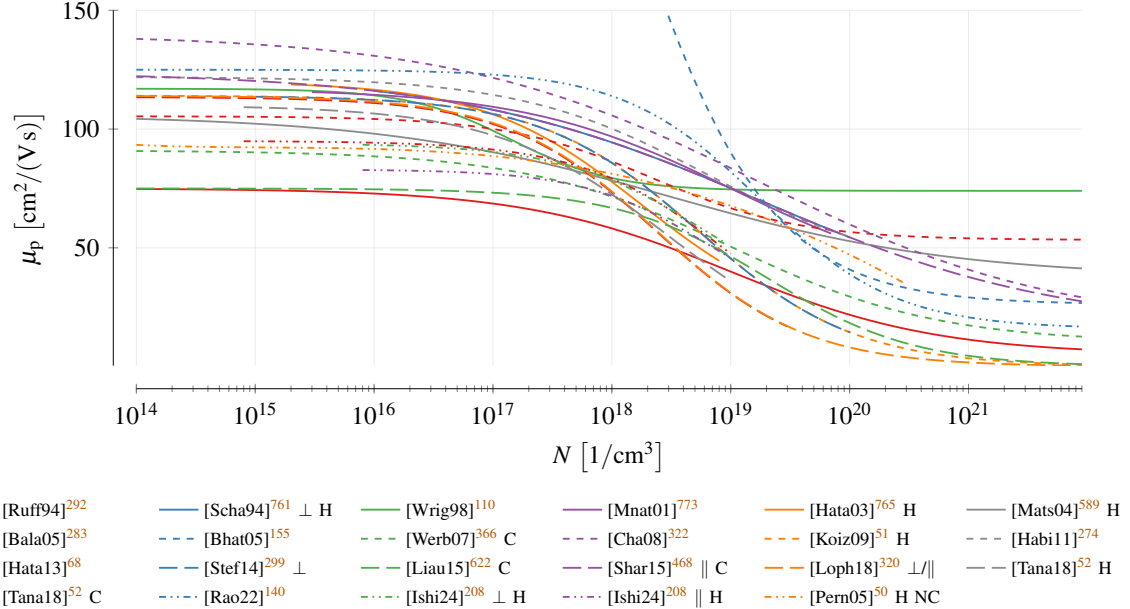


FIG. 41. Hole mobility approximations by the Caughey-Thomas model in Eq. (66) at  $T = 300\text{K}$ . The models are only shown in the region used for characterization.

zero. Exceptional in this regard is the very large value of Wright *et al.*<sup>110</sup> that even exceeded some maximum mobility.  $\mu_{\max}$  also show variations in the range of 75–140  $\text{cm}^2/(\text{Vs})$ .

Besides Eq. (66) we also found a more direct modeling of the mobility as shown in Eq. (89)<sup>111,112</sup>. According to the authors these expressions are, however, based on Ruff, Mitlehner, and Helbig<sup>292</sup> which only contains values on 6H-SiC.

$$\begin{aligned}\mu_n &= \frac{4.05 \times 10^{13} + 20N_D^{0.61}}{3.55 \times 10^{10} + N_D^{0.61}} \\ \mu_p &= \frac{4.05 \times 10^{13} + 10N_A^{0.65}}{3.3 \times 10^{11} + N_A^{0.65}}\end{aligned}\quad (89)$$

A different simplified fitting was proposed Pernot *et al.*<sup>239</sup> who fitted the electron Hall mobility to the free electron density  $n$  as shown in Eq. (90).

$$\mu_H = -39\,000 + 7436 \log(n) - 450.5 \log^2(n) + 8.81 \log^3(n) \quad (90)$$

Some authors also investigated the impact of compensation on the mobility. Pernot, Contreras, and Camassel<sup>50</sup> fitted the Hall mobility using the logarithmic doping concentration for non-compensated (see Eq. (91)) and weakly-compensated (see Eq. (92)) devices. In the graphical representation we only show the former case (denoted by NC), since the latter results in negative

TABLE XXIV. Parameters for the model in Eq. (70).

ref	mob.	$\mu_{\min}$	$\mu_{\min 2}$	$N_{\text{ref}}$	$\delta$	$\mu_1$	$N_{\text{ref}2}$	$\kappa$
		[cm <sup>2</sup> /(Vs)]	[cm <sup>2</sup> /(Vs)]	[1/cm <sup>3</sup> ]	[1]	[cm <sup>2</sup> /(Vs)]	[1/cm <sup>3</sup> ]	[1]
[Zhan18] <sup>469</sup>	$\mu_n$	88	0	$5 \times 10^{18}$	1	43.4	$3.43 \times 10^{20}$	2
	$\mu_p$	44	0	$5 \times 10^{19}$	1	29	$6.1 \times 10^{20}$	2

mobility values. Note that we used  $n = N$  and  $N_A = N$  for the plots.

$$\begin{aligned} \text{non-compensated: } \sigma R_H(292 \text{ K}) &= 2964.3 - 648.72 \log(N_A) + 53.393 \log^2(N_A) \\ &\quad - 1.8717 \log^3(N_A) + 0.002296 \log^4(N_A) \end{aligned} \quad (91)$$

$$\begin{aligned} \text{weakly-compensated: } \sigma R_H(292 \text{ K}) &= 24617 - 5982 \log(N_A) + 536.12 \log^2(N_A) \\ &\quad - 21.151 \log^3(N_A) + 0.30937 \log^4(N_A) \end{aligned} \quad (92)$$

Zhang and You<sup>469</sup> used the Masetti model introduced in Eq. (70) with the parameters shown in Table XXIV. The additional reduction at doping densities around 10<sup>20</sup>/cm<sup>3</sup> are very well visible. Since no values for  $\mu_{\max}$  were provided we used 950 cm<sup>2</sup>/(Vs) for electrons and 80 cm<sup>2</sup>/(Vs) for holes.

*b. Temp Dependency* We found various publications that provide detailed information on the change of the Hall mobility<sup>9,15,23,49–52,62,157,158,202,207,208,210,239,252,265,274,376,391,578,579,582,584,589,594,605,709</sup>, as well as the conductivity mobility<sup>246,577,585,588,622,755</sup> with varying temperature.

For electrons the fitting parameters for Eq. (66) (see Table XXII) show lots of deviations. In some cases not even the sign of the parameters is the same for all models. In a graphical representation for a fixed value of  $N = 1 \times 10^{16}$ /cm<sup>3</sup> some deviations are visible (see Fig. 42). For low temperatures almost all models agree on high mobilities that further increase with decreasing temperature. This contradicts, however, the increasing impact of impurity scattering, that is only covered by the models proposed by Uhnevionak<sup>331</sup> and Neimontas *et al.*<sup>252</sup>. Note that the latter describes the electron mobility in heavily p-doped material (so the minority mobility), which explains the lower values. An increase at low temperatures was also reported by Götz *et al.*<sup>202</sup> who attributed it to impurity limited mobility and the decrease due to phonon limited mobilities. This also corresponds to the majority of measurements we saw, implying once more that the temperature dependency is only valid in a very narrow range for the majority of the available models.

Others observe a dependency of  $T^{-2.1}$  to  $T^{-2.5}$  instead of the expected  $T^{-1.5}$ <sup>376,391,771</sup>. The temperature dependency even shows anisotropy. Schaffer *et al.*<sup>761</sup> proposed a temperature scal-

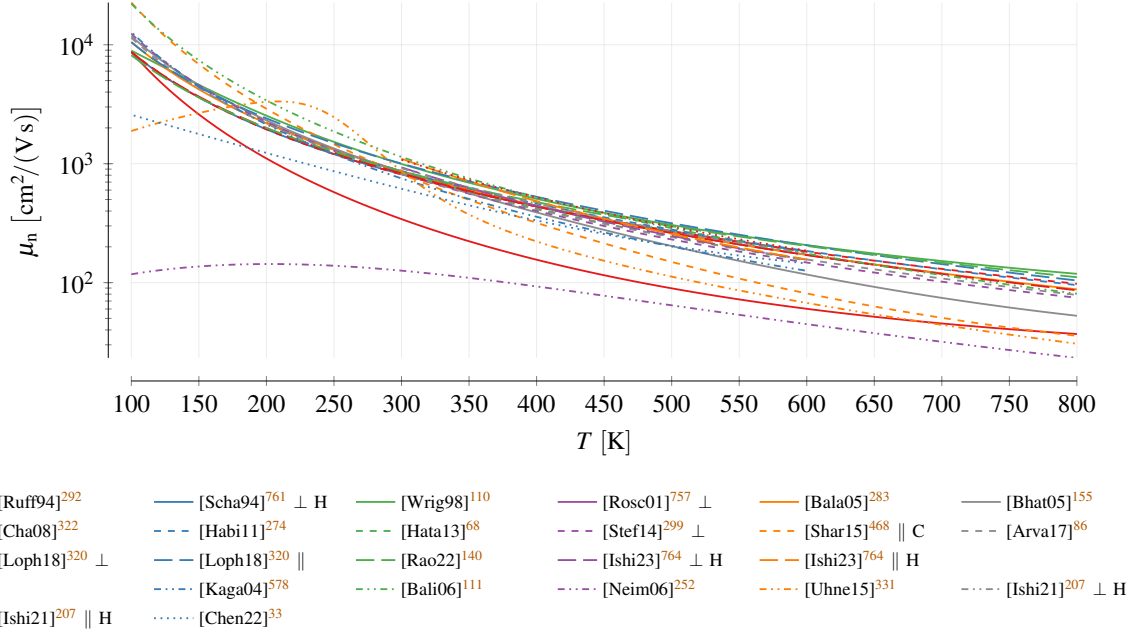


FIG. 42. Description of the electron mobility with varying temperature according to Eq. (66) for a doping of  $1 \times 10^{16}/\text{cm}^3$ . The dash-dot-dotted lines are based on deviating descriptions (see text).

ing parallel to the c-axis of  $T^{-2.4}$  and perpendicular  $T^{-2.15}$  above 200 K. Below that value they get  $T^{-1.2}$  (parallel) and  $T^{-1.18}$  (perpendicular). Ishikawa *et al.*<sup>207</sup> investigated the temperature dependency for three differing dopings, seeing a significant absolute decrease with increasing doping concentration and an anisotropy<sup>208</sup>. In<sup>207</sup> the whole mobility is scaled by  $T^{-\beta}$  whereat  $\beta$  is doping dependent. In Fig. 42 we chose  $\beta = -2.38$  perp. to the c-axis and  $\beta = -2.54$  parallel to it which corresponds to measurements on a doping concentration of  $N_D = 3.6 \times 10^{16}/\text{cm}^3$ .

For holes the fitting parameters for Eq. (66) (see Table XXIII) show the same inconsistencies as the electron data. The graphical representation reveals a much higher agreement among the single models (see Fig. 43). All models predict a continuous decrease with increasing temperature.

Buono<sup>325</sup> argued that the temperature dependency  $\mu_{\max}$  for both charge carriers with  $\gamma_{\max} = -2.15$  is smaller than the ideal factor of  $-1.5$  that is expected from lattice scattering. This was believed to be due to non-polar optical-phonon scattering. Lades<sup>65</sup> achieved  $-1.8 \geq \gamma_{\max} \geq -2.2$ , which lies between acoustical-mode phonon ( $-1.5$ ) and optical-mode phonon ( $-2.5$ ) scattering. Thus they assumed the contribution of other scattering factors contribute less to limit the mobility.

For Eq. 72 and Eq. 73 the parameter values shown in Table XXV were proposed. Note that in this case the temperature coefficient scales with the doping concentration. Kagamihara *et al.*<sup>578</sup> stated that according to theoretical consideration the temperature parameters are 1.5 for low tem-

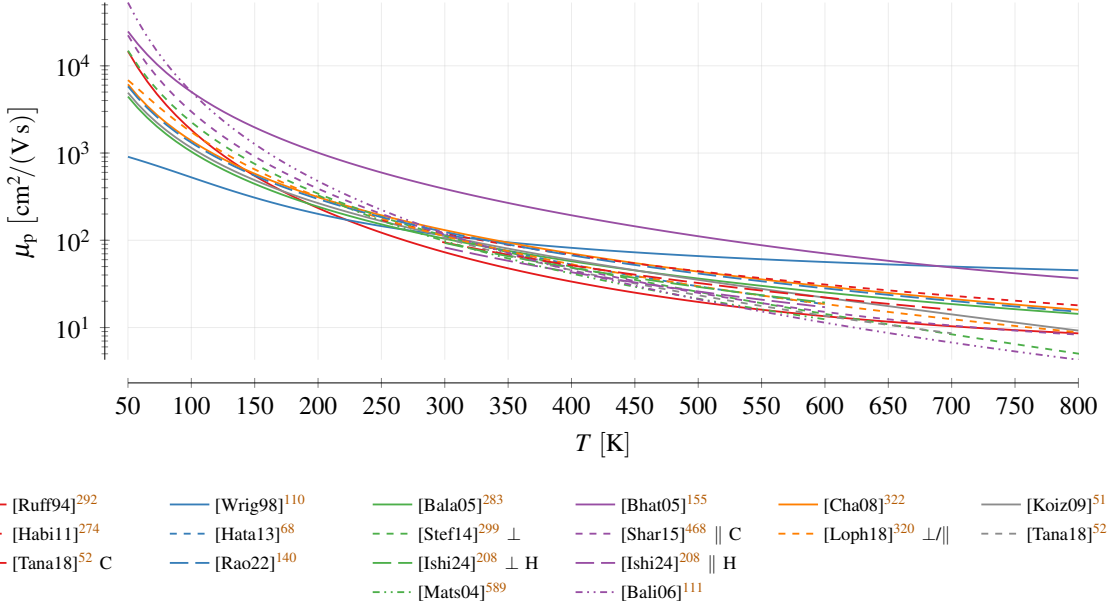


FIG. 43. Description of the hole mobility with varying temperature according to Eq. (66) for a doping of  $1 \times 10^{16}/\text{cm}^3$ .

TABLE XXV. Parameters for the model in Eq. 72 and Eq. 73.

ref	mob.	$\beta_{\min}$	$\beta_{\max}$	$N_p$ [1/cm <sup>3</sup> ]	$\eta$	K	method
		[1]	[1]				
[Kaga04] <sup>578</sup>	$\mu_n$	1.54	2.62	$1.14 \times 10^{17}$	1.35	-	FIT
[Mats04] <sup>589</sup>	$\mu_p$	2.51	3.04	$8.64 \times 10^{17}$	0.456	H	Hall

peratures and 2.6 for high ones, which is close to  $\beta_{\min}$  (1.54) and  $\beta_{\max}$  (2.62) in their fitting.

In contrast to Eq. (66) also more straightforward model for the temperature dependency of the mobility exist. Cheng, Yang, and Zheng<sup>33</sup> fitted the expression shown in Eq. (93) to the measurements of the electron mobility by Schaffer *et al.*<sup>761</sup>.

$$\mu_n(T) = 5422 \exp\left(-\frac{T}{128}\right) + 95 \quad (93)$$

In<sup>111,112</sup> simplified equations that just use a constant mobility combined with a temperature scaling have been presented, which are based on a fitting to data from Koizumi, Suda, and Kimoto<sup>51</sup> and a reference to<sup>110</sup>.

$$\mu_n(T) = 1140 \exp\left(\frac{T}{300}\right)^{-2.7}, \mu_p(T) = 120 \exp\left(\frac{T}{300}\right)^{-3.4} \quad (94)$$

TABLE XXVI. Parameters for the model in Eq. (75) and Eq. (76).

ref	mob.	$\mu_{\min}$	$\mu_{\max}$	$N_{\text{ref}}$	$\delta$	$\gamma_{\max}$	$\gamma$
		[cm <sup>2</sup> /(Vs)]	[cm <sup>2</sup> /(Vs)]	[1/cm <sup>3</sup> ]	[1]	[1]	[1]
[Neim06] <sup>252</sup>	$\mu_n$	100	320	$2 \times 10^{17}$	-0.67 <sup>a</sup>	2.6	0.5

<sup>a</sup> In the paper this value is 0.67 but we changed it to achieve the same results as shown in the paper.

The model proposed by Uhnevionak<sup>331</sup> shown in Eq. (74) that splits  $\mu_{\max}$  in two parts is also shown in the figure using the parameters  $\mu_{\max1} = 500$ ,  $\gamma_{\max1} = -11.6$ ,  $\mu_{\max2} = 450$ ,  $\gamma_{\max2} = -2.74$ ,  $\gamma_{N\text{ref}} = -12.5$  and the remaining parameters according to Roschke and Schwierz<sup>757</sup>.

We also plotted the model proposed in Eq. (75) and Eq. (76) with the parameters introduced by Neimontas *et al.*<sup>252</sup> shown in Table XXVI. These describe the electron mobility in heavily p-doped 4H-SiC.

c. *Analysis* An investigation of the consistency of 4H-SiC mobility models is challenging. In the sequel we want to highlight the most striking issues we encountered. A more complete listing of all inconsistencies is presented in ??.

First of all, we were unable to retrace some values<sup>143,283,284,320</sup> back to scientific publications. In other cases references were provided but the presented values could not be found therein<sup>82,320</sup>. Some publications even present multiple models<sup>59,150,247</sup> that contradict each other.

In the case of electrons sometimes different models seem to be mixed, e.g., using the mobility values from one and the temperature scaling from another. Often a combination of the models by Schaffer *et al.*<sup>761</sup> and Roschke and Schwierz<sup>757</sup> were encountered<sup>86,101,152,177,488</sup> (see Fig. 44). These are also the most influential publications, whereat newer studies have barely been adopted in literature. On the positive side almost all references go back to one of the fundamental studies and almost exclusively 4H values are used. The only exception are the values by Ruff, Mitlehner, and Helbig<sup>292</sup>, which are, however, also seldomly used.

For holes (see Fig. 45) the majority of the values goes back to a single publication by Schaffer *et al.*<sup>761</sup>, whereat, again, newer values do not spread well within the community. We are also unsure about the temperature scaling of the hole mobility in the publications citing<sup>761</sup>, which seem to be taken directly from electrons. There are also various occasions<sup>152,163,324,476,820,821</sup> where  $\mu_{\max}$  was interpreted as  $\mu_0$ , i.e.,  $\mu_{\min}$  is not subtracted.

At last we want to investigate two previous reviews on mobility models in greater details, as

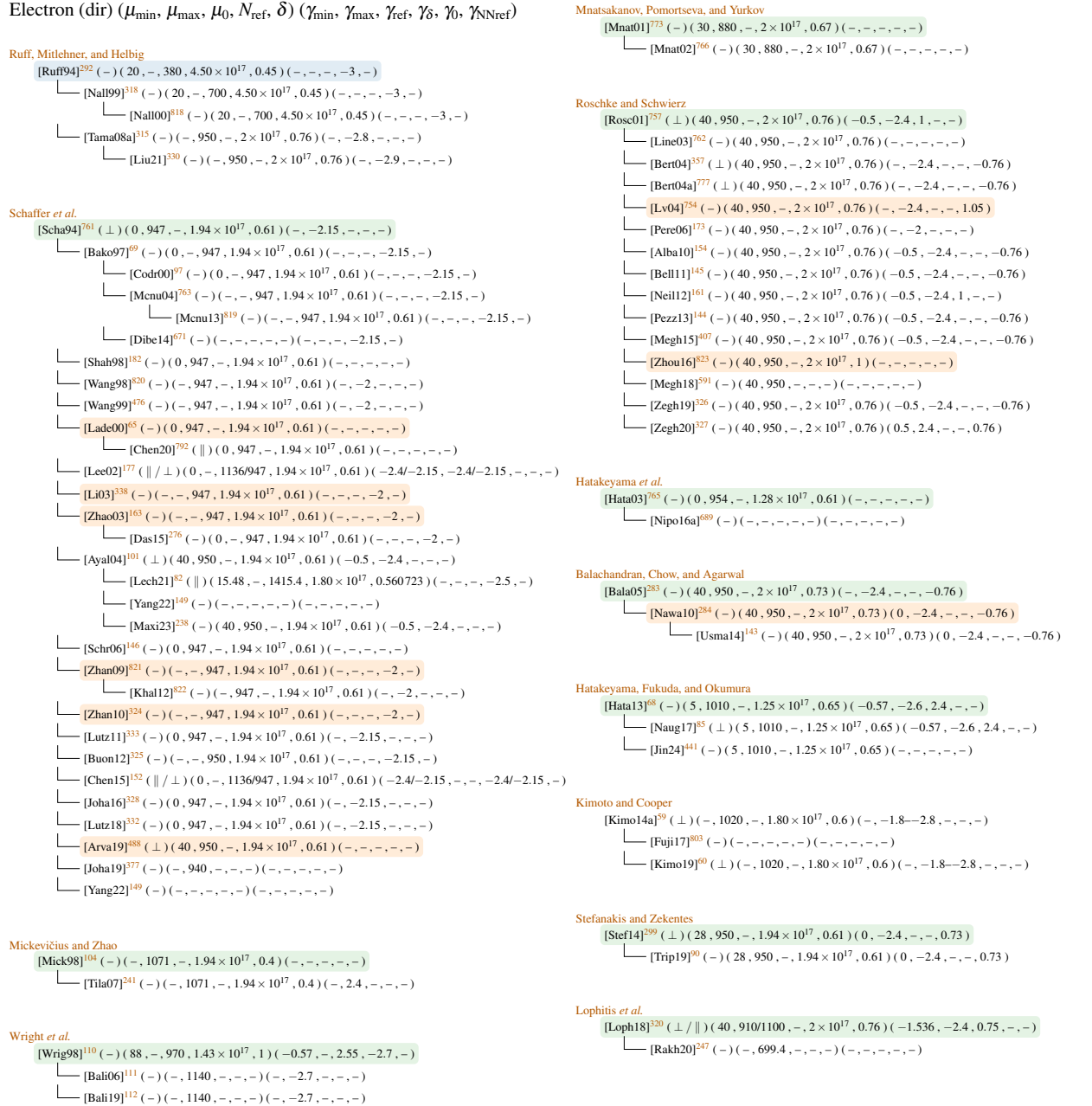


FIG. 44. Reference chain for low field electron mobility models. █ are fundamental investigations, research not focused on 4H and █ connections predicted from the used values.

we encountered problematic parameters that need to be discussed. We begin with the analysis by Stefanakis and Zekentes<sup>299</sup> who investigated six models and fitted a seventh to measurement results for holes. The model denoted as "Reggio Calabria Uni." was cited from Pezzimenti<sup>144</sup> but go back to Schaffer *et al.*<sup>761</sup> for holes and Roschke and Schwierz<sup>757</sup> for electrons. There are also some mistakes with the parameters.  $\delta$  of the electrons should be 0.76 instead of 0.34,



FIG. 45. Reference chain for low field hole mobility models. █ are fundamental investigations, █ are research not focused on 4H and █ connections predicted from the used values.

while  $\gamma_{\text{NNref}}$  of the holes should be  $-0.34$  instead of  $-0.76$ . A similar mistake happened for the values cited from Nawaz <sup>284</sup>, where for the electrons  $\delta = 0.73$  instead of the stated  $0.34$  and  $\gamma_{\text{NNref}} = -0.76$  instead of  $0.73$  were proposed. For holes  $\mu_{\text{min}}$  should be  $53.3 \text{ cm}^2/(\text{Vs})$  instead of the stated  $15.3 \text{ cm}^2/(\text{Vs})$ . In table 3 and 4 the entries by Bakowski, Gustafsson, and Lindefelt <sup>69</sup> and Brosselard <sup>824</sup> were switched, whereat the then appropriate values for the former are still not fully correct since the temperature scaling is regarding to  $\mu_0$  and not  $\mu_{\text{max}}$ . The fitting of  $\gamma_{\text{NNref}}$  for the values presented by Koizumi, Suda, and Kimoto <sup>51</sup> is also questionable as the value proposed

for  $N_{\text{ref}}$  is shown in the measurements for 400 K instead of 300 K and for  $\gamma_{\text{NNref}} = 2.44$  the value of  $N_{\text{ref}}$  effectively decreases with rising temperature, although the measurements show the opposite. Finally, we again want to highlight that the value  $\delta$  for electrons should be 0.61 instead of the proposed  $-0.61$ .

The second overview paper was published by Tian *et al.*<sup>677</sup>. Some mistakes happened for the values cited from Nawaz<sup>284</sup>, where for the electrons  $\delta = 0.73$  instead of the stated 0.34 and  $\gamma_{\text{NNref}} = -0.76$  instead of 0.73 were proposed earlier. For holes  $\mu_{\min}$  should be  $53.3 \text{ cm}^2/(\text{Vs})$  instead of the stated  $15.3 \text{ cm}^2/(\text{Vs})$ . Note that these are the same flaws as discovered in<sup>299</sup>. Despite these variations, this model delivered the best results and was chosen for the simulations. In addition, the maximum mobility for electrons from<sup>325</sup> was changed from  $950 \text{ cm}^2/(\text{Vs})$  to  $947 \text{ cm}^2/(\text{Vs})$ . The model proposed by Megherbi *et al.*<sup>591</sup> was extended by a temperature scaling, which matches an earlier publication by the same authors<sup>407</sup> without, however, the correct value for  $\gamma_{\text{NNref}}$ .

Interesting is also that the origin of the model proposed by Wright<sup>159</sup>, which is denoted as "Brosselard" in<sup>299</sup> and "Gustaffson" in<sup>677</sup> could not yet be fully identified.

### 3. High-Field Mobility

While early publications on SiC had to rely on Silicon parameters<sup>292</sup> later many studies about the dependency of the electron resp. hole velocity on varying electric field were published<sup>1,10,60,104–106,116,428,777,787,792–797</sup>. These led to various parameters to describe the high-field electron mobility with the model introduced in Eq. (77) (see Table XXVII). The saturation velocity parallel to the c-axis is lower compared to the perpendicular direction. Hatakeyama *et al.*<sup>466</sup> estimated the ratio based on impact ionization coefficients (see Section VI), whereat Hatakeyama, Fukuda, and Okumura<sup>68</sup> achieved that the electron velocity parallel to the c-axis is 60 % of the perpendicular one and 80 % for holes. In the table we also added measurements and simulations that only delivered the saturation velocity without any fitting. Overall the values range from a few  $10^6 \text{ V/cm}$  to a few  $10^7 \text{ V/cm}$ .

The hole saturation velocity is marginally lower than the electron one (see Table XXVIII). The key difference, clearly, is the amount of conducted investigations. Often the value of the hole saturation velocity is just assumed<sup>59,86</sup> or set equal to the electron one<sup>86,144,183,247,292,476</sup>.

As already indicated earlier Monte-Carlo simulations reveal a maximum in the charge carrier

TABLE XXVII. High field mobility parameters in Eq. (77) for electrons.

ref.	$v_{\text{sat}}$	$v_{\text{sat}}^{\perp}$	$v_{\text{sat}}^{\parallel}$	$\gamma_{\text{sat}}$	$\beta$	$\gamma_{\beta}$	$T_{\text{sat}}$	$K^{\text{a}}$	method
	[cm/s]	[cm/s]	[cm/s]	[1]	[1]	[1]	[K]		
[Ruff94] <sup>292b</sup>	$2 \times 10^7$	-	-	-	2	-	-	-	-
[Josh95] <sup>246</sup>	-	-	$2.70 \times 10^7$	-	-	-	-	C	MC
[Nils96] <sup>160</sup>	-	$2.10 \times 10^7$	$1.80 \times 10^7$	-	-	-	-	C	MC
[Khan98] <sup>795</sup>	-	$2.08 \times 10^7$	-	-	0.825	-	-	C	NPC
[Mick98] <sup>104</sup>	-	$2 \times 10^7$	$2.50 \times 10^7$	-	1	-	-	C	MC
[Khan00] <sup>797</sup>	-	$2.2 \times 10^7$	-	-	1.2	-	296	C	NPC
	-	$1.6 \times 10^7$	-	-	2.2	-	593	C	NPC
[Lade00] <sup>65c</sup>	-	$2.20 \times 10^7$	-	-0.44	1.2	1	-	-	FIT
[Nils00] <sup>428</sup>	-	$2.26 \times 10^7$	$1.64 \times 10^7$	-	-	-	-	C	MC
[Sank00] <sup>825</sup>	$3.30 \times 10^6$	-	-	-	-	-	-	C	BIV
[Vass00] <sup>826</sup>	-	-	$8 \times 10^6$	-	-	-	300	C	DIV
	-	-	$7.5 \times 10^6$	-	-	-	460	C	DIV
[Zhao00] <sup>105</sup>	-	-	$1.83 \times 10^7$	-	-	-	-	C	MCP
[Bert01] <sup>791</sup>	-	$2.10 \times 10^7$	$1.70 \times 10^7$	-	0.84/1.1 <sup>d</sup>	-	-	C	MC
[Hjel03] <sup>10</sup>	-	$2.12 \times 10^7$	$1.58 \times 10^7$	-	-	-	-	C	EPM
[Bert04] <sup>357</sup>	-	$2 \times 10^7$	$1.70 \times 10^7$	-	-	-	-	C	MC
[Arda05] <sup>794</sup>	-	$1.40 \times 10^7$	-	-	-	-	-	C	NPC
[Aktu09] <sup>106</sup>	$1.60 \times 10^7$	-	-	-	-	-	-	C	MC DFT-DOS
[Hata13] <sup>68e</sup>	-	$2.20 \times 10^7$	-	-0.46	1.20	0.88	-	-	FIT
[Das15] <sup>276</sup>	$2 \times 10^7$	-	-	0.87	1	0.66	-	-	-
[Bela22] <sup>793</sup>	$8.70 \times 10^6$	-	-	-	2	-	-	C	CCh
[Jais24] <sup>798</sup>	$2 \times 10^7$	-	-	-	-	-	-	C	DIV

<sup>a</sup> type of mobility: Hall (H), conductivity (C)

<sup>b</sup>  $\beta$  taken from Silicon

<sup>c</sup> fitted to<sup>797</sup>

<sup>d</sup> values of  $\beta \perp / \parallel$  to c-axis

<sup>e</sup> fitted to<sup>65,797</sup>

TABLE XXVIII. High field mobility parameters in Eq. (77) for holes.

ref.	$v_{\text{sat}}$	$v_{\text{sat}}^{\perp}$	$v_{\text{sat}}^{\parallel}$	$\gamma_{\text{sat}}$	$\beta$	$\gamma_{\beta}$	$T_{\text{sat}}$	$K^a$	method
	[cm/s]	[cm/s]	[cm/s]	[1]	[1]	[1]	[K]		
[Ruff94] <sup>292b</sup>	$2 \times 10^7$	-	-	-	-	-	-	-	-
[Nils00] <sup>428</sup>	-	$1.10 \times 10^7$	$6.50 \times 10^6$	-	-	-	-	C	MC
[Zhao00] <sup>105</sup>	-	-	$8.60 \times 10^6$	-	-	-	-	C	MCP
[Hjel03] <sup>10</sup>	-	$1.08 \times 10^7$	$7.30 \times 10^6$	-	-	-	-	C	EPM
[Aktu09] <sup>106</sup>	$1 \times 10^7$	-	-	-	-	-	-	C	MC DFT-DOS
[Kimo14a] <sup>59</sup>	$1.30 \times 10^7$	-	-	-	-	-	-	-	-
[Das15] <sup>276</sup>	$2 \times 10^7$	-	-	0.52	1.213	0.17	-	-	-

<sup>a</sup> type of mobility: Hall (H), conductivity (C)

<sup>b</sup>  $v_{\text{sat}}$  set equal to electron saturation velocity

velocity, followed by a decrease with increasing field strengths<sup>1,10,104,106,116,160,161,357,428,754,777</sup>. While some then achieve a constant value, others report a steadily decreasing velocity. In all these simulation reports, the peak velocity is highlighted, and even denoted as saturation velocity. Nevertheless, other sources see this as a velocity overshoot<sup>161,247,754</sup>, but also denote that this effect has yet only been seen in simulations and not in experiments<sup>247</sup>.

A graphical representation of the single models for the electron velocity show quite good agreement (see Fig. 46). It can be seen that the first deviations among the model are visible already at a few kV/cm. The mobility starts to change at around 10 kV/cm<sup>112</sup>, which is significantly smaller than the 200 kV/cm proposed by Lophitis *et al.*<sup>320</sup>. We do not explicitly show the results for holes as only a single model could be found.

The description by Lv *et al.*<sup>754</sup> used the model introduced in Eq. (80) with the parameter shown in Eq. (95). Note that we were unable to recreate the plots shown in the paper, which are, considering the provided parameters, not retraceable for us.

$$\begin{aligned} \mu_0 &= 0.17\mu_1, \alpha = -1.95, \beta = 3 \\ F_0 &= 3.05 \times 10^4 \text{ V/cm}, F_1 = 2.8 \times 10^5 \text{ V/cm}, v_{\text{max}} = 4.8 \times 10^7 \text{ cm/s} \end{aligned} \quad (95)$$

In overview listings the electron saturation velocity is dominantly denoted by  $2 \times 10^7$  cm/s (see Fig. 47). This popular value was already reported by V. Muench and Pettenpaul<sup>827</sup> for 6H, as

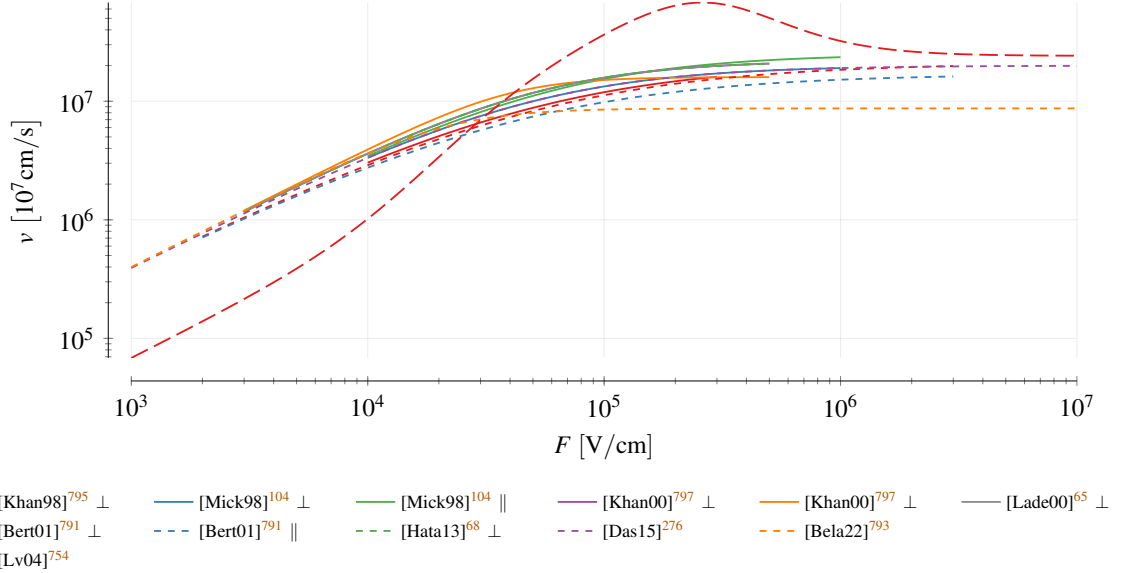


FIG. 46. Electron carrier velocity with varying field for  $\mu_{\text{low}} = 400 \text{ cm}^2/(\text{V s})$ . Long dashed models describe velocity according to Eq. (80).

pointed out by<sup>795</sup>, and then reused for 4H. Nevertheless, later investigations confirmed the validity also for 4H. Slightly lower/higher values are also available but not nearly as prominent. For holes very similar values were proposed (see Fig. 48) but, again, in much less amount.

The temperature dependency of the high-field velocity was measured by Khan and Cooper<sup>795,797</sup> or investigated by simulations<sup>357,777</sup>. Later these results were numerically fitted<sup>65,68</sup>. Note that Lades<sup>65</sup> used a linear fit for the exponent  $\beta$  such that the value published by Khan and Cooper<sup>797</sup> for 620 K could not be perfectly matched (2.2 vs. 2.4).

The results predict a decrease of the saturation velocity with increasing temperature (see Table XXVII and Table XXVIII). The values published by Das and Duttagupta<sup>276</sup>, however, predict the exact opposite. This is also visible in a graphical representation (see Fig. 49). The values by Roschke and Schwierz<sup>757</sup> and Bertilsson, Harris, and Nilsson<sup>777</sup> were described by the model introduced in Eq. (78) and Eq. (79) with the parameters shown in Table XXIX, which were referenced by<sup>154,161,476,685</sup>.

Finally the reference chain (see Fig. 50 for electrons and Fig. 51 for holes) clearly shows that many different publications are referenced in literature.

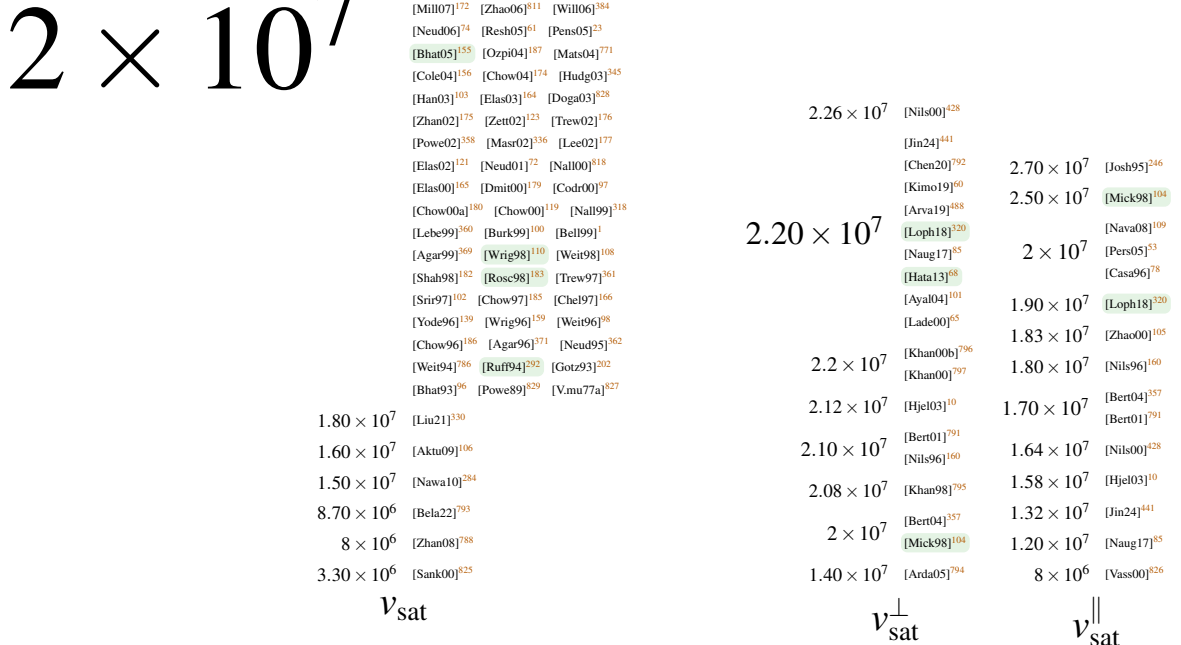


FIG. 47. Electron saturation velocity values used in literature. are fundamental investigations.

TABLE XXIX. Model parameters for temperature dependent carrier velocity in Eq. (78) and Eq. (79).

ref.	dir	$v_{\max}$	$d$	$\beta_0$	$T_{\text{ref}}$	$a$	$b$	$c$
		[cm/s]	[1]	[1]	[K]	[1]	[K]	[1/K]
[Rosc01] <sup>757a</sup>	-	$4.77 \times 10^7$	0.6	0.816	327	$4.27 \times 10^{-2}$	98.4	0
[Bert04a] <sup>777b</sup>	$\perp$	$2.77 \times 10^7$	0.23	0.6	0	0	$\infty$	$10^{-3}$
	$\parallel$	$2.55 \times 10^7$	0.3	1.01	0	0	$\infty$	$3 \times 10^{-4}$

<sup>a</sup> fitted to <sup>160,797</sup>

<sup>b</sup> fitted to simulations by Nilsson, Sannemo, and Petersson <sup>160</sup>

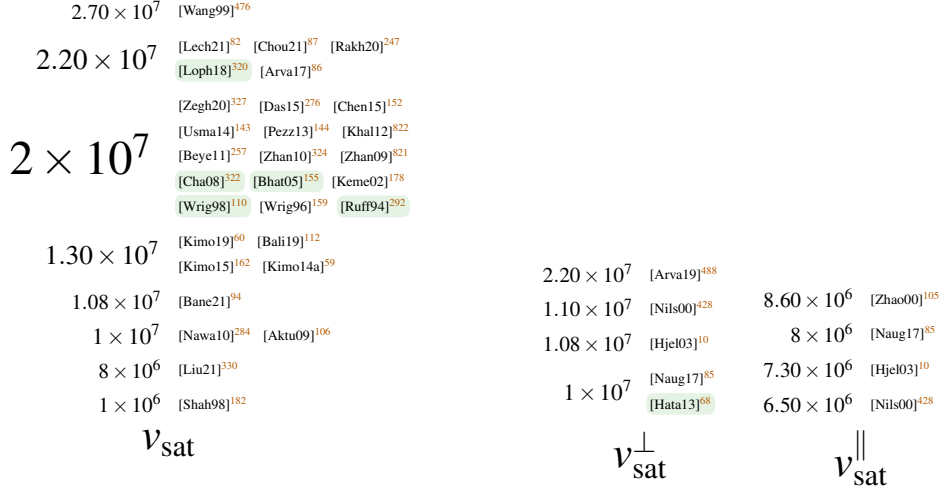


FIG. 48. Hole saturation velocity values used in literature. █ are fundamental investigations.

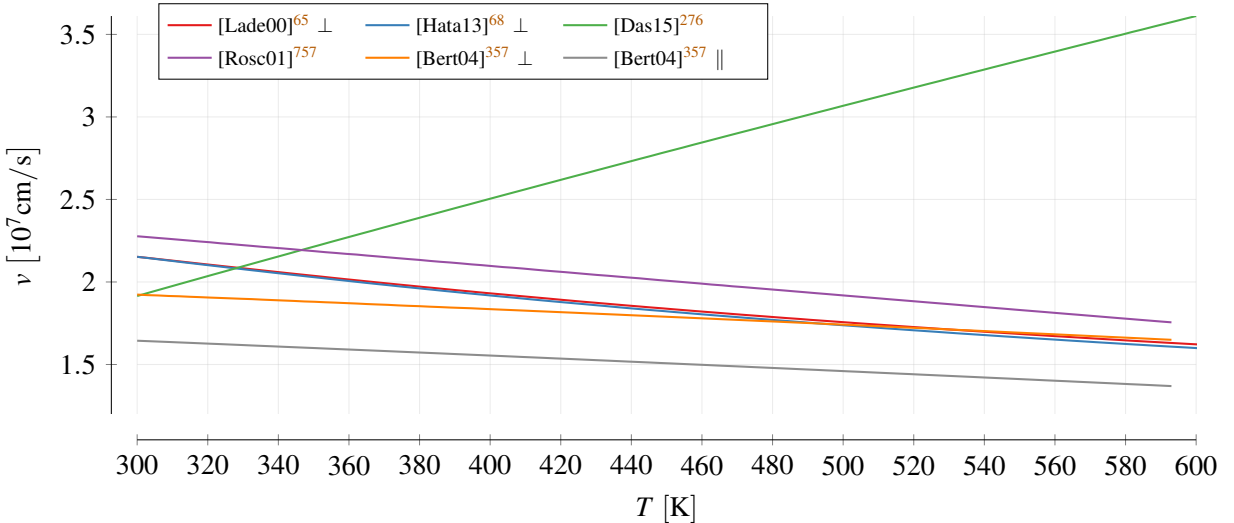


FIG. 49. Temperature dependency of electron velocity for  $F = 10^6$  V/cm and  $\mu_{\text{low}} = 450$  cm<sup>2</sup>/(Vs).

#### 4. Carrier-Carrier Scattering

The only investigation of carrier-carrier scattering in 4H-SiC we found was conducted by Lades<sup>65</sup>, who started from the parameters of Eq. (82) for Silicon and scaled them until the results fit to 4H-SiC measurements. In this fashion the values shown in Eq. (96) were achieved, which are already reused at various occasions<sup>90,101,146</sup>

$$D = 6.9 \times 10^{20} / (\text{cm Vs}), F = 7.452 \times 10^{13} / \text{cm}^2 \quad (96)$$

In addition Onoda *et al.*<sup>783</sup> proposed values for 6H. Bhatnagar *et al.*<sup>155</sup> proposed separate



FIG. 50. High-field mobility reference chain for electrons.

values for electrons and holes but used an equation that was developed by Dorkel and Leturcq<sup>781</sup> for impurity scattering. Lechner<sup>82</sup> referenced the values by Fletcher<sup>830</sup>, which are, however, for Silicon.



FIG. 51. High-field mobility reference chain for holes.

## REFERENCES

- 1 E. Bellotti, *Advanced Modeling of Wide Band Gap Semiconductor Materials and Devices*, Ph.D. thesis, Georgia Institute of Technology (1999).
- 2 V. Komarov, S. Wang, and J. Tang, in *Encyclopedia of RF and Microwave Engineering*, edited by K. Chang (Wiley, 2005) 1st ed.
- 3 S. Adachi, *Properties of Group-IV, III-V and II-VI Semiconductors* (John Wiley, Chichester, England, 2005).
- 4 J. Olivares, M. DeMiguel-Ramos, E. Iborra, M. Clement, T. Mirea, M. Moreira, and I. Katardjiev, in *2013 Joint European Frequency and Time Forum & International Frequency Control Symposium (EFTF/IFC)* (IEEE, Prague, Czech Republic, 2013) pp. 118–121.
- 5 W. Ching, Y.-N. Xu, P. Rulis, and L. Ouyang, *Materials Science and Engineering: A* **422**, 147 (2006).

- <sup>6</sup>L. Patrick and W. J. Choyke, *Physical Review B* **2**, 2255 (1970).
- <sup>7</sup>R. H. Lyddane, R. G. Sachs, and E. Teller, *Physical Review* **59**, 673 (1941).
- <sup>8</sup>R. Ahuja, A. Ferreira Da Silva, C. Persson, J. M. Osorio-Guillén, I. Pepe, K. Järrendahl, O. P. A. Lindquist, N. V. Edwards, Q. Wahab, and B. Johansson, *Journal of Applied Physics* **91**, 2099 (2002).
- <sup>9</sup>H. Iwata and K. M. Itoh, *Journal of Applied Physics* **89**, 6228 (2001).
- <sup>10</sup>M. Hjelm, H.-E. Nilsson, A. Martinez, K. F. Brennan, and E. Bellotti, *Journal of Applied Physics* **93**, 1099 (2003).
- <sup>11</sup>R. Mickevičius and J. H. Zhao, *Materials Science Forum* **264–268**, 291 (1998).
- <sup>12</sup>C. Persson and U. Lindefelt, *Journal of Applied Physics* **82**, 5496 (1997).
- <sup>13</sup>G. L. Harris and Inspec, eds., *Properties of Silicon Carbide*, EMIS Datareviews Series No. 13 (INSPEC, the Inst. of Electrical Engineers, London, 1995).
- <sup>14</sup>M. E. Levinshtein, S. L. Rumyantsev, and M. Shur, eds., *Properties of Advanced Semiconductor Materials: GaN, AlN, InN, BN, SiC, SiGe* (Wiley, New York, 2001).
- <sup>15</sup>I.-R. Arvinte, *Investigation of Dopant Incorporation in Silicon Carbide Epilayers Grown by Chemical Vapor Deposition*, Ph.D. thesis, Universite Cote d'Azur (2017).
- <sup>16</sup>H. Harima, S.-i. Nakashima, and T. Uemura, *Journal of Applied Physics* **78**, 1996 (1995).
- <sup>17</sup>H. Harima, T. Hosoda, and S. Nakashima, *Materials Science Forum* **264–268**, 449 (1998).
- <sup>18</sup>D. W. Feldman, J. H. Parker, W. J. Choyke, and L. Patrick, *Physical Review* **173**, 787 (1968).
- <sup>19</sup>K. Karch, F. Bechstedt, P. Pavone, and D. Strauch, *Physical Review B* **53**, 13400 (1996).
- <sup>20</sup>G. Wellenhofer, K. Karch, P. Pavone, U. Rössler, and D. Strauch, *Physical Review B* **53**, 6071 (1996).
- <sup>21</sup>B. Adolph, K. Tenelsen, V. I. Gavrilenko, and F. Bechstedt, *Physical Review B* **55**, 1422 (1997).
- <sup>22</sup>X. Peng-Shou, X. Chang-Kun, P. Hai-Bin, and X. Fa-Qiang, *Chinese Physics* **13**, 2126 (2004).
- <sup>23</sup>G. Pensl, F. Ciobanu, T. Frank, M. Krieger, S. Reshanov, F. Schmid, and M. Weidner, *International Journal of High Speed Electronics and Systems* **15**, 705 (2005).
- <sup>24</sup>J. Coutinho, V. J. B. Torres, K. Demmouche, and S. Öberg, *Physical Review B* **96**, 174105 (2017).
- <sup>25</sup>I. G. Ivanov, A. Stelmach, M. Kleverman, and E. Janzén, *Physical Review B* **73**, 045205 (2006).
- <sup>26</sup>J. G. Hartnett, D. Mouneyrac, J. Krupka, J.-M. Le Floch, M. E. Tobar, and D. Cros, *Journal of Applied Physics* **109**, 064107 (2011).
- <sup>27</sup>C. R. Jones, J. Dutta, G. Yu, and Y. Gao, *Journal of Infrared, Millimeter, and Terahertz Waves*

**32**, 838 (2011).

- <sup>28</sup>L. Li, S. Reyes, M. J. Asadi, X. Wang, G. Fabi, E. Ozdemir, W. Wu, P. Fay, and J. C. M. Hwang, in *2023 100th ARFTG Microwave Measurement Conference (ARFTG)* (IEEE, Las Vegas, NV, USA, 2023) pp. 1–4.
- <sup>29</sup>M. Naftaly, J. F. Molloy, B. Magnusson, Y. M. Andreev, and G. V. Lanskii, *Optics Express* **24**, 2590 (2016).
- <sup>30</sup>A. T. Tarekegne, B. Zhou, K. Kaltenecker, K. Iwaszczuk, S. Clark, and P. U. Jepsen, *Optics Express* **27**, 3618 (2019).
- <sup>31</sup>M.-m. Gao, L.-y. Fan, X.-y. Gong, J.-l. You, and Z.-z. Chen, *Journal of Applied Physics* **132**, 135702 (2022).
- <sup>32</sup>S. Ninomiya and S. Adachi, *Japanese Journal of Applied Physics* **33**, 2479 (1994).
- <sup>33</sup>L. Cheng, J.-Y. Yang, and W. Zheng, *ACS Applied Electronic Materials* **4**, 4140 (2022).
- <sup>34</sup>M. Ikeda, H. Matsunami, and T. Tanaka, *Physical Review B* **22**, 2842 (1980).
- <sup>35</sup>Q. Yang, Q. Liu, W. Xu, D. Zhou, F. Ren, R. Zhang, Y. Zheng, and H. Lu, *Solid-State Electronics* **187**, 108196 (2022).
- <sup>36</sup>J. M. Dutta, G. Yu, and C. R. Jones, in *2006 Joint 31st International Conference on Infrared Millimeter Waves and 14th International Conference on Terahertz Electronics* (IEEE, Shanghai, China, 2006) pp. 411–411.
- <sup>37</sup>S. Chen, M. Afsar, and D. Sakdatorn, *IEEE Transactions on Instrumentation and Measurement* **57**, 706 (2008).
- <sup>38</sup>L. Li, S. Reyes, M. J. Asadi, P. Fay, and J. C. M. Hwang, *Applied Physics Letters* **123**, 012105 (2023).
- <sup>39</sup>T. Li, L. Li, X. Wang, J. C. M. Hwang, S. Yanagimoto, and Y. Yanagimoto, *IEEE Journal of Microwaves* , 1 (2024).
- <sup>40</sup>Y. Yanagimoto, S. Yanagimoto, T. Li, and J. C. M. Hwang, in *2024 103rd ARFTG Microwave Measurement Conference (ARFTG)* (IEEE, Washington, DC, USA, 2024) pp. 1–4.
- <sup>41</sup>I. G. Ivanov, B. Magnusson, and E. Janzén, *Physical Review B* **67**, 165211 (2003).
- <sup>42</sup>I. G. Ivanov, B. Magnusson, and E. Janzén, *Physical Review B* **67**, 165212 (2003).
- <sup>43</sup>A. Agarwal, S.-H. Ryu, and J. Palmour, in *Silicon Carbide*, edited by W. J. Choyke, H. Matsunami, and G. Pensl (Springer Berlin Heidelberg, Berlin, Heidelberg, 2004) pp. 785–811.
- <sup>44</sup>D. Hofman, J. Lely, and J. Volger, *Physica* **23**, 236 (1957).
- <sup>45</sup>A. Schöner, in *Silicon Carbide*, edited by W. J. Choyke, H. Matsunami, and G. Pensl (Springer

Berlin Heidelberg, Berlin, Heidelberg, 2004) pp. 229–250.

- <sup>46</sup>I. Polaert, N. Benamara, J. Tao, T.-H. Vuong, M. Ferrato, and L. Estel, *Chemical Engineering and Processing: Process Intensification* **122**, 339 (2017).
- <sup>47</sup>J. Chen, Z. H. Levine, and J. W. Wilkins, *Physical Review B* **50**, 11514 (1994).
- <sup>48</sup>U. Lindefelt, *Journal of Applied Physics* **84**, 2628 (1998).
- <sup>49</sup>J. Pernot, W. Zawadzki, S. Contreras, J. L. Robert, E. Neyret, and L. Di Cioccio, *Journal of Applied Physics* **90**, 1869 (2001).
- <sup>50</sup>J. Pernot, S. Contreras, and J. Camassel, *Journal of Applied Physics* **98**, 023706 (2005).
- <sup>51</sup>A. Koizumi, J. Suda, and T. Kimoto, *Journal of Applied Physics* **106**, 013716 (2009).
- <sup>52</sup>H. Tanaka, S. Asada, T. Kimoto, and J. Suda, *Journal of Applied Physics* **123**, 245704 (2018).
- <sup>53</sup>C. Persson and A. Ferreira Da Silva, in *Optoelectronic Devices: III Nitrides* (Elsevier, 2005) pp. 479–559.
- <sup>54</sup>T. A. Baeraky, *Egypt. J. Sol.* **25**, 263 (2002).
- <sup>55</sup>H.-J. Yang, J. Yuan, Y. Li, Z.-L. Hou, H.-B. Jin, X.-Y. Fang, and M.-S. Cao, *Solid State Communications* **163**, 1 (2013).
- <sup>56</sup>T. Chow and R. Tyagi, in *[1993] Proceedings of the 5th International Symposium on Power Semiconductor Devices and ICs* (IEEE, Monterey, CA, USA, 1993) pp. 84–88.
- <sup>57</sup>I. Institute, “Silicon Carbide,” <http://www.ioffe.ru/SVA/NSM/Semicond/SiC/index.html> (2023).
- <sup>58</sup>P. T. B. Shaffer, *Applied Optics* **10**, 1034 (1971).
- <sup>59</sup>T. Kimoto and J. A. Cooper, *Fundamentals of Silicon Carbide Technology: Growth, Characterization, Devices, and Applications*, 1st ed. (Wiley, 2014).
- <sup>60</sup>T. Kimoto, in *Wide Bandgap Semiconductor Power Devices* (Elsevier, 2019) pp. 21–42.
- <sup>61</sup>S. Reshanov, *Device-relevant defect centers and minority carrier lifetime in 3C-, 4H- and 6H-SiC*, Ph.D. thesis, Friedrich-Alexander-Universität, Erlangen-Nürnberg (2005).
- <sup>62</sup>M. Schadt, *Transporteigenschaften von Elektronen Und Löchern in Siliciumkarbid*, Ph.D. thesis, FriedrichAlexander-Universität (1997).
- <sup>63</sup>T. Troffer, *Elektrische und optische Charakterisierung Bauelementrelevanter Dotierstoffe in Siliciumkarbid*, Ph.D. thesis, FriedrichAlexander-Universität (1998).
- <sup>64</sup>N. W. Thibault, American Mineralogist **29**, 327 (1944), <https://pubs.geoscienceworld.org/msa/ammin/article-pdf/29/9-10/327/4243453/am-1944-327.pdf>.

- <sup>65</sup>M. Lades, *Modeling and Simulation of Wide Bandgap Semiconductor Devices: 4H/6H-SiC*, Ph.D. thesis, Technische Universität München (2000).
- <sup>66</sup>C. Persson, U. Lindefelt, and B. E. Sernelius, *Journal of Applied Physics* **86**, 4419 (1999).
- <sup>67</sup>N. T. Son, C. Persson, U. Lindefelt, W. M. Chen, B. K. Meyer, D. M. Hofmann, and E. Janzén, in *Silicon Carbide*, edited by W. J. Choyke, H. Matsunami, and G. Pensl (Springer Berlin Heidelberg, Berlin, Heidelberg, 2004) pp. 437–460.
- <sup>68</sup>T. Hatakeyama, K. Fukuda, and H. Okumura, *IEEE Transactions on Electron Devices* **60**, 613 (2013).
- <sup>69</sup>M. Bakowski, U. Gustafsson, and U. Lindefelt, *physica status solidi (a)* **162**, 421 (1997).
- <sup>70</sup>O. Madelung and R. Poerschke, eds., *Semiconductors: Group IV Elements and III-V Compounds*, Data in Science and Technology (Springer Berlin Heidelberg, Berlin, Heidelberg, 1991).
- <sup>71</sup>B. Wenzien, P. Käckell, F. Bechstedt, and G. Cappellini, *Physical Review B* **52**, 10897 (1995).
- <sup>72</sup>P. Neudeck, in *Encyclopedia of Materials: Science and Technology* (Elsevier, 2001) pp. 8508–8519.
- <sup>73</sup>Y. Choi, H.-Y. Cha, L. Eastman, and M. Spencer, *IEEE Transactions on Electron Devices* **52**, 1940 (2005).
- <sup>74</sup>P. G. Neudeck (CRC Press, 2006).
- <sup>75</sup>X. Zhu, *ALTERNATIVE GROWTH AND INTERFACE PASSIVATION TECHNIQUES FOR SiO<sub>2</sub> ON 4H-SiC*, Ph.D. thesis, Auburn University (2008).
- <sup>76</sup>M. B. Wijesundara and R. Azevedo, *Silicon Carbide Microsystems for Harsh Environments*, MEMS Reference Shelf, Vol. 22 (Springer New York, New York, NY, 2011).
- <sup>77</sup>S. J. Pearton, X. Xia, F. Ren, M. A. J. Rasel, S. Stepanoff, N. Al-Mamun, A. Haque, and D. E. Wolfe, *Journal of Vacuum Science & Technology B* **41**, 030802 (2023).
- <sup>78</sup>J. Casady and R. Johnson, *Solid-State Electronics* **39**, 1409 (1996).
- <sup>79</sup>M. Huang, N. Goldsman, C.-H. Chang, I. Mayergoyz, J. M. McGarrity, and D. Woolard, *Journal of Applied Physics* **84**, 2065 (1998).
- <sup>80</sup>O. Madelung, ed., *Semiconductors — Basic Data* (Springer Berlin Heidelberg, Berlin, Heidelberg, 1996).
- <sup>81</sup>T. Egilsson, J. P. Bergman, I. G. Ivanov, A. Henry, and E. Janzén, *Physical Review B* **59**, 1956 (1999).
- <sup>82</sup>B. Lechner, *Behaviour of 4H-SiC Power Semiconductor Devices under Extreme Operating*

- Conditions*, Ph.D. thesis, Technische Universität München (2021).
- <sup>83</sup>N. Arpatzianis, A. Tsormpatzoglou, C. A. Dimitriadis, K. Zekentes, N. Camara, and M. Godlewski, *physica status solidi (a)* **203**, 2551 (2006).
- <sup>84</sup>R. Scaburri, *The Incomplete Ionization of Substitutional Dopants in Silicon Carbide*, Ph.D. thesis, Università di Bologna, Bologna (2011).
- <sup>85</sup>A. Naugarhiya, P. Wakhadkar, P. N. Kondekar, G. C. Patil, and R. M. Patrikar, *Journal of Computational Electronics* **16**, 190 (2017).
- <sup>86</sup>A. Arvanitopoulos, N. Lophitis, S. Perkins, K. N. Gyftakis, M. Belanche Guadas, and M. Antoniou, in *2017 IEEE 11th International Symposium on Diagnostics for Electrical Machines, Power Electronics and Drives (SDEMPED)* (IEEE, Tinos, Greece, 2017) pp. 565–571.
- <sup>87</sup>R. Choudhary, M. Mehta, R. Singh Shekhawat, S. Singh, and D. Singh, *Materials Today: Proceedings* **46**, 5889 (2021).
- <sup>88</sup>H. Yoshioka and K. Hirata, *AIP Advances* **8**, 045217 (2018).
- <sup>89</sup>C. Miccoli and F. Iucolano, *Materials Science in Semiconductor Processing* **97**, 40 (2019).
- <sup>90</sup>S. Tripathi, C. Upadhyay, C. Nagaraj, A. Venkatesan, and K. Devan, *Nuclear Instruments and Methods in Physics Research Section A: Accelerators, Spectrometers, Detectors and Associated Equipment* **916**, 246 (2019).
- <sup>91</sup>W. M. Klahold, W. J. Choyke, and R. P. Devaty, *Physical Review B* **102**, 205203 (2020).
- <sup>92</sup>A. Kovalchuk, J. Wozny, Z. Lisik, J. Podgorski, L. Ruta, A. Kubiak, and A. Boiadzhian, *Journal of Physics: Conference Series* **1534**, 012006 (2020).
- <sup>93</sup>A. Acharyya, *Applied Physics A* **123**, 629 (2017).
- <sup>94</sup>S. Banerjee, in *Advances in Terahertz Technology and Its Applications*, edited by S. Das, N. Anvesh Kumar, J. Dutta, and A. Biswas (Springer Singapore, Singapore, 2021) pp. 153–172.
- <sup>95</sup>H. Kim, *Transactions on Electrical and Electronic Materials* **25**, 141 (2024).
- <sup>96</sup>M. Bhatnagar and B. Baliga, *IEEE Transactions on Electron Devices* **40**, 645 (1993).
- <sup>97</sup>C. Codreanu, M. Avram, E. Carbunescu, and E. Iliescu, *Materials Science in Semiconductor Processing* **3**, 137 (2000).
- <sup>98</sup>C. Weitzel, J. Palmour, C. Carter, K. Moore, K. Nordquist, S. Allen, C. Thero, and M. Bhatnagar, *IEEE Transactions on Electron Devices* **43**, 1732 (1996).
- <sup>99</sup>H. Morkoç, S. Strite, G. B. Gao, M. E. Lin, B. Sverdlov, and M. Burns, *Journal of Applied Physics* **76**, 1363 (1994).
- <sup>100</sup>A. Burk, M. O'Loughlin, R. Siergiej, A. Agarwal, S. Sriram, R. Clarke, M. MacMillan, V. Bal-

- akrishna, and C. Brandt, *Solid-State Electronics* **43**, 1459 (1999).
- <sup>101</sup>T. Ayalew, *SiC Semiconductor Devices Technology, Modeling, and Simulation*, Ph.D. thesis, TU Wien (2004).
- <sup>102</sup>S. Sriram, R. R. Siergiej, R. C. Clarke, A. K. Agarwal, and C. D. Brandt, *physica status solidi (a)* **162**, 441 (1997).
- <sup>103</sup>R. Han, X. Xu, X. Hu, N. Yu, J. Wang, Y. Tian, and W. Huang, *Optical Materials* **23**, 415 (2003).
- <sup>104</sup>R. Mickevičius and J. H. Zhao, *Journal of Applied Physics* **83**, 3161 (1998).
- <sup>105</sup>J. H. Zhao, V. Gruzinskis, Y. Luo, M. Weiner, M. Pan, P. Shiktorov, and E. Starikov, *Semiconductor Science and Technology* **15**, 1093 (2000).
- <sup>106</sup>A. Akturk, N. Goldsman, S. Potbhare, and A. Lelis, *Journal of Applied Physics* **105**, 033703 (2009).
- <sup>107</sup>B. Zippelius, *Elektrische Charakterisierung Bauelement-relevanter Defekte in 3C- Und 4H-Siliziumkarbid*, Ph.D. thesis, Friedrich-Alexander-Universität Erlangen-Nürnberg (2011).
- <sup>108</sup>C. Weitzel, *Materials Science Forum* **264–268**, 907 (1998).
- <sup>109</sup>F. Nava, G. Bertuccio, A. Cavallini, and E. Vittone, *Measurement Science and Technology* **19**, 102001 (2008).
- <sup>110</sup>N. G. Wright, D. Morrison, C. M. Johnson, and A. G. O'Neill, *Materials Science Forum* **264–268**, 917 (1998).
- <sup>111</sup>B. J. Baliga, *Silicon Carbide Power Devices* (WORLD SCIENTIFIC, 2006).
- <sup>112</sup>B. J. Baliga, *Fundamentals of Power Semiconductor Devices* (Springer International Publishing, Cham, 2019).
- <sup>113</sup>J. Y. Tsao, S. Chowdhury, M. A. Hollis, D. Jena, N. M. Johnson, K. A. Jones, R. J. Kaplar, S. Rajan, C. G. Van De Walle, E. Bellotti, C. L. Chua, R. Collazo, M. E. Coltrin, J. A. Cooper, K. R. Evans, S. Graham, T. A. Grotjohn, E. R. Heller, M. Higashiwaki, M. S. Islam, P. W. Juodawlkis, M. A. Khan, A. D. Koehler, J. H. Leach, U. K. Mishra, R. J. Nemanich, R. C. N. Pilawa-Podgurski, J. B. Shealy, Z. Sitar, M. J. Tadjer, A. F. Witulski, M. Wraback, and J. A. Simmons, *Advanced Electronic Materials* **4**, 1600501 (2018).
- <sup>114</sup>I. N. Jiya and R. Gouws, *Micromachines* **11**, 1116 (2020).
- <sup>115</sup>H.-E. Nilsson, E. Bellotti, M. Hjelm, K. F. Brennan, and C. Petersson, **Proceedings of the IMACS Conference, Sofia, Bulgaria, June 1999** (1999).
- <sup>116</sup>E. Bellotti, H.-E. Nilsson, K. F. Brennan, P. P. Ruden, and R. Trew, *Journal of Applied Physics*

**87**, 3864 (2000).

<sup>117</sup>J. L. Vasconcelos, C. G. Rodrigues, and R. Luzzi, *Materials Science and Engineering: B* **249**, 114426 (2019).

<sup>118</sup>C. G. Rodrigues, *Semiconductors* **55**, 625 (2021).

<sup>119</sup>T. P. Chow, *Materials Science Forum* **338–342**, 1155 (2000).

<sup>120</sup>G. Dhanaraj, K. Byrappa, V. Prasad, and M. Dudley, eds., *Springer Handbook of Crystal Growth* (Springer Berlin Heidelberg, Berlin, Heidelberg, 2010).

<sup>121</sup>A. Elasser and T. Chow, *Proceedings of the IEEE* **90**, 969 (2002).

<sup>122</sup>M. Su, *Power Devices and Integrated Circuits Based on 4H-SiC Lateral JFETs*, Ph.D. thesis, New Brunswick Rutgers, New Jersey (2010).

<sup>123</sup>C.-M. Zetterling, ed., *Process Technology for Silicon Carbide Devices*, EMIS Processing Series No. 2 (Institution of Electrical Engineers, London, 2002).

<sup>124</sup>M. Östling, *Science China Information Sciences* **54**, 1087 (2011).

<sup>125</sup>E. Janzén, A. Gali, A. Henry, I. G. Ivanov, B. Magnusson, and N. T. Son, in *Defects in Micro-electronic Materials and Devices* (CRC Press, 2008) pp. 615–669.

<sup>126</sup>N. Kaminski, 2009 13th European Conference on Power Electronics and Applications **8** (2009).

<sup>127</sup>N. Kaminski and O. Hilt, *IET Circuits, Devices & Systems* **8**, 227 (2014).

<sup>128</sup>C. Buttay, D. Planson, B. Allard, D. Bergogne, P. Bevilacqua, C. Joubert, M. Lazar, C. Martin, H. Morel, D. Tournier, and C. Raynaud, *Materials Science and Engineering: B* **176**, 283 (2011).

<sup>129</sup>S. Fujita, *Japanese Journal of Applied Physics* **54**, 030101 (2015).

<sup>130</sup>P. G. Neudeck, in *Extreme Environment Electronics* (CRC Press, Taylor & Francis Group, 2013) pp. 225–232.

<sup>131</sup>A. Hassan, Y. Savaria, and M. Sawan, *IEEE Access* **6**, 78790 (2018).

<sup>132</sup>M. Higashiwaki, K. Sasaki, A. Kuramata, T. Masui, and S. Yamakoshi, *physica status solidi (a)* **211**, 21 (2014).

<sup>133</sup>G. Liu, B. R. Tuttle, and S. Dhar, *Applied Physics Reviews* **2**, 021307 (2015).

<sup>134</sup>S. Rybalka, E. Yu. Krayushkina, A. Demidov, O. Shishkina, and B. Surin, *International Journal of Physical Research* **5**, 11 (2017).

<sup>135</sup>C. Darmody and N. Goldsman, *Journal of Applied Physics* **126**, 145701 (2019).

<sup>136</sup>V. J. B. Torres, I. Capan, and J. Coutinho, *Physical Review B* **106**, 224112 (2022).

<sup>137</sup>S. J. Pearton, J. Yang, P. H. Cary, F. Ren, J. Kim, M. J. Tadjer, and M. A. Mastro, *Applied Physics Reviews* **5**, 011301 (2018).

- <sup>138</sup>V. Soler, *Design and Process Developments towards an Optimal 6.5 kV SiC Power MOSFET*, Ph.D. thesis, Universitat Politecnica de Catalunya (2019).
- <sup>139</sup>M. Yoder, *IEEE Transactions on Electron Devices* **43**, 1633 (1996).
- <sup>140</sup>S. Rao, E. D. Mallemace, and F. G. Della Corte, *Electronics* **11**, 1839 (2022).
- <sup>141</sup>G. Sozzi, M. Puzzanghera, R. Menozzi, and R. Nipoti, *IEEE Transactions on Electron Devices* **66**, 3028 (2019).
- <sup>142</sup>R. Nipoti, G. Sozzi, M. Puzzanghera, and R. Menozzi, *MRS Advances* **1**, 3637 (2016).
- <sup>143</sup>M. Usman and M. Nawaz, *Solid-State Electronics* **92**, 5 (2014).
- <sup>144</sup>F. Pezzimenti, *IEEE Transactions on Electron Devices* **60**, 1404 (2013).
- <sup>145</sup>S. Bellone, F. G. Della Corte, L. F. Albanese, and F. Pezzimenti, *IEEE Transactions on Power Electronics* **26**, 2835 (2011).
- <sup>146</sup>D. Schröder, *Leistungselektronische Bauelemente* (Springer Berlin Heidelberg, Berlin, Heidelberg, 2006).
- <sup>147</sup>X. Dong, M. Huang, Y. Ma, C. Fu, M. He, Z. Yang, Y. Li, and M. Gong, *IEEE Transactions on Nuclear Science* , 1 (2024).
- <sup>148</sup>T. Yang, C. Fu, W. Song, Y. Tan, S. Xiao, C. Wang, K. Liu, X. Zhang, and X. Shi, *Nuclear Instruments and Methods in Physics Research Section A: Accelerators, Spectrometers, Detectors and Associated Equipment* **1056**, 168677 (2023).
- <sup>149</sup>T. Yang, Y. Tan, C. Wang, X. Zhang, and X. Shi, “Simulation of the 4H-SiC Low Gain Avalanche Diode,” (2022), arXiv:2206.10191 [physics].
- <sup>150</sup>M. De Napoli, *Frontiers in Physics* **10**, 898833 (2022).
- <sup>151</sup>M. Cabello, V. Soler, G. Rius, J. Montserrat, J. Rebollo, and P. Godignon, *Materials Science in Semiconductor Processing* **78**, 22 (2018).
- <sup>152</sup>Q. Chen, L. Yang, S. Wang, Y. Zhang, Y. Dai, and Y. Hao, *Applied Physics A* **118**, 1219 (2015).
- <sup>153</sup>H. A. Mantooth, in *Extreme Environment Electronics* (CRC Press, Taylor & Francis Group, 2013) pp. 243–252.
- <sup>154</sup>L. F. Albanese, *Characterization, Modeling and Simulation of 4H-SiC Power Diodes*, Ph.D. thesis, Universitàdegli Studi di Salerno (2010).
- <sup>155</sup>P. Bhatnagar, A. B. Horsfall, N. G. Wright, C. M. Johnson, K. V. Vassilevski, and A. G. O'Neill, *Solid-State Electronics* **49**, 453 (2005).
- <sup>156</sup>M. W. Cole and P. Joshi, in *Silicon Carbide*, edited by Z. C. Feng and J. H. Zhao (Springer Berlin Heidelberg, Berlin, Heidelberg, 2004) pp. 517–536.

- <sup>157</sup>H. Iwata and K. M. Itoh, *Materials Science Forum* **338–342**, 729 (2000).
- <sup>158</sup>H. Iwata, K. M. Itoh, and G. Pensl, *Journal of Applied Physics* **88**, 1956 (2000).
- <sup>159</sup>N. Wright, in *IEE Colloquium on New Developments in Power Semiconductor Devices*, Vol. 1996 (IEE, London, UK, 1996) pp. 6–6.
- <sup>160</sup>H.-E. Nilsson, U. Sannemo, and C. S. Petersson, *Journal of Applied Physics* **80**, 3365 (1996).
- <sup>161</sup>I. Neila Inglesias, “APPLYING NUMERICAL SIMULATION TO MODELS SiC SEMICONDUCTOR DEVICES,” (2012).
- <sup>162</sup>T. Kimoto, *Japanese Journal of Applied Physics* **54**, 040103 (2015).
- <sup>163</sup>J. Zhao, X. Li, K. Tone, P. Alexandrov, M. Pan, and M. Weiner, *Solid-State Electronics* **47**, 377 (2003).
- <sup>164</sup>A. Elasser, M. Kheraluwala, M. Ghezzo, R. Steigerwald, N. Evers, J. Kretchmer, and T. Chow, *IEEE Transactions on Industry Applications* **39**, 915 (2003).
- <sup>165</sup>A. Elasser, M. Ghezzo, N. Krishnamurthy, J. Kretchmer, A. Clock, D. Brown, and T. Chow, *Solid-State Electronics* **44**, 317 (2000).
- <sup>166</sup>V. Chelnokov and A. Syrkin, *Materials Science and Engineering: B* **46**, 248 (1997).
- <sup>167</sup>F. L. L. Nouketcha, Y. Cui, A. Lelis, R. Green, C. Darmody, J. Schuster, and N. Goldsman, *IEEE Transactions on Electron Devices* **67**, 3999 (2020).
- <sup>168</sup>A. A. Lebedev, *Radiation Effects in Silicon Carbide*, Materials Research Foundations No. volume 6 (2017) (Materials Research Forum LLC, Millersville, PA, USA, 2017).
- <sup>169</sup>T. P. Chow, I. Omura, M. Higashiwaki, H. Kawarada, and V. Pala, *IEEE Transactions on Electron Devices* **64**, 856 (2017).
- <sup>170</sup>J. A. Pellish and L. M. Cohn, in *Extreme Environment Electronics* (CRC Press, Taylor & Francis Group, 2013) pp. 49–58.
- <sup>171</sup>S. M. Sze and K. K. Ng, *Physics of Semiconductor Devices*, 3rd ed. (Wiley-Interscience, Hoboken, N.J, 2007).
- <sup>172</sup>J. Millán, *IET Circuits, Devices & Systems* **1**, 372 (2007).
- <sup>173</sup>A. Pérez-Tomás, P. Brosselard, P. Godignon, J. Millán, N. Mestres, M. R. Jennings, J. A. Covington, and P. A. Mawby, *Journal of Applied Physics* **100**, 114508 (2006).
- <sup>174</sup>T. P. Chow, N. Ramungul, J. Fedison, and Y. Tang, in *Silicon Carbide*, edited by W. J. Choyke, H. Matsunami, and G. Pensl (Springer Berlin Heidelberg, Berlin, Heidelberg, 2004) pp. 737–767.
- <sup>175</sup>N. Zhang, *High Voltage GaN HEMTs with Low On-Resistance for Switching Applications*,

- Ph.D. thesis, UNIVERSITY of CALIFORNIA, Santa Barbara (2002).
- <sup>176</sup>R. Trew, *Proceedings of the IEEE* **90**, 1032 (2002).
- <sup>177</sup>S. K. Lee, *Processing and Characterization of Silicon Carbide (6H-SiC and 4H-SiC) Contacts for High Power and h...* (Mikroelektronik och informationsteknik, Kista, 2002).
- <sup>178</sup>R. Kemerley, H. Wallace, and M. Yoder, *Proceedings of the IEEE* **90**, 1059 (2002).
- <sup>179</sup>V. Dmitriev, T. P. Chow, S. P. DenBaars, M. S. Shur, and M. G. Spencer, “*High-Temperature Electronics in Europe:*,” Tech. Rep. (Defense Technical Information Center, Fort Belvoir, VA, 2000).
- <sup>180</sup>T. Chow, V. Khemka, J. Fedison, N. Ramungul, K. Matocha, Y. Tang, and R. Gutmann, *Solid-State Electronics* **44**, 277 (2000).
- <sup>181</sup>C. M. Zetterling, M. Östling, C. I. Harris, N. Nordell, K. Wongchotigul, and M. G. Spencer, *Materials Science Forum* **264–268**, 877 (1998).
- <sup>182</sup>P. B. Shah and K. A. Jones, *Journal of Applied Physics* **84**, 4625 (1998).
- <sup>183</sup>M. Roschke, F. Schwierz, G. Paasch, and D. Schipanski, *Materials Science Forum* **264–268**, 965 (1998).
- <sup>184</sup>E. Danielsson, C. I. Harris, C. M. Zetterling, and M. Östling, *Materials Science Forum* **264–268**, 805 (1998).
- <sup>185</sup>T. P. Chow, N. Ramungul, and M. Ghezzo, *MRS Proceedings* **483**, 89 (1997).
- <sup>186</sup>T. P. Chow and M. Ghezzo, *MRS Proceedings* **423**, 9 (1996).
- <sup>187</sup>B. Ozpineci, “*Comparison of Wide-Bandgap Semiconductors for Power Electronics Applications,*” Tech. Rep. ORNL/TM-2003/257, 885849 (Oak Ridge National Laboratory, 2004).
- <sup>188</sup>F. Bechstedt, *Materials Science Forum* **264–268**, 265 (1998).
- <sup>189</sup>W. M. Chen, N. T. Son, E. Janzén, D. M. Hofmann, and B. K. Meyer, *physica status solidi (a)* **162**, 79 (1997).
- <sup>190</sup>Y. M. Tairov and Y. A. Vodakov, in *Electroluminescence*, Vol. 17, edited by J. I. Pankove (Springer Berlin Heidelberg, Berlin, Heidelberg, 1977) pp. 31–61.
- <sup>191</sup>G. Wellenhofer and U. Rössler, *physica status solidi (b)* **202**, 107 (1997).
- <sup>192</sup>N. T. Son, P. N. Hai, W. M. Chen, C. Hallin, B. Monemar, and E. Janzén, *Physical Review B* **61**, R10544 (2000).
- <sup>193</sup>C. Persson and U. Lindefelt, *Physical Review B* **54**, 10257 (1996).
- <sup>194</sup>K. Karch, G. Wellenhofer, P. Pavone, U. Rössler, and D. Strauch, “*Structural and electronic properties of SiC polytypes,*” (1995).

- <sup>195</sup>J. Dong and A.-B. Chen, in *SiC Power Materials*, Vol. 73, edited by R. Hull, R. M. Osgood, J. Parisi, H. Warlimont, and Z. C. Feng (Springer Berlin Heidelberg, Berlin, Heidelberg, 2004) pp. 63–87.
- <sup>196</sup>H. P. Iwata, U. Lindefelt, S. Öberg, and P. R. Briddon, *Physical Review B* **68**, 245309 (2003).
- <sup>197</sup>S. Nakashima and H. Harima, *physica status solidi (a)* **162**, 39 (1997).
- <sup>198</sup>Y. Kuroiwa, Y.-i. Matsushita, K. Harada, and F. Oba, *Applied Physics Letters* **115**, 112102 (2019).
- <sup>199</sup>W. Lambrecht, S. Limpijumnong, S. Rashkeev, and B. Segall, *physica status solidi (b)* **202**, 5 (1997).
- <sup>200</sup>C. Raynaud, D. Tournier, H. Morel, and D. Planson, *Diamond and Related Materials* **19**, 1 (2010).
- <sup>201</sup>J. Blakemore, *Semiconductor Statistics* (Elsevier, 1962).
- <sup>202</sup>W. Götz, A. Schöner, G. Pensl, W. Sutrop, W. J. Choyke, R. Stein, and S. Leibenzeder, *Journal of Applied Physics* **73**, 3332 (1993).
- <sup>203</sup>W. Sutrop, *Aluminium, Bor und Stickstoff als Dotierstoffe in einkristallinem Siliziumkarbid SiC(6H)*, Ph.D. thesis, Friedrich-Alexander-Universität, Erlangen-Nürnberg (1991).
- <sup>204</sup>C. Hemmingsson, N. T. Son, O. Kordina, J. P. Bergman, E. Janzén, J. L. Lindström, S. Savage, and N. Nordell, *Journal of Applied Physics* **81**, 6155 (1997).
- <sup>205</sup>P. Ščajev, M. Karaliūnas, E. Kuokštis, and K. Jarašiūnas, *Journal of Luminescence* **134**, 588 (2013).
- <sup>206</sup>V. K. Khanna, *Extreme-Temperature and Harsh-Environment Electronics: Physics, Technology and Applications*, second edition ed. (IOP Publishing, Bristol [England] (Temple Circus, Temple Way, Bristol BS1 6HG, UK), 2023).
- <sup>207</sup>R. Ishikawa, M. Hara, H. Tanaka, M. Kaneko, and T. Kimoto, *Applied Physics Express* **14**, 061005 (2021).
- <sup>208</sup>R. Ishikawa, H. Tanaka, M. Kaneko, and T. Kimoto, *Journal of Applied Physics* **135**, 075704 (2024).
- <sup>209</sup>H. P. Iwata, *Applied Physics Letters* **82**, 598 (2003).
- <sup>210</sup>T. Kinoshita, K. M. Itoh, J. Muto, M. Schadt, G. Pensl, and K. Takeda, *Materials Science Forum* **264–268**, 295 (1998).
- <sup>211</sup>O. Kordina, A. Henry, J. P. Bergman, N. T. Son, W. M. Chen, C. Hallin, and E. Janzén, *Applied Physics Letters* **66**, 1373 (1995).

- <sup>212</sup>J. Camassel and S. Juillaquet, *physica status solidi (b)* **245**, 1337 (2008).
- <sup>213</sup>J. T. Devreese, in *Digital Encyclopedia of Applied Physics*, edited by Wiley-VCH Verlag GmbH & Co. KGaA (Wiley, 2003) 1st ed.
- <sup>214</sup>G. D. Mahan, *Many-Particle Physics* (Springer US, Boston, MA, 1990).
- <sup>215</sup>H. Fröhlich, *Advances in Physics* **3**, 325 (1954).
- <sup>216</sup>K. Takahashi, A. Yoshikawa, and A. Sandhu, eds., *Wide Bandgap Semiconductors* (Springer Berlin Heidelberg, Berlin, Heidelberg, 2007).
- <sup>217</sup>K. Mikami, M. Kaneko, and T. Kimoto, *IEEE Electron Device Letters* , 1 (2024).
- <sup>218</sup>N. T. Son, W. M. Chen, O. Kordina, A. O. Konstantinov, B. Monemar, E. Janzén, D. M. Hofman, D. Volm, M. Drechsler, and B. K. Meyer, *Applied Physics Letters* **66**, 1074 (1995).
- <sup>219</sup>P. Käckell, B. Wenzien, and F. Bechstedt, *Physical Review B* **50**, 10761 (1994).
- <sup>220</sup>L. Lu, H. Zhang, X. Wu, J. Shi, and Y.-Y. Sun, *Chinese Physics B* **30**, 096806 (2021).
- <sup>221</sup>C. Persson and U. Lindefelt, *Journal of Applied Physics* **86**, 5036 (1999).
- <sup>222</sup>G. L. Zhao and D. Bagayoko, *New Journal of Physics* **2**, 16 (2000).
- <sup>223</sup>W. R. L. Lambrecht and B. Segall, *Physical Review B* **52**, R2249 (1995).
- <sup>224</sup>A.-B. Chen and P. Srivikul, *physica status solidi (b)* **202**, 81 (1997).
- <sup>225</sup>G. Pennington and N. Goldsman, *Physical Review B* **64**, 045104 (2001).
- <sup>226</sup>D. Volm, B. K. Meyer, D. M. Hofmann, W. M. Chen, N. T. Son, C. Persson, U. Lindefelt, O. Kordina, E. Sörman, A. O. Konstantinov, B. Monemar, and E. Janzén, *Physical Review B* **53**, 15409 (1996).
- <sup>227</sup>C. Persson and U. Lindefelt, *Journal of Applied Physics* **83**, 266 (1998).
- <sup>228</sup>G. Ng, *Computational Studies of 4H and 6H Silicon Carbide*, Ph.D. thesis, Arizona State University (2010).
- <sup>229</sup>G. Ng, D. Vasileska, and D. Schroder, *Superlattices and Microstructures* **49**, 109 (2011).
- <sup>230</sup>N. T. Son, P. Hai, W. Chen, C. Hallin, B. Monemar, and E. Janzén, *Materials Science Forum* **338–342**, 563 (2000).
- <sup>231</sup>G. Lomakina and Y. A. Vodakov, *Sov. Phys. Solid State* **15**, 83 (1973).
- <sup>232</sup>G. Lomakina, in *In: Silicon Carbide-1973; Proceedings of the Third International Conference* (1974) pp. 520–526.
- <sup>233</sup>L. Patrick, W. J. Choyke, and D. R. Hamilton, *Physical Review* **137**, A1515 (1965).
- <sup>234</sup>M. Schadt, G. Pensl, R. P. Devaty, W. J. Choyke, R. Stein, and D. Stephani, *Applied Physics Letters* **65**, 3120 (1994).

- <sup>235</sup>G. Pensl and W. Choyke, *Physica B: Condensed Matter* **185**, 264 (1993).
- <sup>236</sup>A. Itoh, T. Kimoto, and H. Matsunami, *IEEE Electron Device Letters* **16**, 280 (1995).
- <sup>237</sup>P. A. Ivanov, M. E. Levenshtein, J. W. Palmour, S. L. Rumyantsev, and R. Singh, *Semiconductor Science and Technology* **15**, 908 (2000).
- <sup>238</sup>S. I. Maximenko, *AIP Advances* **13**, 105021 (2023).
- <sup>239</sup>J. Pernot, S. Contreras, J. Camassel, J. L. Robert, W. Zawadzki, E. Neyret, and L. Di Cioccio, *Applied Physics Letters* **77**, 4359 (2000).
- <sup>240</sup>G. Pennington and N. Goldsman, *Journal of Applied Physics* **95**, 4223 (2004).
- <sup>241</sup>V. Tilak, K. Matocha, and G. Dunne, *IEEE Transactions on Electron Devices* **54**, 2823 (2007).
- <sup>242</sup>R. A. Faulkner, *Physical Review* **184**, 713 (1969).
- <sup>243</sup>A. Yang, K. Murata, T. Miyazawa, T. Tawara, and H. Tsuchida, *Journal of Applied Physics* **126**, 055103 (2019).
- <sup>244</sup>N. Kuznetsov and A. Zubrilov, *Materials Science and Engineering: B* **29**, 181 (1995).
- <sup>245</sup>C. Persson, U. Linddefelt, and B. E. Sernelius, *Physical Review B* **60**, 16479 (1999).
- <sup>246</sup>R. P. Joshi, *Journal of Applied Physics* **78**, 5518 (1995).
- <sup>247</sup>S. Rakheja, L. Huang, S. Hau-Riege, S. E. Harrison, L. F. Voss, and A. M. Conway, *IEEE Journal of the Electron Devices Society* **8**, 1118 (2020).
- <sup>248</sup>Y. Negoro, K. Katsumoto, T. Kimoto, and H. Matsunami, *Journal of Applied Physics* **96**, 224 (2004).
- <sup>249</sup>Z. C. Feng and J. H. Zhao, eds., *Silicon Carbide: Materials, Processing, and Devices*, Opto-electronic Properties of Semiconductors and Superlattices No. v. 20 (Taylor & Francis, New York, 2004).
- <sup>250</sup>C. Q. Chen, J. Zeman, F. Engelbrecht, C. Peppermüller, R. Helbig, Z. H. Chen, and G. Martínez, *Journal of Applied Physics* **87**, 3800 (2000).
- <sup>251</sup>R. P. Devaty and W. J. Choyke, *physica status solidi (a)* **162**, 5 (1997).
- <sup>252</sup>K. Neimontas, T. Malinauskas, R. Aleksiejūnas, M. Sūdžius, K. Jarašiūnas, L. Storasta, J. P. Bergman, and E. Janzen, *Semiconductor Science and Technology* **21**, 952 (2006).
- <sup>253</sup>M. Flores, F. Maia, V. Freire, J. Da Costa, and E. Da Silva, *Microelectronics Journal* **34**, 717 (2003).
- <sup>254</sup>H. Van Daal, W. Knippenberg, and J. Wasscher, *Journal of Physics and Chemistry of Solids* **24**, 109 (1963).
- <sup>255</sup>A. Galeckas, J. Linnros, V. Grivickas, U. Linddefelt, and C. Hallin, *Applied Physics Letters* **71**,

3269 (1997).

- <sup>256</sup>S. G. Sridhara, L. L. Clemen, R. P. Devaty, W. J. Choyke, D. J. Larkin, H. S. Kong, T. Troffer, and G. Pensl, *Journal of Applied Physics* **83**, 7909 (1998).
- <sup>257</sup>F. C. Beyer, *Deep Levels in SiC*, Ph.D. thesis, Linköping University (2011).
- <sup>258</sup>A. Gsponer, M. Knopf, P. Gaggl, J. Burin, S. Waid, and T. Bergauer, *Nuclear Instruments and Methods in Physics Research Section A: Accelerators, Spectrometers, Detectors and Associated Equipment* **1064**, 169412 (2024).
- <sup>259</sup>P. Kwasnicki, *Evaluation of Doping in 4H-SiC by Optical Spectroscopies*, Ph.D. thesis, UNIVERSITE MONTPELLIER II (2014).
- <sup>260</sup>D. K. Schroder, *Semiconductor Material and Device Characterization*, 1st ed. (Wiley, 2005).
- <sup>261</sup>J. P. Wolfe and A. Mysyrowicz, *Scientific American* **250**, 98 (1984), 24969326.
- <sup>262</sup>R. J. Elliott, *Physical Review* **108**, 1384 (1957).
- <sup>263</sup>W. Choyke, in *Silicon Carbide–1968* (Elsevier, 1969) pp. S141–S152.
- <sup>264</sup>Ch. Haberstroh, R. Helbig, and R. A. Stein, *Journal of Applied Physics* **76**, 509 (1994).
- <sup>265</sup>A. Itoh, H. Akita, T. Kimoto, and H. Matsunami, *Applied Physics Letters* **65**, 1400 (1994).
- <sup>266</sup>A. Itoh, T. K. Tsunenobu Kimoto, and H. M. Hiroyuki Matsunami, *Japanese Journal of Applied Physics* **35**, 4373 (1996).
- <sup>267</sup>M. Ikeda and H. Matsunami, *Physica Status Solidi (a)* **58**, 657 (1980).
- <sup>268</sup>G. B. Dubrovskii and V. I. Sankin, *Sov. Phys. Solid State* **17**, 1847 (1975).
- <sup>269</sup>W. J. Choyke, L. Patrick, and D. Hamilton, 7th in conference on semicond. physics paris 1964, **7**, 751 (1964).
- <sup>270</sup>W. J. Choyke, D. R. Hamilton, and L. Patrick, *Physical Review* **133**, A1163 (1964).
- <sup>271</sup>G. Zanmarchi, 7th in conference on semicond. physics paris 1964, **7**, 57 (1964).
- <sup>272</sup>W. J. Choyke, H. Matsunami, and G. Pensl, eds., *Silicon Carbide: Recent Major Advances*, Advanced Texts in Physics (Springer Berlin Heidelberg, Berlin, Heidelberg, 2004).
- <sup>273</sup>R. Freer, ed., *The Physics and Chemistry of Carbides, Nitrides and Borides* (Springer Netherlands, Dordrecht, 1990).
- <sup>274</sup>H. Habib, N. G. Wright, and A. B. Horsfall, *Advanced Materials Research* **413**, 229 (2011).
- <sup>275</sup>H. Y. Fan, *Physical Review* **82**, 900 (1951).
- <sup>276</sup>A. Das and S. P. Duttagupta, *Radiation Protection Dosimetry* **167**, 443 (2015).
- <sup>277</sup>R. Pässler, *physica status solidi (b)* **200**, 155 (1997).
- <sup>278</sup>R. Pässler, *Journal of Applied Physics* **83**, 3356 (1998).

- <sup>279</sup>A. Galeckas, P. Grivickas, V. Grivickas, V. Bikbajevs, and J. Linnros, *physica status solidi (a)* **191**, 613 (2002).
- <sup>280</sup>R. Pässler, *Physical Review B* **66**, 085201 (2002).
- <sup>281</sup>K. P. O'Donnell and X. Chen, *Applied Physics Letters* **58**, 2924 (1991).
- <sup>282</sup>Y. P. Varshni, *Physica* **34**, 149 (1967).
- <sup>283</sup>S. Balachandran, T. P. Chow, and A. K. Agarwal, *Materials Science Forum* **483–485**, 909 (2005).
- <sup>284</sup>M. Nawaz, *Microelectronics Journal* **41**, 801 (2010).
- <sup>285</sup>P. Grivickas, V. Grivickas, J. Linnros, and A. Galeckas, *Journal of Applied Physics* **101**, 123521 (2007).
- <sup>286</sup>R. Pässler, *physica status solidi (b)* **216**, 975 (1999).
- <sup>287</sup>L. Viña, S. Logothetidis, and M. Cardona, *Physical Review B* **30**, 1979 (1984).
- <sup>288</sup>R. Pässler, *physica status solidi (b)* **236**, 710 (2003).
- <sup>289</sup>E. F. Schubert, *Doping in III-V Semiconductors*, Cambridge Studies in Semiconductor Physics and Microelectronic Engineering No. 1 (Cambridge University Press, Cambridge [England] ; New York, NY, USA, 1993).
- <sup>290</sup>S. Jain and D. Roulston, *Solid-State Electronics* **34**, 453 (1991).
- <sup>291</sup>G. Donnarumma, V. Palankovski, and S. Selberherr, in *Proceedings of the International Conference on Simulation of Semiconductor Processes and Devices (SISPAD)* (2012) pp. 125–128.
- <sup>292</sup>M. Ruff, H. Mitlehner, and R. Helbig, *IEEE Transactions on Electron Devices* **41**, 1040 (1994).
- <sup>293</sup>M. K. Mainali, P. Dulal, B. Shrestha, E. Amonette, A. Shan, and N. J. Podraza, *Surface Science Spectra* **31**, 026003 (2024).
- <sup>294</sup>W. J. Choyke and L. Patrick, *Physical Review* **105**, 1721 (1957).
- <sup>295</sup>A. O. Ewvaraye, S. R. Smith, and W. C. Mitchel, *Journal of Applied Physics* **79**, 7726 (1996).
- <sup>296</sup>I. G. Ivanov, U. Lindefelt, A. Henry, O. Kordina, C. Hallin, M. Aroyo, T. Egilsson, and E. Janzén, *Physical Review B* **58**, 13634 (1998).
- <sup>297</sup>I. G. Ivanov, J. Zhang, L. Storasta, and E. Janzén, *Materials Science Forum* **389–393**, 613 (2002).
- <sup>298</sup>S. Sridhara, S. Bai, O. Shigiltchoff, R. P. Devaty, and W. J. Choyke, *Materials Science Forum* **338–342**, 567 (2000).
- <sup>299</sup>D. Stefanakis and K. Zekentes, *Microelectronic Engineering* **116**, 65 (2014).
- <sup>300</sup>W. H. Backes, P. A. Bobbert, and W. Van Haeringen, *Physical Review B* **49**, 7564 (1994).

- <sup>301</sup>H.-g. Junginger and W. Van Haeringen, *physica status solidi (b)* **37**, 709 (1970).
- <sup>302</sup>W. Van Haeringen, P. Bobbert, and W. Backes, *physica status solidi (b)* **202**, 63 (1997).
- <sup>303</sup>K. Yamaguchi, D. Kobayashi, T. Yamamoto, and K. Hirose, *Physica B: Condensed Matter* **532**, 99 (2018).
- <sup>304</sup>G. B. Dubrovskii and A. A. Lepneva, Sov. Phys. Solid State **19**, 729 (1977).
- <sup>305</sup>I. Shalish, I. B. Altfeder, and V. Narayanamurti, *Physical Review B* **65**, 073104 (2002).
- <sup>306</sup>Explanation see text.
- <sup>307</sup>According to shown band gap the data were extract from a 21R-SiC device although in<sup>69</sup> argued that it was 6H.
- <sup>308</sup>Solely measurement for lowest temperature shown.
- <sup>309</sup>V. I. Gavrilenko, A. V. Postnikov, N. I. Klyui, and V. G. Litovchenko, *physica status solidi (b)* **162**, 477 (1990).
- <sup>310</sup>C. H. Park, B.-H. Cheong, K.-H. Lee, and K. J. Chang, *Physical Review B* **49**, 4485 (1994).
- <sup>311</sup>J. Käckel, *Siliziumkarbid - Strukturelle und elektronische Eigenschaften verschiedener Polytypen*, Ph.D. thesis, Friedrich-Schiller-Universität Jena (1996).
- <sup>312</sup>Model fitted to 6H-SiC results in<sup>7</sup>.
- <sup>313</sup>Model fitted to results in<sup>263</sup>.
- <sup>314</sup>Origin of Varshni parameters unknown.
- <sup>315</sup>T. Tamaki, G. G. Walden, Y. Sui, and J. A. Cooper, *IEEE Transactions on Electron Devices* **55**, 1920 (2008).
- <sup>316</sup>Y. Huang, R. Wang, Y. Zhang, D. Yang, and X. Pi, *Journal of Applied Physics* **131**, 185703 (2022).
- <sup>317</sup>S. Hagen, A. Van Kemenade, and J. Van Der Does De Bye, *Journal of Luminescence* **8**, 18 (1973).
- <sup>318</sup>F. Nallet, D. Planson, K. Isoird, M. Locatelli, and J. Chante, in *CAS '99 Proceedings. 1999 International Semiconductor Conference (Cat. No.99TH8389)*, Vol. 1 (IEEE, Sinaia, Romania, 1999) pp. 195–198.
- <sup>319</sup>R. Weingärtner, P. J. Wellmann, M. Bickermann, D. Hofmann, T. L. Straubinger, and A. Winacker, *Applied Physics Letters* **80**, 70 (2002).
- <sup>320</sup>N. Lophitis, A. Arvanitopoulos, S. Perkins, and M. Antoniou, in *Disruptive Wide Bandgap Semiconductors, Related Technologies, and Their Applications*, edited by Y. K. Sharma (In-Tech, 2018).

- <sup>321</sup>P. Wellmann, S. Bushevoy, and R. Weingärtner, *Materials Science and Engineering: B* **80**, 352 (2001).
- <sup>322</sup>H.-Y. Cha and P. M. Sandvik, *Japanese Journal of Applied Physics* **47**, 5423 (2008).
- <sup>323</sup>B. Chen, Y. Yang, X. Xie, N. Wang, Z. Ma, K. Song, and X. Zhang, *Chinese Science Bulletin* **57**, 4427 (2012).
- <sup>324</sup>Y.-R. Zhang, B. Zhang, Z.-J. Li, and X.-C. Deng, *Chinese Physics B* **19**, 067102 (2010).
- <sup>325</sup>B. Buono, *Simulation and Characterization of Silicon Carbide Power Bipolar Junction Transistors*, Ph.D. thesis, KTH Royal Institute of Technology (2012).
- <sup>326</sup>K. Zeghdar, L. Dehimi, F. Pezzimenti, S. Rao, and F. G. Della Corte, *Japanese Journal of Applied Physics* **58**, 014002 (2019).
- <sup>327</sup>K. Zeghdar, L. Dehimi, F. Pezzimenti, M. L. Megherbi, and F. G. Della Corte, *Journal of Electronic Materials* **49**, 1322 (2020).
- <sup>328</sup>D. Johannesson and M. Nawaz, *IEEE Transactions on Power Electronics* **31**, 4517 (2016).
- <sup>329</sup>H. Lanyon and R. Tuft, *IEEE Transactions on Electron Devices* **26**, 1014 (1979).
- <sup>330</sup>H. Liu, J. Wang, S. Liang, H. Yu, and W. Deng, *Semiconductor Science and Technology* **36**, 025009 (2021).
- <sup>331</sup>V. Uhnevionak, *Simulation and Modeling of Silicon-Carbide Devices*, Ph.D. thesis, Friedrich-Alexander-Universität (2015).
- <sup>332</sup>J. Lutz, U. Scheuermann, H. Schlangenotto, and R. De Doncker, “Power Semiconductor Devices—Key Components for Efficient Electrical Energy Conversion Systems,” in *Semiconductor Power Devices* (Springer International Publishing, Cham, 2018) pp. 1–20.
- <sup>333</sup>J. Lutz, H. Schlangenotto, U. Scheuermann, and R. De Doncker, *Semiconductor Power Devices: Physics, Characteristics, Reliability* (Springer Berlin Heidelberg, Berlin, Heidelberg, 2011).
- <sup>334</sup>M. Jiménez-Ramos, A. García Osuna, M. Rodriguez-Ramos, E. Viezzer, G. Pellegrini, P. Godignon, J. Rafí, G. Rius, and J. García López, *Radiation Physics and Chemistry* **214**, 111283 (2024).
- <sup>335</sup>T. R. Garcia, A. Kumar, B. Reinke, T. E. Blue, and W. Windl, *Applied Physics Letters* **103**, 152108 (2013).
- <sup>336</sup>P. Masri, *Surface Science Reports* **48**, 1 (2002).
- <sup>337</sup>J. A. Freitas, in *Properties of Silicon Carbide*, EMIS Datareviews Series No. 13, edited by G. L. Harris and Inspec (INSPEC, the Inst. of Electrical Engineers, London, 1995) pp. 29–41.

- <sup>338</sup>X. Li, Y. Luo, L. Fursin, J. Zhao, M. Pan, P. Alexandrov, and M. Weiner, *Solid-State Electronics* **47**, 233 (2003).
- <sup>339</sup>T. Egilsson, I. G. Ivanov, N. T. Son, G. Henry, A., J. P. Bergman, and E. Janzén, in *Silicon Carbide*, edited by Z. C. Feng and J. H. Zhao (Springer Berlin Heidelberg, Berlin, Heidelberg, 2004) pp. 517–536.
- <sup>340</sup>R. C. Marshall, J. W. Faust, C. E. Ryan, A. F. C. R. L. (U.S.), and University of South Carolina, eds., *Silicon Carbide–1973: Proceedings*, 1st ed. (University of South Carolina Press, Columbia, 1974).
- <sup>341</sup>S. Sandeep and R. Komaragiri, in *India International Conference on Power Electronics 2010 (IICPE2010)* (IEEE, New Delhi, India, 2011) pp. 1–5.
- <sup>342</sup>B. Zat’ko, L. Hrubčín, A. Šagátová, J. Osvald, P. Boháček, E. Kováčová, Y. Halahovets, S. V. Rozov, and V. Sandukovskij, *Applied Surface Science* **536**, 147801 (2021).
- <sup>343</sup>G. Rescher, G. Pobegen, T. Aichinger, and T. Grasser, *IEEE Transactions on Electron Devices* **65**, 1419 (2018).
- <sup>344</sup>D. T. Morisette, *Development of Robust Power Schottky Barrier Diodes in Silicon Carbide*, Ph.D. thesis, Purdue University (2001).
- <sup>345</sup>J. Hudgins, G. Simin, E. Santi, and M. Khan, *IEEE Transactions on Power Electronics* **18**, 907 (2003).
- <sup>346</sup>K. C. Mandal, P. G. Muzykov, R. M. Krishna, and J. R. Terry, *IEEE Transactions on Nuclear Science* **59**, 1591 (2012).
- <sup>347</sup>V. V. Afanas’ev, M. Bassler, G. Pensl, M. J. Schulz, and E. Stein Von Kamienski, *Journal of Applied Physics* **79**, 3108 (1996).
- <sup>348</sup>M. Shur, S. L. Rumyantsev, and M. E. Levinshtein, eds., *SiC Materials and Devices*, Selected Topics in Electronics and Systems No. v. 40 (World Scientific, New Jersey ; London, 2006).
- <sup>349</sup>S. J. Bader, H. Lee, R. Chaudhuri, S. Huang, A. Hickman, A. Molnar, H. G. Xing, D. Jena, H. W. Then, N. Chowdhury, and T. Palacios, *IEEE Transactions on Electron Devices* **67**, 4010 (2020).
- <sup>350</sup>D. Mukherjee and M. Neto, *Recent Advances in SiC/Diamond Composite Devices* (IOP Publishing, 2023).
- <sup>351</sup>X. Guo, Q. Xun, Z. Li, and S. Du, *Micromachines* **10**, 406 (2019).
- <sup>352</sup>H. A. Mantooth, K. Peng, E. Santi, and J. L. Hudgins, *IEEE Transactions on Electron Devices* **62**, 423 (2015).

- <sup>353</sup>J. D. Cressler and H. A. Mantooth, *Extreme Environment Electronics* (CRC Press, Taylor & Francis Group, Boca Raton, 2013).
- <sup>354</sup>M. B. J. Wijesundara and R. G. Azevedo, “System Integration,” in *Silicon Carbide Microsystems for Harsh Environments*, Vol. 22 (Springer New York, New York, NY, 2011) pp. 189–230.
- <sup>355</sup>V. Cimalla, J. Pezoldt, and O. Ambacher, *Journal of Physics D: Applied Physics* **40**, S19 (2007).
- <sup>356</sup>M. J. Kumar and V. Parihar, *Microelectronic Engineering* **81**, 90 (2005).
- <sup>357</sup>K. Bertilsson, *Simulation and Optimization of SiC Field Effect Transistors*, Ph.D. thesis, Mikroelektronik och informationsteknik / KTH, Microelectronics and Information Technology, IMIT / KTH, Microelectronics and Information Technology, IMIT (2004).
- <sup>358</sup>A. Powell and L. Rowland, *Proceedings of the IEEE* **90**, 942 (2002).
- <sup>359</sup>Y. Gao, S. I. Soloviev, T. S. Sudarshan, and C.-C. Tin, *Journal of Applied Physics* **90**, 5647 (2001).
- <sup>360</sup>A. A. Lebedev, *Semiconductors* **33**, 107 (1999).
- <sup>361</sup>R. J. Trew, *physica status solidi (a)* **162**, 409 (1997).
- <sup>362</sup>P. G. Neudeck, *Journal of Electronic Materials* **24**, 283 (1995).
- <sup>363</sup>R. Karsthof, M. E. Bathen, A. Galeckas, and L. Vines, *Physical Review B* **102**, 184111 (2020).
- <sup>364</sup>G. Lioliou, M. Mazzillo, A. Sciuto, and A. Barnett, *Optics Express* **23**, 21657 (2015).
- <sup>365</sup>P. B. Klein, *physica status solidi (a)* **206**, 2257 (2009).
- <sup>366</sup>D. Werber, P. Borthen, and G. Wachutka, *Materials Science Forum* **556–557**, 905 (2007).
- <sup>367</sup>P. Ščajev, V. Gudelis, K. Jarašiūnas, and P. B. Klein, *Journal of Applied Physics* **108**, 023705 (2010).
- <sup>368</sup>B. Ng, J. David, D. Massey, R. Tozer, G. Rees, F. Yan, J. H. Zhao, and M. Weiner, *Materials Science Forum* **457–460**, 1069 (2004).
- <sup>369</sup>A. Agarwal, S. Seshadri, J. Casady, S. Mani, M. MacMillan, N. Saks, A. Burk, G. Augustine, V. Balakrishna, P. Sanger, C. Brandt, and R. Rodrigues, *Diamond and Related Materials* **8**, 295 (1999).
- <sup>370</sup>J. Shenoy, J. Cooper, and M. Melloch, *IEEE Electron Device Letters* **18**, 93 (1997).
- <sup>371</sup>A. Agarwal, G. Augustine, V. Balakrishna, C. Brandt, A. Burk, Li-Shu Chen, R. Clarke, P. Eseker, H. Hobgood, R. Hopkins, A. Morse, L. Rowland, S. Seshadri, R. Siergiej, T. Smith, and S. Sriram, in *International Electron Devices Meeting. Technical Digest* (IEEE, San Francisco, CA, USA, 1996) pp. 225–230.

- <sup>372</sup>Wolfspeed, “Silicon Carbide and Nitride Materials Catalog,” (2023).
- <sup>373</sup>C. Langpoklakpam, A.-C. Liu, K.-H. Chu, L.-H. Hsu, W.-C. Lee, S.-C. Chen, C.-W. Sun, M.-H. Shih, K.-Y. Lee, and H.-C. Kuo, *Crystals* **12**, 245 (2022).
- <sup>374</sup>I. Capan, *Electronics* **11**, 532 (2022).
- <sup>375</sup>J. V. Berens, *Carrier Mobility and Reliability of 4H-SiC Trench MOSFETs*, Ph.D. thesis, TU Wien (2021).
- <sup>376</sup>H. Matsunami, *Proceedings of the Japan Academy, Series B* **96**, 235 (2020).
- <sup>377</sup>D. Johannesson, M. Nawaz, and H. P. Nee, *Materials Science Forum* **963**, 670 (2019).
- <sup>378</sup>G. Rescher, *Behavior of SiC-MOSFETs under Temperature and Voltage Stress*, Ph.D. thesis, TU Wien (2018).
- <sup>379</sup>S. Chowdhury, C. Hitchcock, R. Dahal, I. B. Bhat, and T. P. Chow, in *2015 IEEE 27th International Symposium on Power Semiconductor Devices & IC's (ISPSD)* (IEEE, Hong Kong, China, 2015) pp. 353–356.
- <sup>380</sup>M. B. J. Wijesundara and R. G. Azevedo, “Introduction,” in *Silicon Carbide Microsystems for Harsh Environments*, Vol. 22 (Springer New York, New York, NY, 2011) pp. 1–32.
- <sup>381</sup>V. R. Manikam and Kuan Yew Cheong, *IEEE Transactions on Components, Packaging and Manufacturing Technology* **1**, 457 (2011).
- <sup>382</sup>R. Gerhardt, ed., *Properties and Applications of Silicon Carbide* (IntechOpen, 2011).
- <sup>383</sup>C. M. Tanner, J. Choi, and J. P. Chang, *Journal of Applied Physics* **101**, 034108 (2007).
- <sup>384</sup>M. Willander, M. Friesel, Q.-u. Wahab, and B. Straumal, *Journal of Materials Science: Materials in Electronics* **17**, 1 (2006).
- <sup>385</sup>M. Philip and A. O'Neill, in *2006 Conference on Optoelectronic and Microelectronic Materials and Devices* (IEEE, Perth, Australia, 2006) pp. 137–140.
- <sup>386</sup>T. P. Chow, *Microelectronic Engineering* **83**, 112 (2006).
- <sup>387</sup>S. Dhar, Y. W. Song, L. C. Feldman, T. Isaacs-Smith, C. C. Tin, J. R. Williams, G. Chung, T. Nishimura, D. Starodub, T. Gustafsson, and E. Garfunkel, *Applied Physics Letters* **84**, 1498 (2004).
- <sup>388</sup>J. Kohlscheen, Y. N. Emirov, M. M. Beerbom, J. T. Wolan, S. E. Saddow, G. Chung, M. F. MacMillan, and R. Schlaf, *Journal of Applied Physics* **94**, 3931 (2003).
- <sup>389</sup>M. Werner and W. Fahrner, *IEEE Transactions on Industrial Electronics* **48**, 249 (2001).
- <sup>390</sup>A. Hefner, R. Singh, Jih-Sheg Lai, D. Berning, S. Bouche, and C. Chapuy, *IEEE Transactions on Power Electronics* **16**, 273 (2001).

- <sup>391</sup>H. Matsunami and T. Kimoto, *Materials Science and Engineering: R: Reports* **20**, 125 (1997).
- <sup>392</sup>M. V. Rao, J. B. Tucker, M. C. Ridgway, O. W. Holland, N. Papanicolaou, and J. Mittereder, *Journal of Applied Physics* **86**, 752 (1999).
- <sup>393</sup>D. Baierhofer, in *ESSDERC 2019 - 49th European Solid-State Device Research Conference (ESSDERC)* (IEEE, Cracow, Poland, 2019) pp. 31–34.
- <sup>394</sup>J. W. Kleppinger, S. K. Chaudhuri, O. Karadavut, and K. C. Mandal, *Journal of Applied Physics* **129**, 244501 (2021).
- <sup>395</sup>F. Bechstedt, J. Furthmüller, U. Grossner, and C. Raffy, in *Silicon Carbide*, edited by W. J. Choyke, H. Matsunami, and G. Pensl (Springer Berlin Heidelberg, Berlin, Heidelberg, 2004) pp. 3–25.
- <sup>396</sup>H. Choi, “Overview of Silicon Carbide Power Devices,” (2016).
- <sup>397</sup>J. I. Pankove, ed., *Electroluminescence*, softcover reprint of the original 1st ed. 1977 ed. (Springer Berlin, Berlin, 2014).
- <sup>398</sup>I. G. Ivanov, A. Henry, and E. Janzén, *Physical Review B* **71**, 241201 (2005).
- <sup>399</sup>C. Persson and U. Lindefelt, *Materials Science Forum* **264–268**, 275 (1998).
- <sup>400</sup>A. Aditya, S. Khandelwal, C. Mukherjee, A. Khan, S. Panda, and B. Maji, in *2015 International Conference on Recent Developments in Control, Automation and Power Engineering (RDCAPE)* (IEEE, Noida, India, 2015) pp. 61–65.
- <sup>401</sup>S. Zollner, J. G. Chen, E. Duda, T. Wetteroth, S. R. Wilson, and J. N. Hilfiker, *Journal of Applied Physics* **85**, 8353 (1999).
- <sup>402</sup>J. Fan and P. K. Chu, “General Properties of Bulk SiC,” in *Silicon Carbide Nanostructures* (Springer International Publishing, Cham, 2014) pp. 7–114.
- <sup>403</sup>S. Yoshida, in *Properties of Silicon Carbide*, EMIS Datareviews Series No. 13, edited by G. L. Harris and Inspec (INSPEC, the Inst. of Electrical Engineers, London, 1995) pp. 29–41.
- <sup>404</sup>A. Suzuki, H. Matsunami, and T. Tanaka, *Journal of The Electrochemical Society* **124**, 241 (1977).
- <sup>405</sup>L. Patrick, D. R. Hamilton, and W. J. Choyke, *Physical Review* **143**, 526 (1966).
- <sup>406</sup>H. Matsunami, A. Suzuki, and T. Tanaka, in *In: Silicon Carbide-1973; Proceedings of the Third International Conference* (1974) pp. 618–625.
- <sup>407</sup>M. L. Megherbi, L. Dehimi, W. terghini, F. Pezzimenti, and F. G. Della Corte, *Courrier du Savoir* **19**, 71 (2015).
- <sup>408</sup>K. G. Menon, A. Nakajima, L. Ngwendson, and E. M. Sankara Narayanan, *IEEE Electron*

Device Letters **32**, 1272 (2011).

<sup>409</sup>G. Wolfowicz, C. P. Anderson, A. L. Yeats, S. J. Whiteley, J. Niklas, O. G. Poluektov, F. J. Heremans, and D. D. Awschalom, *Nature Communications* **8**, 1876 (2017).

<sup>410</sup>B. Nedzvetskii, B. V. Novikov, N. K. Prokof'eva, and M. B. Reifman, Sov. Phys. Solid State **2**, 914 (1969).

<sup>411</sup>F. Capasso, in *Semiconductors and Semimetals*, Vol. 22 (Elsevier, 1985) pp. 1–172.

<sup>412</sup>S. Selberherr, *Analysis and Simulation of Semiconductor Devices* (Springer Vienna, Vienna, 1984).

<sup>413</sup>A. G. Chynoweth, *Physical Review* **109**, 1537 (1958).

<sup>414</sup>A. G. Chynoweth, *Journal of Applied Physics* **31**, 1161 (1960).

<sup>415</sup>R. Van Overstraeten and H. De Man, *Solid-State Electronics* **13**, 583 (1970).

<sup>416</sup>P. A. Wolff, *Physical Review* **95**, 1415 (1954).

<sup>417</sup>W. Shockley, *Solid-State Electronics* **2**, 35 (1961).

<sup>418</sup>A. O. Konstantinov, Q. Wahab, N. Nordell, and U. Lindefelt, *Applied Physics Letters* **71**, 90 (1997).

<sup>419</sup>T. Lackner, *Solid-State Electronics* **34**, 33 (1991).

<sup>420</sup>G. A. Baraff, *Physical Review* **128**, 2507 (1962).

<sup>421</sup>K. K. Thornber, *Journal of Applied Physics* **52**, 279 (1981).

<sup>422</sup>Y. Okuto and C. R. Crowell, *Physical Review B* **6**, 3076 (1972).

<sup>423</sup>Y. Okuto and C. Crowell, *Solid-State Electronics* **18**, 161 (1975).

<sup>424</sup>M. Valdinoci, D. Ventura, M. Vecchi, M. Rudan, G. Baccarani, F. Illien, A. Stricker, and L. Zullino, in *1999 International Conference on Simulation of Semiconductor Processes and Devices. SISPAD'99 (IEEE Cat. No.99TH8387)* (Japan Soc. Appl. Phys, Kyoto, Japan, 1999) pp. 27–30.

<sup>425</sup>A. Acharyya and J. P. Banerjee, *Journal of Computational Electronics* **13**, 917 (2014).

<sup>426</sup>K. Brennan, E. Bellotti, M. Farahmand, H.-E. Nilsson, P. Ruden, and Yumin Zhang, *IEEE Transactions on Electron Devices* **47**, 1882 (2000).

<sup>427</sup>R. Fujita, K. Konaga, Y. Ueoka, Y. Kamakura, N. Mori, and T. Kotani, in *2017 International Conference on Simulation of Semiconductor Processes and Devices (SISPAD)* (IEEE, Kamakura, Japan, 2017) pp. 289–292.

<sup>428</sup>H.-E. Nilsson, E. Bellotti, K. Brennan, and M. Hjelm, *Materials Science Forum* **338–342**, 765 (2000).

- <sup>429</sup>C. C. Sun, A. H. You, and E. K. Wong, in *MALAYSIA ANNUAL PHYSICS CONFERENCE 2010 (PERFIK-2010)* (Damai Laut, (Malaysia), 2011) pp. 277–280.
- <sup>430</sup>H. Tanaka, T. Kimoto, and N. Mori, *Journal of Applied Physics* **131**, 225701 (2022).
- <sup>431</sup>C. Sun, A. You, and E. Wong, *The European Physical Journal Applied Physics* **60**, 10204 (2012).
- <sup>432</sup>A. Concannon, F. Piccinini, A. Mathewson, and C. Lombardi, in *Proceedings of International Electron Devices Meeting* (IEEE, Washington, DC, USA, 1995) pp. 289–292.
- <sup>433</sup>K. Katayama and T. Toyabe, in *International Technical Digest on Electron Devices Meeting* (IEEE, Washington, DC, USA, 1989) pp. 135–138.
- <sup>434</sup>R. Raghunathan and B. J. Baliga, *Applied Physics Letters* **72**, 3196 (1998).
- <sup>435</sup>P. Mukherjee, S. K. R. Hossain, A. Acharyya, and A. Biswas, *Applied Physics A* **126**, 127 (2020).
- <sup>436</sup>P. Mukherjee, D. Chatterjee, and A. Acharyya, *Journal of Computational Electronics* **16**, 503 (2017).
- <sup>437</sup>W. Bartsch, R. Schörner, and K. O. Dohnke, *Materials Science Forum* **645–648**, 909 (2010).
- <sup>438</sup>Z. Stum, Y. Tang, H. Naik, and T. P. Chow, *Materials Science Forum* **778–780**, 467 (2014).
- <sup>439</sup>S.-i. Nakamura, H. Kumagai, T. Kimoto, and H. Matsunami, *Applied Physics Letters* **80**, 3355 (2002).
- <sup>440</sup>T. Hatakeyama, *physica status solidi (a)* **206**, 2284 (2009).
- <sup>441</sup>S. Jin, K. Lee, W. Choi, C. Park, S. Yi, H. Fujii, J. Yoo, Y. Park, J. Jeong, and D. S. Kim, *IEEE Transactions on Electron Devices*, 1 (2024).
- <sup>442</sup>S. Nida and U. Grossner, *IEEE Transactions on Electron Devices* **66**, 1899 (2019).
- <sup>443</sup>C. R. Crowell and S. M. Sze, *Applied Physics Letters* **9**, 242 (1966).
- <sup>444</sup>H. Niwa, J. Suda, and T. Kimoto, *Materials Science Forum* **778–780**, 461 (2014).
- <sup>445</sup>H. Hamad, C. Raynaud, P. Bevilacqua, S. Scharnholz, and D. Planson, *Materials Science Forum* **821–823**, 223 (2015).
- <sup>446</sup>C. Banc, E. Bano, T. Ouisse, O. Noblanc, and C. Brylinski, *Materials Science Forum* **389–393**, 1371 (2002).
- <sup>447</sup>J. S. Cheong, M. M. Hayat, Xinxin Zhou, and J. P. R. David, *IEEE Transactions on Electron Devices* **62**, 1946 (2015).
- <sup>448</sup>R. Raghunathan and B. Baliga, *Solid-State Electronics* **43**, 199 (1999).
- <sup>449</sup>A. O. Konstantinov, Q. Wahab, N. Nordell, and U. Lindefelt, *Journal of Electronic Materials*

**27**, 335 (1998).

- <sup>450</sup>W. S. Loh, B. K. Ng, J. S. Ng, S. I. Soloviev, H.-Y. Cha, P. M. Sandvik, C. M. Johnson, and J. P. R. David, *IEEE Transactions on Electron Devices* **55**, 1984 (2008).
- <sup>451</sup>B. Ng, J. David, R. Tozer, G. Rees, Feng Yan, Jian H. Zhao, and M. Weiner, *IEEE Transactions on Electron Devices* **50**, 1724 (2003).
- <sup>452</sup>D. Nguyen, C. Raynaud, N. Dheilly, M. Lazar, D. Tournier, P. Brosselard, and D. Planson, *Diamond and Related Materials* **20**, 395 (2011).
- <sup>453</sup>D. Nguyen, C. Raynaud, M. Lazar, G. Pâques, S. Scharnholz, N. Dheilly, D. Tournier, and D. Planson, *Materials Science Forum* **717–720**, 545 (2012).
- <sup>454</sup>D. Stefanakis, X. Chi, T. Maeda, M. Kaneko, and T. Kimoto, *IEEE Transactions on Electron Devices* **67**, 3740 (2020).
- <sup>455</sup>Y. Zhao, H. Niwa, and T. Kimoto, *Japanese Journal of Applied Physics* **58**, 018001 (2019).
- <sup>456</sup>A. S. Kyuregyan, *Semiconductors* **50**, 289 (2016).
- <sup>457</sup>J. E. Green, W. S. Loh, A. R. J. Marshall, B. K. Ng, R. C. Tozer, J. P. R. David, S. I. Soloviev, and P. M. Sandvik, *IEEE Transactions on Electron Devices* **59**, 1030 (2012).
- <sup>458</sup>P. L. Cheang, E. K. Wong, and L. L. Teo, *Journal of Electronic Materials* **50**, 5259 (2021).
- <sup>459</sup>L. Zhu, P. A. Losee, T. P. Chow, K. A. Jones, C. Scozzie, M. H. Ervin, P. B. Shah, M. A. Derenge, R. Vispute, T. Venkatesan, and A. K. Agarwal, *Materials Science Forum* **527–529**, 1367 (2006).
- <sup>460</sup>D. Stefanakis, N. Makris, K. Zekentes, and D. Tassis, *IEEE Transactions on Electron Devices* **68**, 2582 (2021).
- <sup>461</sup>H.-E. Nilsson, A. Martinez, U. Sannemo, M. Hjelm, E. Bellotti, and K. Brennan, *Physica B: Condensed Matter* **314**, 68 (2002).
- <sup>462</sup>H. Niwa, J. Suda, and T. Kimoto, *IEEE Transactions on Electron Devices* **62**, 3326 (2015).
- <sup>463</sup>R. Raghunathan and B. Baliga, in *Proceedings of 9th International Symposium on Power Semiconductor Devices and IC's* (IEEE, Weimar, Germany, 1997) pp. 173–176.
- <sup>464</sup>D. C. Sheridan, G. Niu, J. Merrett, J. D. Cressler, C. Ellis, and C.-C. Tin, *Solid-State Electronics* **44**, 1367 (2000).
- <sup>465</sup>K. Bertilsson, H.-E. Nilsson, and C. Petersson, in *COMPEL 2000. 7th Workshop on Computers in Power Electronics. Proceedings (Cat. No.00TH8535)* (IEEE, Blacksburg, VA, USA, 2000) pp. 118–120.
- <sup>466</sup>T. Hatakeyama, T. Watanabe, T. Shinohe, K. Kojima, K. Arai, and N. Sano, *Applied Physics*

- Letters **85**, 1380 (2004).
- <sup>467</sup>W. Loh, J. David, B. Ng, S. I. Soloviev, P. M. Sandvik, J. Ng, and C. M. Johnson, Materials Science Forum **615–617**, 311 (2009).
- <sup>468</sup>R. K. Sharma, P. Hazdra, and S. Popelka, IEEE Transactions on Nuclear Science **62**, 534 (2015).
- <sup>469</sup>X. Zhang and N. You, in *2018 IEEE 3rd International Conference on Integrated Circuits and Microsystems (ICICM)* (IEEE, Shanghai, 2018) pp. 60–63.
- <sup>470</sup>H.-Y. Cha, S. Soloviev, S. Zelakiewicz, P. Waldrab, and P. M. Sandvik, IEEE Sensors Journal **8**, 233 (2008).
- <sup>471</sup>P. Steinmann, B. Hull, I.-H. Ji, D. Lichtenwalner, and E. Van Brunt, Journal of Applied Physics **133**, 235705 (2023).
- <sup>472</sup>T. Kimoto, M. Kaneko, K. Tachiki, K. Ito, R. Ishikawa, X. Chi, D. Stefanakis, T. Kobayashi, and H. Tanaka, in *2021 IEEE International Electron Devices Meeting (IEDM)* (IEEE, San Francisco, CA, USA, 2021) pp. 36.1.1–36.1.4.
- <sup>473</sup>X. Guo, A. Beck, Xiaowei Li, J. Campbell, D. Emerson, and J. Sumakeris, IEEE Journal of Quantum Electronics **41**, 562 (2005).
- <sup>474</sup>A. Kyuregyan and S. Yurkov, Sov. Phys. Solid State **23**, 1126 (1989).
- <sup>475</sup>R. Trew, J.-B. Yan, and P. Mock, Proceedings of the IEEE **79**, 598 (1991).
- <sup>476</sup>J. Wang and B. W. Williams, Semiconductor Science and Technology **14**, 1088 (1999).
- <sup>477</sup>W. Loh, C. M. Johnson, J. Ng, P. M. Sandvik, S. Arthur, S. I. Soloviev, and J. David, Materials Science Forum **556–557**, 339 (2007).
- <sup>478</sup>W. S. Loh, E. Z. J. Goh, K. Vassilevski, I. Nikitina, J. P. R. David, N. G. Wright, and C. M. Johnson, MRS Proceedings **1069**, 1069 (2008).
- <sup>479</sup>T. Hatakeyama, T. Watanabe, K. Kojima, N. Sano, T. Shinohe, and K. Arai, MRS Proceedings **815**, J9.3 (2004).
- <sup>480</sup>T. Hatakeyama, J. Nishio, C. Ota, and T. Shinohe, in *2005 International Conference On Simulation of Semiconductor Processes and Devices* (IEEE, Tokyo, Japan, 2005) pp. 171–174.
- <sup>481</sup>A. Ivanov, M. Mynbaeva, A. Sadokhin, N. Strokan, and A. Lebedev, Nuclear Instruments and Methods in Physics Research Section A: Accelerators, Spectrometers, Detectors and Associated Equipment **606**, 605 (2009).
- <sup>482</sup>C. Wang, X. Li, L. Li, X. Deng, W. Zhang, L. Zheng, Y. Zou, W. Qian, Z. Li, and B. Zhang, IEEE Electron Device Letters **43**, 2025 (2022).

- <sup>483</sup>Y. Wang, J.-c. Zhou, M. Lin, X.-j. Li, J.-Q. Yang, and F. Cao, *IEEE Journal of the Electron Devices Society* **10**, 373 (2022).
- <sup>484</sup>C. C. Sun, A. H. You, and E. K. Wong, in *2012 10th IEEE International Conference on Semiconductor Electronics (ICSE)* (IEEE, Kuala Lumpur, Malaysia, 2012) pp. 366–369.
- <sup>485</sup>J. Hasegawa, L. Pace, L. V. Phung, M. Hatano, and D. Planson, *IEEE Transactions on Electron Devices* **64**, 1203 (2017).
- <sup>486</sup>J. A. McPherson, C. W. Hitchcock, T. Paul Chow, W. Ji, and A. A. Woodworth, *IEEE Transactions on Nuclear Science* **68**, 651 (2021).
- <sup>487</sup>T. Kimoto, H. Niwa, T. Okuda, E. Saito, Y. Zhao, S. Asada, and J. Suda, *Journal of Physics D: Applied Physics* **51**, 363001 (2018).
- <sup>488</sup>A. E. Arvanitopoulos, M. Antoniou, S. Perkins, M. Jennings, M. B. Guadas, K. N. Gyftakis, and N. Lophitis, *IEEE Transactions on Industry Applications* **55**, 4080 (2019).
- <sup>489</sup>B. Ng, F. Yan, J. David, R. Tozer, G. Rees, C. Qin, and J. Zhao, *IEEE Photonics Technology Letters* **14**, 1342 (2002).
- <sup>490</sup>P. G. Neudeck, *Journal of Electronic Materials* **27**, 317 (1998).
- <sup>491</sup>J. Palmour, R. Singh, R. Glass, O. Kordina, and C. Carter, in *Proceedings of 9th International Symposium on Power Semiconductor Devices and IC's* (IEEE, Weimar, Germany, 1997) pp. 25–32.
- <sup>492</sup>D. Peters, P. Friedrichs, H. Mitlehner, R. Schoerner, U. Weinert, B. Weis, and D. Stephani, in *12th International Symposium on Power Semiconductor Devices & ICs. Proceedings (Cat. No.00CH37094)* (IEEE, Toulouse, France, 2000) pp. 241–244.
- <sup>493</sup>R. Singh, J. Cooper, M. Melloch, T. Chow, and J. Palmour, *IEEE Transactions on Electron Devices* **49**, 665 (2002).
- <sup>494</sup>O. Slobodyan, J. Flicker, J. Dickerson, J. Shoemaker, A. Binder, T. Smith, S. Goodnick, R. Kaplar, and M. Hollis, *Journal of Materials Research* **37**, 849 (2022).
- <sup>495</sup>T. Hayashi, K. Asano, J. Suda, and T. Kimoto, *Journal of Applied Physics* **109**, 114502 (2011).
- <sup>496</sup>T. Hayashi, K. Asano, J. Suda, and T. Kimoto, *Journal of Applied Physics* **109**, 014505 (2011).
- <sup>497</sup>P. Ščajev and K. Jarašiūnas, *Journal of Physics D: Applied Physics* **46**, 265304 (2013).
- <sup>498</sup>Y. Fang, X. Wu, J. Yang, G. Chen, Y. Chen, Q. Wu, and Y. Song, *Applied Physics Letters* **112**, 201904 (2018).
- <sup>499</sup>W. Mao, C. Cui, H. Xiong, N. Zhang, S. Liu, M. Dou, L. Song, D. Yang, and X. Pi, *Semiconductor Science and Technology* **38**, 073001 (2023).

- <sup>500</sup>D. Schroder, *IEEE Transactions on Electron Devices* **29**, 1336 (1982).
- <sup>501</sup>Y. Arafat, F. M. Mohammedy, and M. M. Shahidul Hassan, *International Journal of Optoelectronic Engineering* **2**, 5 (2012).
- <sup>502</sup>K. Nagaya, T. Hirayama, T. Tawara, K. Murata, H. Tsuchida, A. Miyasaka, K. Kojima, T. Kato, H. Okumura, and M. Kato, *Journal of Applied Physics* **128**, 105702 (2020).
- <sup>503</sup>P. T. Landsberg, *Recombination in Semiconductors*, 1st ed. (Cambridge University Press, 1992).
- <sup>504</sup>A. Hangleiter, *Physical Review B* **37**, 2594 (1988).
- <sup>505</sup>W. Shockley and W. T. Read, *Physical Review* **87**, 835 (1952).
- <sup>506</sup>I. D. Booker, *Carrier Lifetime Relevant Deep Levels in SiC*, Linköping Studies in Science and Technology. Dissertations, Vol. 1714 (Linköping University Electronic Press, Linköping, 2015).
- <sup>507</sup>H. C. De Graaff and F. M. Klaassen, *Compact Transistor Modelling for Circuit Design*, edited by S. Selberherr, Computational Microelectronics (Springer Vienna, Vienna, 1990).
- <sup>508</sup>J. Fossum and D. Lee, *Solid-State Electronics* **25**, 741 (1982).
- <sup>509</sup>H. M. Ayedh, R. Nipoti, A. Hallén, and B. G. Svensson, *Journal of Applied Physics* **122**, 025701 (2017).
- <sup>510</sup>J. R. Jenny, D. P. Malta, V. F. Tsvetkov, M. K. Das, H. McD. Hobgood, C. H. Carter, R. J. Kumar, J. M. Borrego, R. J. Gutmann, and R. Aavikko, *Journal of Applied Physics* **100**, 113710 (2006).
- <sup>511</sup>P. Grivickas, A. Galeckas, J. Linnros, M. Syväjärvi, R. Yakimova, V. Grivickas, and J. Tellefsen, *Materials Science in Semiconductor Processing* **4**, 191 (2001).
- <sup>512</sup>L. Lilja, I. D. Booker, J. U. Hassan, E. Janzén, and J. P. Bergman, *Journal of Crystal Growth* **381**, 43 (2013).
- <sup>513</sup>T. Hayashi, K. Asano, J. Suda, and T. Kimoto, *Journal of Applied Physics* **112**, 064503 (2012).
- <sup>514</sup>S. Ichikawa, K. Kawahara, J. Suda, and T. Kimoto, *Applied Physics Express* **5**, 101301 (2012).
- <sup>515</sup>N. Kaji, H. Niwa, J. Suda, and T. Kimoto, *IEEE Transactions on Electron Devices* **62**, 374 (2015).
- <sup>516</sup>K. Kawahara, J. Suda, and T. Kimoto, *Journal of Applied Physics* **111**, 053710 (2012).
- <sup>517</sup>T. Kimoto, K. Danno, and J. Suda, *physica status solidi (b)* **245**, 1327 (2008).
- <sup>518</sup>T. Kimoto, T. Hiyoshi, T. Hayashi, and J. Suda, *Journal of Applied Physics* **108**, 083721 (2010).
- <sup>519</sup>T. Miyazawa and H. Tsuchida, *Journal of Applied Physics* **113**, 083714 (2013).
- <sup>520</sup>T. Okuda, T. Kimoto, and J. Suda, *Applied Physics Express* **6**, 121301 (2013).

- <sup>521</sup>T. Okuda, T. Miyazawa, H. Tsuchida, T. Kimoto, and J. Suda, *Applied Physics Express* **7**, 085501 (2014).
- <sup>522</sup>L. Storasta and H. Tsuchida, *Applied Physics Letters* **90**, 062116 (2007).
- <sup>523</sup>L. Storasta, H. Tsuchida, T. Miyazawa, and T. Ohshima, *Journal of Applied Physics* **103**, 013705 (2008).
- <sup>524</sup>T. Tawara, T. Miyazawa, M. Ryo, M. Miyazato, T. Fujimoto, K. Takenaka, S. Matsunaga, M. Miyajima, A. Otsuki, Y. Yonezawa, T. Kato, H. Okumura, T. Kimoto, and H. Tsuchida, *Journal of Applied Physics* **120**, 115101 (2016).
- <sup>525</sup>H. Tsuchida, I. Kamata, T. Miyazawa, M. Ito, X. Zhang, and M. Nagano, *Materials Science in Semiconductor Processing* **78**, 2 (2018).
- <sup>526</sup>M. Wang, M. Yang, W. Liu, S. Yang, J. Liu, C. Han, L. Geng, and Y. Hao, *Applied Physics Express* **13**, 111002 (2020).
- <sup>527</sup>R. Zhang, R. Hong, J. Han, H. Ting, X. Li, J. Cai, X. Chen, D. Fu, D. Lin, M. Zhang, S. Wu, Y. Zhang, Z. Wu, and F. Zhang, *Chinese Physics B* **32**, 067205 (2023).
- <sup>528</sup>T. Hiyoshi and T. Kimoto, *Applied Physics Express* **2**, 041101 (2009).
- <sup>529</sup>Y. Cui, J. Li, K. Zhou, X. Zhang, and G. Sun, *Diamond and Related Materials* **92**, 25 (2019).
- <sup>530</sup>J. Erlekampf, B. Kallinger, J. Weiße, M. Rommel, P. Berwian, J. Friedrich, and T. Erlbacher, *Journal of Applied Physics* **126**, 045701 (2019).
- <sup>531</sup>J. Erlekampf, M. Rommel, K. Rosshirt-Lilla, B. Kallinger, P. Berwian, J. Friedrich, and T. Erlbacher, *Journal of Crystal Growth* **560–561**, 126033 (2021).
- <sup>532</sup>A. Galeckas, V. Grivickas, J. Linnros, H. Bleichner, and C. Hallin, *Journal of Applied Physics* **81**, 3522 (1997).
- <sup>533</sup>A. Galeckas, J. Linnros, M. Frischholz, K. Rottner, N. Nordell, S. Karlsson, and V. Grivickas, *Materials Science and Engineering: B* **61–62**, 239 (1999).
- <sup>534</sup>A. Galeckas, J. Linnros, M. Frischholz, and V. Grivickas, *Applied Physics Letters* **79**, 365 (2001).
- <sup>535</sup>M. Kato, M. Kawai, T. Mori, M. Ichimura, S. Sumie, and H. Hashizume, *Japanese Journal of Applied Physics* **46**, 5057 (2007).
- <sup>536</sup>P. B. Klein, *Journal of Applied Physics* **103**, 033702 (2008).
- <sup>537</sup>O. Kordina, J. P. Bergman, C. Hallin, and E. Janzén, *Applied Physics Letters* **69**, 679 (1996).
- <sup>538</sup>J. Hassan and J. P. Bergman, *Journal of Applied Physics* **105**, 123518 (2009).
- <sup>539</sup>K. Murata, T. Tawara, A. Yang, R. Takanashi, T. Miyazawa, and H. Tsuchida, *Journal of*

- Applied Physics **126**, 045711 (2019).
- <sup>540</sup>N. A. Mahadik, R. E. Stahlbush, P. B. Klein, A. Khachatrian, S. Buchner, and S. G. Block, Applied Physics Letters **111**, 221904 (2017).
- <sup>541</sup>T. Mori, M. Kato, H. Watanabe, M. Ichimura, E. Arai, S. Sumie, and H. Hashizume, Japanese Journal of Applied Physics **44**, 8333 (2005).
- <sup>542</sup>A. K. Agarwal, P. A. Ivanov, M. E. Levenshtein, J. W. Palmour, S. L. Rumyantsev, and S.-H. Ryu, Semiconductor Science and Technology **16**, 260 (2001).
- <sup>543</sup>P. Ivanov, M. Levenshtein, K. Irvine, O. Kordina, J. Palmour, S. Rumyantsev, and R. Singh, Electronics Letters **35**, 1382 (1999).
- <sup>544</sup>P. Ivanov, M. Levenshtein, A. Agarwal, S. Krishnaswami, and J. Palmour, IEEE Transactions on Electron Devices **53**, 1245 (2006).
- <sup>545</sup>D. Åberg, A. Hallén, and B. Svensson, Physica B: Condensed Matter **273–274**, 672 (1999).
- <sup>546</sup>G. Alfieri, E. V. Monakhov, B. G. Svensson, and M. K. Linnarsson, Journal of Applied Physics **98**, 043518 (2005).
- <sup>547</sup>G. Alfieri and A. Mihaila, Journal of Physics: Condensed Matter **32**, 465703 (2020).
- <sup>548</sup>M. Anikin, A. A. Lebedev, A. Syrkin, and A. Suvorov, Sov. Phys. Semicond. **19**, 1847 (1985).
- <sup>549</sup>T. Ayalew, T. Grasser, H. Kosina, and S. Selberherr, Materials Science Forum **483–485**, 845 (2005).
- <sup>550</sup>H. M. Ayedh, V. Bobal, R. Nipoti, A. Hallén, and B. G. Svensson, Materials Science Forum **858**, 331 (2016).
- <sup>551</sup>M. E. Bathen, A. Galeckas, J. Müting, H. M. Ayedh, U. Grossner, J. Coutinho, Y. K. Frodason, and L. Vines, npj Quantum Information **5**, 111 (2019).
- <sup>552</sup>J. M. Bluet, J. Pernot, J. Camassel, S. Contreras, J. L. Robert, J. F. Michaud, and T. Billon, Journal of Applied Physics **88**, 1971 (2000).
- <sup>553</sup>I. D. Booker, E. Janzén, N. T. Son, J. Hassan, P. Stenberg, and E. Ö. Sveinbjörnsson, Journal of Applied Physics **119**, 235703 (2016).
- <sup>554</sup>T. Brodar, L. Bakrač, I. Capan, T. Ohshima, L. Snoj, V. Radulović, and Ž. Pastuović, Crystals **10**, 845 (2020).
- <sup>555</sup>I. Capan, T. Brodar, J. Coutinho, T. Ohshima, V. P. Markevich, and A. R. Peaker, Journal of Applied Physics **124**, 245701 (2018).
- <sup>556</sup>I. Capan, T. Brodar, Ž. Pastuović, R. Siegele, T. Ohshima, S.-i. Sato, T. Makino, L. Snoj, V. Radulović, J. Coutinho, V. J. B. Torres, and K. Demmouche, Journal of Applied Physics

- 123**, 161597 (2018).
- <sup>557</sup>M. A. Capano, J. A. Cooper, M. R. Melloch, A. Saxler, and W. C. Mitchel, *Journal of Applied Physics* **87**, 8773 (2000).
- <sup>558</sup>A. Castaldini, A. Cavallini, L. Rigutti, and F. Nava, *Applied Physics Letters* **85**, 3780 (2004).
- <sup>559</sup>S. K. Chaudhuri, O. Karadavut, J. W. Kleppinger, and K. C. Mandal, *Journal of Applied Physics* **130**, 074501 (2021).
- <sup>560</sup>W. Choyke and G. Pensl, *MRS Bulletin* **22**, 25 (1997).
- <sup>561</sup>T. Dalibor, G. Pensl, T. Kimoto, H. Matsunami, S. Sridhara, R. P. Devaty, and W. J. Choyke, *Diamond and Related Materials* **6**, 1333 (1997).
- <sup>562</sup>T. Dalibor and M. Schulz, eds., *Numerical Data and Functional Relationships in Science and Technology. Subvol. A2: Gruppe 3: Kristall- Und Festkörperphysik = Group 3: @Crystal and Solid State Physics Vol. 41, Semiconductors Impurities and Defects in Group IV Elements, IV-IV and III-V Compounds. Part Beta: Group IV-IV and III-V Compounds / Ed. by M. Schulz; Authors: T. Dalibor*, Vol. 41 (Springer, Berlin Heidelberg, 2003).
- <sup>563</sup>K. Danno, D. Nakamura, and T. Kimoto, *Applied Physics Letters* **90**, 202109 (2007).
- <sup>564</sup>K. Danno and T. Kimoto, *Journal of Applied Physics* **100**, 113728 (2006).
- <sup>565</sup>M. L. David, G. Alfieri, E. M. Monakhov, A. Hallén, C. Blanchard, B. G. Svensson, and J. F. Barbot, *Journal of Applied Physics* **95**, 4728 (2004).
- <sup>566</sup>J. Doyle, M. Aboelfotoh, B. Svensson, A. Schöner, and N. Nordell, *Diamond and Related Materials* **6**, 1388 (1997).
- <sup>567</sup>S. Greulich-Weber, *physica status solidi (a)* **162**, 95 (1997).
- <sup>568</sup>P. Hazdra and S. Popelka, *Materials Science Forum* **897**, 463 (2017).
- <sup>569</sup>P. Hazdra, P. Smrkovsky, J. Vobecky, and A. Mihaila, *IEEE Transactions on Electron Devices* **68**, 202 (2021).
- <sup>570</sup>C. G. Hemmingsson, N. T. Son, A. Ellison, J. Zhang, and E. Janzén, *Physical Review B* **58**, R10119 (1998).
- <sup>571</sup>H. K. Henisch and R. Roy, *Silicon Carbide—1968: Proceedings of the International Conference on Silicon Carbide, University Park, Pennsylvania, October 20-23, 1968* (Elsevier, 2013).
- <sup>572</sup>T. Hornos, A. Gali, and B. G. Svensson, *Materials Science Forum* **679–680**, 261 (2011).
- <sup>573</sup>Y. Huang, R. Wang, Y. Zhang, D. Yang, and X. Pi, *Chinese Physics B* **31**, 056108 (2022).
- <sup>574</sup>Y. Huang, R. Wang, Y. Qian, Y. Zhang, D. Yang, and X. Pi, *Chinese Physics B* **31**, 046104 (2022).

- <sup>575</sup>S. W. Huh, J. J. Sumakeris, A. Polyakov, M. Skowronski, P. B. Klein, B. Shanabrook, and M. J. O'Loughlin, [Materials Science Forum](#) **527–529**, 493 (2006).
- <sup>576</sup>H. Itoh, T. Troffer, and G. Pensl, [Materials Science Forum](#) **264–268**, 685 (1998).
- <sup>577</sup>G. Izzo, G. Litrico, L. Calcagno, G. Foti, and F. La Via, [Journal of Applied Physics](#) **104**, 093711 (2008).
- <sup>578</sup>S. Kagamihara, H. Matsuura, T. Hatakeyama, T. Watanabe, M. Kushibe, T. Shinohe, and K. Arai, [Journal of Applied Physics](#) **96**, 5601 (2004).
- <sup>579</sup>L. Kasamakova-Kolaklieva, L. Storasta, I. G. Ivanov, B. Magnusson, S. Contreras, C. Consejo, J. Pernot, M. Zielinski, and E. Janzén, [Materials Science Forum](#) **457–460**, 677 (2004).
- <sup>580</sup>T. Kimoto, A. Itoh, H. Matsunami, S. Sridhara, L. L. Clemen, R. P. Devaty, W. J. Choyke, T. Dalibor, C. Peppermüller, and G. Pensl, [Applied Physics Letters](#) **67**, 2833 (1995).
- <sup>581</sup>T. Kimoto, K. Hashimoto, and H. Matsunami, [Japanese Journal of Applied Physics](#) **42**, 7294 (2003).
- <sup>582</sup>T. Kimoto, A. Itoh, and H. Matsunami, [physica status solidi \(b\)](#) **202**, 247 (1997).
- <sup>583</sup>P. B. Klein, B. V. Shanabrook, S. W. Huh, A. Y. Polyakov, M. Skowronski, J. J. Sumakeris, and M. J. O'Loughlin, [Applied Physics Letters](#) **88**, 052110 (2006).
- <sup>584</sup>M. Laube, F. Schmid, K. Semmelroth, G. Pensl, R. P. Devaty, W. J. Choyke, G. Wagner, and M. Maier, in [Silicon Carbide](#), edited by W. J. Choyke, H. Matsunami, and G. Pensl (Springer Berlin Heidelberg, Berlin, Heidelberg, 2004) pp. 493–515.
- <sup>585</sup>F. La Via, G. Galvagno, F. Roccaforte, A. Ruggiero, and L. Calcagno, [Applied Physics Letters](#) **87**, 142105 (2005).
- <sup>586</sup>D. J. Lichtenwalner, J. H. Park, S. Rogers, H. Dixit, A. Scholtze, S. Bubel, and S. H. Ryu, [Materials Science Forum](#) **1089**, 3 (2023).
- <sup>587</sup>K. C. Mandal, J. W. Kleppinger, and S. K. Chaudhuri, [Micromachines](#) **11**, 254 (2020).
- <sup>588</sup>A. Martinez, U. Lindefelt, M. Hjelm, and H.-E. Nilsson, [Journal of Applied Physics](#) **91**, 1359 (2002).
- <sup>589</sup>H. Matsuura, M. Komeda, S. Kagamihara, H. Iwata, R. Ishihara, T. Hatakeyama, T. Watanabe, K. Kojima, T. Shinohe, and K. Arai, [Journal of Applied Physics](#) **96**, 2708 (2004).
- <sup>590</sup>H. Matsuura, T. K. Tsunenobu Kimoto, and H. M. Hiroyuki Matsunami, [Japanese Journal of Applied Physics](#) **38**, 4013 (1999).
- <sup>591</sup>M. L. Megherbi, F. Pezzimenti, L. Dehimi, M. A. Saadoune, and F. G. Della Corte, [IEEE Transactions on Electron Devices](#) **65**, 3371 (2018).

- <sup>592</sup>Y. Negoro, T. Kimoto, and H. Matsunami, *Electronics and Communications in Japan (Part II: Electronics)* **86**, 44 (2003).
- <sup>593</sup>K. V. Nguyen, M. A. Mannan, and K. C. Mandal, *IEEE Transactions on Nuclear Science* **62**, 3199 (2015).
- <sup>594</sup>A. Parisini and R. Nipoti, *Journal of Applied Physics* **114**, 243703 (2013).
- <sup>595</sup>Ž. Pastuović, R. Siegele, I. Capan, T. Brodar, S.-i. Sato, and T. Ohshima, *Journal of Physics: Condensed Matter* **29**, 475701 (2017).
- <sup>596</sup>F. Schmid, M. Krieger, M. Laube, G. Pensl, and G. Wagner, in *Silicon Carbide*, edited by W. J. Choyke, H. Matsunami, and G. Pensl (Springer Berlin Heidelberg, Berlin, Heidelberg, 2004) pp. 517–536.
- <sup>597</sup>S. R. Smith, A. O. Evwaraye, W. C. Mitchel, and M. A. Capano, *Journal of Electronic Materials* **28**, 190 (1999).
- <sup>598</sup>N. T. Son, Mt. Wagner, C. G. Hemmingsson, L. Storasta, B. Magnusson, W. M. Chen, S. Greulich-Weber, J.-M. Spaeth, and E. Janzén, in *Silicon Carbide*, edited by W. J. Choyke, H. Matsunami, and G. Pensl (Springer Berlin Heidelberg, Berlin, Heidelberg, 2004) pp. 461–492.
- <sup>599</sup>N. T. Son, X. T. Trinh, L. S. Løvlie, B. G. Svensson, K. Kawahara, J. Suda, T. Kimoto, T. Umeda, J. Isoya, T. Makino, T. Ohshima, and E. Janzén, *Physical Review Letters* **109**, 187603 (2012).
- <sup>600</sup>L. Storasta, J. P. Bergman, E. Janzén, A. Henry, and J. Lu, *Journal of Applied Physics* **96**, 4909 (2004).
- <sup>601</sup>L. Storasta, P. Bergman, E. Janzén, and C. Hallin, *Materials Science Forum* **389–393**, 549 (2002).
- <sup>602</sup>A. Suzuki, H. Matsunami, and T. Tanaka, *Japanese Journal of Applied Physics* **12**, 1083 (1973).
- <sup>603</sup>Y. Tanaka, N. Kobayashi, H. Okumura, R. Suzuki, T. Ohdaira, M. Hasegawa, M. Ogura, S. Yoshida, and H. Tanoue, *Materials Science Forum* **338–342**, 909 (2000).
- <sup>604</sup>T. Tawara, H. Tsuchida, S. Izumi, I. Kamata, and K. Izumi, *Materials Science Forum* **457–460**, 565 (2004).
- <sup>605</sup>P. Terziyska, C. Blanc, J. Pernot, H. Peyre, S. Contreras, G. Bastide, J. L. Robert, J. Camassel, E. Morvan, C. Dua, and C. C. Brylinski, *physica status solidi (a)* **195**, 243 (2003).
- <sup>606</sup>T. Troffer, M. Schadt, T. Frank, H. Itoh, G. Pensl, J. Heindl, H. P. Strunk, and M. Maier, *physica status solidi (a)* **162**, 277 (1997).

- <sup>607</sup>R. Wang, Y. Huang, D. Yang, and X. Pi, *Applied Physics Letters* **122**, 180501 (2023).
- <sup>608</sup>X. Xu, L. Zhang, L. Li, Z. Li, J. Li, J. Zhang, and P. Dong, *Discover Nano* **18**, 128 (2023).
- <sup>609</sup>X. Yan, P. Li, L. Kang, S.-H. Wei, and B. Huang, *Journal of Applied Physics* **127**, 085702 (2020).
- <sup>610</sup>J. Zhang, L. Storasta, J. P. Bergman, N. T. Son, and E. Janzén, *Journal of Applied Physics* **93**, 4708 (2003).
- <sup>611</sup>B. Zippelius, J. Suda, and T. Kimoto, *Journal of Applied Physics* **111**, 033515 (2012).
- <sup>612</sup>P. Gaggl, J. Burin, A. Gsponer, S.-E. Waid, R. Thalmeier, and T. Bergauer, *Nuclear Instruments and Methods in Physics Research Section A: Accelerators, Spectrometers, Detectors and Associated Equipment* **1070**, 170015 (2025).
- <sup>613</sup>S. Yamashita and T. Kimoto, *Applied Physics Express* **13**, 011006 (2020).
- <sup>614</sup>M. J. Marinella, D. K. Schroder, G. Chung, M. J. Loboda, T. Isaacs-Smith, and J. R. Williams, *IEEE Transactions on Electron Devices* **57**, 1910 (2010).
- <sup>615</sup>M. Kato, A. Ogawa, L. Han, and T. Kato, *Materials Science in Semiconductor Processing* **170**, 107980 (2024).
- <sup>616</sup>R. N. Hall, *Physical Review* **87**, 387 (1952).
- <sup>617</sup>L. Lilja, I. Farkas, I. Booker, J. Ul Hassan, E. Janzén, and J. P. Bergman, *Materials Science Forum* **897**, 238 (2017).
- <sup>618</sup>D. Scharfetter and R. Johnston, *IEEE Transactions on Electron Devices* **14**, 634 (1967).
- <sup>619</sup>D. Roulston, N. Arora, and S. Chamberlain, *IEEE Transactions on Electron Devices* **29**, 284 (1982).
- <sup>620</sup>M. Law, E. Solley, M. Liang, and D. Burk, *IEEE Electron Device Letters* **12**, 401 (1991).
- <sup>621</sup>M. Tyagi and R. Van Overstraeten, *Solid-State Electronics* **26**, 577 (1983).
- <sup>622</sup>G. Liaugaudas, D. Dargis, P. Kwasnicki, H. Peyre, R. Arvinte, S. Juillaguet, M. Zielinski, and K. Jarašiūnas, *Materials Science Forum* **821–823**, 249 (2015).
- <sup>623</sup>H. Shao, X. Yang, D. Wang, X. Li, X. Chen, G. Hu, H. Li, X. Xiong, X. Xie, X. Hu, and X. Xu, *Journal of Electronic Materials* **53**, 2429 (2024).
- <sup>624</sup>S. Sapienza, G. Sozzi, D. Santoro, P. Cova, N. Delmonte, G. Verrini, and G. Chiorboli, *Microelectronics Reliability* **113**, 113937 (2020).
- <sup>625</sup>P. B. Klein, R. Myers-Ward, K.-K. Lew, B. L. VanMil, C. R. Eddy, D. K. Gaskill, A. Srivastava, and T. S. Sudarshan, *Journal of Applied Physics* **108**, 033713 (2010).
- <sup>626</sup>M. E. Levenshtein, P. A. Ivanov, M. S. Boltovets, V. A. Krivutsa, J. W. Palmour, M. K. Das,

- and B. A. Hull, *Solid-State Electronics* **49**, 1228 (2005).
- <sup>627</sup>A. Udal and E. Velmre, *Materials Science Forum* **556–557**, 375 (2007).
- <sup>628</sup>R. Wu and A. Peaker, *Solid-State Electronics* **25**, 643 (1982).
- <sup>629</sup>H. Goebel and K. Hoffmann, in *Proceedings of the 4th International Symposium on Power Semiconductor Devices and Ics* (IEEE, Tokyo, Japan, 1992) pp. 130–135.
- <sup>630</sup>D. Klaassen, *Solid-State Electronics* **35**, 961 (1992).
- <sup>631</sup>A. Schenk, *Solid-State Electronics* **35**, 1585 (1992).
- <sup>632</sup>T. Tamaki, G. G. Walden, Y. Sui, and J. A. Cooper, *IEEE Transactions on Electron Devices* **55**, 1928 (2008).
- <sup>633</sup>K. Gulbinas, V. Grivickas, H. P. Mahabadi, M. Usman, and A. Hallén, *Materials Science* **17**, 119 (2011).
- <sup>634</sup>M. Kato, A. Yoshida, and M. Ichimura, *Japanese Journal of Applied Physics* **51**, 02BP12 (2012).
- <sup>635</sup>M. Kato, Z. Xinchi, K. Kohama, S. Fukaya, and M. Ichimura, *Journal of Applied Physics* **127**, 195702 (2020).
- <sup>636</sup>Y. Mori, M. Kato, and M. Ichimura, *Journal of Physics D: Applied Physics* **47**, 335102 (2014).
- <sup>637</sup>G. Y. Chung, M. J. Loboda, M. Marinella, D. Schroder, T. Isaacs-Smith, and J. R. Williams, *Materials Science Forum* **615–617**, 283 (2009).
- <sup>638</sup>K. Y. Cheong, S. Dimitrijev, and Jisheng Han, *IEEE Transactions on Electron Devices* **50**, 1433 (2003).
- <sup>639</sup>S. Asada, J. Suda, and T. Kimoto, *IEEE Transactions on Electron Devices* **65**, 4786 (2018).
- <sup>640</sup>T. Hayashi, T. Okuda, J. Suda, and T. Kimoto, *Japanese Journal of Applied Physics* **53**, 111301 (2014).
- <sup>641</sup>Y. Ichikawa, M. Ichimura, T. Kimoto, and M. Kato, *ECS Journal of Solid State Science and Technology* **7**, Q127 (2018).
- <sup>642</sup>T. Kimoto, Y. Nanen, T. Hayashi, and J. Suda, *Applied Physics Express* **3**, 121201 (2010).
- <sup>643</sup>K. Nonaka, A. Horiuchi, Y. Negoro, K. Iwanaga, S. Yokoyama, H. Hashimoto, M. Sato, Y. Maeyama, M. Shimizu, and H. Iwakuro, *physica status solidi (a)* **206**, 2457 (2009).
- <sup>644</sup>B. Buono, R. Ghandi, M. Domeij, B. G. Malm, C.-M. Zetterling, and M. Ostling, *IEEE Transactions on Electron Devices* **57**, 704 (2010).
- <sup>645</sup>V. V. Afanasev, M. Bassler, G. Pensl, and M. Schulz, *physica status solidi (a)* **162**, 321 (1997).
- <sup>646</sup>D. Fitzgerald and A. Grove, *Surface Science* **9**, 347 (1968).

- <sup>647</sup>E. Yablonovitch, D. L. Allara, C. C. Chang, T. Gmitter, and T. B. Bright, *Physical Review Letters* **57**, 249 (1986).
- <sup>648</sup>K. Murata, T. Tawara, A. Yang, R. Takanashi, T. Miyazawa, and H. Tsuchida, *Journal of Applied Physics* **129**, 025702 (2021).
- <sup>649</sup>K. Tanaka and M. Kato, *Japanese Journal of Applied Physics* **63**, 011002 (2024).
- <sup>650</sup>J. Fossum, R. Mertens, D. Lee, and J. Nijs, *Solid-State Electronics* **26**, 569 (1983).
- <sup>651</sup>J. Linnros, *Journal of Applied Physics* **84**, 275 (1998).
- <sup>652</sup>K. Tanaka, K. Nagaya, and M. Kato, *Japanese Journal of Applied Physics* **62**, SC1017 (2023).
- <sup>653</sup>P. T. Landsberg and G. S. Kousik, *Journal of Applied Physics* **56**, 1696 (1984).
- <sup>654</sup>J. Dziewior and W. Schmid, *Applied Physics Letters* **31**, 346 (1977).
- <sup>655</sup>G. Y. Chung, M. J. Loboda, M. Marinella, D. Schroder, P. B. Klein, T. Isaacs-Smith, and J. Williams, *Materials Science Forum* **600–603**, 485 (2008).
- <sup>656</sup>M. Ruff, *Elektronische Bauelemente Aus Siliziumkarbid (SiC) : Physikalische Grundlagen Und Numerische Simulation*, Ph.D. thesis, Friedrich-Alexander-Universität, Erlangen-Nürnberg (1993).
- <sup>657</sup>C. Hettler, C. James, J. Dickens, and A. Neuber, in *2010 IEEE International Power Modulator and High Voltage Conference* (IEEE, Atlanta, GA, USA, 2010) pp. 34–37.
- <sup>658</sup>C. Hettler, W. W. Sullivan Iii, and J. Dickens, *Materials Science Forum* **717–720**, 301 (2012).
- <sup>659</sup>S. S. Suvanam, K. Gulbinas, M. Usman, M. K. Linnarson, D. M. Martin, J. Linnros, V. Grivickas, and A. Hallén, *Journal of Applied Physics* **117**, 105309 (2015).
- <sup>660</sup>K. Tanaka and M. Kato, *AIP Advances* **13**, 085220 (2023).
- <sup>661</sup>H. Tsuchida, I. Kamata, M. Ito, T. Miyazawa, H. Uehigashi, K. Fukada, H. Fujibayashi, M. Naitou, K. Hara, H. Osawa, T. Sugiura, and T. Kozawa, *Materials Science Forum* **858**, 119 (2016).
- <sup>662</sup>T. Miyazawa, M. Ito, and H. Tsuchida, *Applied Physics Letters* **97**, 202106 (2010).
- <sup>663</sup>T. Okuda, T. Kobayashi, T. Kimoto, and J. Suda, *Applied Physics Express* **9**, 051301 (2016).
- <sup>664</sup>E. Saito, J. Suda, and T. Kimoto, *Applied Physics Express* **9**, 061303 (2016).
- <sup>665</sup>T. Kimoto, N. Miyamoto, and H. Matsunami, *Materials Science and Engineering: B* **61–62**, 349 (1999).
- <sup>666</sup>A. Udal and E. Velmre, *Materials Science Forum* **338–342**, 781 (2000).
- <sup>667</sup>S. A. Reshanov, W. Bartsch, B. Zippelius, and G. Pensl, *Materials Science Forum* **615–617**, 699 (2009).

- <sup>668</sup>P. A. Ivanov, M. E. Levenshtein, J. W. Palmour, M. K. Das, and B. A. Hull, *Solid-State Electronics* **50**, 1368 (2006).
- <sup>669</sup>M. E. Levenshtein, T. T. Mnatsakanov, P. A. Ivanov, R. Singh, J. W. Palmour, and S. N. Yurkov, *Solid-State Electronics* **48**, 807 (2004).
- <sup>670</sup>G. Sozzi, S. Sapienza, G. Chiorboli, L. Vines, A. Hallén, and R. Nipoti, *IEEE Access* , 1 (2024).
- <sup>671</sup>L. Di Benedetto, G. D. Licciardo, R. Nipoti, and S. Bellone, *IEEE Electron Device Letters* **35**, 244 (2014).
- <sup>672</sup>M. Puzzanghera and R. Nipoti, *Materials Science Forum* **858**, 773 (2016).
- <sup>673</sup>M. Domeij, E. Danielsson, W. Liu, U. Zimmermann, C.-M. Zetterling, and M. Ostling, in *ISPSD '03. 2003 IEEE 15th International Symposium on Power Semiconductor Devices and ICs, 2003. Proceedings.* (IEEE, Cambridge, UK, 2003) pp. 375–378.
- <sup>674</sup>A. Koyama, M. Sometani, K. Takenaka, K. Nakayama, A. Miyasaka, K. Kojima, K. Eto, T. Kato, J. Senzaki, Y. Yonezawa, and H. Okumura, *Japanese Journal of Applied Physics* **59**, SGGD14 (2020).
- <sup>675</sup>M. Kato, Y. Mori, and M. Ichimura, *Materials Science Forum* **778–780**, 293 (2014).
- <sup>676</sup>A. K. Tiwari, M. Antoniou, N. Lophitis, S. Perkin, T. Trajkovic, and F. Udrea, *IEEE Transactions on Electron Devices* **66**, 3066 (2019).
- <sup>677</sup>K. Tian, J. Xia, K. Elgammal, A. Schöner, W. Kaplan, R. Karhu, J. Ul-Hassan, and A. Hallén, *Materials Science in Semiconductor Processing* **115**, 105097 (2020).
- <sup>678</sup>M. E. Levenshtein, T. T. Mnatsakanov, P. A. Ivanov, A. K. Agarwal, J. W. Palmour, S. L. Rumyantsev, A. G. Tandoev, and S. N. Yurkov, *Solid-State Electronics* **45**, 453 (2001).
- <sup>679</sup>S. Bellone, L. F. Albanese, and G.-D. Licciardo, *IEEE Transactions on Electron Devices* **56**, 2902 (2009).
- <sup>680</sup>M. Usman, B. Buono, and A. Hallen, *IEEE Transactions on Electron Devices* **59**, 3371 (2012).
- <sup>681</sup>T. Kimoto, K. Yamada, H. Niwa, and J. Suda, *Energies* **9**, 908 (2016).
- <sup>682</sup>K. Naydenov, N. Donato, and F. Udrea, *Engineering Research Express* **3**, 035008 (2021).
- <sup>683</sup>A. Galeckas, J. Linnros, V. Grivickas, U. Lindefelt, and C. Hallin, *Materials Science Forum* **264–268**, 533 (1998).
- <sup>684</sup>B. Kakarla, A. Tsibizov, R. Stark, I. K. Badstubner, and U. Grossner, in *2020 32nd International Symposium on Power Semiconductor Devices and ICs (ISPSD)* (IEEE, Vienna, Austria, 2020) pp. 234–237.

- <sup>685</sup>S. Bellone and L. Di Benedetto, *IEEE Transactions on Power Electronics* **29**, 2174 (2014).
- <sup>686</sup>L. Di Benedetto, N. Rinaldi, G. D. Licciardo, R. Liguori, A. Rubino, A. May, and M. Rommel, in *2024 International Semiconductor Conference (CAS)* (IEEE, Sinaia, Romania, 2024) pp. 23–28.
- <sup>687</sup>S. Asada, T. Miyazawa, and H. Tsuchida, *IEEE Transactions on Electron Devices* **68**, 3468 (2021).
- <sup>688</sup>N. Ramungul, V. Khemka, T. P. Chow, M. Ghezzo, and J. W. Kretchmer, *Materials Science Forum* **264–268**, 1065 (1998).
- <sup>689</sup>R. Nipoti, A. Parisini, G. Sozzi, M. Puzzanghera, A. Parisini, and A. Carnera, *ECS Journal of Solid State Science and Technology* **5**, P621 (2016).
- <sup>690</sup>T. Grasser, B. Kaczer, W. Goes, Th. Aichinger, Ph. Hehenberger, and M. Nelhiebel, in *2009 IEEE International Reliability Physics Symposium* (IEEE, Montreal, QC, Canada, 2009) pp. 33–44.
- <sup>691</sup>H. Pourbagheri Mahabadi, *Optical Studies of Surface Recombination Velocity in 4H-SiC Epitaxial Layer*, Master's thesis, KTH, School of Information and Communication Technology (ICT) / KTH, School of Information and Communication Technology (ICT) (2011).
- <sup>692</sup>A. Xiang, *IEEE Transactions on Nanotechnology* **20**, 28 (2021).
- <sup>693</sup>Y. Negoro, T. Kimoto, H. Matsunami, F. Schmid, and G. Pensl, *Journal of Applied Physics* **96**, 4916 (2004).
- <sup>694</sup>I. G. Atabaev, Kh. N. Juraev, and M. U. Hajiev, *Journal of Spectroscopy* **2018**, 1 (2018).
- <sup>695</sup>V. Heera, D. Panknin, and W. Skorupa, *Applied Surface Science* **184**, 307 (2001).
- <sup>696</sup>M. Miyata, Y. Higashiguchi, and Y. Hayafuji, *Journal of Applied Physics* **104**, 123702 (2008).
- <sup>697</sup>J. Senzaki, K. Fukuda, Y. Ishida, Y. Tanaka, H. Tanoue, N. Kobayashi, T. Tanaka, and K. Arai, *MRS Proceedings* **622**, T6.7.1 (2000).
- <sup>698</sup>T. Troffer, G. Pensl, A. Schöner, A. Henry, C. Hallin, Kordina, and E. Janzén, *Materials Science Forum* **264–268** (1998), 10.4028/www.scientific.net/MSF.264-268.557.
- <sup>699</sup>M. Krieger, M. Rühl, T. Sledziewski, G. Ellrott, T. Palm, H. B. Weber, and M. Bockstedte, *Materials Science Forum* **858**, 301 (2016).
- <sup>700</sup>E. M. Handy, M. V. Rao, O. W. Holland, K. A. Jones, M. A. Derenge, and N. Papanicolaou, *Journal of Applied Physics* **88**, 5630 (2000).
- <sup>701</sup>G. Xiao, J. Lee, J. Liou, and A. Ortiz-Conde, *Microelectronics Reliability* **39**, 1299 (1999).
- <sup>702</sup>N. Donato and F. Udrea, *IEEE Transactions on Electron Devices* **65**, 4469 (2018).

- <sup>703</sup>R. Nipoti, H. M. Ayedh, and B. G. Svensson, *Materials Science in Semiconductor Processing* **78**, 13 (2018).
- <sup>704</sup>Q. Chen, W. He, C. Cheng, and Y. Xue, *Journal of Physics: Conference Series* **1649**, 012048 (2020).
- <sup>705</sup>M. Laube, F. Schmid, G. Pensl, G. Wagner, M. Linnarsson, and M. Maier, *Journal of Applied Physics* **92**, 549 (2002).
- <sup>706</sup>Z. Lv, J. Li, L. Dong, and J. Zang, in *2023 International Conference on Telecommunications, Electronics and Informatics (ICTEI)* (IEEE, Lisbon, Portugal, 2023) pp. 269–273.
- <sup>707</sup>H. Matsuura, *Materials Science Forum* **389–393**, 679 (2002).
- <sup>708</sup>G. L. Pearson and J. Bardeen, *Physical Review* **75**, 865 (1949).
- <sup>709</sup>A. Schöner, *Elektrische Charakterisierung von Flächen Und Tiefen Störstellen in 4H-, 6H- Und 15R-Siliziumkarbid*, Ph.D. thesis, FriedrichAlexander-Universität (1994).
- <sup>710</sup>P. Achatz, J. Pernot, C. Marcenat, J. Kacmarcik, G. Ferro, and E. Bustarret, *Applied Physics Letters* **92**, 072103 (2008).
- <sup>711</sup>J. Weiße, M. Hauck, T. Sledziewski, M. Tschiesche, M. Krieger, A. J. Bauer, H. Mitlehner, L. Frey, and T. Erlbacher, *Materials Science Forum* **924**, 184 (2018).
- <sup>712</sup>Y. Kajikawa, *Journal of Electronic Materials* **50**, 1247 (2021).
- <sup>713</sup>M. Rambach, A. J. Bauer, and H. Ryssel, *physica status solidi (b)* **245**, 1315 (2008).
- <sup>714</sup>R. Scaburri, A. Desalvo, and R. Nipoti, *Materials Science Forum* **679–680**, 397 (2011).
- <sup>715</sup>P. P. Altermatt, A. Schenk, and G. Heiser, *Journal of Applied Physics* **100**, 113714 (2006).
- <sup>716</sup>P. P. Altermatt, A. Schenk, B. Schmithüsen, and G. Heiser, *Journal of Applied Physics* **100**, 113715 (2006).
- <sup>717</sup>P. T. Landsberg, *physica status solidi (b)* **41**, 457 (1970).
- <sup>718</sup>B. K. Ridley, *Journal of Physics C: Solid State Physics* **11**, 2323 (1978).
- <sup>719</sup>M. Lades, W. Kaindl, N. Kaminski, E. Niemann, and G. Wachutka, *IEEE Transactions on Electron Devices* **46**, 598 (1999).
- <sup>720</sup>M. Lax, *Physical Review* **119**, 1502 (1960).
- <sup>721</sup>V. N. Abakumov, V. I. Perel, and I. N. Yassievich, *Nonradiative Recombination in Semiconductors*, Modern Problems in Condensed Matter Sciences No. v. 33 (North-Holland ; Sole distributors for the USA and Canada, Elsevier Science Pub. Co, Amsterdam ; New York : New York, NY, USA, 1991).
- <sup>722</sup>W. Kaindl, M. Lades, N. Kaminski, E. Niemann, and G. Wachutka, *Journal of Electronic*

Materials **28**, 154 (1999).

<sup>723</sup>I. S. Gorban, A. P. Krokhmal', V. I. Levin, A. S. Skirda, Yu. M. Tairov, and V. F. Tsetkov, Sov. Phys. Semiconductors **21**, 119 (1987).

<sup>724</sup>S. Asada, T. Okuda, T. Kimoto, and J. Suda, Applied Physics Express **9**, 041301 (2016).

<sup>725</sup>S. Contreras, L. Konczewicz, P. Kwasnicki, R. Arvinte, H. Peyre, T. Chassagne, M. Zielinski, M. Kayambaki, S. Juillaguet, and K. Zekentes, Materials Science Forum **858**, 249 (2016).

<sup>726</sup>C. Hitchcock, R. Ghandi, P. Deeb, S. Kennerly, M. Torky, and T. P. Chow, Materials Science Forum **1062**, 422 (2022).

<sup>727</sup>R. Nipoti, R. Scaburri, A. Hallén, and A. Parisini, Journal of Materials Research **28**, 17 (2013).

<sup>728</sup>M. Obernhofer, M. Krieger, F. Schmid, H. B. Weber, G. Pensl, and A. Schöner, Materials Science Forum **556–557**, 343 (2007).

<sup>729</sup>G. Pensl, F. Schmid, F. Ciobanu, M. Laube, S. A. Reshanov, N. Schulze, K. Semmelroth, A. Schöner, G. Wagner, and H. Nagasawa, Materials Science Forum **433–436**, 365 (2003).

<sup>730</sup>M. Rambach, L. Frey, A. J. Bauer, and H. Ryssel, Materials Science Forum **527–529**, 827 (2006).

<sup>731</sup>S. Rao, T. P. Chow, and I. Bhat, Materials Science Forum **527–529**, 597 (2006).

<sup>732</sup>G. Rutsch, R. P. Devaty, W. J. Choyke, D. W. Langer, and L. B. Rowland, Journal of Applied Physics **84**, 2062 (1998).

<sup>733</sup>N. S. Saks, A. K. Agarwal, S.-H. Ryu, and J. W. Palmour, Journal of Applied Physics **90**, 2796 (2001).

<sup>734</sup>N. S. Saks, A. V. Suvorov, and D. C. Capell, Applied Physics Letters **84**, 5195 (2004).

<sup>735</sup>F. Schmid, M. Laube, G. Pensl, G. Wagner, and M. Maier, Journal of Applied Physics **91**, 9182 (2002).

<sup>736</sup>A. Schöner, S. Karlsson, T. Schmitt, N. Nordell, M. Linnarsson, and K. Rottner, Materials Science and Engineering: B **61–62**, 389 (1999).

<sup>737</sup>G. Wagner, W. Leitenberger, K. Irmscher, F. Schmid, M. Laube, and G. Pensl, Materials Science Forum **389–393**, 207 (2002).

<sup>738</sup>R. Wang, I. B. Bhat, and T. P. Chow, Journal of Applied Physics **92**, 7587 (2002).

<sup>739</sup>S. Y. Ji, K. Kojima, Y. Ishida, H. Tsuchida, S. Yoshida, and H. Okumura, Materials Science Forum **740–742**, 181 (2013).

<sup>740</sup>H. Matsuura, K. Aso, S. Kagamihara, H. Iwata, T. Ishida, and K. Nishikawa, Applied Physics Letters **83**, 4981 (2003).

- <sup>741</sup>S. Smith, A. Evwaraye, and W. Mitchel, *MRS Proceedings* **510**, 193 (1998).
- <sup>742</sup>K. Kawahara, H. Watanabe, N. Miura, S. Nakata, and S. Yamakawa, *Materials Science Forum* **821–823**, 403 (2015).
- <sup>743</sup>S. Beljakowa, S. A. Reshanov, B. Zippelius, M. Krieger, G. Pensl, K. Danno, T. Kimoto, S. Onoda, T. Ohshima, F. Yan, R. P. Devaty, and W. J. Choyke, *Materials Science Forum* **645–648**, 427 (2010).
- <sup>744</sup>C. Kisielowski, K. Maier, J. Schneider, and V. Oding, *Materials Science Forum* **83–87**, 1171 (1992).
- <sup>745</sup>M. Kato, J. Di, Y. Ohkouchi, T. Mizuno, M. Ichimura, and K. Kojima, *Materials Today Communications* **31**, 103648 (2022).
- <sup>746</sup>N. T. Son, A. Henry, J. Isoya, M. Katagiri, T. Umeda, A. Gali, and E. Janzén, *Physical Review B* **73**, 075201 (2006).
- <sup>747</sup>M. Bockstedte, A. Mattausch, and O. Pankratov, *Applied Physics Letters* **85**, 58 (2004).
- <sup>748</sup>A. K. Tiwari, F. Udrea, N. Lophitis, and M. Antoniou, in *2019 31st International Symposium on Power Semiconductor Devices and ICs (ISPSD)* (IEEE, Shanghai, China, 2019) pp. 175–178.
- <sup>749</sup>J. Sullivan and J. Stanley, *IEEE Transactions on Plasma Science* **36**, 2528 (2008).
- <sup>750</sup>F. Pezzimenti, L. F. Albanese, S. Bellone, and F. G. D. Corte, in *2009 IEEE Bipolar/BiCMOS Circuits and Technology Meeting* (IEEE, Capri, Italy, 2009) pp. 214–217.
- <sup>751</sup>G. Pensl, ed., *Silicon Carbide, III-nitrides and Related Materials: Proceedings of the 7th International Conference on Silicon Carbide, III-Nitrides and Related Materials, Stockholm, Sweden, September 1997*, Materials Science Forum No. 264/268 (1998).
- <sup>752</sup>K. Adachi, *Simulation and Modelling of Power Devices Based on 4H Silicon Carbide*, Ph.D. thesis, University of Newcastle (2003).
- <sup>753</sup>A. Gali, P. Deák, R. P. Devaty, and W. J. Choyke, *Physical Review B* **60**, 10620 (1999).
- <sup>754</sup>H. Lv, Y. Zhang, Y. Zhang, and L.-A. Yang, *IEEE Transactions on Electron Devices* **51**, 1065 (2004).
- <sup>755</sup>B. K. Meyer, D. M. Hofmann, D. Volm, W. M. Chen, N. T. Son, and E. Janzén, *Physical Review B* **61**, 4844 (2000).
- <sup>756</sup>H. Matsuura, A. Takeshita, T. Imamura, K. Takano, K. Okuda, A. Hidaka, S. Ji, K. Eto, K. Kojima, T. Kato, S. Yoshida, and H. Okumura, *Applied Physics Express* **11**, 101302 (2018).
- <sup>757</sup>M. Roschke and F. Schwierz, *IEEE Transactions on Electron Devices* **48**, 1442 (2001).
- <sup>758</sup>D. Caughey and R. Thomas, *Proceedings of the IEEE* **55**, 2192 (1967).

- <sup>759</sup>N. Arora, J. Hauser, and D. Roulston, *IEEE Transactions on Electron Devices* **29**, 292 (1982).
- <sup>760</sup>K. Vasilevskiy, S. K. Roy, N. Wood, A. B. Horsfall, and N. G. Wright, *Materials Science Forum* **897**, 254 (2017).
- <sup>761</sup>W. J. Schaffer, G. H. Negley, K. G. Irvine, and J. W. Palmour, *MRS Proceedings* **339**, 595 (1994).
- <sup>762</sup>H. Linewih, S. Dimitrijev, and K. Y. Cheong, *Microelectronics Reliability* **43**, 405 (2003).
- <sup>763</sup>T. McNutt, A. Hefner, H. Mantooth, J. Duliere, D. Berning, and R. Singh, *IEEE Transactions on Power Electronics* **19**, 573 (2004).
- <sup>764</sup>R. Ishikawa, H. Tanaka, M. Kaneko, and T. Kimoto, *physica status solidi (b)* **260**, 2300275 (2023).
- <sup>765</sup>T. Hatakeyama, T. Watanabe, M. Kushibe, K. Kojima, S. Imai, T. Suzuki, T. Shinohe, T. Tanaka, and K. Arai, *Materials Science Forum* **433–436**, 443 (2003).
- <sup>766</sup>T. T. Mnatsakanov, M. E. Levenshtein, L. I. Pomortseva, and S. N. Yurkov, *Semiconductor Science and Technology* **17**, 974 (2002).
- <sup>767</sup>S. N. Mohammad, A. V. Bemis, R. L. Carter, and R. B. Renbeck, *Solid-State Electronics* **36**, 1677 (1993).
- <sup>768</sup>M. Sotoodeh, A. H. Khalid, and A. A. Rezazadeh, *Journal of Applied Physics* **87**, 2890 (2000).
- <sup>769</sup>G. Masetti, M. Severi, and S. Solmi, *IEEE Transactions on Electron Devices* **30**, 764 (1983).
- <sup>770</sup>C. Lombardi, S. Manzini, A. Saporito, and M. Vanzi, *IEEE Transactions on Computer-Aided Design of Integrated Circuits and Systems* **7**, 1164 (1988).
- <sup>771</sup>H. Matsunami, *Japanese Journal of Applied Physics* **43**, 6835 (2004).
- <sup>772</sup>H. Dixit, D. J. Lichtenwalner, A. Scholtze, J. H. Park, S. Rogers, S. Bubel, and S. H. Ryu, *Materials Science Forum* **1090**, 153 (2023).
- <sup>773</sup>T. T. Mnatsakanov, L. I. Pomortseva, and S. N. Yurkov, *Semiconductors* **35**, 394 (2001).
- <sup>774</sup>D. Klaassen, *Solid-State Electronics* **35**, 953 (1992).
- <sup>775</sup>C. Canali, G. Majni, R. Minder, and G. Ottaviani, *IEEE Transactions on Electron Devices* **22**, 1045 (1975).
- <sup>776</sup>C. Jacoboni, C. Canali, G. Ottaviani, and A. Alberigi Quaranta, *Solid-State Electronics* **20**, 77 (1977).
- <sup>777</sup>K. Bertilsson, C. Harris, and H.-E. Nilsson, *Solid-State Electronics* **48**, 2103 (2004).
- <sup>778</sup>B. Foutz, S. O’Leary, and M. Shur, in *High Power, Broadband, Linear, Solid State Amplifier* (Cornell University, 1998) p. 57.

- 779 V. Polyakov and F. Schwierz, *IEEE Transactions on Electron Devices* **48**, 512 (2001).
- 780 V. O. Turin, *Solid-State Electronics* **49**, 1678 (2005).
- 781 J. Dorkel and Ph. Leturcq, *Solid-State Electronics* **24**, 821 (1981).
- 782 S. C. Choo, *IEEE Transactions on Electron Devices* **19**, 954 (1972).
- 783 S. Onoda, T. Ohshima, T. Hirao, K. Mishima, S. Hishiki, N. Iwamoto, and K. Kawano, *IEEE Transactions on Nuclear Science* **54**, 2706 (2007).
- 784 M. Noguchi, T. Iwamatsu, H. Amishiro, H. Watanabe, K. Kita, and S. Yamakawa, in *2017 IEEE International Electron Devices Meeting (IEDM)* (IEEE, San Francisco, CA, USA, 2017) pp. 9.3.1–9.3.4.
- 785 H. Tanaka and N. Mori, in *2024 International VLSI Symposium on Technology, Systems and Applications (VLSI TSA)* (IEEE, HsinChu, Taiwan, 2024) pp. 1–2.
- 786 C. Weitzel, J. Palmour, C. Carter, and K. Nordquist, *IEEE Electron Device Letters* **15**, 406 (1994).
- 787 H.-Y. Cha, Y. C. Choi, L. F. Eastman, M. G. Spencer, L. Ardaravicius, A. Matulionis, and O. Kiprijanovic, *Journal of Electronic Materials* **34**, 330 (2005).
- 788 Q. Zhang, A. Q. Huang, J. Wang, C. Jonas, R. Callanan, J. J. Sumakeris, S.-H. Ryu, M. Das, A. Agarwal, and J. Palmour, *IEEE Transactions on Electron Devices* **55**, 1912 (2008).
- 789 S. Murray and K. Roenker, *Solid-State Electronics* **46**, 1495 (2002).
- 790 J. Vobecky, P. Hazdra, S. Popelka, and R. K. Sharma, *IEEE Transactions on Electron Devices* **62**, 1964 (2015).
- 791 K. Bertilsson, H.-E. Nilsson, M. Hjelm, C. Petersson, P. Käckell, and C. Persson, *Solid-State Electronics* **45**, 645 (2001).
- 792 C.-Y. Cheng and D. Vasileska, *Journal of Applied Physics* **127**, 155702 (2020).
- 793 E. Belas, M. Betušiak, R. Grill, P. Praus, M. Brynza, J. Pipek, and P. Moravec, *Journal of Alloys and Compounds* **904**, 164078 (2022).
- 794 L. Ardaravičius, A. Matulionis, O. Kiprijanovic, J. Liberis, H.-Y. Cha, L. F. Eastman, and M. G. Spencer, *Applied Physics Letters* **86**, 022107 (2005).
- 795 I. Khan and J. A. Cooper, *Materials Science Forum* **264–268**, 509 (1998).
- 796 I. Khan and J. A. Cooper, *Materials Science Forum* **338–342**, 761 (2000).
- 797 I. Khan and J. Cooper, *IEEE Transactions on Electron Devices* **47**, 269 (2000).
- 798 V. Jaiswal and P. Vigneshwara Raja, *IEEE Transactions on Nuclear Science* , 1 (2024).
- 799 V. I. Sankin, *Semiconductors* **36**, 717 (2002).

- 800 D. L. Barrett and R. B. Campbell, *Journal of Applied Physics* **38**, 53 (1967).
- 801 A. A. Burk, M. J. O'Loughlin, and S. Mani, *Materials Science Forum* **264–268**, 83 (1998).
- 802 S. Contreras, M. Zielinski, L. Konczewicz, C. Blanc, S. Juillaguet, R. Müller, U. Künecke, P. J. Wellmann, and J. Camassel, *Materials Science Forum* **527–529**, 633 (2006).
- 803 H. Fujihara, J. Suda, and T. Kimoto, *Japanese Journal of Applied Physics* **56**, 070306 (2017).
- 804 T. Kimoto, S. Nakazawa, K. Hashimoto, and H. Matsunami, *Applied Physics Letters* **79**, 2761 (2001).
- 805 G. Lomakina, G. F. Kholuyanov, R. Verenehikova, E. Mokhov, and Y. A. Vodakov, *Sov. Phys. Semiconductors* **6**, 988 (1972).
- 806 R. Siergiej, R. Clarke, S. Sriram, A. Agarwal, R. Bojko, A. Morse, V. Balakrishna, M. MacMilan, A. Burk, Jr., and C. Brandt, *Materials Science and Engineering: B* **61–62**, 9 (1999).
- 807 G. Rutsch, R. P. Devaty, W. J. Choyke, D. Langer, L. Rowland, E. Niemann, and F. Wischmeyer, *Materials Science Forum* **338–342**, 733 (2000).
- 808 G. Pacchioni, L. Skuja, and D. L. Griscom, eds., *Defects in SiO<sub>2</sub> and Related Dielectrics: Science and Technology* (Springer Netherlands, Dordrecht, 2000).
- 809 V. V. Afanas'ev, A. Stesmans, M. Bassler, G. Pensl, and M. J. Schulz, *Applied Physics Letters* **76**, 336 (2000).
- 810 W.J. Choyke and L. Patrick, in *In: Silicon Carbide-1973; Proceedings of the Third International Conference* (1974) pp. 261–283.
- 811 J. H. Zhao, K. Sheng, and R. C. Lebron-Velilla, “SILICON CARBIDE SCHOTTKY BARRIER DIODE,” in *Sic Materials and Devices*, Vol. 40 (WORLD SCIENTIFIC, 2006) pp. 117–162.
- 812 N. S. Saks, S. S. Mani, and A. K. Agarwal, *Applied Physics Letters* **76**, 2250 (2000).
- 813 P. Luo and S. N. E. Madathil, *IEEE Transactions on Electron Devices* **67**, 5621 (2020).
- 814 M. Ostling, R. Ghandi, and C.-M. Zetterling, in *2011 IEEE 23rd International Symposium on Power Semiconductor Devices and ICs* (IEEE, San Diego, CA, USA, 2011) pp. 10–15.
- 815 R. Raghunathan and B. Baliga, *IEEE Electron Device Letters* **19**, 71 (1998).
- 816 C. Carter, Jr., V. Tsvetkov, R. Glass, D. Henshall, M. Brady, St.G. Müller, O. Kordina, K. Irvine, J. Edmond, H.-S. Kong, R. Singh, S. Allen, and J. Palmour, *Materials Science and Engineering: B* **61–62**, 1 (1999).
- 817 S. Nakashima and H. Harima, *SILICON CARBIDE AND RELATED MATERIALS 1995* **142**, 269 (1996).

- 81<sup>8</sup>F. Nallet, A. Senes, D. Planson, M. Locatelli, J. Chante, and J. Taboy, in *Proceedings IPEMC 2000. Third International Power Electronics and Motion Control Conference (IEEE Cat. No.00EX435)*, Vol. 1 (Int. Acad. Publishers, Beijing, China, 2000) pp. 396–401.
- 81<sup>9</sup>T. R. McNutt, in *Extreme Environment Electronics* (CRC Press, Taylor & Francis Group, 2013) pp. 409–416.
- 82<sup>0</sup>J. Wang and B. W. Williams, *Semiconductor Science and Technology* **13**, 806 (1998).
- 82<sup>1</sup>Y.-R. zhang, b. zhang, Z.-J. Li, X.-C. Deng, and X.-L. liu, *Chinese Physics B* **18**, 3995 (2009).
- 82<sup>2</sup>M. Khalid, S. Riaz, and S. Naseem, *Communications in Theoretical Physics* **58**, 577 (2012).
- 82<sup>3</sup>Y. Zhou, Y. Li, and B. Wang, in *2016 IEEE 4th Workshop on Wide Bandgap Power Devices and Applications (WiPDA)* (IEEE, Fayetteville, AR, 2016) pp. 1–7.
- 82<sup>4</sup>D. Brosselard, Pierre ; Planson, *Conception, Réalisation et Caractérisation d'interrupteurs (Thyristors et JFETs) Haute Tension (5kV) En Carbure de Silicium*, Ph.D. thesis (2004).
- 82<sup>5</sup>V. I. Sankin and A. A. Lepneva, *Materials Science Forum* **338–342**, 769 (2000).
- 82<sup>6</sup>K. Vassilevski, K. Zekentes, A. Zorenko, and L. Romanov, *IEEE Electron Device Letters* **21**, 485 (2000).
- 82<sup>7</sup>W. V. Muench and E. Pettenpaul, *Journal of Applied Physics* **48**, 4823 (1977).
- 82<sup>8</sup>S. Doğan, F. Yun, C. Roberts, J. Parish, D. Huang, R. E. Myers, M. Smith, S. E. Saddow, B. Ganguly, and H. Morkoç, *MRS Proceedings* **764**, C7.2 (2003).
- 82<sup>9</sup>J. A. Powell and L. G. Matus, in *Amorphous and Crystalline Silicon Carbide II*, Vol. 43, edited by H. K. V. Lotsch, M. M. Rahman, C. Y.-W. Yang, and G. L. Harris (Springer Berlin Heidelberg, Berlin, Heidelberg, 1989) pp. 14–19.
- 83<sup>0</sup>N. Fletcher, *Proceedings of the IRE* **45**, 862 (1957).